



University of
Nottingham
UK | CHINA | MALAYSIA



TCES-UKSB 2019 11-13 June

East Midlands Conference Centre
University of Nottingham, UK

Abstract Book



Foreward:

We are delighted to welcome you to Nottingham for the first joint conference of TCES and UKSB. We have a fantastic line up of internationally recognised keynote speakers coupled with more than thirty selected oral presentations and twenty turbo-talks. Both TCES and UKSB take pride in their engagement with up and coming researchers and this is reflected in the breadth and diversity of this year's scientific programme. The programme is organised as thirteen broad sessions, focussed on recent developments in imaging, innovation in biomaterials chemistry and characterisation, advances in sensing and controlling cell behaviour and translational research.

There will be widespread opportunities for networking and interaction across a range of exhibitors, keynote speakers and abstract presenters. We hope that this joint conference of TCES and UKSB provides excellent opportunities for both developing new networks and collaborations and renewing old links. To that end, we hope that you will join us in the social opportunities including the Welcome Reception, 6 – 8 pm on Tuesday 11th June and the conference gala on Wednesday 12th June. In addition, all Early Career Researchers are invited to the TCES-UKSB Early Career Researchers Social event, held in Mooch Bar at the Student's Union from 8 pm on Tuesday.

Please come to the registration desk for any additional information or visit our website: <https://www.nottingham.ac.uk/conference/fac-sci/pharmacy/tcesanduksb/index.aspx>

We hope you enjoy our scientific programme and social events!

Dr Lisa White, Chair TCES-UKSB 2019

TCES-UKSB 2019 Local committee

Dr Lisa White – Chair
Dr Ifty Ahmed
Dr Mahetab Amer
Ms Anannya Chatterjee
Dr Hadi Hajjali
Mr Joshua Jones
Dr I-Ning Lee
Ms Rabea Loczenski
Dr Jane McLaren
Dr Robert Owen
Mr Francesco Pappalardo
Mr Jopeth Ramis
Ms Natalija Tatic
Ms Kathryn Thomas
Mr Matthew Wadge



University of
Nottingham
UK | CHINA | MALAYSIA



TCES



UK Society for Biomaterials

TCES-UKSB 2019 11-13 June

East Midlands Conference Centre
University of Nottingham, UK



TCES-UKSB 2019 Official Sponsors:



Biomaterials
Discovery

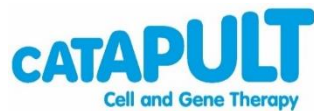
Think Possible



Life Science Innovator Since 1966



biopharma
group



don whitley
scientific
www.dwscientific.com



UK Regenerative
Medicine Platform



ElectroForce®



WORLD
PRECISION
INSTRUMENTS
Instrumenting scientific ideas

Tuesday 11th June 2019:

Development of New Models, Tools and Technologies

08:00 – 10:00 TCES-UKSB 2019 Registration and Poster Set-up

10:00 – 10:15 Welcome and Introduction to TCES-UKSB 2019

Dr Lisa White, University of Nottingham

10:15 – 11:15 SESSION 1: IMAGING IN TERM

Chair: A/Prof Colin Scotchford, University of Nottingham

10:15 – 10:45 **Keynote - Professor Chris Sammon**, Sheffield Hallam University
Using infrared imaging and spectroscopy to support the development of regenerative therapies

10:45 – 11:00 Mr Dan Merryweather, Loughborough University
Influence of sample preparation methods on the organizational presentation of collagen fibrils in hydrogel electron microscopy

11:00 – 11:15 Prof Elisa Budyn, ENS Paris-Saclay
Reforming the Haversian network in a bone-on-chip

11:15 – 12:15 SESSION 2: Turbo Talks I

1. Ms Lydia Beeken, University of Nottingham (Poster No. 144)
Development of a topical cell therapy for ocular surface disorders
2. Ms Charlotte Lee-Reeves, Imperial College London (Poster No. 264)
Improving stem cell therapies for traumatic brain injury using bioactive ECM scaffolds to attenuate inflammation
3. Mr David Hiram Ramos Rodriguez, University of Sheffield (Poster No. 136)
Development of topographically controlled electrospun scaffolds to deliver proangiogenic agents for wound healing
4. Ms Man Li, University of Liverpool (Poster No. 54)
Nitric oxide releasing electrospun nanofibers for antimicrobial bone tissue engineering
5. Ms Kathryn Thomas, University of Nottingham (Poster No. 240)
Phosphate based glass coatings for rapid Ga³⁺ release: the challenges of balancing cytocompatibility with antimicrobial effects
6. Mrs Shirin Hanaei, Nottingham Trent University (Poster No. 109)
Modelling and emulating 3D multi-tissue interactions by microfluidic chip technology
7. Ms Flavia Bonalumi, University of Brighton (Poster No. 104)
Development of a multi-layered cryogel bioreactor with optimised fluid dynamics for bioartificial liver application
8. Mrs Alison Wilson, University of York (Poster No. 73)
Clinical translation of regenerative medicines: a regulatory primer
9. Mr Paul Mardling, Sheffield Hallam University (Poster No. 194)
Auxetic and composite scaffolds show potential for use in tissue engineering
10. Ms Thunyaporn Srisubin, University of Manchester (Poster No. 80)
Phosphonate-modified graphene-laponite composites for bone repair

12:15 – 13:30 Lunch and UKSB Annual General Meeting

13:30 – 15:15 SESSION 3: NEXT GENERATION BIOMATERIALS DISCOVERY

Chair: Prof Morgan Alexander, University of Nottingham

- 13:30 – 14:00 **Keynote - Professor Jan de Boer**, Eindhoven University of Technology
Life at the cell-material interface
- 14:00 – 14:15 Dr Mahetab Amer, University of Nottingham
Differentiation by design: Varying surface topographical features of polymeric microparticles influences mesenchymal stem cell fate
- 14:15 – 14:30 Mr Chinnawich Phamornnak, University of Manchester
Non-woven mats of electroactive composites of silk-PEDOT:PSS for peripheral nerve regeneration
- 14:30 – 14:45 Dr Jenny Aveyard, University of Liverpool
Nitric oxide releasing contact lens bandages
- 14:45 – 15:00 Mr David Richards, University of Manchester
Utilising a novel photoresponsive hydrogel with defined surface topography and photoswitchable stiffness to analyse the biophysical regulation of mesenchymal stem cells
- 15:00 – 15:15 Dr Laura Ruiz, University of Nottingham.
Rapid screening of inks for 3D printing personalised drug delivery implants
- 15:15 – 16:15 Coffee Break and Posters

16:15 – 18:00 SESSION 4: INNOVATIVE BIOMATERIALS

Chair: Dr Jude Curran, University of Liverpool

- 16:15 – 16:30 Platinum Exhibitor: **Jellagen**
- 16:30 – 17:00 **Keynote - Professor Sandra Van Vlierberghe**, University of Ghent
Versatile hydrogel platform for 3D printing applications
- 17:00 – 17:15 Dr Maxine Chan, Imperial College London
Fabrication and characterisation of endometrial extracellular matrix hydrogel for endometrial regeneration
- 17:15 – 17:30 Mr George Fleming, University of Liverpool.
Dual-action nitric oxide-releasing micropatterned antibacterial PDMS surfaces
- 17:30 – 17:45 Dr Richard Balint, University of Manchester.
Graphene-polymer composites for the engineering of cardiac tissue
- 17:45 – 18:00 Prof Bikramjit Basu, Indian Institute of Science
3D inkjet printing of biomaterials with strength reliability and cytocompatibility: Quantitative process strategy for Ti-6Al-4V

18:00 – 20:00 TCES-UKSB Welcome Reception

20:00 onward TCES-UKSB Early Career Researchers Social, Mooch, Students Union

Wednesday 12th June 2019:
Translational Research: Barriers and Breakthroughs

08:00 – 09:00 Meet the Mentor 1

09:00 – 10:45 SESSION 5: BIOMATERIALS AND TERM

Chair: Dr Araida Hidalgo-Bastida, Manchester Metropolitan University

09:00 – 09:15 Platinum Exhibitor: **TA Electroforce**

09:15 – 09:45 **Keynote - Professor Stephen Badylak**, University of Pittsburgh
Clinical Translation of an acellular therapy for Barrett's Oesophagus

09:45 – 10:00 Dr Victoria Roberton, University College London
Local suppression of the T cell response to peripheral nerve allografts using drug-eluting PCL fibres

10:00 – 10:15 Mr James Reid, University of Edinburgh
Biofunctionalizing tailored electrospun scaffolds for influencing vascular cellular performance

10:15 – 10:30 Ms Azadeh Rezaei, University College London
Role of silicate and silicate-bioactive glasses in bone nodule formation

10:30 – 10:45 Ms Roxanna Ramnarine, University of Southampton
Self-assembling structured laponite hydrogels with spontaneous 3D micropatterning of bioactive factors for tissue regeneration

10:45 – 11:15 Coffee break

11:15 – 12:45 SESSION 6: ADVANCES IN TERM

Chair: Dr James Phillips, University College London

11:15 – 11:30 Platinum Exhibitor: **Cell and Gene Therapy Catapult**

11:30 – 12:00 **Keynote - Professor Alicia El Haj**, University of Birmingham
Translation of cell therapy control platforms to the clinic

12:00 – 12:15 Dr Lucy Bosworth, University of Liverpool
Electrospun scaffolds containing decellularised tissue matrix support conjunctival epithelial and goblet cells

12:15 – 12:30 Dr Emily Britchford, University of Nottingham/NuVision Biotherapies
Validation and assessment of an antibiotic decontamination manufacturing protocol for vacuum-dried human amniotic membrane

12:30 – 12:45 Mr Jonathan May, University of Southampton
Study of the effects of microbubbles on bone formation using micro-CT

12:45 – 14:00 Lunch and TCES Annual General Meeting

14:00 – 15:30 SESSION 7: DEVELOPMENT OF TRANSLATIONAL & 3D MODELS

Chair: Dr Paul Roach, Loughborough University

14:00 – 14:15 Platinum Exhibitor: **BioTek**

- 14:15 – 14:45 **Keynote - Professor Katja Schenke-Layland**, University of Tübingen
Non-invasive high content analysis of 3D in vitro test systems
- 14:45 – 15:00 Ms Bethany Ollington, University of Sheffield
Generation of an immuno-responsive tissue engineered oral mucosal equivalent containing primary human macrophages
- 15:00 – 15:15 Dr Laura Macri-Pellizzeri, University of Nottingham
Porous glass microspheres show biocompatibility, tissue ingrowth and osteogenic onset in vivo
- 15:15 – 15:30 Mr Jeremy Mortimer, University of Edinburgh
Investigations of human tendon width for the anatomical design of an in vitro flexor digitorum profundus enthesis model
- 15:30 – 16:30 Coffee and Posters
- 16:30 – 18:00 SESSION 8: ROBERT BROWN EARLY STAGE INVESTIGATOR AND UKSB PRIZES**
Chair: Dr Nick Evans, University of Southampton
- 16:30 – 16:45 Dr Jennifer Ashworth, University of Nottingham
Peptide gels of fully-defined composition and mechanics for modelling cell-matrix interactions in breast cancer
- 16:45 – 17:00 Dr Nazia Mehrban, University College London
In vivo response to injectable hydrogels: from decellularised ECM to de novo peptides
- 17:00 – 17:30 **Alan Wilson Memorial Lecture – Professor David Wood**, University of Leeds
The Minimata convention: challenges and opportunities for aesthetic dental materials
- 17:30 – 18:00 **UKSB President's Prize – Professor Kevin Shakesheff**, University of Nottingham
Minimally invasive delivery of temperature sensitive biomaterials
- 19:00 – 23:00 TCES-UKSB Conference Gala Dinner** *Drinks reception in Council Room (A21); dinner in the Senate Chamber at 20:00, Trent Building.*

Thursday 13th June 2019:
Emerging Research and New Frontiers

08:00 – 09:00 Meet the Mentor 2

09:00 – 09:45 SESSION 9: SENSING & CONTROLLING CELL BEHAVIOUR I

Chair: Prof Sarah Cartmell, University of Manchester

09:00 – 09:30 **Keynote - Dr Roisin Owens**, University of Cambridge
A 3D bioelectronics model of the human gut

09:30 – 09:45 Dr Frankie Rawson, University of Nottingham
Stimulative 3D conducting architectures to modulate cellular phenotype

09:45 – 10:45 SESSION 10: TURBO TALKS II

1. Ms Jazz Stening, University of Nottingham (Poster No. 243)
Optimisation of microparticle formulations for cytokine delivery for macrophage modulation for potential application in spinal cord injury
2. Ms Rina Maruta, Kyoto Institute of Technology (Poster No. 150)
3D culture of epidermis by use of recombinant silk materials containing FGF-7 protein microcrystals
3. Ms Eleanor Porges, University of Southampton (Poster No. 148)
Stable encapsulation of rifampicin and doxycycline in polymersome nanoparticles for delivery to intracellular bacteria
4. Mr George Bullock, University of Sheffield (Poster No. 159)
Bisphosphonate toxicity to the oral mucosa is inhibited in vitro by hydroxyapatite granules
5. Ms Jamie Thompson, University of Nottingham (Poster No. 161)
Investigating glycosaminoglycans in development and disease using fully defined 3D cell culture environments and human pluripotent stem cells
6. Mr Alexander Sturtivant, University of Edinburgh (Poster No. 182)
Use of antifreeze proteins to modify pores in directionally frozen alginate sponges for cartilage tissue engineering
7. Ms Anastasia Polydorou, University of Southampton (Poster No. 122)
Acoustically-stimulated drug carriers for bone fracture repair
8. Dr Valentina Barrera, NHS Blood and Transplant, Tissue and Eye Services R&D (Poster No. 236)
Decellularisation of human femoral nerves in a closed system: towards introducing a new nerve allograft in healthcare in the UK
9. Mr Jordan Roe, Loughborough University (Poster No. 197)
Magnetic hydrogels: tissue engineering constructs with switchable stiffness
10. Ms Michaela Petaroudi, University of Glasgow (Poster No. 149)
Bacterial engineering for the ex-vivo expansion of HSCs

10:45 – 11:45 Coffee and Posters

11:45 – 12:30 SESSION 11: SENSING & CONTROLLING CELL BEHAVIOUR II

Chair: Dr Adam Celiz, Imperial College London

11:45 – 12:00 Dr Nuria Oliva Jorge, Imperial College London
Bioinspired nanomaterials for cell-selective activation of growth factors

- 12:00 – 12:15 Mr Manohar Prasad Koduri, University of Liverpool
Cytotoxicity and functionality of nano oxy-ph sensors in HMSC environment
- 12:15 – 12:30 Mrs Eva Barcelona, University of Glasgow
Engineering ligand mobility in the adhesive crosstalk to control stem cell differentiation
- 12:30 – 13:30 Lunch and Meet the Mentor 3

13:30 – 14:45 SESSION 12: BIOMATERIALS CHEMISTRY AND CHARACTERISATION I
Chair: Dr Cheryl Miller, University of Sheffield

- 13:30 – 14:00 **Keynote - Professor Elizabeth Cosgriff-Hernandez**, University of Texas
Integrin-targeting materials in regenerative medicine
- 14:00 – 14:15 Dr Caroline Taylor, University of Sheffield
The potential of pressurised gyration to fabricate polyhydroxyalkanoate aligned fibre scaffolds for peripheral nerve repair
- 14:15 – 14:30 Mr Morgan Lowther, University of Birmingham
Formulation of an antimicrobial silver-doped magnesium oxychloride cement
- 14:30 – 14:45 Dr Rachel McCormick, University of Liverpool
Designing a novel bioengineered substrate as a treatment for AMD
- 14:45 – 15:15 Coffee break

15:15 – 16:00 SESSION 13: BIOMATERIALS CHEMISTRY AND CHARACTERISATION II
Chair: Prof Felicity Rose, University of Nottingham

- 15:15 – 15:45 **Larry Hench Young Investigators Prize – Dr Asha Patel**, Imperial College London
Chemically diverse materials for cell and gene therapy applications
- 15:45 – 16:00 Ms Maha Omran, University of Sheffield
Evaluating two powder-based 3d printing techniques for the manufacture of implants for orbital floor repair
- 16:00 – 17:00 Prizes and Closing Address**

TCES-UKSB 2019 Keynote Lecture

USING INFRARED IMAGING AND SPECTROSCOPY TO SUPPORT THE DEVELOPMENT OF REGENERATIVE THERAPIES

Professor Chris Sammon¹

¹Sheffield Hallam University, UK

Infrared (IR) spectroscopy is a non-destructive analytical tool commonly used in materials characterisation and forensics, providing a 'chemical fingerprint' based on the vibrations of covalent bonds. These vibrations are sensitive to both the chemistry and environment of the species under investigation. Consequently it is possible to use IR to provide an abundance of information pertinent to TERM applications beyond facile materials identification. In this presentation I will show how IR spectroscopy and imaging can play an important role in biomaterials development and tissue engineering using examples from my lab.

I will present data to show how IR spectroscopy can provide information about the gelation, hydration, swelling and dehydration properties of a family of Laponite[®] crosslinked pNIPAM hydrogels. These materials have thermal responsive properties close to body temperature and, by careful selection of the hydrogel composition, can drive the differentiation of human mesenchymal stem cells towards predetermined phenotypes for a range of clinical applications.

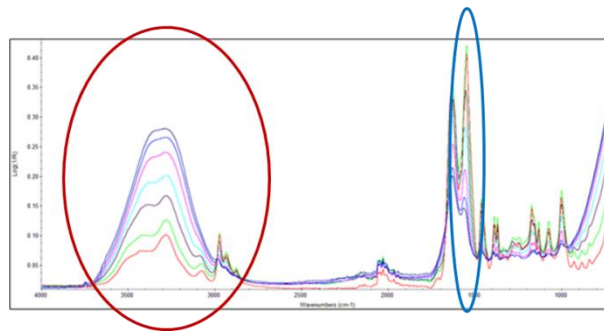


Fig 1: Typical IR data showing the dehydration of a L-pNIPAM hydrogel with time

I will also provide examples of how we use IR imaging to generate pseudo immunohistological stains from tissue sections based on changes in the chemistry. This has some advantages over more traditional IHC approaches such as obtaining multiple 'stains' from the same section and the ability to use the same protocols across species. This approach has been used to characterise the diseased state in both human and goat IVDs and we are currently applying this to assess the efficacy of regeneration of samples using an organ culture system.

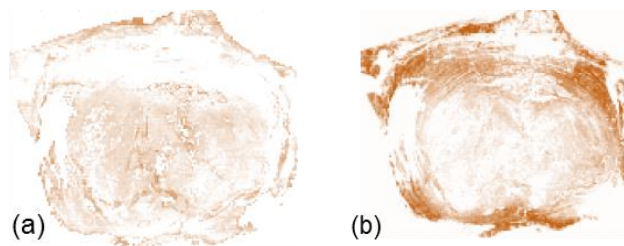


Fig 2: Typical IR images showing the distribution of (a) Col I and (b) Col II from a single goat IVD section

TCES-UKSB 2019 Keynote Lecture

LIFE AT THE CELL-MATERIAL INTERFACE

Professor Jan de Boer¹

¹*Laboratory of BioInterface Science, Institute for Complex Molecular Systems and Dept. of Biomedical Engineering, Eindhoven University of Technology, The Netherlands.
www.jandeboerlab.com*

In my seminar I will present our latest work on controlling the interaction of cells with biomaterials through design of surface topography. For instance, we are interested in the bone-inducing properties of a subset of porous calcium phosphate ceramics and show how through reverse engineering, we are uncovering an interesting and complex response of cells to materials. Inspired by this, we have started to design high throughput screening strategies of biomaterials libraries, and in particular libraries of surface topographies. Using a design algorithm, we have generated numerous different patterns, which can first be reproduced on a silicon mold and then imprinted onto polymers using microfabrication. After cell seeding, we use quantitative high content imaging and machine learning algorithms to characterize the response of the cells to the thousands of different surfaces and learn more about the relation between surface topography and cell response. For instance, we have identified surfaces which stimulate osteogenic differentiation of mesenchymal stem cells and we are currently testing whether these surfaces can be applied in orthopedic surgery. The focus of my seminar will be on our effort to digitize life at the interface of biomaterials and cells through parameterization of biomaterial properties, –omics based approaches to analyse cell response and computational science to understand and design bio-active biomaterials.

TCES-UKSB 2019 Keynote Lecture

VERSATILE HYDROGEL PLATFORM FOR 3D PRINTING APPLICATIONS

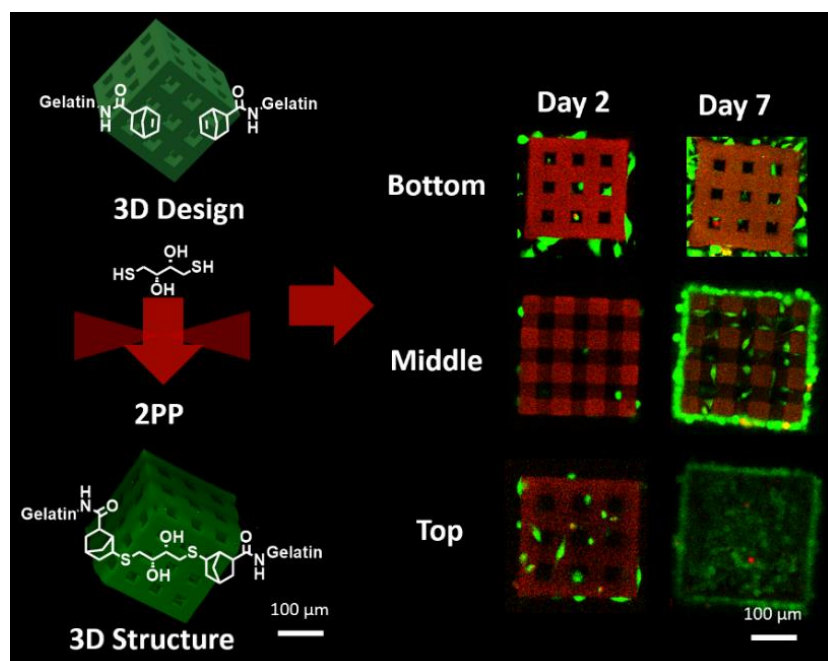
Professor Sandra Van Vlierberghe¹

¹University of Ghent

Biofabrication is a specific area within the field of tissue engineering which takes advantage of rapid manufacturing (RM) techniques to generate 3D structures which mimic the natural extracellular matrix (ECM). A popular material in this respect is gelatin, as it is a cost-effective collagen derivative, which is the major constituent of the natural ECM. The material is characterized by an upper critical solution temperature making the material soluble at physiological conditions. To tackle this problem, the present work focusses on different gelatin functionalization strategies which enable covalent stabilization of 3D gelatin structures [1, 2].

In a second part, synthetic acrylate-endcapped, urethane-based precursors will be discussed with exceptional solid state crosslinking behaviour compared to conventional hydrogels [3].

Several polymer processing techniques will be covered including conventional 3D printing using the Bioscaffolder 3.1, two-photon polymerization (see Fig.) and electrospinning starting from crosslinkable hydrogels. A number of biomedical applications will be tackled including adipose tissue engineering [4], vascularization [5], ocular applications [6], etc. The results show that chemistry is a valuable tool to tailor the properties of hydrogels towards processing while preserving the material biocompatibility.



References

- [1] J. Van Hoorick *et al.*, *Macromolecular Rapid Communications* (2018) 39 : 1800181, doi: 10.1002/marc.201800181.
- [2] J. Van Hoorick *et al.*, *Biomacromolecules* (2017) 18 : 3260-3272, doi: 10.1021/acs.biomac.7b00905.
- [3] A. Houben *et al.*, WO 2017/005613.
- [4] L. Tytgat *et al.*, *Acta Biomaterialia* (2019) accepted.
- [5] T. Qazi *et al.*, *Biofabrication* (2019) submitted.
- [6] J. Van Hoorick *et al.*, *Advanced Healthcare Materials* (2019) submitted.

TCES-UKSB 2019 Keynote Lecture

CLINICAL TRANSLATION OF AN ACELLULAR THERAPY FOR BARRETT'S ESOPHAGUS

Professor Stephen Badyak, DVM, PhD, MD¹

¹McGowan Institute for Regenerative Medicine, University of Pittsburgh

The clinical translation of any medical technology, including regenerative medicine technology, is dependent upon the ability to overcome recognized barriers including: a genuine clinical need with a sound solution, intellectual property protection, convincing preclinical studies, and regulatory hurdles, among others. Esophageal disease represents a major societal problem which begins with gastric reflux and, in a significant number of cases, progress to esophageal cancer and esophagectomy. This presentation will review the preclinical and clinical studies that resulted in the development of an ECM-based hydrogel for the treatment of esophageal disease. A review of initial human studies and next steps in clinical translation will be discussed.

TCES-UKSB 2019 Keynote Lecture

CELLS IN THEIR DYNAMIC ENVIRONMENT – IMPLICATIONS FOR CELL THERAPY AND REGENERATIVE MEDICINE

Professor Alicia El Haj¹

¹Healthcare Technology Institute, University of Birmingham

A variety of cell types respond and adapt to their mechanical environment. These mechanical cues are responsible for maintaining homeostasis, turnover and growth of developmental and adult tissues. Connective tissues are well known for their mechanical functions and a variety of cell types within these tissues have been shown to be mechano-responsive. Our studies on single cell analysis of the biomechanical properties of chondrocytes and the effects of the surrounding matrix in integrating the biomechanical responses demonstrates the challenges for tissue engineers for mimicking natural dynamic cell matrix interactions. Our 3D studies have begun to define the ways we can use bioreactor growth environments to mimic the in vivo environment. Using magnetic nanoparticles approaches, we have begun to target specific mechano-receptors and control cell behaviour remotely. The challenge lies in translating our findings into the clinical setting – can we use biomechanical cues/receptor tagging as therapeutic treatments and if so how? Regenerative medicine gives us a route to explore ways we can define new mechano-active therapies. This presentation will identify the role of physical cues in cell behaviour and stem cell differentiation and the potential for utilising these biomechanical signalling cues ultimately in cell therapy.

TCES-UKSB 2019 Keynote Lecture

NON-INVASIVE HIGH CONTENT ANALYSIS OF 3D IN VITRO TEST SYSTEMS

Professor Katja Schenke-Layland^{1,2,3}

¹ Department of Women's Health, Research Institute for Women's Health, Eberhard Karls University Tübingen, Tübingen, Germany

² The Natural and Medical Sciences Institute (NMI) at the University of Tübingen, Reutlingen, Germany

³ Department of Medicine/Cardiology, Cardiovascular Research Laboratories (CVRL), University of California (UCLA), Los Angeles, CA, USA

As the field of regenerative and personalized medicine matures, the need for novel enabling technologies to characterize cells and engineered constructs (i.e. cells/tissue combined with scaffolds and/or growth factors) as well as their individual components in a more insightful, quantitative and preferably non-invasive manner becomes imperative. Raman microspectroscopy is an emerging technique based on light scattering that allows assessing molecular interactions and the biochemical structure of a sample in a non-invasive manner. Specifically for tissue engineering applications, it has been proven to allow determining biochemical information on cells, tissues and/or material-cell tissue constructs without the need for labels.

The aim of this talk is to show the applicability of Raman microspectroscopy for regenerative and personalized medicine applications, and to discuss the added value of the generated data for tissue engineering construct design optimization and preclinical as well as clinical applications.

TCES-UKSB 2019 Keynote Lecture

A 3D BIOELECTRONICS MODEL OF THE HUMAN GUT

Dr Roisin M. Owens¹

¹Department of Chemical Engineering and Biotechnology, University of Cambridge, Cambridge CB3 0AS, United Kingdom

In vitro models of biological systems are essential for our understanding of biological systems. In many cases where animal models have failed to translate to useful data for human diseases, physiologically relevant in vitro models can bridge the gap. Many difficulties exist in interfacing complex, 3D models with technology adapted for monitoring function. Polymeric electroactive materials and devices can bridge the gap between hard inflexible materials used for physical transducers and soft, compliant biological tissues. An additional advantage of these electronic materials is their flexibility for processing and fabrication in a wide range of formats.(1) In this presentation, I will discuss our recent progress in adapting conducting polymer devices, including simple electrodes and transistors, to integrate with 3D cell models. We go further, by generating 3D electroactive scaffolds capable of hosting and monitoring cells.(2) We are currently working on adapting these scaffolds for a 3D model of the human gut to study microbiome interactions.

Bibliography

1. J. Rivnay *et al.*, Organic electrochemical transistors. *Nat. Rev. Mater.* **3**, 17086 (2018).
2. C. Pitsalidis *et al.*, Transistor in a tube: A route to three-dimensional bioelectronics. *Sci. Adv.* **4**, eaat4253 (2018).

TCES-UKSB 2019 Keynote Lecture

INTEGRIN-TARGETING MATERIALS IN REGENERATIVE MEDICINE

Professor Elizabeth Cosgriff-Hernandez¹

¹Biomedical Engineering, The University of Texas at Austin, Austin, Texas

The ability to direct cell behavior has been central to the success of numerous therapeutics to regenerate tissue or facilitate device integration. Collagen often serves as a design basis for bioactive materials due to its putative role in regulating cell adhesion and phenotype, which occurs in part through $\alpha1\beta1$ and $\alpha2\beta1$ integrin adhesion signals it presents to cells. These integrins are involved in an array of cell activities including angiogenesis, cell migration, adhesion, and proliferation. However, all collagen-containing products on the market today utilize materials from slaughterhouses with the associated disadvantages including no means to optimize the molecular composition of the collagen to guide regeneration. We propose to circumvent these limitations by generating novel bioactive materials using a collagen-mimetic protein engineered to have enhanced therapeutic action and improved scale-up potential. Initial sequence design was based on the collagen-like protein, Scl2 in *Streptococcus pyogenes*. Whereas native collagen has numerous binding sites for integrins present on a wide range of cells, the Scl2 protein acts as a biological blank slate that only displays the selected receptor-binding sequences programmed in by site-directed mutagenesis. We used site directed mutagenesis to introduce human integrin binding sites into this protein and have provided evidence that human integrin binding sites function within the engineered protein bind and activate $\alpha1\beta1/\alpha2\beta1$. To generate robust materials based on this technology, the collagen-mimetic protein was conjugated into a poly(ethylene glycol) (PEG) based hydrogel to generate bioactive hydrogels. This platform technology is currently being explored in several tissue engineering applications including chronic wound dressings, bone grafts, and vascular grafts. It also provides a unique opportunity to investigate the contribution of collagen binding integrins in a variety of regenerative processes and disease pathogenesis.

UKSB Prizes

ALAN WILSON MEMORIAL LECTURE

THE MINIMATA CONVENTION: CHALLENGES AND OPPORTUNITIES FOR AESTHETIC DENTAL MATERIALS

Professor David Wood¹

¹School of Dentistry, University of Leeds
Corresponding author: d.j.wood@leeds.ac.uk

Introduction: Interest in developing new materials to replace amalgam in stress-bearing posterior restorations remains high following the introduction of the Minimata Convention which aims to reduce global environmental mercury levels. The implication for dentistry of the Minimata Convention is a phased reduction in the use of dental amalgam, which for many dentists, particularly in the NHS, is their go-to material for posterior fillings. This opens up the possibility of further developments in the field of direct aesthetic filling materials, including glass-ionomer cements and dental composites. At the other end of the translational pipeline it will be important to understand the barriers to uptake and routine use of these amalgam alternatives.

Materials and Methods: Mechanical properties of commercial and model amalgam replacement materials were assessed with a focus on flexural strength and fracture toughness which are claimed to be key materials properties when trying to project how a material will perform clinically. The barriers to the uptake of new materials were addressed using a mixed methods approach; the qualitative study involved semi-structured interviews and focus groups with GDPs (private and NHS), dental school teaching leads and NHS dental commissioners.

Results and Discussion: Several of the newly launched amalgam replacement materials and an experimental dental composite exhibited similar/enhanced mechanical properties compared to a highly filled conventional resin composite and significantly higher values compared to a glass hybrid material. Barriers to amalgam phase down included lack of suitable alternatives, costs, time and training in use of alternative materials. Of concern, NHS GDPs considered extraction of teeth as a treatment option in the absence of amalgam and commissioners were concerned that GDP time constraints in the absence of amalgam would lead to reduced access to dental services. Dental schools had reduced teaching of dental amalgam but newly qualified GDPs felt disadvantaged as amalgam was the material of choice for NHS restorations.

Conclusions: The continued development of aesthetic directly placed filling materials suitable for the posterior of the mouth is encouraging. Our data suggest that a complete phase out of amalgam is not currently feasible unless appropriate measures are in place to ensure cheaper, long-lasting and easy to use alternatives are available and can be readily adopted by primary care oral health providers.

UKSB PRESIDENT'S PRIZE

MINIMALLY INVASIVE DELIVERY OF TEMPERATURE SENSITIVE BIOMATERIALS

Professor Kevin Shakesheff¹

¹UK Regenerative Medicine Platform for Acellular Materials, School of Pharmacy, University of Nottingham

Corresponding author: kevin.shakesheff@nottingham.ac.uk

There are many emerging opportunities in the fields of cell therapy and regenerative medicine to improve efficacy and safety using biomaterials. For example, the use of cell therapies to regenerate tissues is hampered by low retention efficiencies after injection into target tissue sites. Biomaterials can optimize the local environment after administration to protect cells from unwanted physical stresses, provide surfaces for attachment and release molecules to guide cell fate.

For applications in the musculoskeletal system, CNS, liver, eye and other tissues there is a need for minimally invasive delivery of the cell therapy. This places an extra demand on the design of the biomaterials that can be administered through narrow bore needles and acquire their functional structure post-delivery within the body. The Nottingham teams over the last 2 decades have invented new materials and processes to create technologies for cell and drug delivery after minimally-invasive administration. A new class of particulate materials that undergo a process called liquid sintering provide a platform technology for many cell and regenerative medicines. The underlying materials science and potential applications of these materials will be explored in this presentation.

LARRY HENCH YOUNG INVESTIGATORS PRIZE

CHEMICALLY DIVERSE MATERIALS FOR CELL AND GENE THERAPY APPLICATIONS

Dr Asha Kumari Patel^{1*}

¹National Heart & Lung Institute, Imperial College London, UK.
Corresponding author: asha.patel@imperial.ac.uk

Introduction

The development of defined biomaterials for cell & gene therapy could overcome issues associated with scalability and reproducibility that hinder biologically derived systems. However, rationale design of biomaterials is difficult without fully understanding cell-material interactions, therefore to enable identification of novel chemical ligands capable of cellular interaction, we employed parallel screening approaches that correlate biological response with materials chemistry [1].

Two key areas that my research has focussed on to date are developing synthetic materials that can support cell culture [2] and non-viral vectors that encourage cell uptake and gene delivery [3,4]. More recently we have demonstrated that physical properties such as polymer topology can influence gene delivery, broadening the toolkit to manipulate material properties for control of cellular interaction.

My current research investigates how chemically diverse messenger RNA constructs can alter pharmacokinetic profile to enable controlled protein expression.

Methods

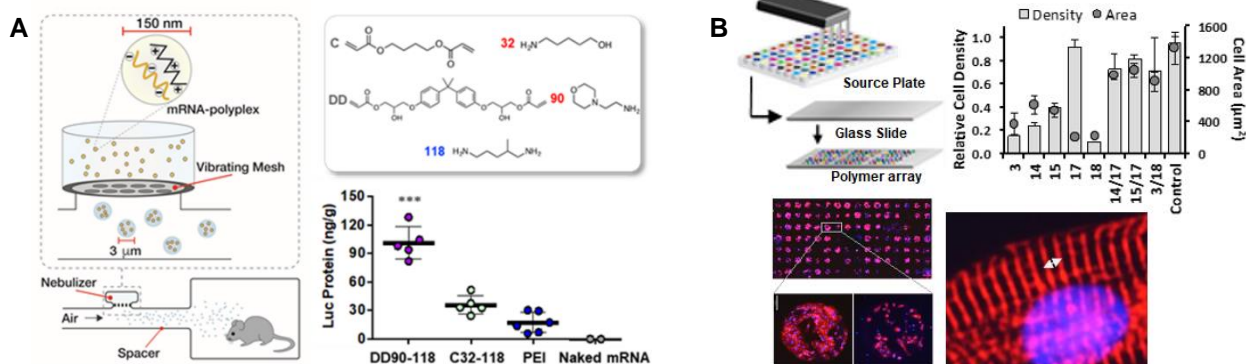
Nanoformulated polyplexes for gene delivery

Chemically diverse acrylate and amine monomers were reacted via Michael Addition to generate linear or hyperbranched cationic polymers. The ability of these materials to complex with and protect nucleic acids such as DNA and mRNA was assessed, as well as transfection efficiency for intracellular gene delivery.

Chemically defined substrates for cell culture

Acrylate monomers with diverse side chain chemistry were pin printed onto glass slides and polymerised in situ via free-radical polymerisation. Cells of interest such as human pluripotent stem cells and cardiomyocytes were cultured on the slides to identify materials capable of supporting cell survival in the absence of undefined components such as Matrigel™ or fetal bovine serum.

Results & Discussion



A) Cationic amine polymers were synthesised for nebulised messenger RNA delivery. Chemical modification of the polymer greatly influenced gene transfection in vivo, with DD90-118 based polymers able to generate greater luciferase protein in the lung compared to C32-118 polymers [3].

B) Chemically diverse microarrays were seeded with human pluripotent stem cell derived cardiomyocytes. Cardiomyocyte attachment density, as well as cell morphology and sarcomere alignment were influenced by surface chemistry [2].

References

1. Patel AK, Tibbitt MW, Celiz AD *et al.* Current Opinion in Solid State & Material Science 2016
2. Patel AK, Celiz AD, Rajamohan D *et al.* Biomaterials 61: 257-265, 2015
3. Patel AK, Kaczmarek JC, Bose S *et al.* Advanced Materials. 31: 1805116, 2019
4. Kaczmarek JC, Patel AK, Kauffman K *et al.* Angewandte Chemie Int Ed. 55: 1-6, 2016

Acknowledgements

I'd like to express my sincere gratitude to generous mentors including David Williams, Chris Denning, Morgan Alexander, Martyn Davies, Sian Harding, Bob Langer, Dan Anderson. I'd like to acknowledge recent contributions from Skye Quinn, Rafaela Konstantinidi and Emmanuel Okwelogu and previous funding from the Engineering & Physical Sciences Research Council (EPSRC) EP/I017801/1.

Table of Contents

ORAL

Biofunctionalizing Tailored Electrospun Scaffolds for Influencing Vascular Cellular Performance	2
<u>Mr. James Reid</u> ¹ , <u>Dr. Alison McDonald</u> ¹ , <u>Dr. Anthony Callanan</u> ²	
<i>1. The University of Edinburgh, 2. University of Edinburgh</i>	
BIOINSPIRED NANOMATERIALS FOR CELL-SELECTIVE ACTIVATION OF GROWTH FACTORS	3
<u>Dr. Nuria Oliva Jorge</u> ¹ , <u>Dr. Benjamin Almquist</u> ¹	
<i>1. Imperial College London</i>	
CYTOTOXICITY AND FUNCTIONALITY OF NANO OXY-PH SENSORS IN HMSC ENVIRONMENT	4
<u>Mr. Manohar Prasad Koduri</u> ¹ , <u>Dr. James Henstock</u> ¹ , <u>Prof. John Hunt</u> ² , <u>Prof. Fan- Gang Tseng</u> ³ , <u>Dr. Judith Curran</u> ¹	
<i>1. University of Liverpool, 2. Nottingham Trent University, 3. National Tsing Hua University</i>	
Designing a novel bioengineered substrate as a treatment for AMD	5
<u>Dr. Rachel McCormick</u> ¹ , <u>Mr. Ian Pearce</u> ² , <u>Dr. Atikah Haneef</u> ¹	
<i>1. University of Liverpool, 2. Royal Liverpool University Hospital, St Paul's Eye Unit</i>	
Differentiation by design: Varying surface topographical features of polymeric microparticles influences mesenchymal stem cell fate	6
<u>Dr. Mahetab Amer</u> ¹ , <u>Dr. Marta Alvarez Paino</u> ¹ , <u>Prof. Kevin M Shakesheff</u> ¹ , <u>Prof. David Needham</u> ¹ , <u>Prof. Morgan Alexander</u> ¹ , <u>Prof. Cameron Alexander</u> ¹ , <u>Prof. Felicity Rose</u> ¹	
<i>1. University of Nottingham</i>	
Dual-action Nitric Oxide-releasing Micropatterned Antibacterial PDMS Surfaces	7
<u>Mr. George Fleming</u> ¹ , <u>Dr. Jenny Aveyard</u> ¹ , <u>Dr. Jo Fothergill</u> ¹ , <u>Dr. Fiona McBride</u> ¹ , <u>Prof. Rasmita Raval</u> ¹ , <u>Dr. Raechelle D'Sa</u> ¹	
<i>1. University of Liverpool</i>	
Electrospun scaffolds containing decellularised tissue matrix support conjunctival epithelial and goblet cells	8
<u>Dr. Lucy Bosworth</u> ¹ , <u>Dr. Catalina Pineda Molina</u> ² , <u>Dr. Valentina Barrera</u> ³ , <u>Dr. Lisa White</u> ⁴ , <u>Dr. Kyle Doherty</u> ¹ , <u>Dr. Raechelle D'Sa</u> ¹ , <u>Prof. Paul Rooney</u> ³ , <u>Prof. Stephen Badylak</u> ² , <u>Prof. Rachel Williams</u> ¹	
<i>1. University of Liverpool, 2. University of Pittsburgh, 3. NHS Blood and Transplant, 4. University of Nottingham</i>	
Engineering ligand mobility in the adhesive crosstalk to control stem cell differentiation	9
<u>Mrs. Eva Barcelona</u> ¹ , <u>Dr. Marco Cantini</u> ¹ , <u>Prof. Matthew Dalby</u> ¹ , <u>Prof. Manuel Salmeron-Sanchez</u> ¹	
<i>1. University of Glasgow</i>	
EVALUATING TWO POWDER-BASED 3D PRINTING TECHNIQUES FOR THE MANUFACTURE OF IMPLANTS FOR ORBITAL FLOOR REPAIR	10
<u>Ms. maha omran</u> ¹ , <u>Dr. Caroline Harrison</u> ² , <u>Dr. Candice Majewski</u> ² , <u>Dr. Robert Moorehead</u> ² , <u>Dr. Joey Shepherd</u> ² , <u>Dr. Iain Varley</u> ² , <u>Dr. cheryl miller</u> ³	
<i>1. University of She, 2. University of Sheffield, 3. The University of Sheffield</i>	

Fabrication and Characterisation of Endometrial Extracellular Matrix Hydrogel for Endometrial Regeneration	11
<i>Dr. Maxine Chan¹, Dr. Tim Keane¹, Dr. Srdjan Saso¹, Mr. Richard Smith¹, Prof. Molly Stevens¹</i>	
<i>1. Imperial College London</i>	
FORMULATION OF AN ANTIMICROBIAL SILVER-DOPED MAGNESIUM OXYCHLORIDE CEMENT	12
<i>Mr. Morgan Lowther¹, Prof. Liam Grover², Dr. Sophie Cox²</i>	
<i>1. School of Chemical Engineering, University of Birmingham, 2. University of Birmingham</i>	
Generation of an immuno-responsive tissue engineered oral mucosal equivalent containing primary human macrophages	13
<i>Ms. Bethany Ollington¹, Dr. Helen Colley¹, Prof. Craig Murdoch¹</i>	
<i>1. University of Sheffield</i>	
Graphene-Polymer Composites for the Engineering of Cardiac Tissue	14
<i>Dr. Richard Balint¹, Dr. Araida Hidalgo-Bastida²</i>	
<i>1. The University of Manchester, 2. Manchester Metropolitan University</i>	
In vivo Response to Injectable Hydrogels: from Decellularised ECM to de novo Peptides	15
<i>Dr. Nazia Mehrban¹, Dr. Catalina Pineda Molina², Dr. Lina Quijano², Dr. James Bowen³, Mr. Scott Johnson², Dr. Joseph Bartolacci², Mr. Jordan Chang², Mr. Arne Scott⁴, Prof. Derek Woolfson⁴, Prof. Martin Birchall¹, Prof. Stephen Badylak²</i>	
<i>1. University College London, 2. University of Pittsburgh, 3. The Open University, 4. University of Bristol</i>	
Influence of sample preparation methods on the organizational presentation of collagen fibrils in hydrogel electron microscopy	16
<i>Mr. Dan Merryweather¹, Ms. Nicola Weston², Dr. Chris Parmenter², Prof. Mark Lewis¹, Dr. Paul Roach¹</i>	
<i>1. Loughborough University, 2. University of Nottingham</i>	
Investigations Of Human Tendon Width For The Anatomical Design Of An In Vitro Flexor Digitorum Profundus Enthesis Model	17
<i>Mr. Jeremy Mortimer¹, Mr. Mario Macia¹, Ms. Nika Vonk¹, Ms. Philippa Rust¹, Dr. Jennifer Paxton²</i>	
<i>1. University of Edinburgh, 2. The University of Edinburgh</i>	
Local suppression of the T cell response to peripheral nerve allografts using drug-eluting PCL fibers	18
<i>Dr. Victoria Robertson¹, Dr. Ukrit Angkawinitwong¹, Ms. Holly Gregory¹, Dr. Gareth Williams¹, Dr. James Phillips¹</i>	
<i>1. School of Pharmacy, University College London</i>	
NITRIC OXIDE RELEASING CONTACT LENS BANDAGES	19
<i>Dr. Jenny Aveyard¹, Dr. Robert Deller¹, Dr. Rebecca Lace¹, Prof. Rachel Williams¹, Dr. Raechelle D'Sa¹</i>	
<i>1. University of Liverpool</i>	
Non-woven mats of electroactive composites of silk-PEDOT:PSS for peripheral nerve regeneration	20
<i>Mr. Chinnawich Phamornnak¹, Mr. Jie Ma¹, Dr. John Hardy², Dr. Jonny Blaker¹, Prof. Sarah Cartmell³</i>	
<i>1. University of Manchester, 2. Lancaster University, 3. The University of Manchester</i>	
Peptide Gels of Fully-Defined Composition and Mechanics for Modelling Cell-Matrix Interactions in Breast Cancer	21
<i>Dr. Jennifer Ashworth¹, Ms. Charlotte Slater¹, Dr. Gillian Farnie², Prof. Catherine Merry¹</i>	
<i>1. University of Nottingham, 2. University of Oxford</i>	

POROUS GLASS MICROSPHERES SHOW BIOCOMPATIBILITY, TISSUE INGROWTH AND OSTEOGENIC ON-SET IN VIVO.	22
Dr. JANE McLAREN ¹ , Dr. Laura Macri-Pellizzeri ¹ , Dr. Kazi Zakir Hossain ¹ , Dr. Uresha Patel ¹ , Prof. David Grant ² , Prof. Brigitte Scammell ¹ , Dr. Ifty Ahmed ² , Dr. Virginie Sottile ¹	
<i>1. University of Nottingham, 2. University of Nottingham, United Kingdom</i>	
RAPID SCREENING OF INKS FOR 3D PRINTING PERSONALISED DRUG DELIVERY IMPLANTS	23
Dr. Laura Ruiz ¹ , Dr. Vincenzo Taresco ¹ , Dr. Zuoxin Zhou ¹ , Prof. Richard Hague ¹ , Prof. Clive Roberts ¹ , Prof. Christopher Tuck ¹ , Prof. Morgan Alexander ¹ , Prof. Derek Irvine ¹ , Prof. Ricky Wildman ¹	
<i>1. University of Nottingham</i>	
Reforming the Haversian network in a bone-on-chip	24
Prof. Elisa Budyn ¹ , Dr. Bertrand Cinquin ¹ , Dr. Morad Bensidhoum ² , Dr. Hugues Portier ³	
<i>1. ENS Paris-Saclay, 2. University Paris 7, 3. University of Orleans</i>	
ROLE OF SILICATE AND SILICATE-BIOACTIVE GLASSES IN BONE NODULE FORMATION	25
Ms. Azadeh Rezaei ¹ , Dr. Yutong Li ¹ , Ms. Sofia Petta ¹ , Dr. Kaveh Shakib ¹ , Dr. gavin jell ¹	
<i>1. University College London</i>	
Self-Assembling structured Laponite Hydrogels with Spontaneous 3D Micropatterning of Bioactive Factors for Tissue Regeneration	26
Ms. Roxanna Ramnarine ¹ , Dr. Nick Evans ² , Prof. Richard Oreffo ¹ , Dr. Jon Dawson ¹	
<i>1. University of Southampton, 2. southampton</i>	
Stimulative 3D Conducting Architectures to Modulate Cellular Phenotype	27
Dr. Frankie Rawson ¹ , Dr. Jayasheelan Vaithilingam ² , Dr. Paola Sanjuan Alberte ¹ , Dr. Simona Campora ³ , Dr. Graham Rance ¹ , Dr. Long Jiang ¹ , Prof. Christopher Tuck ¹ , Prof. Chris Denning ¹ , Prof. Ricky Wildman ¹ , Prof. Richard Hague ¹ , Prof. Morgan Alexander ¹	
<i>1. University of Nottingham, 2. Johnson Matthey, 3. ABIEL</i>	
Study of the effects of microbubbles on bone formation using micro-CT	28
Mr. Jonathan May ¹ , Mr. Jehan Zaib ¹ , Ms. Sara Ferri ¹ , Ms. Anastasia Polydorou ¹ , Dr. Stuart Lanham ¹ , Dr. Janos Kanczler ¹ , Dr. Robin Rumney ² , Prof. Eleanor Stride ³ , Dr. Dario Carugo ¹ , Dr. Nick Evans ¹	
<i>1. University of Southampton, 2. University of Portsmouth, 3. Oxford University</i>	
The Potential of Pressurised Gyration to fabricate Polyhydroxyalkanoate Aligned fibre Scaffolds for Peripheral Nerve Repair	29
Dr. Caroline Taylor ¹ , Ms. Mehrie Behbehani ¹ , Dr. Pooja Basnett ² , Ms. Barbara Lukasiewicz ² , Dr. Eranka Illangakoon ³ , Dr. Suntharavathanan Mahalingam ³ , Prof. Mohan Edirisinghe ³ , Prof. Ipsita Roy ² , Prof. John Haycock ⁴	
<i>1. The University of Sheffield, 2. University of Westminster, 3. University College London, 4. University of Sheffield</i>	
Utilising a Novel Photoresponsive Hydrogel with Defined Surface Topography and Photoswitchable Stiffness to Analyse the Biophysical Regulation of Mesenchymal Stem Cells	30
Mr. David Richards ¹	
<i>1. University of Manchester</i>	
Validation and assessment of an antibiotic decontamination manufacturing protocol for vacuum-dried human amniotic membrane	31
Dr. Emily Britchford ¹ , Dr. Nagi Marsit ² , Dr. Laura Sidney ² , Mr. Owen McIntosh ² , Dr. Claire Allen ² , Mr. Waheed Ashraf ² , Prof. Roger Bayston ² , Dr. Andrew Hopkinson ¹	
<i>1. University of Nottingham / NuVision Biotherapies, 2. University of Nottingham</i>	

TURBOTALK + POSTER

- 3D culture of epidermis by use of recombinant silk materials containing FGF-7 protein microcrystals** 33
Ms. Rina Maruta¹, Ms. Keiko Takaki ¹, Prof. Eiji Kotani ¹, Dr. Christian Pernstich ², Dr. Michael Jones ², Prof. Hajime Mori ¹
1. Kyoto Institute of technology, 2. Cell Guidance Systems
- Acoustically-stimulated drug carriers for bone fracture repair** 34
Ms. Anastasia Polydorou¹, Mr. Jonathan May ¹, Ms. Sara Ferri ¹, Dr. Qiang Wu ², Prof. Eleanor Stride ², Dr. Dario Carugo ¹, Dr. Nick Evans ¹
1. University of Southampton, 2. Oxford University
- Auxetic and Composite Scaffolds Show Potential for use in Tissue Engineering** 35
Mr. Paul Mardling¹, Prof. Christine Le Maitre ¹, Prof. Andrew Alderson ¹, Dr. Nikki Jordan-Mahy ¹
1. Sheffield Hallam University
- Bacterial engineering for the ex-vivo expansion of HSCs** 36
Ms. Michaela Petaroudi¹, Dr. Aleixandre Rodrigo-Navarro ¹, Dr. Ewan Ross ¹, Prof. Matthew Dalby ¹, Prof. Manuel Salmeron-Sanchez ¹
1. University of Glasgow
- Bisphosphonate toxicity to the oral mucosa is inhibited in vitro by hydroxyapatite granules** 37
Mr. George Bullock¹, Dr. Cheryl Miller ¹, Mr. Alasdair McKechnie ², Dr. Vanessa Hearnden ³
1. The University of Sheffield, 2. University of Leeds, 3. University of Sheffield
- Clinical Translation of Regenerative Medicines: A Regulatory Primer** 38
Mrs. Alison Wilson¹
1. University of York
- Decellularisation of Human Femoral Nerves in a Closed System: Towards Introducing a New Nerve Allograft in Healthcare in the UK** 39
Dr. Valentina Barrera¹, Ms. Georgina Webster ², Ms. Agatha Joseph ¹, Dr. Penny Hogg ¹, Prof. John Kearney ³, Prof. Paul Rooney ³
1. NHS Blood and Transplant, Tissue and Eye Services R&D, 2. iMBE, University of Leeds, 3. NHS Blood and Transplant
- DEVELOPMENT OF A MULTI-LAYERED CRYOGEL BIOREACTOR WITH OPTIMISED FLUID DYNAMICS FOR BIOARTIFICIAL LIVER APPLICATION** 40
Ms. Flavia Bonalumi¹, Prof. Cyril Crua ¹, Dr. Irina Savina ¹, Dr. Nathan Davies ², Prof. Maurizio Santini ³, Dr. Stephanie Fest-Santini ³, Dr. Susan Sandeman ¹
1. University of Brighton, 2. University College London, 3. Università degli Studi di Bergamo
- DEVELOPMENT OF A TOPICAL CELL THERAPY FOR OCULAR SURFACE DISORDERS** 41
Ms. Lydia Beeken¹, Dr. Laura Sidney ¹, Prof. Cameron Alexander ¹, Prof. Felicity Rose ¹
1. University of Nottingham
- Development of topographically controlled electrospun scaffolds to deliver proangiogenic agents for wound healing** 42
Mr. David Hiram Ramos Rodriguez¹, Prof. Sheila MacNeil ¹, Dr. Frederik Claeysens ¹, Dr. Ildia Ortega Asencio ¹
1. University of Sheffield

Improving stem cell therapies for traumatic brain injury using bioactive ECM scaffolds to attenuate inflammation	43
<i>Ms. Charlotte Lee-Reeves¹, Dr. Tim Keane¹, Dr. James Phillips², Prof. Molly Stevens¹</i>	
<i>1. Imperial College London, 2. School of Pharmacy, University College London</i>	
Investigating glycosaminoglycans in development and disease using fully defined 3D cell culture environments and human pluripotent stem cells	44
<i>Ms. Jamie Thompson¹, Dr. Sara Pijuan-Galitó², Dr. Jennifer Ashworth¹, Ms. Kate Dowding¹, Prof. Morgan Alexander¹, Prof. Cathy Merry¹</i>	
<i>1. University of Nottingham, 2. Jamie L Thompspm</i>	
Magnetic hydrogels: Tissue engineering constructs with switchable stiffness	45
<i>Mr. Jordan Roe¹, Ms. Pippa Baynham¹, Dr. Helen Willcock¹, Dr. Paul Roach¹</i>	
<i>1. Loughborough University</i>	
Modelling and emulating 3D multi-tissue interactions by microfluidic chip technology	46
<i>Mrs. Shirin Hanaei¹, Prof. Carole Perry¹, Dr. Yvonne Reinwald¹, Dr. Livia Santos¹</i>	
<i>1. Nottingham Trent University</i>	
NITRIC OXIDE RELEASING ELECTROSPUN NANOFIBERS FOR ANTIMICROBIAL BONE TISSUE ENGINEERING	47
<i>Ms. Man Li¹, Dr. Jenny Aveyard¹, Dr. Fiona McBride¹, Prof. Rasmita Raval¹, Dr. Judith Curran¹, Dr. Raechelle D'Sa¹</i>	
<i>1. University of Liverpool</i>	
Optimisation of Microparticle Formulations for Cytokine Delivery for Macrophage Modulation for Potential Application in Spinal Cord Injury	48
<i>Ms. Jazz Stening¹, Dr. Felicity R. J. A. Rose¹, Dr. Lisa J. White¹</i>	
<i>1. University of Nottingham</i>	
PHOSPHATE BASED GLASS COATINGS FOR RAPID GA3+ RELEASE: THE CHALLENGES OF BALANCING CYTOTOXICITY WITH ANTIMICROBIAL EFFECTS	49
<i>Ms. Kathryn Thomas¹, Dr. Bryan Stuart², Dr. Steve Atkinson¹, Dr. Colin Scotchford¹, Prof. David Grant³</i>	
<i>1. University of Nottingham, 2. Oxford University, 3. University of Nottingham, United Kingdom</i>	
Phosphonate-modified graphene–Laponite composites for bone repair	50
<i>Ms. Thunyaporn Srisubin¹, Prof. Julie Gough¹, Dr. Christopher Blanford¹</i>	
<i>1. The University of Manchester</i>	
Stable encapsulation of rifampicin and doxycycline in polymersome nanoparticles for delivery to intracellular bacteria	51
<i>Ms. Eleanor Porges¹, Mr. Antonio De Grazia¹, Mr. Adam Taylor², Dr. Dominic Jenner², Dr. Caroline Rowland², Dr. Tracey Newman¹, Dr. Nick Evans¹</i>	
<i>1. University of Southampton, 2. DSTL</i>	
Use of Antifreeze Proteins to Modify Pores in Directionally Frozen Alginate Sponges for Cartilage Tissue Engineering	52
<i>Mr. Alexander Sturtivant¹, Dr. Anthony Callanan¹</i>	
<i>1. University of Edinburgh</i>	

POSTER

- 3D PRINTED SCAFFOLDS FOR FUNCTIONAL EX VIVO CARDIAC TISSUE MODELS** 54
Mr. Aidan Meenagh¹, Prof. Brian Meenan¹
1. *University of Ulster*
- A caprine model of intervertebral disc degeneration: a testing platform for an injectable hydrogel** 55
Dr. Joseph Snuggs¹
1. *Sheffield Hallam University*
- A comparative study to evaluate bioactive surfaces to deliver NGF and BDNF on neuronal cells** 56
Ms. Ana Sandoval¹, Dr. Frederik Claeysens¹, Prof. John Haycock¹
1. *University of Sheffield*
- A NEW METHOD TO QUANTIFY BIOFILM FORMATION ON BIOMATERIALS SURFACES** 57
. Sophie Mountcastle¹, Dr. Nina Vyas¹, Dr. Richard Shelton¹, Dr. Rachel Sammons¹, Dr. Sophie Cox¹, Dr. Sara Jabbari¹, Prof. Damien Walmsley¹, Dr. Sarah Kuehne¹
1. *University of Birmingham*
- A NOVEL ORGANIC-INORGANIC HYBRID HYDROGEL FOR CELL ENCAPSULATION AND DRUG DELIVERY** 58
Dr. Soher Jayash¹, Prof. Paul Cooper¹, Dr. Richard Shelton¹, Dr. Gowsihan Poologasundarampillai¹
1. *University of Birmingham*
- A NOVEL WEIGHT-BEARING ANTIBIOTIC ELUTING TEMPORARY HIP SPACER MANUFACTURED BY SELECTIVE LASER MELTING** 59
Ms. Sophie Louth¹, Dr. Parastoo Jamshidi¹, Dr. Neil Eisenstein², Dr. Mark Webber¹, Prof. Moataz Attallah¹, Prof. Duncan Shepherd¹, Prof. Owen Addison¹, Prof. Liam Grover¹, Dr. Kenneth Nai³, Dr. Sophie Cox¹
1. *University of Birmingham*, 2. *Royal Centre for Defence Medicine*, 3. *Renishaw PLC*
- A zero-order drug eluting material to improve nerve grafting** 60
Ms. Holly Gregory¹, Dr. Ukrit Angkawinitwong¹, Dr. Victoria Roberton¹, Dr. Gareth Williams¹, Dr. James Phillips¹
1. *School of Pharmacy, University College London*
- Accelerating collagen deposition with macromolecular crowding can disrupt collagen fibre alignment** 61
Ms. Danielle O'Loughlin¹, Dr. Hannah Levis¹, Dr. Victoria Kearns¹, Dr. Carl Sheridan¹, Dr. Elizabeth Canty-Laird¹
1. *University of Liverpool*
- ACELULAR GELATINE-ALGINATE SCAFFOLDS FOR DENTINE-PULP REGENERATION** 62
Mr. Ignacio Medina-Fernandez¹, Dr. Adam Celiz²
1. *Imperial College London*, 2. *Imperial College*
- Airway smooth muscle cell morphology, proliferation, and α -smooth muscle actin is modulated by substrate stiffness** 63
Mr. Jopeth Ramis¹, Prof. Dominick Shaw¹, Prof. Felicity Rose¹, Dr. Lee Buttery¹, Dr. Amanda Tatler¹
1. *University of Nottingham*
- An ex vivo tissue assay to reduce animal use in advanced genetic therapy testing** 64
Ms. Lauren Smith¹, Prof. Kevin M Shakesheff¹, Dr. Amanda Tatler¹, Dr. James Dixon¹
1. *University of Nottingham*
-

Anti-Inflammatory Properties of Corneal Stroma-Derived Stem Cells: Potential as a Topical Therapy for the Ocular Surface	65
<u>Mr. Owen McIntosh</u> ¹ , Ms. Lizeth Orozco Gil ¹ , Dr. Nagi Marsit ¹ , Dr. Andrew Hopkinson ¹ , Dr. Laura Sidney ¹	
<i>1. University of Nottingham</i>	
Antibacterial efficacy of nitric oxide releasing hydrogels on 2D and 3D human skin models	66
<u>Dr. Robert Deller</u> ¹ , Dr. Jenny Aveyard ¹ , Prof. Rachel Williams ¹ , Dr. Raechelle D'Sa ¹	
<i>1. University of Liverpool</i>	
Armoured growth factors for tissue engineering	67
<u>Dr. Ciara Whitty</u> ¹ , Dr. Julia Oswald ² , Dr. Christian Pernstich ¹ , Prof. Petr Baranov ² , Dr. Michael Jones ¹	
<i>1. Cell Guidance Systems, 2. Harvard Medical School</i>	
Assessing the paracrine effects of fat on dermal fibrosis	68
<u>Mr. Samuel Higginbotham</u> ¹ , Dr. Victoria Workman ² , Dr. Nicola Green ² , Dr. Daniel Lambert ¹ , Dr. Vanessa Hearnden ²	
<i>1. The University of Sheffield, 2. University of Sheffield</i>	
Assessment of lithium exposure in an ex vivo chick femur culture model	69
<u>Mr. Nasseem Salam</u> ¹ , Prof. Stefan Hoppler ¹ , Prof. Iain Gibson ¹	
<i>1. University of Aberdeen</i>	
Association of Environmental Cues with Mesenchymal Stem Cell Fate	70
<u>Ms. Rawiya Al Hosni</u> ¹ , Dr. Umber Cheema ¹ , Dr. Scott Roberts ¹	
<i>1. University College London</i>	
Biocompatibility of Graphene for Regenerative Medicine Applications using Dental Pulp Stem Cells	72
<u>Mr. Iain Slinn</u> ¹ , Prof. Craig Banks ¹ , Dr. Araida Hidalgo-Bastida ¹	
<i>1. Manchester Metropolitan University</i>	
BIOENGINEERING 3D MICROENVIRONMENTS TO STUDY MECHANOTRANSDUCTION AND VASCULARIZATION IN BONE REGENERATION	73
<u>Ms. Sofia Perea Ruiz</u> ¹	
<i>1. University of Glasgow</i>	
Bioengineering Dual Gradient Platforms for the Control of Cell Behaviour and Differentiation	74
<u>Ms. Laurissa Havins</u> ¹ , Dr. Paul Roach ¹	
<i>1. Loughborough University</i>	
Bioresponsive hydrogels for on-demand modulation of elastase activity	75
<u>Ms. Rebeca Obenza Otero</u> ¹ , Mr. Emanuele Russo ¹ , Dr. Debbie Clements ¹ , Prof. Simon Johnson ¹ , Dr. Marianne Ashford ² , Dr. Paul Gellert ² , Dr. Weng Chan ¹ , Dr. Giuseppe Mantovani ¹ , Dr. Mischa Zelzer ¹	
<i>1. University of Nottingham, 2. Astrazeneca</i>	
Blended PCL/PLA/GO grooved nerve guide conduit for the treatment of peripheral nerve injury	76
<u>Ms. Ying Lu</u> ¹ , Dr. Christopher Blanford ¹ , Dr. Adam Reid ¹ , Prof. Julie Gough ¹	
<i>1. The University of Manchester</i>	
Can We Fine-tune Mesenchymal Stem Cells for Therapeutic Angiogenesis? – Preliminary Study on the use of Hypoxic Pre-conditioned Cells	77
<u>Dr. Jasmine Ho</u> ¹ , Dr. Umber Cheema ¹ , Prof. Mark Lowdell ¹ , Prof. Paolo De Coppi ¹ , Prof. Martin Birchall ¹	
<i>1. University College London</i>	

Characterization of a low-cost synthetic mesh for abdominal wall repair	78
<i>Ms. Alessandra Grillo¹, Dr. Vivek Mudera¹, Dr. Alvena Kureshi¹</i>	
<i>1. University College London</i>	
Characterization of Detachable Gelatin/Chitosan Hydrogels for Tissue Engineering Applications	79
<i>Ms. Kayla Kret¹, Dr. Alastair Campbell Ritchie¹, Dr. Colin Scotchford¹</i>	
<i>1. University of Nottingham</i>	
Combined bio-ink and supportive bath strategies for bio-mimetic 3-dimensional printing	80
<i>Dr. Julian Dye¹, Mr. Zhuoran Jiang¹, Prof. Zhanfeng Cui¹</i>	
<i>1. University of Oxford</i>	
Control of Topographical Features on PCL Electrospun Nanofibre Scaffolds for Liver Tissue Engineering	82
<i>Ms. Yunxi Gao¹, Dr. Anthony Callanan¹</i>	
<i>1. University of Edinburgh</i>	
Controllable dehydration of cell-seeded type I collagen hydrogels using sodium polyacrylate.	83
<i>Ms. Laura Beattie¹, Mrs. Catherine Henderson¹, Prof. Simon Mackay¹, Dr. Philip Riches¹, Prof. Helen Grant¹</i>	
<i>1. University of Strathclyde</i>	
Cross-linking of bone derived extracellular matrix hydrogels to alter mechanical properties	84
<i>Mr. Joshua Jones¹, Mr. Simon Kellaway², Dr. Lisa White¹</i>	
<i>1. University of Nottingham, 2. University College London</i>	
Decellularized materials support Schwann cell growth and alignment in engineered neural tissue	85
<i>Mr. Simon Kellaway¹, Dr. James Phillips², Dr. Lisa White³</i>	
<i>1. University College London, 2. School of Pharmacy, University College London, 3. University of Nottingham</i>	
Design of nerve repair conduits with the aid of an in silico model	86
<i>Dr. Simao Laranjeira¹, Mr. Kulraj Singh Bhangra¹, Dr. James Phillips², Dr. Rebecca Shipley¹</i>	
<i>1. UCL, 2. School of Pharmacy, University College London</i>	
Designing An Angled Interface For An In Vitro Flexor Digitorum Profundus Enthesis Model Through Human Histological Investigation	87
<i>Mr. Jeremy Mortimer¹, Mr. Subashan Vadibeler¹, Mr. Mario Macia¹, Ms. Miriam Graute¹, Ms. Philippa Rust¹, Dr. Jennifer Paxton²</i>	
<i>1. University of Edinburgh, 2. The University of Edinburgh</i>	
Developing a human blood-brain barrier model using 3D-biomaterials and iPSC derived brain microvascular endothelial cells	88
<i>Mr. Geoffrey Potjewyd¹, Ms. Wenjun Zhang¹, Dr. Samuel Moxon¹, Dr. Kate Fisher¹, Prof. Tao Wang¹, Dr. Marco Domingos¹, Prof. Nigel Hooper¹</i>	
<i>1. The University of Manchester</i>	
Developing an Oral Insulin Delivery System using GET-peptide-mediated transcytosis	89
<i>Ms. Sahrish Rehmani¹, Prof. Kevin Shakesheff¹, Dr. James Dixon¹</i>	
<i>1. University of Nottingham</i>	
Development of 3D Tumour Models for Ameloblastoma	90
<i>Ms. Deniz Bakkalci¹, Dr. Umber Cheema¹, Dr. Gavin Jell¹, Prof. Stefano Fedele¹</i>	
<i>1. University College London</i>	

DEVELOPMENT OF A BIOPROCESS FOR THE EXPANSION AND DIFFERENTIATION OF IPSCS	91
<u>Mr. Fritz de la Raga</u> ¹	
<i>1. Aston University</i>	
Development of a composite hydrogel-decellularised scaffold intervention for chondrocyte implantation	92
<u>Mr. Patrick Lawson-Statham</u> ¹ , Dr. Louise Jennings ¹ , Dr. Hazel Fermor ¹ , Dr. James Warren ¹ , Dr. Elena Jones ² , Mr. Mike Izon ³	
<i>1. Institute of Medical and Biological Engineering, University of Leeds, 2. University of Leeds, 3. Tissue Regenix</i>	
DEVELOPMENT OF A HYDROXYAPATITE-BASED INK FOR THE 3D PRINTING OF BONE TISSUE-LIKE SCAFFOLDS	93
<u>Mr. Michael Moore</u> ¹ , Prof. Brian Meenan ¹	
<i>1. University of Ulster</i>	
Discovering novel immune-modulatory monosaccharides using high-throughput screening strategies	94
<u>Mr. Meshal Alobaid</u> ¹ , Dr. Sarah-Jane Richards ² , Prof. Mathew Gibson ² , Prof. Morgan Alexander ¹ , Prof. Amir Ghaemmaghami ¹	
<i>1. University of Nottingham, 2. University of warwick</i>	
Effect of conditioned media from adipose-derived stromal cells, adipose tissue and emulsified fat on endothelial cells	95
<u>Mrs. Alejandra Penuelas Alvarez</u> ¹ , Dr. Vanessa Hearnden ¹ , Dr. Joey Shepherd ¹	
<i>1. University of Sheffield</i>	
EMBEDDED BIOPRINTING AN IN VITRO COCHLEA MODEL FOR STUDYING COCHLEAR IMPLANTS	96
<u>Ms. Iek Man Lei</u> ¹ , Dr. Chen Jiang ¹ , Prof. Manohar Bance ¹ , Dr. Yan Yan Shery Huang ¹	
<i>1. University of Cambridge</i>	
Engineering the Liver Using Self-assembled Peptide Hydrogels	97
<u>Ms. Yu Xin</u> ¹ , Prof. Alberto Saiani ¹ , Prof. Aline Miller ¹ , Prof. Julie Gough ¹	
<i>1. The University of Manchester</i>	
Enhanced proliferation and osteogenic differentiation of MC3T3-E1 cells on piezoelectric polymeric scaffolds	98
<u>Mr. BIRANCHE TANDON</u> ¹ , Dr. Jonny Blaker ² , Prof. Sarah Cartmell ¹	
<i>1. The University of Manchester, 2. University of Manchester</i>	
EXAMINATION OF THE SUITABILITY OF LIPIODOL AS A CONTRAST AGENT FOR POLYETHYLENE BIOMATERIALS	99
<u>Ms. Parnian f.zaribaf@bath.ac.uk</u> ¹ , Prof. Richie Gill ¹ , Dr. Elise Pegg ¹	
<i>1. University of Bath</i>	
Experimental investigation on the impact of an Engineered Bioactive Microenvironment using Growth factors on PEEK Osteoinduction	100
<u>Dr. Noura Alotaibi</u> ¹ , Dr. Kurt Naudi ¹ , Prof. Manuel Salmeron-Sanchez ² , Prof. Matthew Dalby ² , Prof. Ashraf Ayoub ¹	
<i>1. University of Glasgow/Glasgow dental hospital & school, 2. University of Glasgow</i>	
Feeder-free Culture of Naïve Human Pluripotent Stem Cells in Normoxic Conditions	101
<u>Dr. Sara Pijuan-Galitó</u> ¹ , Ms. Jamie Thompson ² , Dr. Lara C Lewis ² , Dr. Christoffer Tamm ³ , Prof. Chris Denning ¹ , Dr. Cecilia Anneren ³ , Prof. Cathy Merry ²	
<i>1. University of Nottingham, 2. University of Nottingham, United Kingdom, 3. Uppsala University</i>	

GELATIN MICROPARTICLES AS CARRIERS FOR THE DELIVERY OF ANTIMICROBIAL PEPTIDES	102
<u>Ms. Kiran Mann</u> ¹ , Dr. Jenny Aveyard ¹ , Mr. Graeme Pitt ¹ , Dr. Raechelle D'Sa ¹	
<i>1. University of Liverpool</i>	
Generating Intrafusal Skeletal Muscle Fibres In-Vitro	103
<u>Mr. Philip Barrett</u> ¹ , Dr. Vivek Mudera ¹ , Dr. Darren Player ¹	
<i>1. University College London</i>	
Human Extracellular Matrix Powder Hydrogels: Development of a New Human Tissue-Specific Product in NHSBT	104
<u>Prof. Paul Rooney</u> ¹ , Dr. Sarah Rathbone ¹ , Dr. Valentina Barrera ¹ , Prof. Eileen Ingham ² , Prof. John Kearney ¹	
<i>1. NHS Blood and Transplant, 2. University of Leeds</i>	
IDENTIFICATION OF SCALABLE POLYMERS CAPABLE OF MODULATING MACROPHAGE POLARISATION	105
<u>Mrs. Chidimma Mbadugha</u> ¹ , Prof. Morgan Alexander ² , Prof. Amir Ghaemmaghani ²	
<i>1. University of Nottingham, United Kingdom, 2. University of Nottingham</i>	
Immune Instructive Polymers for Dendritic Cell Modulation	106
<u>Ms. Lisa Kammerling</u> ¹ , Prof. Morgan Alexander ¹ , Prof. Amir Ghaemmaghani ¹	
<i>1. University of Nottingham</i>	
In vivo-like ramified morphologies are induced in neural immune cells (microglia) when cultured in 3D collagen hydrogels	107
<u>Mr. Jonathan Goldfinch</u> ¹ , Ms. Bushra Kabiri ¹ , Mr. Kyle Storey ¹ , Dr. Stuart Jenkins ¹	
<i>1. Keele University</i>	
Incorporation of antioxidant into structurally organised PCL scaffolds for cartilage tissue engineering	108
<u>Ms. Nimrah Munir</u> ¹ , Dr. Alison McDonald ¹ , Dr. Anthony Callanan ²	
<i>1. The University of Edinburgh, 2. University of Edinburgh</i>	
Incorporation of Laminin into Polymeric Scaffolds for Kidney Tissue Engineering	109
<u>Ms. Busra Baskapan</u> ¹ , Dr. Anthony Callanan ²	
<i>1. The University of Edinburgh, 2. University of Edinburgh</i>	
INVESTIGATIONS INTO NOVEL TITANATE CONVERSION OF DC MAGNETRON SPUTTERED TITANIUM THIN FILMS FOR BIOMEDICAL APPLICATIONS	110
<u>Mr. Matthew Wadge</u> ¹ , Mr. Burhan Turgut ¹ , Dr. Reda Felfel ¹ , Dr. Ifty Ahmed ¹ , Prof. David Grant ¹	
<i>1. University of Nottingham, United Kingdom</i>	
Mathematical modelling informing tissue engineering protocols for a microcarrier bone culture	111
<u>Ms. Iva Burova</u> ¹ , Prof. Ivan Wall ² , Dr. Rebecca Shipley ¹	
<i>1. UCL, 2. Aston University</i>	
Mechanical loading attenuates atrophy in tissue engineered skeletal muscle.	112
<u>Ms. Kathryn Aguilar-Agon</u> ¹ , Dr. Andrew Capel ¹ , Dr. Neil Martin ¹ , Dr. Darren Player ² , Prof. Mark Lewis ¹	
<i>1. Loughborough University, 2. University College London</i>	
Micro-computed tomography as a predictive tool in the cell-sieving capabilities of structurally graded lyophilised collagen scaffolds	113
<u>Dr. Jennifer Shepherd</u> ¹ , Dr. Daniel Howard ² , Dr. Cedric Ghevaert ² , Prof. Serena Best ² , Prof. Ruth Cameron ²	
<i>1. University of Leicester, 2. University of Cambridge</i>	

Microvessel-on-chip model	114
<u>Ms. Jenny O'Dowd¹, Ms. Magda Gerigk¹, Dr. Yan Yan Shery Huang¹</u>	
<i>1. University of Cambridge</i>	
Modulating fibroblast behaviour using microparticle systems	115
<u>Mr. Arsalan Latif¹, Dr. Adam Dundas¹, Mrs. Valentina Crucitti¹, Prof. Ricky Wildman¹, Prof. Derek Irvine¹, Prof. Morgan Alexander¹, Prof. Amir Ghaemmaghami¹</u>	
<i>1. University of Nottingham</i>	
Morphological control of liver ECM-PCL electrospun scaffolds	116
<u>Mr. Thomas Bate¹, Dr. Anthony Callanan¹, Prof. Stuart Forbes¹</u>	
<i>1. University of Edinburgh</i>	
MULTICELLULAR AGGREGATES GENERATED USING DROPLET MICROFLUIDICS FOR CARTILAGE TISSUE ENGINEERING	117
<u>Mr. Juan Aviles Milan¹, Dr. Jon Dawson¹, Dr. Xize Niu¹, Dr. Rahul S. Tare¹, Dr. Jonathan J. West¹</u>	
<i>1. University of Southampton</i>	
Musculoskeletal Tissue Interface Development	118
<u>Ms. Wendy Balestri¹, Dr. Rob Morris¹, Prof. John Hunt¹, Dr. Yvonne Reinwald¹</u>	
<i>1. Nottingham Trent University</i>	
NANOCOMPOSITE HYDROGEL SYSTEM FOR BIOMEDICAL APPLICATIONS	119
<u>Mrs. Nathalie Sallstrom¹, Dr. Andrew Capel¹, Prof. Mark Lewis¹, Dr. Daniel Engstrom¹, Dr. Simon Martin¹</u>	
<i>1. Loughborough University</i>	
NANOPOROUS ENTEROSORBENT YAQ001 AS AN ORAL TREATMENT FOR LIVER DISEASE THROUGH EN-DOTOXIN ADSORPTION AND MODERATION OF IMMUNE DYSREGULATION	120
<u>Ms. Tochukwu Ozulumba¹, Dr. Ganesh Ingavle², Dr. Jane Macnaughtan³, Dr. Nathan Davies³, Prof. Rajiv Jalan³, Dr. susan sandeman¹</u>	
<i>1. University of Brighton, 2. Symbiosis International University, 3. University College London</i>	
NANOVIBRATION INDUCED MESENCHYMAL STEM CELLS FOR 3D OSTEOGENESIS IN FREEZE DRIED COLLAGEN SPONGE- HYDROGELS COMPOSITE FOR BONE TISSUE ENGINEERING	121
<u>Mr. Wich Orapiriyakul¹, Dr. Penelope Tsimbouri¹, Dr. Peter Childs¹, Prof. Dominic Meek², Prof. Elizabeth Tanner³, Prof. Manuel Salmeron-Sanchez¹, Prof. Richard Oreffo⁴, Prof. Stuart Reid⁵, Prof. Matthew Dalby¹</u>	
<i>1. University of Glasgow, 2. Southern General Hospital, Glasgow, 3. Queen Mary University of London, 4. University of Southampton, 5. University of Strathclyde</i>	
Novel approach for wound healing processes	122
<u>Mr. Abed Ali¹, Dr. Yvonne Reinwald¹</u>	
<i>1. Nottingham Trent University</i>	
NOVEL POROUS STRUCTURES FOR ENHANCED OSTEOINTEGRATION IN ORTHOPAEDIC DEVICES	123
<u>Mr. Ian Richards¹, Prof. Christopher Sutcliffe¹, Dr. Judith Curran¹, Dr. Simon Tew¹</u>	
<i>1. University of Liverpool</i>	
Optimisation of Cell Ratio and Medium composition for the tri-culture of cells in wound-healing	124
<u>Ms. Vinuri Abeygunawardana¹, Mr. Abed Ali², Dr. Yvonne Reinwald²</u>	
<i>1. Griffith University, 2. Nottingham Trent University</i>	

Optimisation of Microfabricated Devices for Human Neuronal Modelling	125
<u>Ms. Sophie Oakley</u> ¹ , Dr. Paul Roach ¹ , Prof. Mark Lewis ¹	
<i>1. Loughborough University</i>	
Optimising a Method to Study the effect of Autologous Fat on Skin Graft Contraction	126
<u>Dr. Victoria Workman</u> ¹ , Dr. Nicola Green ¹ , Prof. Sheila MacNeil ¹ , Dr. Vanessa Hearnden ¹	
<i>1. University of Sheffield</i>	
PCL & PGS Poly HIPE scaffolds for osteochondral regeneration	127
<u>Ms. Maria Velazquez</u> ¹	
<i>1. University of Sheffield</i>	
PEG-based hydrogels for minimally invasive cartilage therapies	128
<u>Ms. Nicola Foster</u> ¹ , <u>Dr. Richard Moakes</u> ¹ , Prof. Alicia El Haj ¹ , Prof. Liam Grover ¹	
<i>1. University of Birmingham</i>	
Porous poly-ε-lysine for an artificial cornea application	129
<u>Ms. Georgia Duffy</u> ¹ , Dr. Don Wellings ² , Dr. Kate Black ¹ , Prof. Rachel Williams ¹	
<i>1. University of Liverpool, 2. Spheritech Ltd</i>	
REGULATION OF THE HIF PATHWAY FOR CONTROLLED BONE REMODELLING IN PATIENTS WITH IMPAIRED FRACTURE REPAIR	130
<u>Dr. Yutong Li</u> ¹ , <u>Ms. Adriana-Monica Radu</u> ¹ , Mr. Joel Turner ² , Ms. Azadeh Rezaei ¹ , Dr. gavin jell ¹	
<i>1. University College London, 2. UCL</i>	
Serum-free cryopreservation of engineered neural tissue	131
<u>Mr. Kulraj Singh Bhangra</u> ¹ , Prof. Jonathan Knowles ¹ , Dr. Rebecca Shipley ¹ , Mr. David Choi ¹ , Dr. James Phillips ²	
<i>1. UCL, 2. School of Pharmacy, University College London</i>	
Short-time oxygen plasma treatment of a polyethylene terephthalate anterior cruciate ligament graft.	132
<u>Ms. Tania Choreño Machain</u> ¹ , Mr. Sujith Konan ² , Dr. Umber Cheema ¹	
<i>1. University College London, 2. University College London / University College Hospital NHS-Trust (UCLH)</i>	
STRUCTURAL AND MECHANICAL CHANGES IN PLLA-BASED POLYMER BLENDS DURING HYDROLYTIC DEGRADATION	133
<u>Mr. Reece Oosterbeek</u> ¹ , Dr. Patrick Duffy ² , Dr. Sean McMahon ² , Prof. Xiang Zhang ³ , Prof. Serena Best ¹ , Prof. Ruth Cameron ¹	
<i>1. University of Cambridge, 2. Ashland Specialties Ireland Ltd, 3. Lucideon Ltd.</i>	
Structure –Function Correlation and Precision Bio-Manipulation of Leukaemic Cell-Matrix Interactions	134
<u>Ms. Jenna James</u> ¹ , Dr. Jennifer Ashworth ¹ , Ms. Devapriya Murukesan ¹ , Dr. Kenton Arkil ¹ , Prof. Cathy Merry ¹ , Dr. Amanda Wright ¹ , Dr. Alexander Thompson ¹	
<i>1. University of Nottingham</i>	
Substrate mechanical properties modify bone marrow stem cell behaviour	135
<u>Ms. Maria Luisa Hernandez Miranda</u> ¹ , Dr. Bram Sengers ¹ , Dr. Nick Evans ²	
<i>1. University of Southampton, 2. southampton</i>	

Surface modification and functionalisation of electrically conductive electrospun PLCL/PANI biomaterials using atmospheric dielectric barrier plasma discharge (DBD) for tissue engineering applications	136
Dr. Gareth Menagh ¹ , Dr. Dorian Dixon ¹ , Dr. George Burke ¹	
<i>1. University of Ulster</i>	
SUSPENDED LAYER ADDITIVE MANUFACTURE OF A TRI-LAYER SKIN MODEL	137
Ms. Jessica Senior ¹ , Dr. Alan Smith ¹	
<i>1. University of Huddersfield</i>	
Synthesis of various calcium phosphate nanoparticles from a magnesium-free simulated body fluid.	138
Ms. Ting Yan Ng ¹ , Prof. Jan Skakle ¹ , Prof. Iain Gibson ¹	
<i>1. University of Aberdeen</i>	
THE APPLICATION OF COLD ATMOSPHERIC PLASMA GAS TO DIRECT WOUND HEALING IN EQUINES	139
Ms. Laura Bowker ¹ , Dr. Carol Hall ¹ , Prof. John Hunt ¹	
<i>1. Nottingham Trent University</i>	
The Interaction between Cancer and the Stroma within a Tumouroid	140
Ms. Judith Pape ¹ , Prof. Mark Emberton ¹ , Dr. Umber Cheema ¹	
<i>1. University College London</i>	
Thermosetting decellularised nerve hydrogels for spinal cord injury repair	141
Ms. Roxanne Dyer ¹ , Dr. Jessica Kwok ¹ , Dr. Stacy-Paul Wilshaw ² , Dr. Helen Berry ¹ , Prof. Richard Hall ¹ , Dr. Ronaldo Ichiyama ¹	
<i>1. University of Leeds, 2. University of Bradford</i>	
TISSUE CULTURE BIOREACTOR OPTIMISATION USING COMPUTATIONAL FLUID DYNAMICS TECHNIQUES	142
Ms. Kerry Chaplin ¹ , Dr. Andrew Capel ¹ , Dr. Steve Christie ¹ , Dr. Hemaka Bandulasena ¹ , Prof. Mark Lewis ¹	
<i>1. Loughborough University</i>	
Tissue Engineering the tendon synovial sheath for anti-adhesive properties	143
Ms. Angela Imere ¹ , Dr. Jason Wong ¹ , Dr. Marco Domingos ¹ , Prof. Sarah Cartmell ¹	
<i>1. The University of Manchester</i>	
Tissue-engineered models to study extracellular matrix: tumour interactions in oral cancer	144
Ms. Amy Harding ¹ , Dr. Daniel Frankel ² , Dr. Daniel Lambert ¹ , Dr. Helen Colley ³	
<i>1. The University of Sheffield, 2. The University of Newcastle, 3. University of Sheffield</i>	
TOWARDS THE DEVELOPMENT OF A IMPLANTABLE BIODEGRADABLE SENSOR FOR THE ELECTROCHEMICAL MONITORING OF THERAPEUTICS	145
Mr. Steven Gibney ¹ , Dr. Paul Smith ¹ , Dr. Andrew Hook ¹ , Dr. Peter Hoelig ² , Dr. Christian Moers ² , Dr. Alexander Bernhardt ² , Dr. Frankie Rawson ¹	
<i>1. University of Nottingham, 2. Evonik Nutrition & Care GmbH</i>	
TOWARDS TRANSMUCOSAL PEPTIDE DELIVERY: INCORPORATION OF AN ACTIVE MODEL PROTEIN INTO A MUCODAHESIVE NANOFIBRE PATCH USING UNIAXIAL ELECTROSPINNING	146
Mr. Jake Edmans ¹ , Dr. Sebastian Spain ¹ , Prof. Craig Murdoch ¹ , Prof. Paul Hatton ¹ , Dr. Helen Colley ¹ , Dr. Martin Santocildes-Romero ¹ , Dr. Lars Madsen ¹	
<i>1. University of Sheffield</i>	

Towards understanding why nanoclays are osteogenic	147
<u>Mr. Mohamed Mousa</u> ¹ , Dr. Oscar Kelly ² , Dr. Jane Doyle ² , Dr. Nick Evans ³ , Prof. Richard Oreffo ¹ , Dr. Jon Dawson ¹	
<i>1. University of Southampton, 2. BYK Additives Ltd., 3. southampton</i>	
Tuning adenosine release from biodegradable microspheres for bone regeneration	148
<u>Dr. Hadi Hajiali</u> ¹ , Prof. Manuel Salmeron-Sanchez ² , Prof. Matthew Dalby ² , Prof. Felicity Rose ¹	
<i>1. University of Nottingham, 2. University of Glasgow</i>	
ULTRA-SHORT CONSTRAINED BETA-SHEET FORMING PEPTIDES FOR THE FABRICATION OF VERSATILE SOFT BIOMATERIALS	149
<u>Dr. Mohamed Elsayy</u> ¹ , Mr. Ronak Patel ¹ , Dr. Jacek Wychowanec ² , Mx. Claire-Marie Nuttegg ³ , Dr. Araida Hidalgo-Bastida ³	
<i>1. School of Pharmacy and Biomedical Sciences, University of Central Lancashire, 2. School of Chemistry, University College Dublin, 3. Centre for Biomedicine, School of Healthcare Science, Manchester Metropolitan University</i>	
Uncovering the Role of Heparan Sulphate Proteoglycans in Extracellular Vesicle Biogenesis: Potential Tools for Improved Therapies	150
<u>Ms. Rebecca Morgan</u> ¹ , Dr. Rebecca Holley ² , Dr. Jason Webber ³ , Dr. David Onion ¹ , Prof. Cathy Merry ⁴ , Dr. Oksana Kehoe ⁵	
<i>1. University of Nottingham, 2. University of Manchester, 3. Cardiff University, 4. University of Nottingham, United Kingdom, 5. Keele University</i>	
UNDERSTANDING AMELOBLASTOMA-INDUCED BONE REMODELLING	151
<u>Ms. Deniz Bakkalci</u> ¹ , Ms. Kiren Malik ¹ , Dr. Umber Cheema ¹ , Dr. gavin jell ¹ , Prof. Stefano Fedele ¹	
<i>1. University College London</i>	
Understanding Cadherin Mechanisms Using Single Molecule Force Spectroscopy	152
<u>Mr. Adam Studd</u> ¹ , Prof. Phil Williams ¹ , Prof. Cathy Merry ¹ , Prof. Stephanie Allen ¹	
<i>1. University of Nottingham</i>	
UNDERSTANDING CELLULAR UPTAKE OF SILICATE SPECIES IN BONE CELLS	153
<u>Mr. Joel Turner</u> ¹ , Ms. Azadeh Rezaei ¹ , Mrs. Akiko Obata ² , Mrs. Alexandra Porter ³ , Prof. Julian Jones ³ , Dr. gavin jell ¹	
<i>1. University College London, 2. Nagoya Institute of Technology, 3. Imperial College London</i>	
UNDERSTANDING NEURAL NETWORKS: THE DEVELOPMENT OF SINGLE NEURON-NEURON BRAIN-ON-A-CHIP MODELS	154
<u>Mr. James Kinsella</u> ¹ , Dr. Paul Roach ¹ , Dr. Steve Christie ¹	
<i>1. Loughborough University</i>	
Unique patterns of elastin degradation in ascending aortic aneurysms in bicuspid aortic valve patients	155
<u>Dr. Ya Hua Chim</u> ¹ , Dr. Hannah Davies ¹ , Dr. Riaz Akhtar ¹ , Dr. Jill Madine ¹	
<i>1. University of Liverpool</i>	
Utilising self-assembling peptide hydrogels for MSC mechanobiology research	156
<u>Mr. Joshua Shaw</u> ¹ , Dr. Stephen Richardson ¹ , Dr. Joe Swift ¹ , Dr. Mhairi Harper ²	
<i>1. University of Manchester, 2. Biogelx Ltd</i>	
Vascularisation Bioreactor: A step towards “plug-and-play” vascularised tissue	157
<u>Dr. Richard Balint</u> ¹ , Dr. Araida Hidalgo-Bastida ²	
<i>1. University of Manchester, 2. Manchester Metropolitan University</i>	

ORAL

Biofunctionalizing Tailored Electrospun Scaffolds for Influencing Vascular Cellular Performance

J. A. Reid, A. McDonald, A. Callanan

The Institute for Bioengineering, School of Engineering, The University of Edinburgh, UK

INTRODUCTION: Arterial disease accounted for approximately 45% of all cardiovascular disease (CVD) related incidence in Europe in 2015¹. To treat this there are currently a large variety of vascular tissue engineering strategies utilized². The current gold standard is the use of transplanted materials such as the saphenous vein, mammary artery and full scale heart transplants³. Increasing shortage of available transplants has led to the advancement of synthetic alternatives⁴. Finding solutions that promote vascular regeneration is paramount to the field of vascular tissue engineering. Herein, we propose biofunctionalizing scaffolds with cell secretome to improve their ability to host Human Umbilical Vein Endothelial Cells (HUVECs).

METHODS: Electrospun scaffold design was optimized using a combination of polycaprolactone (PCL) and native Extracellular Matrices (ECM). Briefly, bovine aorta was decellularized and added to a PCL/solvent mixture at varying ECM concentrations. Alongside this, differing concentrations of PCL were electrospun to find the ideal platform for HUVEC growth.

The most suitable scaffold was functionalized with HUVEC secretome. Briefly, 70% confluent HUVECs were put onto serum free medium for 24h for the collection of secretome. Scaffolds were plasma coated and soaked in 5mM of EDC and NHS for 1h to enable the binding of the cell secretome. The secretome filled medium was lifted from the cells and bound to the electrospun scaffolds via soaking. Controls were run alongside the secretome functionalized scaffolds (soaking in non-functionalized serum free medium and soaking in PBS). HUVECs were then seeded onto the scaffolds and grown using serum free medium. Biochemical and biomechanical quantification was performed at 12h, 24h and 48h.

RESULTS: Scaffolds were successfully electrospun (Figure 1A) and culture medium protein was successfully bound to the scaffolds via soaking (Table 1). The protein content of the serum free medium increased by 12.8% after 24h

of cell culture (Table 1), suggesting that the cells were secreting various paracrine factors into the medium. Subsequent soaking showed that approximately 22% of the protein was bound to the scaffolds. Increases in cell viability were noted across all groups (Figure 1B). Trends were noted in gene expression.

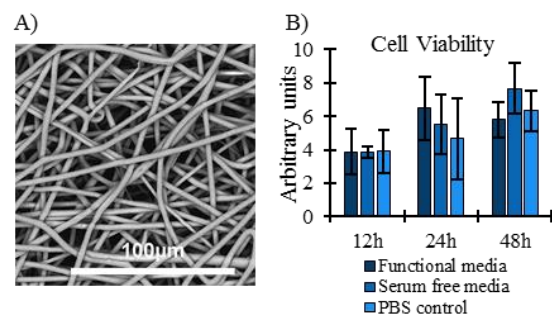


Figure 1: A) SEM image showing random orientation of scaffold fibres. B) Cell viability on each scaffold. $N=5$, error bars = SD.

Table 1: Protein secretome bound to scaffolds.

		Secretome media	Serum free media
Protein content of media (ng/ml)	Before protein binding	782 ± 35	693 ± 29
	After protein binding	620 ± 40	542 ± 37
Protein bound/absorbed (ng)		40.6 ± 3.2	37.7 ± 3.0

DISCUSSION & CONCLUSIONS: This systematic study has shown that cellular secretome can be bound/absorbed onto synthetic polymer scaffolds and does have an effect on cellular performance. Further study is required to see how the secretome can be tailored.

ACKNOWLEDGEMENTS: ESPRC no. EP/N509644/1. MRC grant MR/L012766/1.

REFERENCES: ¹E. Wilkins, *et al.* (2017) *EHN*. ²S. Ravi, *et al.* (2010) *Regen Med* **5**: 1-21. ³S. Pashneh-Tala, *et al.* (2016) *Tissue Eng Part B Rev* **22**(1): 68-100. ⁴L. Altinay, *et al.* (2018) *JOSAM* **2**(2): 130-138.

BIOINSPIRED NANOMATERIALS FOR CELL-SELECTIVE ACTIVATION OF GROWTH FACTORS

Nuria Oliva^{1,2*}, Benjamin D. Almquist^{1*}

¹Department of Bioengineering, Imperial College London, ²Grup d'Enginyeria de Materials, Institut Químic de Sarrià
 Corresponding authors: n.oliva-jorge@imperial.ac.uk – Postdoctoral Fellow, b.almquist@imperial.ac.uk

Introduction

Tissue healing is a highly dynamic process involving multiple cell types and transient biological signalling.^{1,2} Efforts in the field of tissue engineering have been focused on developing biomaterials that incorporate dynamic biological information,^{3,4} activated by either passive (pH or enzymes) or active (light) triggers. Passive triggers lack spatiotemporal control over release, while active triggers have the challenge of requiring external manipulation. Looking at nature for inspiration, we have developed a novel aptamer-based technology platform that harnesses cellular traction forces to activate growth factors, called Traction Force-Activated Payloads (TrAPs), inspired by the naturally occurring process of activation of TGF- β 1 during the healing process (**Fig. 1A-D**).⁵

Materials and Methods

Oligos were synthesised in-house using solid-phase phosphoramidite chemistry, followed by on-column chemical conversions. DBCO-peptides were conjugated to the azide end of aptamers through click chemistry, and the thiol end was conjugated to maleimides on 2D (glass coverslip or polyacrylamide gel) or 3D (collagen sponges) surfaces. Cell proliferation was measured as either metabolic activity (Presto Blue) or viable cell number/field (Cell Tracker Green CMFDA). Established cell culture protocols were used for all cells (human dermal fibroblasts - HDF, human microvascular endothelial cells - HMEC-1 and smooth muscle cells - SMC).

Results and Discussion

This work demonstrates that TrAP technology harnesses cellular traction forces to activate growth factors by unfolding the aptamer. We synthesized aptamers in which one end is attached to a cell-adhesive peptide (e.g., the integrin binding peptide RGD), and the other end has a chemical group that facilitates facile conjugation to any scaffold of interest (e.g., thiol) (**Fig. 1C-D**). We showed that TrAPs platform enables various cells (HFD, HMEC-1 and SMC) to mechanically unfold the aptamers and release active forms of various growth factors (PDGF, VEGF). We demonstrated that the TrAP technology is easy to integrate within a variety of cell culture systems and biomaterials that span both 2D – glass coverslips and polyacrylamide gels – and 3D collagen scaffolds, enabling the addition of cell-activated growth factors to virtually any existing biomaterial of interest. Furthermore, this is the first ever demonstration of cell-selective activation of growth factors – e.g., activation by SMCs but not HDFs after one (**Fig 1E**) and two weeks (**Fig 1F**), by tailoring cell adhesive-peptides to specific cell types (i.e. VAPG to SMCs).

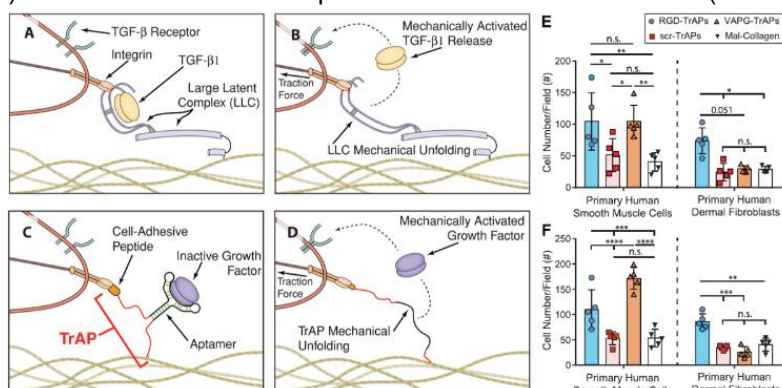


Figure 1. A,B) Natural TGF- β 1 activation from LLC. **C,D)** Aptamer-based synthetic mimic of LLC. Selective GF activation by SMC but not HDF using VAPG TrAPs after **E)** one and **F)** two weeks. Adapted from ref. 5 under CC-BY permission.

(**Fig. 1C-D**). We showed that TrAPs platform enables various cells (HFD, HMEC-1 and SMC) to mechanically unfold the aptamers and release active forms of various growth factors (PDGF, VEGF). We demonstrated that the TrAP technology is easy to integrate within a variety of cell culture systems and biomaterials that span both 2D – glass coverslips and polyacrylamide gels – and 3D collagen scaffolds, enabling the addition of cell-activated growth factors to virtually any existing biomaterial of interest. Furthermore, this is the first ever demonstration of cell-selective activation of growth factors – e.g., activation by SMCs but not HDFs after one (**Fig 1E**) and two weeks (**Fig 1F**), by tailoring cell adhesive-peptides to specific cell types (i.e. VAPG to SMCs).

Conclusions

TrAP technology platform harnesses cellular traction forces as a biophysical trigger to activate and release therapeutics without the need of passive or external triggers, unlocking the potential to develop highly dynamic biomaterials that enable spatiotemporal, cell-selective activation of localized bioactivity for regenerative medicine. Multiplexing different TrAPs (for various growth factors and/or selective for specific cell types) within a scaffold will allow to tune the activation of defined growth factors to the arrival of specific cell types within a local microenvironment, mimicking the complex and dynamic natural healing process.

References

- Nelson C M. *Biochim. Biophys. Acta, Mol. Cell Res.* 1793: 903, 2009.
- Enyedi B & Niethammer P. *Trends Cell Biol.* 25: 398, 2015.
- Zhang YS & Khademhosseini A. *Science.* 356: eaaf3627, 2017.
- Stejskalová A & Almquist BD. *Biomater. Sci.* 5: 1421, 2017.
- Stejskalová A, Oliva N, England FJ, Almquist BD. *Adv. Mater.* 31(7): 1806380, 2019.

Acknowledgements

This work was supported by the Wellcome Trust [109838/Z/15/Z], Engineering and Physical Science Research Council [EP/R041628/1], and the Department of Bioengineering at Imperial College London. N.O. acknowledges support from a TECNIOspring PLUS fellowship, part of the European Union's Horizon 2020 research and innovation programme under the Marie Skłodowska-Curie grant agreement no. 712949.

CYTOTOXICITY AND FUNCTIONALITY OF NANO OXY-PH SENSORS IN HMSC ENVIRONMENT

Manohar Prasad Koduri^{1, 2*}, James Henstock³, John Hunt⁴, Fan-Gang Tseng^{1, 5}, Jude Curran²

¹ International Intercollegiate PhD Program, NTHU, Hsinchu, Taiwan

²Department of Mechanical, Materials and Aerospace, School of Engineering, University of Liverpool, UK

³Institute of Ageing and Chronic Disease University of Liverpool, UK

⁴School of Science and Technology, Nottingham Trent University, Nottingham NG11 8NS, UK.

⁵Engineering and System Science, NTHU, Hsinchu, Taiwan

Corresponding author: mfgtjch@liverpool.ac.uk (PhD student 3rd year)

Introduction:

Oxygen levels have been identified as an important parameter in stem cell cultivation and differentiation. In addition pH level levels can also be used as an indicator of the physiological conditions associated with the cell environment [1]. Therefore real-time monitoring of these factors, in spatially defined locations within a tissue/cell construct can provide abundant and valuable information directly relating to the optimal physiological conditions required to control cell function and performance within a 3D construct in vitro. For implantable medical devices and in vitro cell modeling this information can be used to optimize/develop novel materials and culture scenarios that can be used to control cell function, eliminating the need for supplementation with exogenous biological factors. In addition, the sensors must not affect cell viability or induce changes in cell function or phenotype whilst optimizing sensitivity, accuracy, resolution, linearity, dynamic range and hysteresis. To validate the use of this technology in Human Mesenchymal Stem Cell culture systems viability and cytotoxic effect of Nano Sensors to monitor oxygen and pH levels in real time in vitro was assessed.

Material and Methods

Nano Oxygen and Nano pH sensors were fabricated using Polystyrene Nano beads (PSB) with surface modified by carboxyl groups (Thermo SCIENTIFIC, W050C) s. For Nano Oxygen sensors Pluronic F127 (a triblock copolymer), was employed (all are from Aldrich Sigma) and attached onto the surface of PSB by an esterification process. Oxygen-sensitive red fluorescent molecule Ru (dpp)₃Cl₂, (C₇₂H₄₈Cl₂N₆Ru) (Fluka, excitation at 470-490 nm and emission at 613 nm), was attached to the structure of a hydrophobic polymer Pluronic F-127 [2] in ethanol. For Nano pH sensors, initially, an intermediate sulpho NHS ester was formed with the help of EDAC/ NHS coupling reaction. The intermediate compound was further mixed with amine conjugated FITC fluorophore resulting in the synthesis of Nano pH sensors as shown in figure 1.

Results and Discussion

Three different concentrations (0.1, 1, and 10 µL/mL) of each sensor was tested and measured using live cell and MTT assays in 96 well plates. Cells cultured in 96 well plates at a seeding density of 5000 cells/ cm² are as shown in figure 2 and 3. Control cells, grown in the absence of any sensors, demonstrated a normal gradient of increase in cell number and the same profile was shown with 10µL/mL of both Oxygen and pH sensors. In contrast w 1µL/mL of both sensors shows an increased growth rate at day 11, indicating a reaction to the presence of the sensors. At a sensor concentration of 0.1µL/mL of both sensors a Gaussian distribution of cell proliferation was observed.

Conclusion

In this study we demonstrate a novel O₂ and pH sensor synthesis and its cytotoxic effect in HMSC cellular environment.

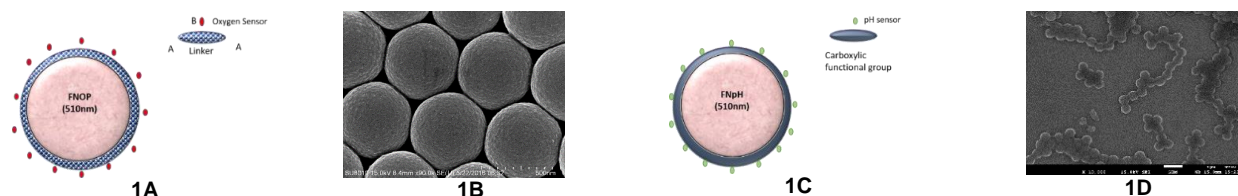


Figure 1 Schematic and SEM image of Nano-Oxygen sensor (A,B) and Nano- pH Sensor (C, D)

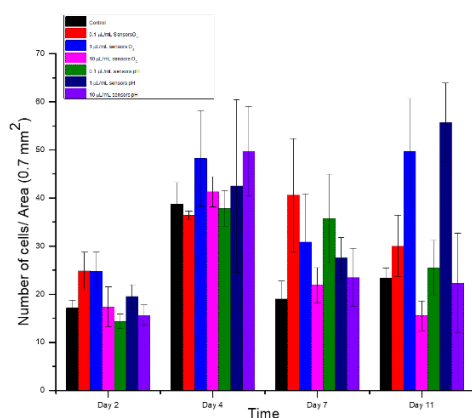


Figure 2: Cell Viability assay (Calcein Green)

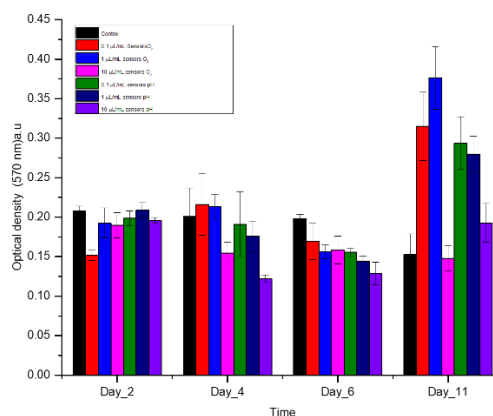


Figure 3 MTT Assay

Reference:

- Wang et al. Chemical Society Reviews 43.10, 3666-3761, 2014.
- Koduri, Manohar Prasad, et al. ACS applied materials & interfaces 10.36, 30163-30171 2018

Designing a novel bioengineered substrate as a treatment for AMD

R McCormick¹, I Pearce², and A Haneef¹

¹Eye and vision department, Institute of Ageing and Chronic Disease, University of Liverpool, William Duncan Building, 6 West Derby Street, Liverpool L7 8TX

²Royal Liverpool University Hospital, St Paul's Eye Unit, Prescot Street, Liverpool, L7 8XP.

INTRODUCTION: Age related macular degeneration (AMD) is the third most prevalent cause of blindness worldwide. In AMD, the Bruch's membrane, a section of the retina, thickens with age, resulting in impaired waste/nutrient exchange between the retinal pigment epithelial (RPE) cells and the choroid. This leads to photoreceptor death and eventually permanent central vision loss. There are two types of AMD, wet and dry. Dry AMD is the most common affecting 90% of AMD patients and there is no effective treatment [1]. Considering there is no treatment for dry AMD and with its prevalence anticipated to rise due to increasing life span, a treatment for this debilitating condition is essential. Here we have optimised the production of a bioengineered substrate to act as an artificial Bruch's membrane, suitable for growing RPE cells as well as a bioactive layer that will deliver active molecules at a controlled rate to break down the drusen in the diseased native Bruch's membrane.

METHODS: 25% w/v PET (polyethylene terephthalate) dissolved in hexafluoro-2 propanol (HFIP) scaffolds, capable of growing ARPE-19 cells in their native role, were produced through electrospinning as optimised by Haneef et al [2]. ARPE-19 cells were seeded on 2cm² scaffolds at a density of 80,000 cells. Electrospun PET was also subjected to tensile testing. For nanoparticle production PLGA (poly(lactic-co-glycolic acid, 2% chloroform) was subjected to different working distances and voltages to ensure the formation of nanoparticles, using SEM images as a confirmation. Following on from this, nanoparticles were tested for their ability to encapsulate, protect and release biological moieties.

RESULTS: Our results have shown that electrospinning 25% PET can produce nanoscale fibres and confirm that electrospun PET is a suitable scaffold for ARPE-19 cells.

ARPE-19 cells are able to form a monolayer on top of the material as they do natively, and do not pass through the material. Water contact measurements show that electrospun PET is very hydrophilic (average contact angle of 28°). Tensile testing of PET fibres show electrospun PET has a high elasticity compared with cast PET sheets which are extremely brittle. The average porosity of the material is 86% and barrier assays showed that FITC (fluorescein isothiocyanate) was able to pass through the material within 10 minutes to an hour. We have also shown that electrospaying of PLGA is able to form reproducible nanoparticles that are capable of encapsulating biological moieties. Degradation studies using FITC (fluorescein isothiocyanate) tagged bovine serum albumin (BSA) and enzymes have shown that these nanoparticles are capable of releasing BSA and enzymes (lipases, collagenases), at a controlled rate. Gel enzyme assays show the nanoparticles do not affect the function of enzymes and are likely to protect the enzymes from degradation.

DISCUSSION & CONCLUSIONS: This work shows that PET is a suitable scaffold for ARPE-19 cells and has properties that can allow it to act as an artificial Bruch's membrane. Electrospayed biodegradable nanoparticles are able to encapsulate, protect and sustain the release of biological enzymes. Future work will focus on the optimisation of the specific cocktail and release of enzymes suitable for the breakdown of drusen for replacing the RPE and Bruch's membrane, as a treatment for dry AMD.

ACKNOWLEDGEMENTS: Financial support was received from EPSRC

REFERENCES: [1] Gehrs K et al (2016). *Annals of Medicine*, 36 (7), 450-471.[2] Haneef, A et al. *International Journal of Polymeric Materials and Polymeric Biomaterials*, 64(6), 320-33

Differentiation by design: Varying surface topographical features of polymeric microparticles influences mesenchymal stem cell fate

M Amer¹, M Alvarez-Paino¹, K Shakesheff¹, D Needham^{1,2}, M R Alexander¹, C Alexander¹ and F RAJ Rose¹

¹School of Pharmacy, University of Nottingham, Nottingham, UK; ²Department of Mechanical Engineering and Material Science, Duke University, North Carolina, USA

INTRODUCTION: Material properties are capable of influencing cell behaviour. The aim of this study was to examine the influence of tailored microparticle design by varying surface topography on stem cell response, which is critical for their use as cell delivery systems for regenerative medicine applications.

METHODS: Textured PLA microparticles were produced by exploiting phase separation of fusidic acid from PLA during loss of solvent from an oil-in-water emulsion. Fusidic acid then dissolves leaving textured surfaces (Fig 1A). By varying emulsion settings, microparticles of two key morphologies were produced: dimpled ‘golf ball’-like and angular morphologies. To investigate the influence of microparticle topography on cell response, a planar presentation of the particles was developed by heat sintering them into discs before cell culture. The influence of topographical features on attachment and proliferation of primary human mesenchymal stem cell (hMSCs) was investigated. Markers of osteogenesis, metabolomics and comparative gene expression analysis were also assessed in the absence of osteo-inductive supplements.

RESULTS: Cell morphology was influenced by different topographies, with cells spreading on smooth surfaces and adopting more rounded morphologies on dimpled microparticles (Fig. 1A). In the absence of osteo-inductive supplements, cells cultured on microparticles with dimples exhibited notably increased expression of osteocalcin (Fig. 1B & C) and mineralisation levels relative to smooth microparticles. Differential gene expression was observed for hMSCs on microparticles compared to 2D-cultured controls. A number of osteogenesis-related genes were differentially expressed between smooth and dimpled microparticles. Metabolomics revealed that the dimpled microparticles group was significantly separated from the smooth microparticles group by orthogonal partial least-squares discriminant

analysis models, indicating that metabolic state of hMSCs cultured on dimpled microparticles was changed relative to smooth ones (Fig 2).

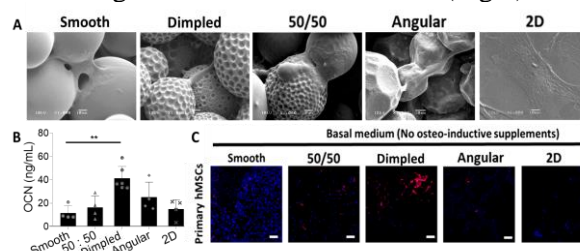


Fig. 1: (A) SEM images of hMSCs attached to microparticle surfaces 4hr post-seeding. (B) OCN levels in culture media, measured by ELISA, of hMSCs (2 donors) on various topographies 21d post-seeding ($n \geq 4$; $**p \leq 0.01$). (C) Osteocalcin (red) and nuclear (blue) staining of hMSCs cultured in basal media 14d post-seeding (scale bar=100 μ m).

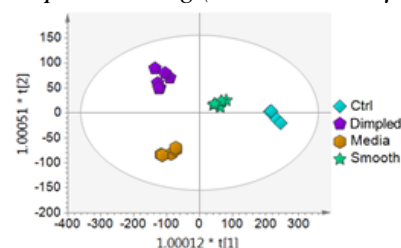


Fig. 2: OPLS-DA scores plot of hMSCs culture media on smooth & dimpled microparticles ($n=6$), 2D control & blank media 14d post-seeding ($R^2=0.936$ & $Q^2=0.651$ (Simca-P)).

DISCUSSION & CONCLUSIONS: Topographically-textured microparticles of varying microscale features were used to investigate stem cell adhesion and subsequent differentiation. This study highlights the importance of tailoring topographical design of microparticles and offers the opportunity to control stem cell fate by inducing osteogenesis without exogenous osteo-inductive factors.

ACKNOWLEDGMENTS

This work was supported by the Engineering and Physical Sciences Research Council [EP/N006615/1]; EPSRC Programme Grant for Next Generation Biomaterials Discovery.

Dual-action Nitric Oxide-releasing Micropatterned Antibacterial PDMS Surfaces

George Fleming^{1*}, Jenny Aveyard¹, Joanne L Fothergill², Fiona McBride³, Rasmita Raval³, Raechelle A D'Sa¹

1: Department of Mechanical, Materials and Aerospace Engineering, University of Liverpool, Liverpool, L69 3GH.

2: Institute of Infection and Global Health, University of Liverpool, 8 West Derby Street, Liverpool, L7 3EA.

3: The Open Innovation Hub for Antimicrobial Surfaces, Surface Science Research Centre, Department of Chemistry, University of Liverpool, Liverpool, L69 3BX.

*sggflemi@liverpool.ac.uk

INTRODUCTION

As medicine and technology develops so does life expectancy and the prevalence of age-related diseases. Due to this, implantable medical devices, such as: pacemakers, catheters and orthopaedic prostheses have become paramount in modern healthcare and are necessary for prolonging and improving the life of critically ill patients. The increased use of such devices is not without significant problems; one being their susceptibility to bacterial adhesion and subsequent biofilm formation. In this work dual-action micropatterned PDMS surfaces that release nitric oxide (NO) have been fabricated with the aim of controlling bacterial response with both physical and chemical surface modifications, for the potential use in medical implant applications.

MATERIALS & METHODS

PDMS replicas were moulded over micropatterned silicon wafers to give PDMS with defined microtopographical features (rectangles, rectangles, inverted rectangles). Aminosilanisation of these surfaces was then carried out using N-(3-trimethoxysilylpropyl)diethylenetriamine (DET3). The amine groups in DET3 facilitated the formation of the NO donor groups, *N*-diazoniumdiolates, when in the presence of high pressures of NO. Planktonic and adhered cell colony forming unit (CFU) assays were carried out against a lab strain of *Pseudomonas aeruginosa* (PA14), to assess the bactericidal and anti-adhesion abilities of the surfaces, respectively. Scanning electron microscopy (SEM) was used to image surface adhered bacterial cells.

RESULTS & DISCUSSION

XPS confirmed the presence of the *N*-diazoniumdiolate groups and AFM analysis showed the well-defined microtopographical features on the PDMS surface. NO release was monitored by chemiluminescence detection and surfaces released up to 981 μmol over 20 hrs at pH 7.4. Planktonic and adhered cell colony forming unit (CFU) assays were carried out against a lab strain of *Pseudomonas aeruginosa* (PA14), to assess the bactericidal and anti-adhesion abilities of the surfaces, respectively. In the presence of non-structured NO-releasing PDMS a bactericidal effect resulted in the complete eradication of bacteria by 4 hrs, due to large NO payloads. Structured NO-releasing PDMS was bactericidal due to NO (62 % reduction) and anti-adhesive due to microtopography (52 % reduction). The results are in agreement with findings reported by Lu *et al.*,¹ that microtopography controls bacterial response, through alterations in the cell-surface contact area; when the diameter of surface features are smaller than the diameter of the bacterial cell, cell-surface contact area is minimised and a reduction in adhesion is observed.

CONCLUSION

Novel dual-action surfaces have been engineered to control bacterial response through multiple mechanisms. Micropatterned PDMS surfaces that release bactericidal concentrations of NO over 20 hrs were successfully fabricated. At 24 hrs, dual-action PDMS surfaces were bactericidal due to NO release and anti-adhesive due to their distinct microtopography.

REFERENCES

[1] Lu, N *et al.*, Food Control, 68:344-351, 2016.

Electrospun scaffolds containing decellularised tissue matrix support conjunctival epithelial and goblet cells

LA. Bosworth¹, C. Pineda Molina², V. Barrera³, LJ. White⁴, KG. Doherty¹, RA. D'Sa⁵, P. Rooney³, SF. Badylak², RL. Williams¹

¹Department of Eye and Vision Science, University of Liverpool, Liverpool L7 8TX;

²McGowan Institute for Regenerative Medicine, University of Pittsburgh, Pittsburgh, PA 15219, USA; ³NHS Blood and Transplant, Tissue and Eye Services R&D, Speke, Liverpool L24 8RB; ⁴School of Pharmacy, University of Nottingham, Nottingham NG7 2RD; ⁵School of Engineering, University of Liverpool, Liverpool L69 3BX

INTRODUCTION: The conjunctiva lines the sclera and inside of the eyelids, and is essential for maintaining homeostasis of the ocular surface¹. Persistent damage can cause chronic ocular discomfort leading to secondary corneal blindness. This study investigates the viability of conjunctival epithelial and goblet cells when cultured on electrospun fibres containing decellularised tissue matrix as a potential new substrate for conjunctiva regeneration.

METHODS: Powdered decellularised small intestine submucosa (SIS) porcine tissue was received following processing² and used as a source of natural extracellular matrix. Poly(ϵ -caprolactone) (PCL; 12 % w/v) was dissolved in 1,1,1,3,3,3-hexafluoroisopropanol plus 1% or 10% SIS and stirred continuously for 48 hours. Solutions were electrospun using parameters: needle voltage +15kV, collector voltage -4kV, flow rate 1ml/hr, distance 17cm, and rotating mandrel target (100RPM).

Fibre scaffolds were mounted in 24-well CellCrowns, disinfected in 70% ethanol, washed in sterile phosphate buffered saline and pre-soaked in culture medium overnight. Scaffolds were seeded with either 3×10^4 human conjunctival epithelial (HCjE) cells³ or 1×10^4 goblet HT29 MTX cells⁴ and cultured for 7 days. For Scanning Electron Microscopy (SEM) imaging of HCjE cells, scaffolds were fixed in 1.5% glutaraldehyde and chemically dehydrated. Confocal microscopy of HT29 MTX cells, scaffolds were fixed in 10% neutral buffered formalin and stained with primary (and secondary) antibodies: MUC5AC (AlexaFluor 488nm) and CK19 (AlexaFluor 597nm), both positive markers of goblet cells.

RESULTS: Electrospun fibres were fabricated for all solutions investigated. HCjE cells adhered and proliferated on the surface of the fibre scaffolds (Fig. 1). Positive expression of MUC5AC (green) and CK19 (magenta) was

observed for HT29 MTX cells cultured on all electrospun fibre scaffolds.

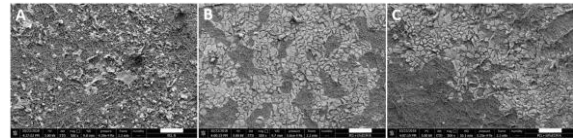


Fig. 1: SEM images of HCjE cells on (A) random, (B) random +1% SIS and (C) random +10% SIS ($\times 500$, scale = 100 μ m)

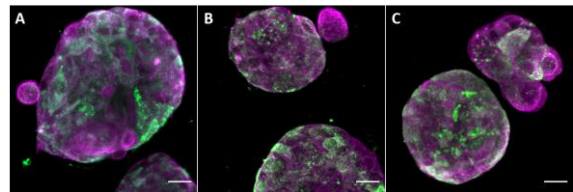


Fig. 2: Z-stack confocal microscopy images of HT29 MTX cell clusters on (A) random, (B) random +1% SIS and (C) random +10% SIS ($\times 40$, scale = 20 μ m); CK19 expression (magenta) and MUC5AC (green)

DISCUSSION & CONCLUSIONS: Solutions of PCL containing SIS were successfully electrospun to create fibrous scaffolds. Fibre scaffolds containing SIS supported the adhesion of HCjE cells with an epithelial-like morphology. Similarly, goblet cells retained their phenotype with positive expression of MUC5AC and CK19 following 7 days in culture. Further *in vitro* studies will be undertaken to explore the effect of different matrices of decellularised tissues combined with electrospun fibres on cell phenotype.

ACKNOWLEDGEMENTS: Special thanks to The Ulverscroft Foundation and The Pauline and Geoffrey Martin Trust for supporting this research.

REFERENCES: ¹Williams RL, et al. *Adv Health Mat.* 2018;7(10):1701328. ²Keane TJ, et al. *Methods.* 2015;84:25-34. ³Gipson IK, et al. *IOVS.* 2003;44(6):2496-2506. ⁴Lesuffleur T, et al. *Cancer Research.* 1990;50:6334-6343.

Engineering ligand mobility in the adhesive crosstalk to control stem cell differentiation

Eva Barcelona-Estaje¹, Marco Cantini¹, Matthew Dalby¹, Manuel Salmeron-Sanchez¹

¹Center for the Cellular Microenvironment, University of Glasgow

Corresponding author: e.barcelona.1@research.gla.ac.uk – PhD student (2nd year)

Introduction

The behaviour of mesenchymal stem cell (MSCs) is strongly influenced by their local surroundings, which provide them with biochemical and physical signals. The biochemical cues are mediated by interactions with the extracellular matrix (ECM) through integrins and by interactions between cells via cadherins. On the other hand, cells are equally sensitive to the physical properties of the microenvironment, such as stiffness or viscosity (1). The metabolic pathways involved in the adhesive crosstalk converge to regulate MSCs mechanosensing, provoking changes in their behaviour and eventually determining cell fate (2). Nevertheless, these mechanisms are not fully understood yet.

In this work, we address the role of ligand mobility in cell fate, and how it affects the adhesive crosstalk between integrins (RGD receptors) and cadherins (HAVDI-containing proteins) to ultimately elucidate stem cell mechanosensing of viscosity.

Materials and Methods

We used a model system based on supported lipid bilayers made by following the vesicle fusion method. To determine how ligand mobility and hence viscosity affects MSCs behaviour, two kind of bilayers were used: one of lipids that present a fluid phase (DOPC) and the other one made of lipids with gel phase (DPPC) at cell culture conditions. Glass is used as a non-mobile control surface. All the surfaces are functionalised with varying ratios of RGD and HAVDI which mimic cell-ECM and cell-cell contacts respectively.

Then, human MSCs are cultured on these biointerfaces and parameters such as cell adhesion, protein translocation or expression of transcription factors are investigated. To achieve this, several techniques are being used such as immunostaining, atomic force microscopy or in-cell western.

Results and Discussion

An increase in cell area and cell adhesion, in particular its strength, is observed when the viscosity of the surface and the amount of RGD increases. Nevertheless, when HAVDI is included in the bilayers, cell spreading is reduced and changes in the location of mechanosensitive proteins (i.e. YAP) are observed, revealing an altered sensing of viscosity (Figure 1).

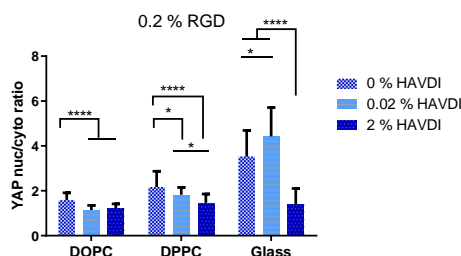


Figure 1: YAP/TAZ ratio of hMSCs cultured on surfaces with different viscosities and different amounts of HAVDI.

The presence of HAVDI provokes not only differences in adhesion and mechanosensing in a viscosity-dependent manner, but also in the expression of transcription factors (e.g. osteogenic), which is an indicator of the influence of viscosity in cell fate.

Conclusions

Our findings reveal not only that there is an influence of viscosity in the adhesive crosstalk between integrins and cadherins, but also that the mobility of the ligands affects stem cell differentiation.

These results show that, when cell-cell interactions are involved, MSCs have a different perception of the mechanical properties of their surroundings compared to when only cell-ECM interactions are present. This altered sensing of the physical cues (viscosity, in this case) provokes changes in cell behaviour and cell fate. Further investigations of these changes in cell behaviour will allow to establish a paradigm to understand and exploit cell response to viscous interactions.

References

1. Bennett M. *et al.* P. Natl. Acad. Sci. USA. 115(6), 1192-1197, 2018
2. Cosgrove B.D *et al.* Nat. Commun, 15(12), 1297, 2016

Acknowledgements

The authors acknowledge funding from EPSRC (EP/P001114/1) and MRC (MR/S005412/1). This work was also funded by a grant from the UK Regenerative Medicine Platform.

EVALUATING TWO POWDER-BASED 3D PRINTING TECHNIQUES FOR THE MANUFACTURE OF IMPLANTS FOR ORBITAL FLOOR REPAIR

M. Omran¹, C.J. Harrison¹, C. Majewski², R. Moorehead¹, J. Shepherd¹, I. Varley¹, and C.A. Miller¹

¹ School of Clinical Dentistry, The University of Sheffield, 19 Claremont Crescent, Sheffield, S10 2TA.

² Department of Mechanical Engineering, The University of Sheffield, Mappin Street, Sheffield, S1 3JD.

Corresponding author: momran1@sheffield.ac.uk – PhD student (3rd year)

Introduction

The delicate structure of the orbital floor makes it prone to fractures. Titanium mesh is often used for repair as it can be tailored to the estimated size and shape of the defect by the surgeon, however, sharp edges are common which can cause pain and discomfort to the patient¹. Incorrectly shaping or positioning the implant are other drawbacks which can lead to additional surgeries. 3D printing offers customisable implants based on patient scan data, aiming to reduce inaccuracies in implant shaping in-situ. Two possible techniques for manufacturing such an implant are laser sintering (LS) and high speed sintering (HSS). LS sinters powders using a laser while HSS utilises an ink and an infrared lamp to sinter powders layer by layer². One problem with these techniques is that the polymer commonly used, polyamide 12 (PA12), is not osteoconductive, and can limit bone regeneration. Hydroxyapatite (HA) is a widely used osteoconductive material, similar in composition to natural bone³. Therefore, this project aims to assess the feasibility LS and HSS for the manufacture of implants with osteoconductive properties for orbital floor regeneration.

Materials and methods

HA was added to PA12 in wt% of 0, 5, 10, 20, 30 and 40 wt% and mixed for 45 min. Discs and bars were manufactured by LS and HSS. Tensile testing and 3-point bending was performed on all printed compositions to determine their mechanical properties. Biocompatibility was evaluated by seeding MG63 cells on discs which were incubated for up to 7 days. PrestoBlue™, PicoGreen™ and alkaline phosphatase assays were used to determine *in vitro* cell viability, quantify DNA and assess osteogenic activity, respectively. Scanning electron microscopy (SEM) was used to study the surface topography of the samples.

Results and discussion

For higher wt% of HA, parts were printed more reliably with HSS than LS. SEM images showed that HSS samples were more porous than LS samples, which is likely to have influenced the mechanical properties as shown by Figure 1. T-tests showed that LS samples had a significantly higher ultimate tensile strength (UTS) than HSS samples, therefore, LS implants can potentially withstand more strain before failure. Additionally, laser sintered samples with HA equal to or greater than 20 wt%, had a significantly lower UTS than the control. This trend was not seen for HSS samples. Initial cell viability studies showed that the samples were biocompatible.

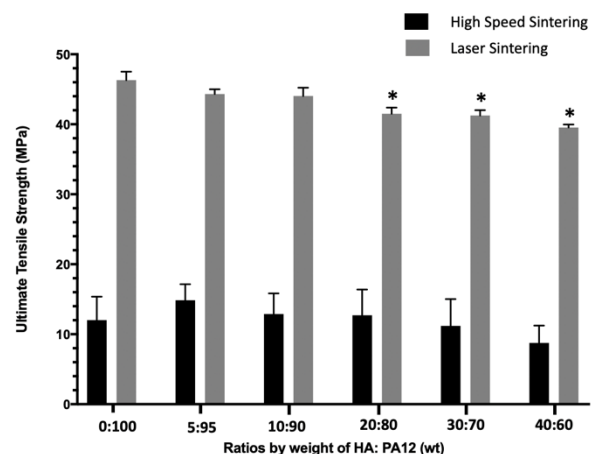


Figure 1: UTS of LS and HSS samples composed of different ratios of HA: PA12 from tensile testing. One-way ANOVA was used to statistically analyse the samples at different ratios manufactured using the same fabrication technique. Statistical significance ($p < 0.05$) compared to 100 wt% PA12 is indicated by *.

Conclusions

LS samples had superior mechanical properties to HSS samples, however, as the orbital floor is a non-load bearing bone, a high mechanical strength is not critical, thus, both techniques have the potential for the fabrication of patient specific implant for orbital floor repair. Initial biocompatibility results suggest that both techniques produce biocompatible materials, however further work is required to eliminate the use of potentially carcinogenic inks from HSS.

References

- Strong EB, *et al.* Otolaryngology-Head and Neck Surgery. 149 (1): 60-66, 2013.
- Ellis A, *et al.* Surface Topography-Metrology and Properties. 3 (3), 2015.
- Wei J, *et al.* Journal of Materials Science. 38 (15): 3303-3306, 2003.

Acknowledgements

We are grateful to Wendy Birtwisle and Kurt Bonser for their assistance in the 3D printing processes. Thank you to University of Sheffield for financial support as part of institutional commitment to the EPSRC Centre for Innovative Manufacturing in Medical Devices (MeDe Innovation) grant: EP/K029592/1.

Fabrication and Characterisation of Endometrial Extracellular Matrix Hydrogel for Endometrial Regeneration

M. Chan¹, T. Keane Jr¹, JR. Smith², S. Saso², MM. Stevens¹

¹Department of Materials, Imperial College London, ²Department of Surgery and Cancer, Imperial College London

INTRODUCTION: Intrauterine adhesions and endometrial scarring can lead to absolute uterine factor infertility. Currently, there are limited effective preventative or fertility-restoring treatments. Extracellular matrix (ECM) as a biomaterial has been shown to promote healthy tissue regeneration in many different organs and clinical applications. We describe the fabrication and characterisation of an innovative, injectable and sprayable endometrial ECM hydrogel. We hypothesise that this hydrogel could target scar tissue caused by surgical trauma and stimulate healthy endometrial repair.

METHODS: Endometrial tissue isolated from porcine uteri was decellularized using sodium deoxycholate, sodium chloride, deoxyribonuclease and peracetic acid. Decellularized endometrium was characterised by histology, nuclear staining with DAPI, immunofluorescence for ECM proteins, DNA quantification and Raman spectroscopy. Endometrial ECM was lyophilised, Pepsin-digested and neutralised to form an injectable and sprayable hydrogel. The gelation properties of the endometrial ECM hydrogel were determined by rheometry. Cell viability was assessed with Live/Dead® staining of endometrial stromal cells cultured on an ECM hydrogel coating.

RESULTS: Histological analysis of the decellularized endometrium showed absence of cells and preservation of the matrix architecture (Fig.1). Staining with DAPI revealed absence of nuclear material whilst immunofluorescence showed presence of Collagen I, Laminin, Fibronectin and Collagen IV (Fig.2). The ECM DNA content was reduced by 94.4% compared to native tissue. The Raman spectrum of decellularized endometrial ECM showed biochemical similarities to small intestinal submucosal ECM and urinary bladder matrix ECMs. Rheological testing of the ECM hydrogel showed formation of a stable gel at 37 degrees Celsius within clinically relevant

timepoints, including after injection and spraying. Primary mouse endometrial stromal cells cultured on endometrial ECM hydrogel coatings and labelled with Live/Dead® stain showed 87% live cells (control 79%).

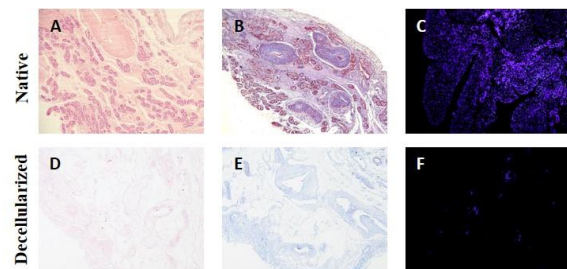


Fig. 1 Histology sections of native endometrium vs. decellularized endometrial ECM. Images A, B and C show native tissue stained by H&E, Masson's Trichrome and DAPI respectively. D, E and F show the corresponding stains in decellularized ECM.

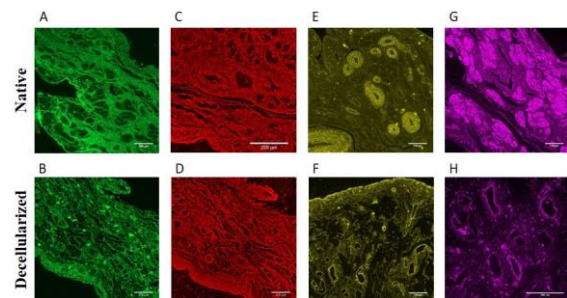


Fig. 2 Immunofluorescence of native and decellularized endometrial tissue sections. Images in the top row represent native endometrium and the bottom row shows decellularized endometrial ECM. Collagen I (A,B), Fibronectin (C,D), Collagen IV (E,F) and Laminin (G,H) are found in both native and decellularized tissue.

DISCUSSION & CONCLUSIONS: We report an effective method for decellularizing endometrium to produce an endometrial hydrogel that retains key ECM proteins. This injectable and sprayable gel allows versatility for clinical application. Further studies will be done to characterise its effects on endometrial fibrosis *in vitro* and in an animal model.

ACKNOWLEDGEMENTS: Funding from Wellbeing of Women (RG2123).

FORMULATION OF AN ANTIMICROBIAL SILVER-DOPED MAGNESIUM OXYCHLORIDE CEMENT

Morgan Lowther,*¹ Prof Liam Grover¹, Dr Sophie Cox¹

¹School of Chemical Engineering, University of Birmingham (UK)

Corresponding author: mxl782@bham.ac.uk – PhD student (2nd year)

Introduction

There is great interest in developing cement formulations with high strength and easy preparation for bone regeneration. In comparison to existing materials such as calcium phosphates (CaP), magnesium oxychloride cements (MOC) offer greater resorbability and can be tailored by the addition of phosphoric acid.

Excess MgO is frequently added to MOC mixes for improved strength. Interestingly, this could lead to inherent antimicrobial and antifungal functionality due to the efficacy of micron scale MgO powders [1]. Current prophylaxes are often face difficulties penetrating biofilms. Supplementing with an inorganic antimicrobial such as silver can disrupt biofilm formation, enhancing the efficacy of conventional antibiotic treatments [2].

In this work, the potential for antimicrobial MOC formulations has been investigated. Both the mechanism of any inherent antimicrobial behaviour and the addition of a silver phosphate to increase efficacy have been studied. Importantly, correlations between critical cement requirements have been explored, identifying a formulation that balances mechanical properties and efficacy.

Materials and Methods

Cements were manufactured by mixing light MgO powder with MgCl brine [3], with a range of formulations with excess MgO produced. Phosphate-modification was by addition of H₃PO₄ to the brine. When producing silver-modified cements, Ag₃PO₄ was added to the dry MgO. For a subset of formulations, deliberate porosity was induced by addition of a porogen.

Samples were produced by extrusion into moulds of 6 mm diameter and 12 mm height, curing for 48 hours before demoulding. Compression testing was performed with load rate 1 mm/min. Helium pycnometry and X-ray diffraction (XRD) were performed on ground cements. Semi-quantitative assessment of spectra was made and normalised based on the ratios of reagents used. Perfusion and elution assessments were made, with elutants assessed by inductively coupled plasma spectroscopy (ICP-OES).

Antibacterial efficacy was assessed compared to CaP controls. Zones of inhibition were assessed for *S. aureus* and *E. coli* on tryptic soy agar (TSA) after 24 hours incubation. Efficacy against planktonic bacteria in broth was assessed by serial dilutions inoculated on TSA for overnight culture.

Results and Discussion

Dry compressive strength was comparable to CaP ceramic cements, with ultimate compressive strength (UCS) up to 30 MPa. Increasing the powder to liquid ratio had no significant effect on UCS, but increased relative density, suggesting critical flaw size remained consistent. Addition of Ag₃PO₄ had negligible effect on UCS, however addition of H₃PO₄ to the brine reduced strength by a factor of a half, and prevented extrusion at powder/liquid ratio of 1.6.

XRD results indicate retardation of 5Mg(OH)₂.MgCl₂.8H₂O (5-phase) formation by orthophosphate modification, with associated brine acidification reducing Mg(OH)₂ to MgO. Silver modification also reduced the yield of 5-phase, however this was associated with depletion of chloride ions by formation of AgCl.

Antibacterial efficacy was shown both by the formation of zones of inhibition, and reduced viability of both planktonic and adhered bacteria in broth versus CaP controls. Unmodified cements showed significant reduction in viability, suggesting that MOC shows some inherent antimicrobial efficacy.

Conclusions

Magnesium oxychloride cements have been shown to possess a degree of inherent antimicrobial efficacy associated with MgO. Addition of a porogen and silver phosphate improved efficacy, both against adhered and planktonic bacteria in broth. This formulation shows promise as an antimicrobial cement that exhibits more rapid degradation than calcium phosphate cements.

References

1. Sawai, J. et al. World J. Microbiol. Biotechnol. 16, 187–194 (2000).
2. Park, H.-J. et al. J. Ind. Eng. Chem. 19, 614–619 (2013).
3. Tan, Y et al. J. Biomed. Mater. Res. Part A 103, 194–202 (2015)

Generation of an immuno-responsive tissue engineered oral mucosal equivalent containing primary human macrophages

B. Ollington, H. E. Colley, C. Murdoch

School of Clinical Dentistry, University of Sheffield, Sheffield, UK

INTRODUCTION: Complex tissue engineered models are used extensively to mimic the oral mucosa¹. However, to date only one study has included an immune component², and none have incorporated primary immune cells. An immune component is important as these cells have key roles in surveillance, and orchestrating the innate and adaptive responses to invading organisms and molecules not recognised as ‘self’. This study seeks to address this knowledge gap by generating reproducible tissue engineered oral mucosal models containing functional immune cells that can be used as an improved model system to investigate immunity, and immune-mediated disorders in the oral mucosa.

METHODS: Human peripheral blood monocytes were isolated from whole blood, differentiated into monocyte-derived macrophages (MDM) and cultured as monolayers or in a tissue engineered oral mucosal equivalent (OME). OME were generated by incorporating primary oral fibroblasts in a type 1 collagen hydrogel, seeding with immortalised buccal mucosal keratinocytes (FNB6 cell line) and culturing for 10 days at an air to liquid interface (ALI)¹. MDM were incorporated into the collagen hydrogel alongside oral fibroblasts to generate MDM-OME. Immune functionality was interrogated by stimulation with oral bacterial lipopolysaccharide (LPS) and induced release of pro-inflammatory cytokines compared to unstimulated controls. Mucosal models were disaggregated with type 1 collagenase and purified cells analysed by flow cytometry for immune cell surface markers.

RESULTS: MDM responded to LPS from oral bacteria when cultured in 2D with increased cytokine gene expression and secretion with the following potency *Porphyromonas gingivalis* > *Aggregatibacter actinomycetemcomitans* > *Tannerella forsythia*. When cultured within a 3D collagen hydrogel, MDM remained viable over 21 days as assessed by viability staining and lactate dehydrogenase release.

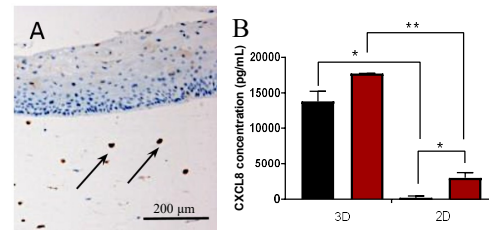


Fig. 1: CD68+ MDM in an OME collagen matrix (A). Secretion of CXCL8 in response to *P. gingivalis* LPS (red) and control (black) by MDM in 3D collagen and in 2D (B).

Both OME and MDM-OME contained a full thickness differentiated epithelium (Fig 1A) and responded to *P. gingivalis* LPS with increased secretion of IL-6 and CXCL8 compared to unstimulated controls (Fig 1B). Upon disaggregation MDM could be distinguished from other cells present in the OME by CD11c. In addition, these isolated MDM displayed increased cell surface expression of immune activation markers compared to unstimulated controls.

DISCUSSION & CONCLUSIONS: These data show long-term functionality of MDM both in monolayer and when incorporated within an OME. Phenotypic cellular changes and increased cytokine secretion following stimuli show the MDM-OME models are immune-responsive. It is hoped that these models will be beneficial in future studies monitoring the immune response in the oral mucosa to potentially inflammatory molecules in pathogenic or drug discovery studies.

ACKNOWLEDGEMENTS: The authors would like to thank Dr Graham Stafford, Mr Ashley Gains and Mrs Katherine Ansbro for assistance with isolating oral bacteria LPS, Professor Keith Hunter for the kind donation of the FNB6 cell line and the MRC DiMeN DTP for funding this work.

REFERENCES: 1. Jennings L.R et al (2016), *Tissue Eng Part C*, 22 (12), pp. 1108-1117.
2. Kosten I. J et al (2016), *Altex*, 33(4), pp. 423-434.

Graphene-Polymer Composites for the Engineering of Cardiac Tissue

R. Balint¹, L. A. Hidalgo-Bastida^{2,3,4}

¹Manchester Institute of Biotechnology (MIB), University of Manchester, United Kingdom,

²Centre for Biomedicine, ³Centre for Advanced Materials and Surface Engineering, ⁴Centre for Musculoskeletal Science and Sports Medicine, Manchester Metropolitan University, UK

INTRODUCTION: Electroactive biomaterials are of interest for the engineering of excitable tissues and implantable devices. Metals, such as gold and titanium, are commonly used, but can be expensive and suffer from mechanical incompatibility with most tissue types. Intrinsically conductive polymers (e.g PPy, PEDOT) have been extensively investigated, but are difficult to process once synthesised and also lose their conductivity (and often mechanical integrity) with repeated cycles of electrical stimulation [1]. In this study, we aimed to explore whether compositing the highly electrically conductive 2D material graphene with polymers could yield a material suitable for the engineering of excitable tissue, with a focus on cardiac cells.

METHODS: A custom bioreactor system was designed and built for effective electrical stimulation of cells cultured on a biomaterial surface. FEM computer simulations were performed to assess the behaviour of the electrical field and current inside the bioreactor chamber. Polycaprolactone (PCL) and polyurethane (PU) were composited with four types of commercially available graphene at weight percentages ranging from 0 to 75%. These composites were tested for electrical conductivity, wettability, mechanical properties and surface morphology. Biocompatibility was tested with C2C12 mural myoblasts and RN22 rat Schwann cells. The composites' performance was further explored with human cardiac progenitors and iPSC-derived cardiomyocytes, with and without fibronectin coating, and with and without 2 and 20 ms mono- and bi-phasic electrical stimulation. Response was tested using PicoGreen, Vybrant DiD staining, qRT-PCR for 9 cardiac marker genes and superarrays.

RESULTS: Computer simulations determined 1.7 S/m as the critical electrical conductivity for the substrates. All four graphene-polymer types were able to achieve conductivities exceeding this value. Conductivity was not decreased after 6 days of continuous stimulation. It was found

that addition of polycarboxylate-functionalised graphene decreased contact angle to approx. 60°, while all other types increased it. Material roughness, porosity, reduced modulus and hardness were also increased by the addition of graphene. C2C12 and RN22 cells adhered and proliferated on hydrophilic graphene composites to an equivalent or greater extent than on pure polymers. Fibronectin coated hydrophilic composites showed excellent performance with cardiac cells, reaching 5 times greater cell number within only 5 days of *in vitro* culture.

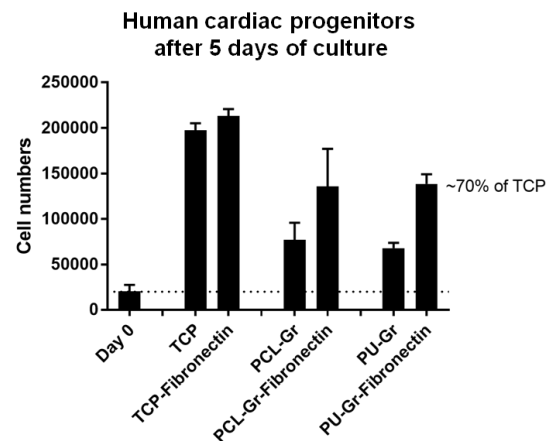


Fig. 1: The growth of human primary cardiac progenitors on composites formed from PCL or PU and polycarboxylate-functionalised graphene with or without fibronectin coating.

DISCUSSION & CONCLUSIONS: This study demonstrates that graphene-polymer composites offer a valuable alternative to conductive polymers in engineering of cardiac tissues.

ACKNOWLEDGEMENTS: We thank the EPSRC Doctoral Prize Fellowship and the EPSRC Postdoctoral Fellowship (EP/P016898/1) funding for financial support.

REFERENCES: [1] Balint R et al. Acta Biomater. 2014; 10:2341-53.

***In vivo* Response to Injectable Hydrogels: from Decellularised ECM to *de novo* Peptides**

N. Mehrban¹, C. Pineda Molina², L.M. Quijano², J. Bowen³, S.A. Johnson², J. Bartolacci², J.T. Chang², A. Scott², D.N. Woolfson⁴, M.A. Birchall¹, S.F. Badylak²

¹UCL Ear Institute, University College London, London, UK ²McGowan Institute for Regenerative Medicine, University of Pittsburgh, Pittsburgh, USA ³School of Engineering & Innovation, The Open University, Milton Keynes, UK ⁴School of Chemistry, University of Bristol, Bristol, UK

INTRODUCTION: Tissue engineering materials are not only expected to mimic tissue architecture and support cells but to also induce cell infiltration and tissue integration towards full functional restoration. These materials must be chemically and physically complex and controllable. Here the response of two hydrogel systems, decellularised tissue ECM and α -helical peptide hydrogels, is investigated after injection into rat abdominal wall defects.

METHODS: Partial thickness abdominal wall defects of Sprague Dawley rats were injected with rheologically-comparable bovine collagen (type I) gels, decellularised urinary bladder matrix gels, decellularised small intestine submucosa gels¹ and hydrogelating self-assembling fibre (hSAF) gels.² The *in vivo* response was measured over 28 days through scanning electron microscopy, histology macrophage response (immunolabeling and gene expression).

RESULTS: The acute host response to the injected gels was characterised by increased mononuclear cell infiltration and no foreign body reaction at the gel-tissue interface by day 28. A progression of cellular infiltration within the gels was observed over time, without evidence of gel encapsulation or formation of multinucleate giant cells. All hydrogels were associated with pro-remodeling outcomes, as indicated by the upregulation of myogenic differentiation markers and the expression of anti-inflammatory markers (M2-like) Arginase 1, IL-10, and CD206. The macrophage response to all hydrogels was favourable, with hSAF hydrogels inducing a steady increase of an anti-inflammatory environment compared to the decellularised ECM hydrogels which induced a stable M2-like phenotype after an initial spike in the M1-like (pro-inflammatory) phenotype. None of the hydrogels could be detected from the surrounding healthy tissue, indicating full integration after 28 days (Figure 1).

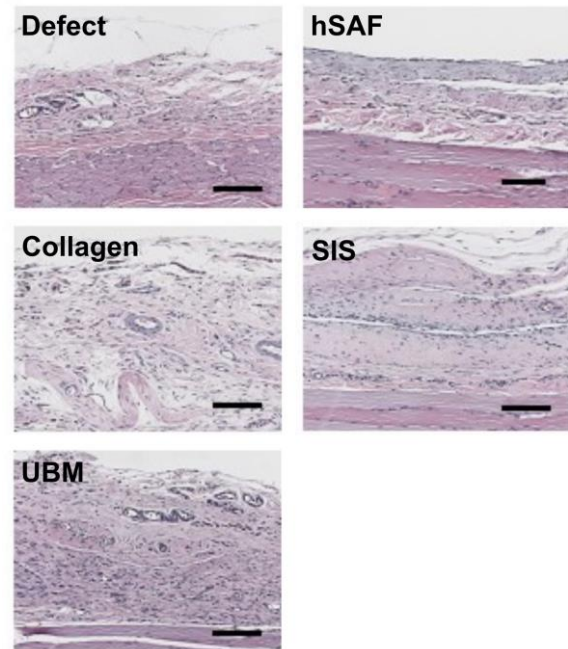


Fig. 1: Histomorphologic characterisation of implanted hydrogels on day 28 with haematoxylin (purple) and eosin (pink). Scale bar: 100 μ m.

DISCUSSION & CONCLUSIONS: Over 28 days all hydrogels indicated pro-modelling at the defect site with no evidence of foreign body reaction, encapsulation or multinucleate giant cells. The macrophage response in the remodelled tissue across all hydrogels was indicative of an anti-inflammatory environment by day 28. The results indicate that injected decellularised ECM hydrogels and synthesised peptide-based hydrogels are suitable for muscle repair *in vivo*.

ACKNOWLEDGEMENTS: This template was modified with kind permission from eCM conferences Open Access online periodical & eCM annual conferences

REFERENCES: (1) Badylak SF et al. *J. Surg. Res.* 1989; 47:74-80. (2) Mehrban N et al. *Adv. Health. Mat.* 2014; 3:1387-91.

Investigation of the impact of sample preparation methods and imaging technique on the organizational presentation of collagen fibrils in hydrogel electron microscopy

Daniel Merryweather*,¹ Nicola Weston,² Chris Parmenter,² Paul Roach¹

¹Department of Chemistry, Loughborough University, ²Nano- and Microscale Research Center, Nottingham University
Corresponding author: d.merryweather@lboro.ac.uk – PhD student (3rd year)

Introduction

Type-I collagen is the most abundant of the collagens and one of the most common biopolymers found in nature, increasingly employed as the basis of 3D cell scaffolds. The collagen-I molecule forms large fibrillar structures comprised of α -helical collagen molecules arranged into larger microfibrils, the interaction and organization of which determine the mechanical properties of the material. Electron microscopy remains a gold-standard method of analysing the nanostructures of a material. Preparation for electron microscopy may itself induce widespread conformational changes in the polymeric constituent of a gel. We here present a systematic comparison of various electron microscopy techniques and preparation methods on the conformational structure of collagen fibrils within gels.

Methods

Collagen hydrogels were fabricated from an acid-dissociated solution at 2.0mg/ml collagen content. The acidic collagen solution was mixed 9:1 with MEM to serve as a pH indicator. This solution was then neutralized by dropwise addition of sodium hydroxide with regular mixing. Once neutralized the solution was held at 37°C for 30 minutes in order to induce gelation and run to completion. Collagen gel samples were loaded onto a pre-cooled -15C sample stand for ESEM and low-vacuum electron microscopy. Dehydrated gel samples were sputter-coated with platinum and imaged via a field-emission gun. Finally, a hydrated gel-state was imaged by slam-freezing collagen gel on a cryogenically-cooled gold-coated copper plate. This sample was transferred to a pre-cooled sample preparation airlock in liquid nitrogen to maintain the frozen state of the gel. This was sputter-coated with platinum within the airlock and transferred to the microscopy stage under vacuum at -190°C. Further platinum was added via gas-injection of methylcyclopentadienyl platinum trimethyl onto the frozen sample surface. A 15 μ m deep trench was milled into the gel bulk using a focused ion beam. The sample was then warmed to -90°C for 30 minutes to remove gel water content. The sample was returned to -190°C and the observable fibril matrix imaged.

Results

Collagen fibrils were readily visible within dehydrated gel samples. Low-vacuum SEM of uncoated gels revealed an increasingly dense network of fibrillar structures as the sample-chamber pressure was dropped and gel water content reduced via sublimation. Dehydrated gel samples presented a densely matted net of collagen fibrils between 70 to 150nm in diameter, with visible structural organizational features such as triplicate braiding of collagen fibrils readily observable under ESEM and FEG-SEM conditions. Under low-vacuum conditions initial fibrils observed presented as isolated structures >200nm in diameter. As pressure was reduced, an increased density of fibrils could be observed. FIB-milling of platinum-coated slam-frozen collagen gels and subsequent sublimation of the gel water content revealed a highly organized network of fibrillar structures in the range of 70-100nm in diameter connecting to form 3D porous structures.

Discussion & Conclusions

The collagen molecule is around 300nm in length and 1.6nm in diameter according to crystal studies. [1] In biological systems these molecules form a helical microfibril formed from three collagen molecules. These microfibrils in turn may form much larger structures, with size dependent on tissue and cellular population. Water is key in stabilizing the structure of the collagen fibril, forming stabilizing bridges between hydroxyproline residues that interconnect adjacent collagen molecules and microfibrils to form the larger observed structures. [2] As the water content is increasingly restricted to more tightly-bound water directly interacting with the collagen surface, individual collagen fibrils are brought into increasing contact in order to maintain the stable structure imparted by this hydration shell. Increasing density results in increased collagen-collagen interaction with fewer intermediary layers of bound and free water.

References

- [1] – Gautieri, A., *et al.*, Nano Letters 11.2, 757-766, 2011.
[2] – Bella, J., *et al.*, Structure 3.9, 893-906, 1995.

INVESTIGATIONS OF HUMAN TENDON WIDTH FOR THE ANATOMICAL DESIGN OF AN IN VITRO FLEXOR DIGITORUM PROFUNDUS ENTHESIS MODEL

Jeremy W Mortimer*¹, Mario Macia¹, Nika P Vonk¹, Philippa A Rust², Jennifer Z Paxton¹

¹Deanery of Biomedical Sciences, University of Edinburgh, UK, ²Department of Plastic Surgery, St. John's Hospital, Livingston, UK

*Corresponding author: j.w.mortimer@sms.ed.ac.uk - PhD student (3rd year)

Introduction

Interfacial tissue engineering between soft tissue and bone aims to rapidly generate a matched soft tissue bony insertion (the enthesis) for implantation in an injured area. Our laboratory is designing a model particular to avulsion injuries of the human flexor digitorum profundus (FDP) at the distal phalanx, the most common closed flexor tendon injury in the hand.¹ In repair of flexor tendon injuries, size-matched tendon ends in tenorrhaphy are crucial for smooth tendon glide in the flexor sheath tunnel. This highlights the importance of correct sizing of the tendon analogue for a clinically-applicable *in vitro* model, and we are developing our design from real human FDP morphometric data. Tendon analogue formation is based on an established basic suture to suture fibroblast-seeded fibrin model,² and the current study examines how manipulation of suture anchor orientation and size, referencing anatomical data, affects the *in vitro* tendon analogue development over time.

Materials and Methods

64 fresh-frozen human fingers from 8 cadavers donated to The University of Edinburgh Medical School were dissected to expose the FDP tendon insertion onto the distal phalanx. Digital images were taken to measure the tendon width at 12mm and 6mm distances proximal to the bony insertion using ImageJ software. Suture anchor constructs consisted of a fibrin gel seeded with 100,000 rat tendon fibroblasts contracting between 2 suture anchors in 35mm wells. Suture anchors were set up 12mm apart with an intermediate suture size based on the human 12mm proximal tendon width data (5mm) in horizontal vs. vertical or vertical vs. vertical orientations. Larger (10mm) and smaller (2mm) suture sizes were also trialled in vertical positions. Digital photographs of triplicate repeats at multiple time points between days 0-21 were analysed with ImageJ software, measuring gel width at the suture anchor points and midway between them.

Results and Discussion

The mean width (\pm SEM) of the FDP tendon at 12mm and 6mm distances proximal to its bony insertion was 4.69mm (\pm 0.20mm) and 6.05mm (\pm 0.25mm), respectively, for all fingers and genders combined. Fibroblast-seeded fibrin gel contracted to conform to suture anchor orientation and length, however even by day 21 the gel width was never equal to (or less than) the suture size when measured at the suture anchor point. Standard errors of gel width means were tightest the later the time point and the larger the sutures used in the constructs, suggesting predictability of gel size increases with time and size of anchor. For vertical vs. vertical suture anchor constructs, the gel width midway between 10mm sutures became less than suture size between days 14-17, continuing to decrease with time (**Fig.1**). The equivalent midway measurement between smaller vertical vs. vertical suture anchors had not decreased beyond suture size by day 21, showing that larger anchors may require an intermediate anchoring point to prevent gel/tendon analogue bowing at shorter growth periods.

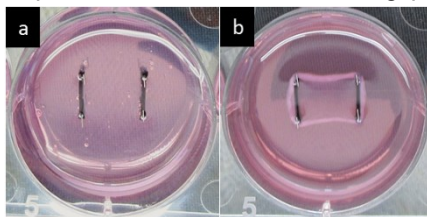


Figure 1. 10mm vs 10mm vertical suture construct; 35mm well. Gel contraction from day 0 (a) (gel covers the entire well) to day 21 (b) where gel conforms to anchor length and positioning. Continued gel contraction causes bowing between suture anchors in this design.

Conclusions

We have quantitatively assessed the tendon morphology at the human FDP insertion to guide tendon analogue design in an anatomically sized *in vitro* FDP enthesis construct. To recreate these tendon sizes we have begun manipulation and assessment of suture anchor constructs to inform contraction pattern predictability and maturation of the *in vitro* tendon analogue over time. This data will form the basis of more finely focused anatomical anchor designs.

References

1. Freilich A. Clin Sports Med. 34: 151-166, 2015.
2. Paxton J *et al.* Tissue Eng Part A. 15:1201-1209, 2009.

Acknowledgements

Orthopaedic Research UK: grant 528.

Special acknowledgement to the body donors of The University of Edinburgh Medical School.

Local suppression of the T cell response to peripheral nerve allografts using drug-eluting PCL fibers

V.H. Robertson, U. Angkawinitwong, H. Gregory, G. Williams, J.B. Phillips

¹*UCL Centre for Nerve Engineering, UCL School of Pharmacy, University College London, UK*

INTRODUCTION: Nerve autografts, the current standard repair for disabling nerve gaps, are associated with donor site morbidity and limited tissue supply. Alternatives including nerve allografts from organ donors, or engineered tissues containing allogeneic therapeutic cells are not currently used due to immunological rejection. This can be avoided with systemic immunosuppression, though side effects are too severe for use in a non-life threatening condition. We have developed a tacrolimus-loaded fibre mat for local sustained release of immunosuppressant (tacrolimus) at the site of a nerve allograft, and present in vivo data testing this in a rat peripheral nerve allograft model.

METHODS: Electrospun poly-caprolactone (PCL) fibres¹ were prepared either loaded with tacrolimus² or drug-free (control) and cut into 1 cm² sheets. Male Lewis rats (n=32) were randomised to one of 4 experimental groups: 1) autograft with control fibre wrap; 2) autograft with tacrolimus fibre wrap; 3) allograft with control fibre wrap; 4) allograft with tacrolimus fibre wrap (n=8 per group). Rats received 1 cm² sciatic nerve grafts, either rotated autografts, or allografts from donor rats of a different strain with mismatched MHC (Dark Agouti). Fibre mats were wrapped around nerve grafts prior to wound closure (Fig 1). Nerves were harvested at 3 or 8 weeks post-transplantation (n=4 per group per time-point). Electrophysiological assessment of nerve conduction and histological analyses were carried out to compare the immune response to nerve grafts (T cell markers) and assess nerve regeneration (neurofilament).



Fig. 1: Wrapping of tacrolimus loaded fibre sheets around a rat nerve allograft

RESULTS: Nerve wraps were well tolerated by the animals with no adverse effects with or without drug. At 3 weeks there was increased T cell infiltration of nerve allografts compared to autografts, which was reduced in allografts wrapped with tacrolimus loaded fibre mats (Fig 2). Electrophysiology at 8 weeks showed return of nerve conduction continuity in all animals.

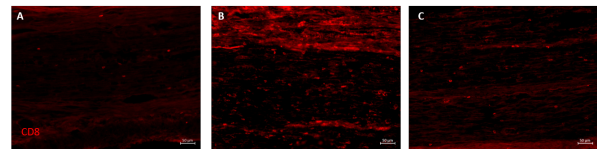


Fig. 2: CD8 T cell response to nerve autografts with control fibres (A), allografts with control fibres (B) and allografts with tacrolimus-loaded fibres (C)

DISCUSSION & CONCLUSIONS: We have demonstrated proof-of-concept for the use of tacrolimus-loaded PCL nanofibers to deliver local immunosuppression sufficient to reduce the host immune response to mis-matched allografts in a rodent peripheral nerve model. Tacrolimus loaded fibre mats can be safely wrapped around nerve allografts to suppress the host immunological response.

ACKNOWLEDGEMENTS: The authors are grateful for the 2018 UCL Rosetrees/Stoneygate Prize to fund this research, the MRC Confidence in Concept Fund (UA) and EPSRC CDT in Advanced Therapeutics and Nanomedicines; EP/L01646X/1 (HG).

REFERENCES:

- [1] Angkawinitwong, U., Awwad, S., Khaw, P.T., Brocchini, S., Williams, G.R., (2017). Electrospun formulations of bevacizumab for sustained release in the eye. *Acta Biomater.* 64, 126–136.
- [2] See poster: Gregory, H., Angkawinitwong, A., Robertson V.H., Williams, G., Phillips J.B. A zero-order drug eluting material to improve nerve grafting

NITRIC OXIDE RELEASING CONTACT LENS BANDAGES

J. Aveyard¹, R. C. Deller¹, R. Lace², R. L Williams², R. A. D'Sa^{1*}

¹ University of Liverpool, Department of Mechanical, Materials and Aerospace Engineering, Liverpool.

² University of Liverpool, Institute of Ageing and Chronic Disease, Department of Eye and Vision Science, Liverpool.
 rdsa@liverpool.ac.uk

Introduction

Blindness due to corneal ulcers represent 5% of all cases worldwide. ^{1,2} These ulcers are caused by a range of conditions from autoimmune diseases to infections such as fungal and bacterial keratitis. ³ Bacterial keratitis is often contracted through the improper use of contact lenses and treatment regimens often include broad spectrum antibiotic drops, and sometimes the application of a bandage lens to protect the wound. ⁴ This method of delivery of the drug however is not efficacious as less than 7% of the active agent reaches the site of injury due to the method of administration. Moreover, in recent years, there has been a drive to reduce the use of antibiotics owing to the growing epidemic of antimicrobial resistance.

Nitric oxide (NO) acts as an antimicrobial agent by interacting with simultaneously produced reactive oxygen species such as hydrogen peroxide (H₂O₂) and superoxide (O₂⁻) to generate reactive nitrogen species such as peroxyxynitrite (OONO⁻), S-nitrosothiols (RSNO), nitrogen dioxide (NO₂), dinitrogen trioxide (N₂O₃), and dinitrogen tetroxide (N₂O₄).^{5,6} It has been shown that these reactive intermediates target DNA, causing deamination, oxidative damage, strand breaks, and other DNA alterations.

Compounds containing the diazeniumdiolate [N(O)=NO]⁻ functional group have shown great potential in a variety of medical applications requiring the controlled and sustained release of NO ⁷ Described herein are environmentally friendly methods to develop NO donor contact lenses capable of releasing a controlled and sustained dose of NO to target biofilms on infected wounds.

Materials and methods

In this work poly-ε-lysine (pεK) is cross-linked with bis-carboxy fatty acids and functionalised with diazeniumdiolate to produce nitric oxide releasing contact lens gels with a high water content and excellent transparency. The chemical properties of the gels were determined using X-ray photoelectron spectroscopy, Fourier transform infrared spectroscopy and UV vis spectroscopy. The NO released was determined using a chemiluminescent NO detector. The antimicrobial efficacy of the gels against *S. aureus* and *P. aeruginosa* was determined after 4 and 24 hr incubation and an indirect cytotoxicity assay was carried out to determine if released NO negatively affected a human corneal epithelial cell line (HCE-T cells).

Results and discussion

NO release from the functionalised contact lens bandages was evaluated at varying pHs in three different solutions; buffer, cell culture media and nutrient broth. The gels demonstrated a burst release at pH 4, and a lower and more sustained release profile at physiological pH 's (pH 7). The antimicrobial efficacy of the contact lenses was observed as reduction colony forming units of *S. aureus* and *P. aeruginosa* using a bactericidal assay. A 3-4 log reduction in *S. aureus* and up to 1 log reduction with *P. aeruginosa* was observed after incubation with the NO releasing gels. The indirect cytotoxicity assay demonstrated that released NO did not negatively affect a human corneal epithelial cell line (HCE-T cells).

Conclusion

The fabrication and functionalisation of nitric oxide (NO) releasing contact lens gel bandages is reported. The contact lens gels exhibit excellent optical and mechanical properties and can release NO under physiological conditions. The gels displayed excellent antimicrobial activity against two of the most common pathogens associated with bacterial keratitis- *S. aureus* and *P. aeruginosa* and did not exhibit significant cytotoxicity against a human corneal epithelial cell line. These contact lens gels could be a promising alternative to current antibiotic eyedrop treatments, that are often inefficient and laborious. The use of NO would not contribute to the growing epidemic of antimicrobial resistance and as the delivery of the treatment is direct to the site of infection, less treatments would be required which would ultimately improve patient compliance.

References

1. Sengupta, S. *et al.* Ophthal. Epidemiol. 2012, 19, 297
2. Whitcher, J.P. *et al.* Bull. W.H.O., 2001, 79, 214
3. Weiner, G., Confronting corneal ulcers, www.aao.org/eyenet/article/confronting-corneal-ulcers?july-2012
4. Upadhyay, M.P., *et al.* Int. Ophthalmol. Clin. 2007, 47,17.
5. Weller, R.B., J Invest Dermatol. 2009, 129, 2335.
6. Wahl, C *et al.* Appl Microbiol Biotechnol. 2010, 88, 401.
7. Schoenfisch, M.H *et al.* Chem. Soc. Rev. 2012, 41, 3753.

Acknowledgements

The authors gratefully acknowledge the funding for this project which was provided by a Health Impact Partnership grant from the EPSRC (EP/P023223/1). The authors also thank SpheriTech Ltd (Runcorn, Cheshire, UK) for providing the PεK used in this work.

Non-woven mats of electroactive composites of silk-PEDOT:PSS for peripheral nerve regeneration

C. Phamornnak¹, J. Ma¹, J.G. Hardy*², J.J. Blaker*¹, S.H. Cartmell*¹

¹*School of Materials, University of Manchester, United Kingdom.* ²*Department of Chemistry and Materials Science Institute, Lancaster University, United Kingdom.*

INTRODUCTION: Peripheral nerve injury is a severe problem in traumas with over 1 million patients around the world [1]. Electrically conductive nerve tissue scaffolds are promising materials for the regeneration of fully functional nerves post trauma [2, 3]. Here, we describe the optimization of a protocol for electrospinning *Bombyx mori* silk fibroin (SF) integrated with poly(3,4-ethylenedioxythiophene) polystyrene sulfonate (PEDOT:PSS) to generate novel peripheral nerve tissue scaffolds as sub-micron fibre non-woven mats.

METHODS: Solutions of 10% w/v SF in formic acid (FA) and calcium chloride (CaCl₂) were electrospun under various conditions of electrical potentials (25, 30, and 35 kV), relative humidity (35% and 50% R.H.), and speeds of the rotating collector (3.14 and 4.96 m/s). The electrospun fibre mats were treated with ethanol and methanol to induce β -sheet formation in the silk (confirmed by FTIR). Additionally, the alignment and diameter of fibres were characterised by SEM. Next, the optimal material was functionalized with PEDOT:PSS via the interpenetrating polymer network (IPN) technique. Neuron-like cells (NG108-15) were cultured on the electrospun silk fibres for 7 days to test the biocompatibility of the non-woven mats. Prior to cell culture, the fibre mats were attached to glass cover slips and then subsequently coated with laminin. Initial cell seeding density was 5,000 cells/cm². Cell viability and DNA concentration were ascertained at 3, 5 and 7 days.

RESULTS: Electrospinning conditions of 35 kV, 35% R.H. yielded the most consistent fibres that were smooth and aligned. The average fibre diameter was 180 ± 60 nm using a solution flux of 0.4 mL/h and 4.96 m/s collection speed. The β -sheet content of the electrospun fibres is significantly increased by ethanol and methanol treatment compared to untreated fibres. The β -sheet content decreased

when the fibres were immersed in water. Cell viability and DNA concentration of NG108-15 cells cultured on SF fibres were observed to increase from day 3 through to day 7.

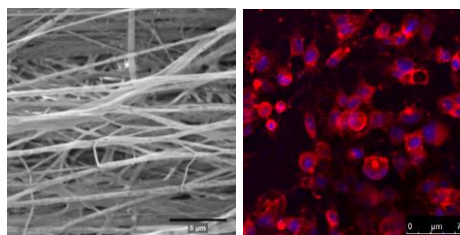


Fig. 1: Electrospun SF fibres (left) and NG108-15 on laminin coated SF with PEDOT:PSS fibre mats (right): nucleus – blue and cell membrane – red

DISCUSSION & CONCLUSIONS: Electrospinning SF in FA and CaCl₂ can provide nanofibres which have similar diameters to the neurites. These fibres can support cell proliferation. In case of PEDOT:PSS functionalized fibres, our initial results suggest that these electroactive fibres can also promote cell proliferation compared to the non-electroactive SF fibres. Current work involves optimizing the PEDOT:PSS phase within the SF as an IPN, and correlating this to cell morphology and neurite outgrowth.

ACKNOWLEDGEMENTS: The Royal Thai Government Scholarship and Adrián Magaz, Bio-Active Materials Group, School of Materials, The University of Manchester and A*STAR (A*STAR Research Attachment Program, Singapore)

REFERENCES:

- [1] Magaz et al. *Adv Healthc Mater.* 2018.
- [2] Balint et al. *Acta Biomaterialia.* 2014.
- [3] Zhou et al. *Biomaterials Science.* 2018

Peptide Gels of Fully-Defined Composition and Mechanics for Modelling Cell-Matrix Interactions in Breast Cancer

JC Ashworth^{1,2}, CE Slater¹, G Farnie^{2,3} & CLR Merry¹

¹Stem Cell Glycobiology Group, Division of Cancer & Stem Cells, University of Nottingham, UK; ²Manchester Cancer Research Centre, University of Manchester, UK; ³Botnar Research Centre, NDORMS, University of Oxford, UK

INTRODUCTION: Current materials used for *in vitro* 3D disease models are often limited by their poor similarity to human tissue, batch-to-batch variability and complexity of composition and manufacture. We have developed a “blank slate” culture environment based on a self-assembling peptide gel free from matrix motifs [1]. This gel can be customised by incorporating matrix components selected to match the target tissue, with independent control of mechanical properties. Here, we present optimisation of these peptide gels to support cell models of breast cancer progression.

METHODS: Peptide gels are initially synthesised as a matrix-free precursor, containing no organic components other than the octapeptide gelator FEFEFKFK. The gelator concentration may be tuned from 5-15 mg/mL, which controls the final peptide gel stiffness between ~500 Pa (normal breast) and ~5 kPa (breast tumour). Bespoke environments matching the target tissue are then created by physically mixing this precursor with cells and matrix components of interest, yielding a final peptide gel with user-defined stiffness, matrix composition and cellularity.

RESULTS: Our defined peptide gel system allows the separate influences of tissue composition and stiffness to be probed independently. As proof-of-concept, human mammary fibroblasts were cultured for 7 days in peptide gels with and without collagen I functionalisation. Whereas the matrix-free gels were inert to adherent cells, causing them to cluster rather than elongate, peptide gels containing collagen I additions allowed the fibroblasts to elongate and spread in 3D.

Peptide gel + collagen (x µg/ml)

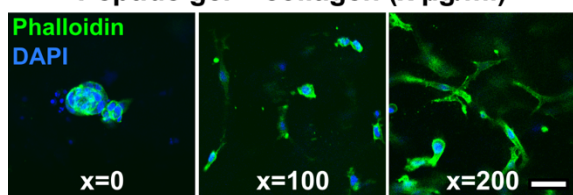


Fig. 1: Human mammary fibroblasts (HMF) cultured to day 7 in 6 mg/mL peptide gels with varying levels of collagen I functionalisation (scale bar 50 µm).

Doubling collagen concentration from 100 to 200 µg/mL also increased the extent of cell spreading, whilst maintaining a constant peptide gel stiffness on cell encapsulation. This approach demonstrates how simple functionalisation can alter the behaviour of encapsulated cells in response to their matrix environment.

Changes in the matrix in response to remodelling or organisation by encapsulated cells may also be examined. MCF10A mammary epithelial cells (normal breast) cultured for 14 days in a collagen-modified peptide gel grew into dense clusters, distorting the surrounding collagen and excluding it entirely from the cell cluster.

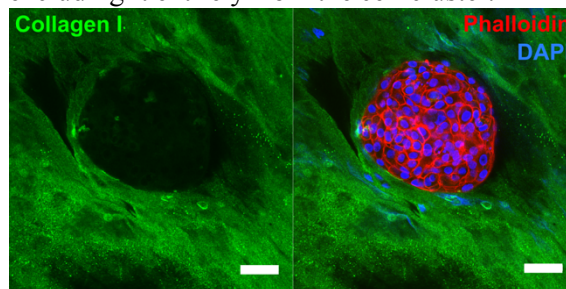


Fig. 2: MCF10A mammary epithelial cells cultured to day 14 in 10 mg/mL peptide gels with 200 µg/mL collagen I (scale bar 50 µm).

DISCUSSION & CONCLUSIONS: The self-assembling peptide gel presented here allows the independent control of two critical factors: matrix composition and bulk stiffness. Using this method we are developing bespoke models of the human breast, informed by proteomic analysis of human tissue. Multiple cell types, including epithelial, stromal and immune cell compartments, may also be incorporated into this system, allowing the role of extracellular regulation to be investigated in a multicellular, tissue-mimetic environment.

ACKNOWLEDGEMENTS: This research was funded by the National Centre for the Replacement, Refinement and Reduction of Animals in Research (NC3Rs) grant NC/N001583/1.

REFERENCES: 1. Ashworth *et al.*, Matrix Biology (Accepted for publication April 2019).

POROUS GLASS MICROSPHERES SHOW BIOCOMPATIBILITY, TISSUE INGROWTH AND OSTEOGENIC ONSET IN VIVO.

Jane McLaren^{1†}, Laura Macri-Pellizzeri^{2†}, Kazi Zakir Hossain³, Uresha Patel³, David Grant³, Brigitte Scammell^{1*}, Iffy Ahmed^{3*}, Virginie Sottile^{2,4*}

¹Academic Orthopaedics, Trauma and Sports Medicine, School of Medicine, University of Nottingham, UK

²Wolfson STEM Centre, Division of Cancer & Stem Cells, School of Medicine, University of Nottingham, UK

³Advanced Materials Research Group, Faculty of Engineering, University of Nottingham, UK

⁴Arthritis Research UK Pain Centre, University of Nottingham, Nottingham, UK

*Corresponding author: virginie.sottile@nottingham.ac.uk

Introduction: Phosphate-based glasses (PBG) are bioactive and fully degradable materials with tailorable degradation rates. PBGs can be produced as porous microspheres through a single-step process, using changes in their formulation and geometry to produce varying pore sizes and interconnectivity for use in a range of applications, including biomedical use. Calcium phosphate PBG have recently been proposed as orthobiologics, based on their *in vitro* cytocompatibility and ion release profile^{1,2}.

Materials and Methods: In this study, porous microspheres made of two PBG formulations, either containing TiO₂ (P40Ti) or without (P40), were implanted *in vivo* in a sheep model of bone defect. A cylindrical bone defect (8 mm width x 15 mm depth) was created in medial femoral condyles and microspheres were delivered to fill the defect site, with or without bone marrow concentrate. The biocompatibility and osteogenic potential of these porous materials were assessed 13 weeks post-implantation and compared to empty defects and to autologous bone grafts, used as negative and positive controls respectively.

Results and Discussion: Histological analysis showed marked differences between the two formulations, as lower trabeculae-like interconnection and higher fatty bone marrow content were observed in the faster degrading P40-implanted defects, whilst the slower degrading P40Ti material promoted dense interconnected tissue³. Autologous bone marrow concentrate (BMC) was also incorporated within the P40 and P40Ti microspheres in some defects, however no significant differences were observed in comparison to microspheres implanted alone. Both formulations induced the formation of a collagen-enriched matrix, from 20 % to 40 % for P40 and P40Ti2.5 groups, suggesting commitment towards the bone lineage. With the faster degrading P40 formulation, mineralisation of the tissue matrix was observed both with and without BMC. Some lymphocyte-like cells and foreign body multinucleated giant cells were observed with P40Ti2.5, suggesting this more durable formulation might be linked to an inflammatory response.

Conclusions: These first *in vivo* results indicate that PBG microspheres could be useful candidates for bone repair and regenerative medicine strategies, and highlight the role of material degradation in the process of tissue formation and maturation.

References: 1. Hossain KMZ *et al.* Acta Biomater. 72:396-406, 2018. 2. Patel U *et al.* J Tissue Eng Regen Med. 13(3):396-405, 2019. 3. McLaren *et al.* ACS Appl Mater Interfaces, 2019 (in press).

Acknowledgements: This work was supported by the Engineering and Physical Sciences Research Council [Grant Number EPSRC EP/K503800/1]. We are grateful for the expertise and invaluable support of M. Baker and D. Surgay (University of Nottingham), and to D. Storer for veterinary input.

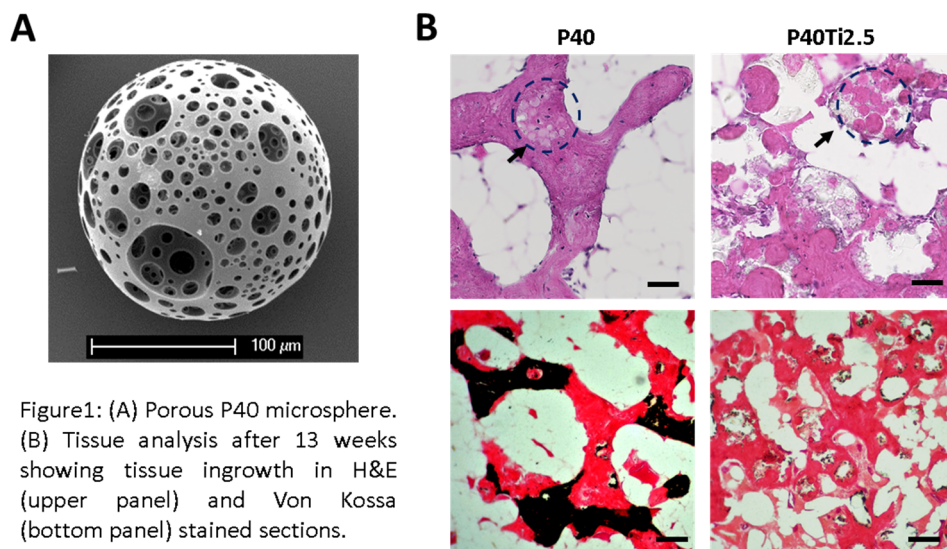


Figure1: (A) Porous P40 microsphere. (B) Tissue analysis after 13 weeks showing tissue ingrowth in H&E (upper panel) and Von Kossa (bottom panel) stained sections.

RAPID SCREENING OF INKS FOR 3D PRINTING PERSONALISED DRUG DELIVERY IMPLANTS

Laura Ruiz,¹ Vincenzo Taresco,² Zuoxin Zhou¹, Richard Hague¹, Clive Roberts³, Christopher Tuck¹, Morgan Alexander³, Derek Irvine¹ and Ricky Wildman^{1*}

¹Centre for Additive Manufacturing/University of Nottingham, ²Molecular Therapeutics and Formulation Division/ University of Nottingham, The Advance Materials and Healthcare Technologies Division/ University of Nottingham
Corresponding author: Ricky.Wildman@nottingham.ac.uk

Introduction

The technology of 3D printing (3DP) is rapidly gaining traction in multiple industrial sectors with some of the most exciting applications being within the pharmaceutical industry. However, the lack of materials able to be successfully 3D printed is constraining the wider adoption of 3DP into industrial processes and consequently stifling the proliferation of these new technologies. Future development pipelines would benefit immensely from a systematic, robust and rapid system for determining the utility of a material for 3DP pharmaceuticals and to establish that information into a materials library.

The aim of this study was to identify, assess and characterise in a rapid way candidate materials for inkjet 3D printing using high throughput (HT) methodologies. The primary goal is to create a library of bioerodible, biocompatible and photocurable materials for the pharmaceutical industry that could be used to 3D print personalised drug eluting implants for heart disease.

Materials and Methods

Polycaprolactone (PCL), poly (lactic acid) (PLA) and poly trimethylene carbonate (PTMC) macromers were synthesised with different methacrylate and acrylate end functionalities and then mixed with two different reactive solvents resulting in a total of 134 different formulations. Materials synthesis was evaluated with NMR. A base library of 18 formulations and a total of 134 combinations were screened using HT methods. The materials were screened for printability, phase separation, mechanical properties, in vitro weight loss, cytotoxicity and drug release. Phase separation and surface mechanical properties were tested in micro array format using ToF SIMS and AFM as described by Louzao et al at 2018. The printability of the materials was tested using an automated liquid handler. The 'hit' formulations were used to inkjet 3D print a dual subdermal implant containing the drugs trandolapril and pitavastatin. Drug release was determined with HPLC.

Results and Discussion

The printability results showed that all the base materials combined with NVP and PEGDA were printable at temperatures ranging from 40 °C – 70 °C with the exception of two of them mixed with PEGDA. The phase separation studies showed that PCL and TMC based materials present more phase separation than PLA based materials when mixed with the solvents. This behaviour could help to incorporate hydrophilic and hydrophobic drugs in the same implant avoiding interaction between them. These studies also demonstrated the different surface mechanical properties presented when mixing a non-functionalised material with a di-end functional material. The drug release studies showed that the trandolapril loaded implants were able to continuously deliver the drug for a period of four months.

Conclusions

A HT method for testing printability of materials in a rapid and fully automated way using small amounts of material was developed for the first time in this project. Additionally, by using this rapid screening method we created a library printable biodegradable materials with different degradation times, mechanical properties and drug release behaviour. Formulations were successfully printed and continuous drug release from dual drug implants has been demonstrated.

References

1. Louzao, I. *et al.* J. ACS Appl. Mater. Interfaces. 2: 5-11, 2018.

Reforming the Haversian network in a bone-on-chip

E. Budyn¹, B. Cinquin², M. Bensidhoum³, H. Portier³

¹ LMT CNR UMR 8535 Laboratory, ENS Paris-Saclay, Cachan, France, ² LBPA CNR UMR 8113 Laboratory, ENS Paris-Saclay, Cachan, France, ³ B2OA CNR UMR 7052 Laboratory, University Paris 7, Paris, France,

INTRODUCTION: Osteocytes orchestrate healthy bone homeostasis. They coordinate bone resorption by osteoclasts and bone formation initiated by mesenchymal stem cells (MSCs) that differentiate into osteoblasts laying collagen fibers and further differentiate into osteocytes mineralizing the collagen fibers. Osteocytes bear numerous processes to detect their mechanical environment. However quantification of human bone cells *in situ* 3D mechanical environment is challenging but essential to understand the effects of mechanical forces on the cell mechanobiology, differentiation and secretome quality.

METHODS: A bone-on-chip including one or multiple bone samples provides *in situ* 3D environment for human bone cells to grow, differentiate and form new bone. These systems also made it possible to track by microscopy the spatial reorganization of the bone samples by the contraction of the matrix formed by the cells. In a bone-on-chip, human MSCs were reseeded on decellularized human bones and cultured for a long period of time to obtain stem cell derived osteocytes (SCDOs) (up 26 months). The systems were mechanically stimulated in either 3-point bending or compression to mimic human walk or run. The cell mechanobiology was measured by simultaneously recording the cell calcium responses in the mechanically stimulated bone-on-chip and by modeling their 3D mechanical environment using image-based FEM (finite element method) at the cell and tissue scales in the same bone-on-chip. The MSCs differentiation marker secretion and morphological changes were tracked by *in situ* immuno-histology using confocal microscopy. The secretome proteomics and mechanical properties were measured *in situ* by immunofluorescence and mechanical tests.

RESULTS: The mechanobiology of bone stromal cells showed cytoplasmic calcium response adapts to the expected *in vivo* mechanical load at the successive differentiation stages. The cell morphology of

SCDOs exhibited long processes organized in a network at 19 months among multiple bone cells populations. The cell organized in layers of alternate orientation up to 45°. *In situ* immuno-fluorescence under confocal microscopy at 547 days revealed the presence of osteocytes markers such as E11 and sclerostin of which the amounts were correlated to exercise and local stresses. The neo-formed bone displayed a strength nearly a quarter of native bone strength at 109 days and contained calcium minerals at 39 days and type I collagen at 256 days. Three types of bone samples were prepared with respect to the orientation of the osteons. The cells assembled the bone samples in space in order to recreate an Haversian system in Fig. 1.

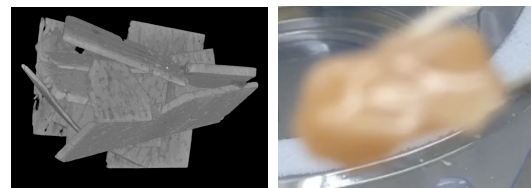


Fig. 1: SCDOs creating a 3D spatial assembly of bones with longitudinal osteons: micro CT (left) vs. full-field (right).

DISCUSSION & CONCLUSIONS: The bone-on-chip made it possible to grow SCDOs and study *in vitro* the effect of mechanical forces on human osteocytes on a physiologically relevant substrate. The observed spatial bone assembly created by the cells provides an insight on the role of cells ability to mechanically move bones in the early stages of repair of a bone defect or a fracture.

ACKNOWLEDGEMENTS: The authors are grateful to NSF CMMI BMMB 1214816 EAGER award, Ola, Bone Labs, Bonoclisflum, BoneOnTheMov awards from the Farman Institute, CG94 CNRS award.

REFERENCES: Budyn E, Gaci N, Sanders S et al. *MRS Advances*, vol. 3(36), p. 1443-1455, (2018) doi.org/10.1557/adv.2018.278.

ROLE OF SILICATE AND SILICATE-BIOACTIVE GLASSES IN BONE NODULE FORMATION

Azadeh Rezaei¹, Yutong Li¹, Sofia Petta¹, Kaveh Shakib¹, Gavin Jell¹

¹Division of Surgery, University College London.

Corresponding author: azadeh.rezaei.14@ucl.ac.uk

Introduction

Silicate-based bioactive glasses (SiBGs) have been reported to promote bone regeneration through the controlled release of ions such as calcium, phosphate and silicate¹. SiBGs have also exhibited improved bone forming capability compared to non-Si bioceramics², which is believed to be due to the biological activity of Si. Dissolution products from 45S5BG have been shown to activate bone-related genes *in vitro*³, whilst Si can promote angiogenesis, proliferation and collagen production⁴. Considering the invention of SiBGs was over 50 years ago and the commercial use of Si containing materials in dental and orthopaedic applications⁵, there is still relatively little known about the cellular mechanism of Si on bone formation or the effect of different concentrations of Si on bone formation. To address and investigate the role of Si and SiBGs in bone formation, we developed an *in vitro* bone nodule model and characterisation approach that included biological, biochemical, ultrastructure and microstructure quantitative techniques.

Materials and Methods

Calvarial osteoblasts were isolated from neonatal rats and seeded in α -MEM with 2 mM β -glycerophosphate, 10 nM dexamethasone, and 50 μ g/ml ascorbate. Cells were treated with Si (0.5, 1, 2 mM) or dissolution products from 45S5BG diluted to achieve similar levels as Si (referred as 0.5SiBG, 1SiBG, 2SiBG). Ion release profiles, metabolic activity, proliferation, VEGF expression and ALP activity of the cells were measured. Nodules were characterised using Alizarin Red staining, SEM and TEM. Raman spectroscopy and interferometry were also used for compositional profiling and quantitative dimensional measurements, respectively.

Results and Discussion

Osteoblasts cultured in all concentrations of Si and SiBGs were capable of forming bone, but a Si concentration-dependent response was observed (Fig1). Si 0.5mM increased the maximum nodule height ($P \leq 0.05$) compared to normoxia. Controlled release of ions and bone nodule formation within the biologically relevant range of SiBGs confirm the role of BG as an ion delivery system and the potential of these materials in tissue engineering applications. TEM showed mineralised nodules formed in all conditions (Fig2); however, nodules seemed to cover larger area in Si 0.5mM and 0.5SiBG compared to Si 2mM and 2SiBG (in accordance with interferometry measurements). A Si concentration-dependent effect on ALP production was observed. Si and SiBG exhibited increased VEGF production compared to control (normoxia) on day 1.

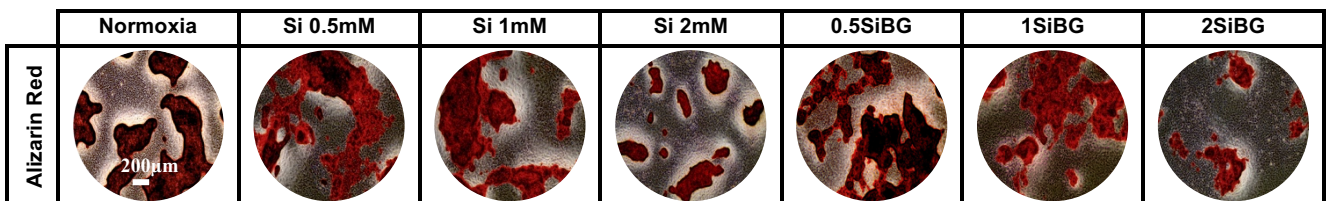


Figure1. Alizarin Red and SEM images of osteoblasts. Neither Si nor SiBGs did not inhibit nodule formation and showed nodules raised from the culture surface; however, a concentration-dependant effect was observed in both Si and SiBGs. 0.5SiBG exhibited denser nodules (dark red) compared to Si 0.5mM which might be due to the presence of other ions.

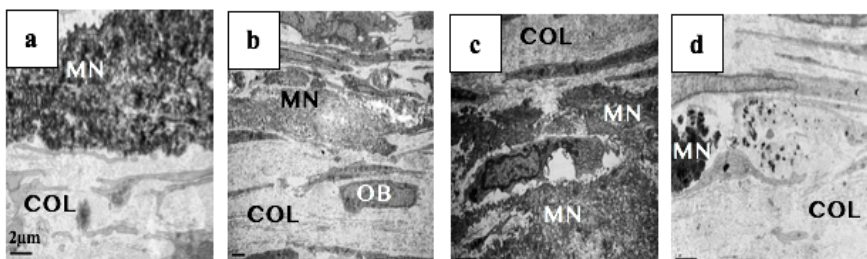


Figure2. TEM micrographs of a) Si 0.5, b) Si 2, c)0.5SiBG, d)2SiBG. Osteoblasts in all conditions were embedded within a fibrous ECM with collagen fibres. Si 0.5 and 0.5SiBG showed denser and larger nodules.

Conclusions

For the first time, we presented quantification and biochemical characterisation of bone nodules using different amounts of Si and Si containing BG conditioned media. This could allow us to use different therapeutic ion concentrations to target different stages of healthy bone regeneration.

References

1. Jones J.R. *et al.* J. Elements. 3(6):393-399, 2007.
2. Oonishi H., *et al.* J. Biomed Mater Res. 51(1):37-46, 2000.
3. Xynos I.D., *et al.* J. Biomed Mater Res. 55(2):151-157, 2001.
4. Shie M *et al.* J. Acta Biomater. 7(6):2604-2614, 2011.
5. Cerruti M. J. Rev Mineral Geochem. 64(1):283-313, 2006.

Self-Assembling structured Laponite Hydrogels with Spontaneous 3D Micropatterning of Bioactive Factors for Tissue Regeneration

R.S. Ramnarine¹, N. Evans¹, R. Oreffo¹, J. Dawson¹.

¹Bone & Joint Research Group, Centre for Human Development, Stem Cells & Regeneration, Institute of Developmental Sciences, University of Southampton, Southampton, SO16 6YD, United Kingdom.

INTRODUCTION: Mimicking the three dimensional (3D) hierarchical organization of physical and/or biochemical cues found in the native cellular microenvironment is likely to be key to building biomaterials with higher levels of functionality¹. Despite advances in Tissue Engineering (TE), true 3D patterning of biochemical cues has proved difficult². In this regard, clay nanoparticle gels offer potential in TE for their ability to sequester proteins for sustained localized bioactivity³. The current study reports a simple and biomimetic method for applying self-assembling clay hydrogels to achieve spontaneous 3D micropatterning of bioactive proteins under physiological conditions.

METHODS: Hydrous suspensions of smectite clay; Laponite, were added to a master solution containing defined concentrations of biomolecules and ions present in blood plasma to initiate the self-assembly of hydrogel scaffolds mediated by a diffusion-reaction process. The structures were analyzed using a range of microscopy techniques and tested for their ability to pattern model proteins (serum albumin, avidin, streptavidin, immunoglobulin G and casein) and localize the activity of bone morphogenetic protein *in vivo*.

RESULTS: the Laponite/protein hydrogels displayed an internal degree of order able to template concentration gradients of fluorescently labelled model proteins. Characterization of the structures using confocal microscopy demonstrated micron resolution control of 3D protein patterning which could be tuned with the assembly time and protein concentration. In contrast, non-structured gels assembled in saline, adsorbed model proteins on the gel surface³. Polarized light imaging revealed radial birefringence patterns indicating a nanoscale periodical arrangement. Scanning Electron Microscopy and rheological studies show rearrangement of nanoparticles upon interaction with proteins.

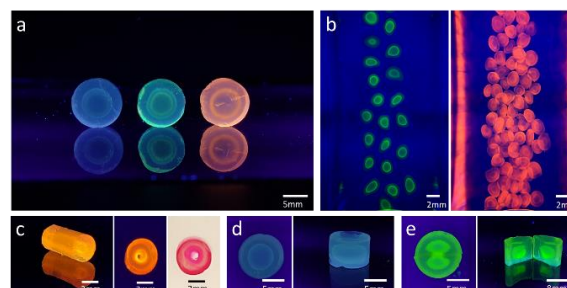


Figure 1: Self-assembled protein patterning in nanoclay colloidal hydrogels. Anisotropic concentration gradients stabilized in stiff colloidal hydrogels (>97% water) of various dimensions (tubes (a, c-e) and spheres (b) and incorporating various model proteins - FITC-streptavidin (a, left and d), FITC-BSA (b, left and e) and Rhoda-BSA (b, right and c).

Proof-of-concept murine subcutaneous implantation studies confirmed structured hydrogels could localize active BMP2 to induce ectopic bone formation *in vivo*.

DISCUSSION & CONCLUSIONS: This study reveals, for the first time, the opportunity to harness interactions between clay nanoparticles, biomolecules and ions present in physiological fluids to trigger the assembly of supramolecular structures of physical and biochemical cues. This bottom up approach affords new opportunities for 3D protein micropatterning and delivery of growth factors for tissue engineering of hard and soft tissues.

ACKNOWLEDGEMENTS: Funded by EPSRC (EP/L010259/1) and University of Southampton, Faculty of Medicine and Faculty of Engineering & Environment postgraduate awards to JI Dawson.

REFERENCES:

- [1] Chow LW et al. *Exp. Biol. Med.* 2015; 241: 1025-1032.
- [2] Wylie RG, et al. *Nat. Mater.* 2011; 10: 799-806.
- [3] Dawson JI, et al. *Adv. Mater.* 2013; 23: 3304-3308.

STIMULATIVE 3D CONDUCTING ARCHITECTURES TO MODULATE CELLULAR PHENOTYPE

Frankie J. Rawson^{1*}, Jayasheelan Vaithilingam^{‡2}, Paola Sanjuán-Alberte^{‡1,2}, Simona Campora^{3,4}, Graham A. Rance⁵, Long Jiang¹, Christopher J. Tuck², Ricky D. Wildman², Richard J.M. Hague², Morgan R. Alexander¹, Chris Denning⁶

¹ School of Pharmacy, University of Nottingham, Nottingham, NG7 2RD, UK.

² Centre for Additive Manufacturing, Faculty of Engineering, University of Nottingham, Nottingham, NG7 2RD, UK.

³ Scienze e Tecnologie Biologiche, Chimiche e Farmaceutiche (STEBICEF), University of Palermo, Viale delle scienze Ed. 16, 90128 Palermo, Italy.

⁴ ABIEL S.r.l., c/o Arca incubatore di Imprese, viale delle Scienze ed.16 90128 Palermo, Italy.

⁵ Nanoscale and Microscale Research Centre, University of Nottingham, Nottingham, NG7 2RD, UK

⁶ Department of Stem Cell Biology, Faculty of Medicine & Health Sciences, University of Nottingham, Nottingham, NG7 2RD, UK

Introduction

Biology carefully orchestrates the building of 3 dimensional (3D) architectures and physical-chemical cues which, include electrical, chemical, topographical and mechanical stimuli to carefully modulate cellular function. There is a pressing need for the development of new materials that will allow us to manufacture artificial structures that mimic these biological instructive characteristics. We address this challenge by development of a new conductive composite material compatible with two photon polymerisation (TPP) manufacturing.

Methods

A new biomaterial based on Pentaerythritol triacrylate (PETrA) was polymerised with MWCNTs forming conductive structures. This was printed using TPP and material properties and topography was characterised using impedance spectroscopy, Raman IR, AFM and SEM. Human pluripotent stem cell-derived cardiomyocytes (hPSC-CMs) were cultured on the new material and structures printed. These were tested for their ability to modulate phenotype by analysing aspect ratio, sarcomere length and contractile frequency via microscopy of the cells.

Results

The developed ink and printed composite structures were shown to be conductive and the MWCNTs were well dispersed. In addition to being biocompatible when 1% photo initiator was used. The hPSC-CMs were cultured on printed structures that had nano-groves printed, and electrical input was applied using AC at 2V at 30 KHz (Figure 1). Cells aligned in the groves. When different structures were tested in the presence and absence of electrical input, the presence and absence of MWCNTs in the composite material we could modulate the sarcomere length up to 2.2 μm . This is similar to mature adult cardiomyocytes.

Discussions and conclusions

The PETrA-MWCNT materials developed was noted to promote hiPSC-CMs maturation in serum free conditions. The biomimetic myofibril-like 3D architecture and the presence of MWCNTs further improved the maturation measured. The application of electromechanical stimulus, superseded the maturation achieved.

Study of the effects of microbubbles on bone formation using micro-CT

J.P. May¹, J. Zaib¹, S. Ferri¹, A. Polydorou¹, S.A. Lanham¹, J.M. Kanczler¹, R. Rumney², E. Stride³, D. Carugo¹, N.D. Evans¹

¹Human Development and Health, University of Southampton, Southampton; ²University of Portsmouth, Portsmouth; ³Institute of Biomedical Engineering, University of Oxford, Oxford.

INTRODUCTION: There are many reports in the literature on the effects of oxygen on the bone healing process, although the exact mechanisms by which this takes place are still a matter of debate.¹ Gas microbubbles (MBs) stabilised by a lipid shell can travel systemically throughout the body, providing an approach to transport bioactive gases or drugs. This study set out to determine the effects of oxygen microbubbles (O2MBs) on bone formation, relative to nitrogen microbubbles (N2MBs) and vehicle control.

METHODS: MBs were prepared containing either O₂ or N₂ gas and a range of lipid shell formulations (including: 1,2-dibehenoyl-sn-glycero-3-phosphocholine [DBPC], 1,2-distearoyl-sn-glycero-3-phosphoethanolamine-N-[methoxy (polyethyleneglycol)-2000] [DSPE-PEG], 1,2-distearoyl-sn-glycero-3-phosphocholine [DSPC], polyoxyethylene(40) stearate [PEG40s]). MBs were tested for their relative stability at 37°C. MB formulations with optimal stability profiles were then prepared aseptically, in both O₂ and N₂ gas forms, for use in vitro and in vivo. These MBs were studied for their effects on cells in vitro, with a particular emphasis on the bone remodelling processes (osteoclast and osteoblast activity). MBs were subsequently studied using in vivo murine models, to assess the relative effects from O2MBs and N2MBs compared to a control cohort. Mice were injected twice weekly with O2MBs, N2MBs or control formulations and effects on the mouse skeleton were observed using micro-CT (35 µm). Bone structure was studied in more detail post-termination using high resolution CT scans (9 µm) and histology. All formulations were analysed for potential signs of toxicity via body weight measurements, histology and serology.

RESULTS: From the lipid combinations studied, a DBPC/DSPE-PEG (9:1) MB formulation (diameter range: 1-5 µm) was demonstrated to be the most suitable for further

study, based on the relative stability of the MBs formed (for >2 h in PBS/FBS at 37°C). Human bone marrow stromal cells (HBMSCs, STRO-1 +ve) exposed to increasing doses of O2MBs displayed increased osteogenic differentiation in both basal and osteogenic media (alkaline phosphatase assay). In vivo, all mice showed good tolerance to multiple doses of the MB formulations over the study period (increased body weight, no signs of toxicity observed with histology/serology). However, there were no demonstrable changes in skeletal structure during the course of the study (*Fig. 1*, 35 µm µCT scans), or after detailed analysis of the tibia and femur at high resolution (9 µm).

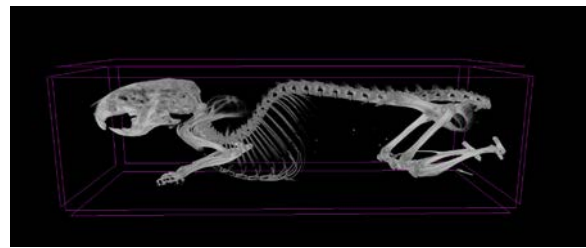


Fig. 1: Mouse skeleton microCT image taken 4 weeks into the study.

DISCUSSION & CONCLUSIONS: A relatively stable MB formulation was prepared, suitable for carrying O₂ and N₂ gases. O2MBs were shown to stimulate osteoblastic differentiation in vitro. However, in a murine model, O2MBs did not appear to stimulate bone formation over and above that observed for N2MBs or vehicle control formulations. Possible reasons for this disconnection between in vitro and in vivo data will be discussed.

ACKNOWLEDGEMENTS: Gratefully supported by an EPSRC grant (EP/R013624/1).

REFERENCES:

- Lu et al *Bone* **2013**, *52*, 220-229; Hirao et al *J Bone Miner Metab* **2007**, *25*, 266-276; Tuncay et al *Am J Orthod Dentofac Orthop* **1994**, *105*, 457-463; McCauley et al *Bone* **1989**, *10*, 29-34.

The Potential of Pressurised Gyration to fabricate Polyhydroxyalkanoate Aligned fibre Scaffolds for Peripheral Nerve Repair

C. S Taylor¹, M Behbehani¹, P. Basnett², B. Lukaszewicz², U. Illangakoon³, S. Mahalingam³, M. Edirisinghe³, I. Roy² and J.W. Haycock¹

¹Department Materials Science & Engineering, University of Sheffield, UK

²Applied Biotechnology Research Group, School of Life Sciences, University of Westminster, London, UK

³Department of Mechanical Engineering, University College London, UK

INTRODUCTION: 2.8% of all trauma patients will occur a Peripheral Nerve Injury (PNI). Current hollow Nerve Guide Conduits (NGCs) are still not comparable with autografts. The addition of guidance scaffolds, such as polymer fibres to NGCs, has been shown to increase nerve regeneration distances¹. Pressurised gyration is a relatively new technique to fabricate fibrous scaffolds for tissue engineering purposes. Polyhydroxyalkanoates (PHAs) are used widely in many tissue engineering applications. PHAs are biocompatible, biodegradable and can be tailored to a specific application.

METHODS: PHAs were produced by bacterial fermentation and characterised as per the methods by Basnett *et al*². Purified PHA was used to generate aligned fibres by pressurized gyration³. Fibres were quantified by scanning electron microscope. NG108-15 neuronal cells, and rat primary Schwann cells were cultured on PHA fibres for 6 days. Chick Dorsal Root Ganglion (DRG) bodies were extracted and explanted whole on to the ends of a 3D *in vitro* fibre testing method⁴. Chick DRGs and NG108-15 neuronal cells were labelled for β III tubulin, and primary Schwann cells labelled using S100 β .

RESULTS: PHA gyrate fibres supported NG108-15 neuronal and primary Schwann cell adhesion and growth. The longest average neurite lengths were detected on blended fibres ($83.90 \pm 20.35\mu\text{m}$), followed by P(3HB) fibres ($76.89 \pm 19.80\mu\text{m}$). Primary Schwann cell phenotype was maintained on both fibre blends. When investigated using a novel 3D *ex vivo* model, average neurite outgrowth length was measured as 0.59 ± 0.16 mm and 0.49 ± 0.19 mm on P(3HB) and P(3HB)/P(3HO-co-3HD) 80:20 blend fibres, respectively. Maximum

neurite lengths of 1.39 ± 0.41 mm were detected on P(3HB) fibres.

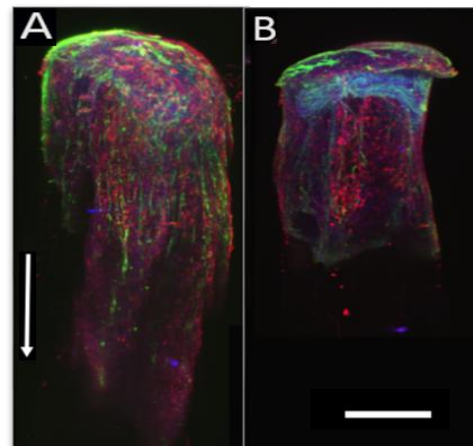


Figure 1. PEG tubes containing gyrate A) P(3HB) fibres and B) PHA blend fibres were evaluated using a 3D chick dorsal root ganglion model by light sheet microscopy (scale bar = 0.5mm)

DISCUSSION & CONCLUSIONS: PHAs are a very promising material for fabricating intraluminal fibre scaffolds to aid and improve nerve regeneration. An increasing need exists for scalable fabrication methods for nerve regeneration. Significant potential exists for pressurised gyration as a method to fabricate aligned fibres.

ACKNOWLEDGEMENTS: We acknowledge the University of Sheffield for funding. Also, The University of Westminster and University College London for their contributions.

REFERENCES:

1. Bell J et al. Tissue Eng Part B Rev. 18: 116-128, 2012.
2. Basnett et al. Microbial Biotechnology 10(12), 2017.
3. Basnett P et al. Front. Bioeng. Biotechnol. Conference Abstract: 10th World Biomaterials Congress. 2016.
4. Behbehani et al. Int J Bioprint, 4(1):123, 2018.

Utilising a Novel Photoresponsive Hydrogel with Defined Surface Topography and Photoswitchable Stiffness to Analyse the Biophysical Regulation of Mesenchymal Stem Cells

D. Richards¹, J. Swift², LS. Wong³, SM. Richardson¹

¹*Division of Cell Matrix Biology and Regenerative Medicine*, ²*Wellcome Trust Centre for Cell Matrix Research*, ³*Manchester Institute of Biotechnology, University of Manchester, UK*

INTRODUCTION: Mesenchymal stem cell (MSC) morphology responds to hydrogel stiffness and topography both in isolation and combination.¹ However, in addition to static hydrogel stiffness, MSC morphology also responds to in situ stiffness modulation.² We previously reported the development of a photoresponsive hydrogel with photoswitchable stiffness and demonstrated its potential for studying the dynamic response of MSCs to extracellular stiffening.² Here we demonstrate that by modulating the fabrication of this novel photoresponsive hydrogel we were able to probe the morphological response of both primary human bone-marrow derived MSCs and the immortalized, mechanoresponsive Y201 MSC cell line to extracellular stiffening in the presence of a defined surface topography. Understanding the combined regulatory effects of multiple static and dynamic material stimuli will improve the regulation of MSCs for tissue engineering and regenerative medicine.^{1,3}

METHODS: Fibronectin coated hydrogels were prepared with defined surface topography and softened via exposure to 30 mins UV light. Hydrogels were seeded with either primary MSCs or Y201s and cultured for 24 hours before being exposed to 60 minutes blue light irradiation, to stimulate hydrogel stiffening, and cultured for a further 24 hours. Samples were fixed and stained with DAPI and phalloidin before being imaged and subjected to quantitative morphometric analysis using CellProfilerTM software. Hydrogel topography on both softened and subsequently stiffened samples was characterised via bright-field, fluorescence (following fibronectin staining) and atomic force microscopy.

RESULTS: Hydrogel topography is composed of microscale surface creases which remained constant during irradiation and stiffness modulation, with no significant change in crease width and depth, surface area ratio, or

branch number, length, and angle. Both primary MSCs and Y201s showed a significant and conserved morphological response to hydrogel stiffening. Primary MSCs whole cell and nuclear area increased by ~33% and ~20% respectively, while cell circularity decreased by ~12%. Y201 whole cell and nuclear area increased by ~34% and ~22% respectively, while cell circularity, roundness, and nuclear aspect ratio decreased by ~18%, ~4%, and ~5% respectively.

DISCUSSION & CONCLUSIONS: These data demonstrate that hydrogel topography is composed of microscale surface creases which remain unchanged throughout irradiation and stiffening. Furthermore, both primary MSCs and Y201s show a conserved morphological response to extracellular stiffening, even in the presence of a defined surface topography, in particular highlighting the conserved mechanosensitivity of the nucleus and further indicating a mechanosensitive link between the cell and nucleus, supporting the existing literature. We now aim to study the effect modifying surface topography has on this morphological response to stiffening, and utilise the Y201 line to perform time-resolved analysis via live-cell time-lapse fluorescence microscopy.

ACKNOWLEDGEMENTS: D Richards is supported by an EPSRC & MRC funded CDT in Regenerative Medicine studentship (EP/L014904/1). The Bioimaging Facility microscopes used in this study were purchased with grants from BBSRC, Wellcome, Walgreen Boots Alliance and the University of Manchester Strategic Fund. Special thanks go to Dr Nigel Hodson (BioAFM Facility).

REFERENCES: 1. Donnelly et al (2018) *J. R. Soc. Interface*. 15:20180388. 2. Lee et al (2018) *ACS Appl Mater Interfaces* 10:7765–7776. 3. Akhmanova et al (2015) *Stem. Cells. Int.* 167025.

Validation and assessment of an antibiotic decontamination manufacturing protocol for vacuum-dried human amniotic membrane

ER. Britchford^{1,3}, NM. Marsit¹, LE. Sidney¹, OD. McIntosh¹, C. Allen¹, W. Ashraf², R. Bayston², and A. Hopkinson^{1,3}

¹ Academic Ophthalmology, Division of Clinical Neuroscience, School of Medicine, University of Nottingham, Nottingham, UK; ² Biomaterials Related Infection Group, Academic Orthopaedics, School of Medicine, University of Nottingham, Nottingham, UK; ³ NuVision Biotherapies, MediCity, Nottingham, UK

INTRODUCTION: Amniotic membrane (amnion) is used to treat a range of ocular surface and wound care situations, but must be presented in a non-contaminated state. AM from elective caesarean (C-) sections contains natural microbial bioburden, requiring decontamination during clinical processing. In this study, we assess the ability of antibiotic decontamination of amnion, during processing by innovative low-temperature vacuum-drying, used to produce the commercial product Omnigen® (NuVision Biotherapies, UK).

METHODS: Bioburden of 10 fresh amnion obtained by C-section was assessed using *in vitro* microbial culture. Subsequently, the processing steps used to produce low temperature vacuum-dried AM (VDAM), was assessed for decontamination ability. Five isolated amnions were artificially loaded (10^6 CFU/mL) with *Staphylococcus epidermidis* at three different stages of processing; i) before the full manufacture processing; ii) prior to antibiotic treatment; and iii) immediately before drying, and resulting products assessed by microbial cultures. The long-term stability and antimicrobial activity of 10 different antibiotic treated amnions was assessed after 2-3 year storage; antibacterial activity of non-antibiotic treated amnion compared to VDAM was evaluated using minimum inhibitory / biocidal concentrations (MIC/MBC), and disc diffusion assays against methicillin-resistant *Staphylococcus aureus*, methicillin-resistant *Staphylococcus epidermidis*, *Escherichia coli*, *Pseudomonas aeruginosa* and *Enterococcus faecalis*.

RESULTS: Bioburden of fresh C-section amnion was found to be very low. The amnion processing protocol (Tereo® process at NuVision) was highly efficient at removing bioburden introduced at any stage of processing. The combined process was comparable to a sterilising process. Amnion not treated with

antibiotics was shown not to be antimicrobial. However, VDAM with antibiotic demonstrated effective antibacterial capacity against all bacteria tested. Antimicrobial activity of VDAM was not reduced after 2-year storage.

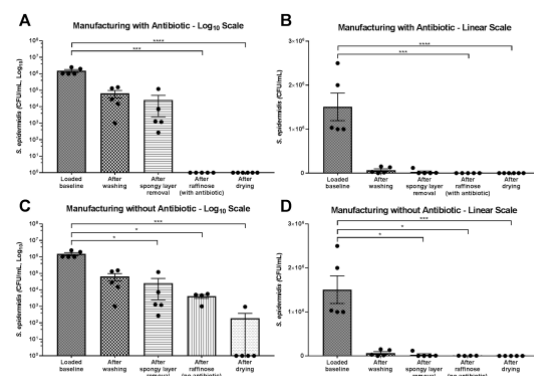


Figure 2: Effect of VDAM processing on reduction of artificially loaded *Staphylococcus epidermidis* bacterial counts.

DISCUSSION & CONCLUSIONS: Antibiotic decontamination is a reliable method for sterilisation of amnions and the resultant antibiotic reservoir is effective against *gram*-positive and -negative bacteria. The research suggests, amnion products manufactured without the use of antibiotics possess little antimicrobial activity. However, VDAM (Omnigen) may be useful in the treatment of ocular surface conditions where infection is a risk.

ACKNOWLEDGEMENTS: This study was funded by The Authority for Research, Science and Technology of the Ministry of Higher Education and Scientific Research-Libya (Scholarship 404/2013), an Innovate UK Biomedical Catalyst Feasibility Award (132044) and the Defense Science & Technology Laboratory, UK.

TURBOTALK + POSTER

3D culture of epidermis by use of recombinant silk materials containing FGF-7 protein microcrystals

R. Maruta¹, K. Takaki¹, E. Kotani¹, C. Pernstich², M. Jones², H. Mori¹

¹Kyoto Institute of Technology, ²Cell Guidance Systems

INTRODUCTION: The epidermis is composed of differentiated keratinocytes, resulting in four epidermal layers: stratum basale, stratum spinosum, stratum granulosum, and stratum corneum (Fig. 1). The epidermal layer is made up of cells generated by proliferating keratinocytes of the stratum basale that move upwards while they differentiate. The protein microcrystals called polyhedra derived from an insect virus (cytovirus) can be used for encapsulation of cargo proteins and the sustained slow release. We call this strategy **POlyhedra Delivery Systems (PODS®)**. We have previously reported that fibroblast growth factor-7 (FGF-7) PODS® crystals induced proliferation of keratinocytes [1]. To construct 3D culture of keratinocytes, we have developed a new culture method by using silk materials containing PODS® FGF-7 crystals. In the silk gland (SG) of a transgenic silkworm, *Bombyx mori*, PODS® FGF-7 crystals are produced. It is known that SG has a high potential for protein biosynthesis and can be used as cell culture matrix.

In this study, we examined the construction of epidermis consisting of stratum basale, stratum spinosum, stratum granulosum, and stratum corneum by use of SG containing PODS® FGF-7 crystals.

METHODS: Transgenic silkworm expressing PODS® FGF-7 crystals in SG was generated by PiggyBac Transposon Vector System. The production of FGF-7 PODS® crystals was confirmed by western blotting and immunostaining. The SG containing PODS® FGF-7 crystals was freeze-dried and crushed into fine silk gland powders (SGP). The bioactivity of SGP incorporating PODS® FGF-7 crystals was examined by WST-8 assay. For 3D culture, SGP was mixed in collagen type I-A and keratinocytes were seeded on the collagen gel. Keratinocytes were submerged in culture medium for 2 days. Then the composite cultures were raised to the air-liquid interface for 14 days. Each differentiation marker of the four layers was detected in the 3D culture with SGP by immunostaining (Fig. 1).

RESULTS: Western blotting and immunostaining revealed that SG of transgenic silkworm contained PODS® FGF-7 crystals. Moreover, it was confirmed that SGP incorporating PODS® FGF-7 crystals induced cell proliferation of keratinocytes in a dose dependent manner. Lastly, induction of a reconstruction of four layers of epidermis was observed and expression of each differential marker was confirmed immunostaining with antibodies against Keratin14, Keratin10, Filaggrin and Loricrin (Fig. 2).

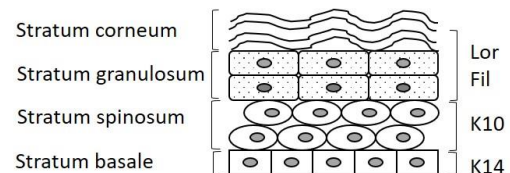


Fig. 1: Diagram of human skin showing differentiated keratinocytes of the epidermis and expression of stratification markers Keratin 10 (K10), Keratin 14 (K14), Filaggrin (Fil) and Loricrin (Lor).

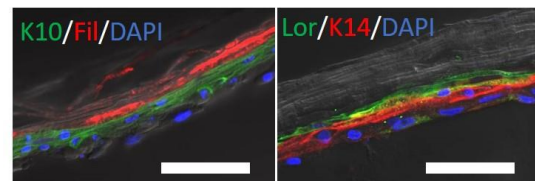


Fig. 2: HE stain in 3D cultures of keratinocytes. Scar bar = 50 μ m

DISCUSSION & CONCLUSIONS: The new silk materials incorporating PODS® FGF-7 crystals were useful for the assembly of a 3D model of epidermis. SGP contained free FGF-7 as well as FGF-7 encapsulated in PODS® crystals, from which FGF-7 was sustainably released over time, resulting in the differentiation of keratinocytes into a 3D culture of epidermis.

ACKNOWLEDGEMENTS: This work was supported by Japan society for the promotion of science.

REFERENCES: [1] Ijiri, H et al, Biomaterials 30 (2009) 4297–4308.

Acoustically-stimulated drug carriers for bone fracture repair

A.E. Polydorou¹, J. P. May², S. Ferri², Q. Wu³, E. Stride³, D. Carugo¹, N.D. Evans^{1,2}

¹Bioengineering Science Research Group, Faculty of Engineering and Physical Sciences, University of Southampton, UK; ²Human Development and Health, Southampton General Hospital, UK; ³Institute of Biomedical Engineering, University of Oxford, UK

INTRODUCTION: Impaired fracture healing is a major financial burden for healthcare services, and has a significant physical and mental impact on patients. Progress of the development of therapeutic agents has been limited by pharmacokinetic issues and costs. The aim of this study is to overcome these limitations by developing a targeted drug delivery system using acoustically-stimulated microbubbles (MBs) [1] and nanodroplets (NDs) [2]. The combination of ultrasound (US) and MBs enhances the delivery, release and uptake of drugs by cells. Therefore, in this study, we tested the hypothesis that MB and ND preparations are non-toxic, promote osteoblastic differentiation and induce mechanostimulation of human bone marrow stromal cells (BMSCs).

METHODS: A 9:1 molar ratio of 1,2-distearoyl-sn-glycero-3-phosphocholine (DSPC) to polyoxyethylene(40) stearate (PEG40S), hydrated in PBS, was sonicated to form a MB suspension. NDs were formed in a similar way using PFP for the core as opposed to room air. Cytotoxicity was tested on MG63 osteocarcinoma cells for up to 72 hours, using an Alamar Blue® assay, as an indicator of cell viability. Each shell constituent was also tested to determine cytotoxic effects individually. The effect of MBs on osteogenic differentiation of BMSCs, was also investigated using room-air filled MBs in a 14 day culture. Osteoblastic differentiation was tested using alkaline phosphatase (ALP) and gene expression studies. An acoustofluidic device was employed to test the effect of US-induced shear stress by measuring the expression of downstream targets of the YAP/TAZ mechanotransduction pathway – *ANKRD* and *CTGF*.

RESULTS: A dose-dependent effect was observed with 72 hours exposure; metabolic activity decreased with increasing MB concentration which was only significant at 0.5 dilution ($63\% \pm 6\%$, $p < 0.0001$). The cytotoxic effects were attributed to PEG40s as metabolic activity was reduced to $2\% \pm 7\%$ at 0.5 dilution

with 72 hours exposure. Up to 24 hours, neither MBs nor NDs had any cytotoxic effects. MBs in the presence of osteoinductive factors induced the expression of osteoinductive markers (*Runx2*) and US-induced shear stress for 1 hour, was not sufficient to rescue mechanostimulation in levitating BMSCs.

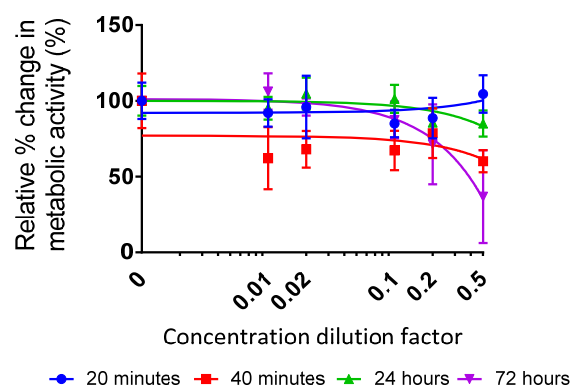


Fig. 1: MBs are non-cytotoxic to MG63 cells, with exposure up to 24 hours. When applied for up to 72 hours, significant reductions in cell metabolic activity were observed.

DISCUSSION & CONCLUSIONS: Based on the *in-vitro* effects observed on MG63 cells, DSPC:PEG40s MBs and NDs are a safe drug delivery method. No cytotoxicity was observed up to 3×10^7 MBs/ml at clinically relevant time frames. The effect of MBs on osteoblastic differentiation will be further assessed by gene expression studies and further tests with longer exposure to US will be carried out.

ACKNOWLEDGEMENTS: We are grateful to EPSRC (EP/R013624/1), the MRC, and the IfLS, Southampton, for funding.

REFERENCES: [1] Sirsi SR and Borden MA. *Advanced Drug Delivery Reviews*. 2014; 72: 3-14. [2] Sheeran PS et al. *Langmuir*. 2011; 27(17): 10412-10420.

Auxetic and Composite Scaffolds Show Potential for use in Tissue Engineering

P Mardling¹, N Jordan-Mahy¹, A Alderson², C Sammon², P Godbole³, CL Le Maitre¹

¹ The Biomolecular Sciences Research Centre, Sheffield Hallam University, ² Materials and Engineering Research Institute, Sheffield Hallam University, ³ Sheffield Children's Hospital and Pioneer Healthcare, UK.

INTRODUCTION: Tissue engineering scaffolds for regenerative medicine have to withstand a variety of loading conditions, as well as support and stimulate cell growth. A number of biological tissues display auxetic properties where upon stretching they become thicker which corresponds with a negative Poisson's ratio. A porous auxetic scaffold has the potential to mimic the properties of natural tissue which would enable a more natural environment to support cells for eventual use in tissue engineering. Here we investigate the mechanical properties of fabricated auxetic and composite scaffolds (polyurethane and pNIPAM-Laponite® (1C10) hydrogel), and biological tissue using 3D digital image correlation (DIC) to determine the suitability of these scaffolds for use as tissue engineering scaffolds.

METHODS: Auxetic scaffolds were manufactured from polyurethane foam using a previously developed thermomechanical technique. Duplicate scaffolds were filled with pNIPAM-Laponite® hydrogel (1C10). The auxetic properties of the scaffolds were assessed by uniaxial tensile testing on an Instron 3367 and 3D DIC (LaVision Strainmaster) was carried out simultaneously. Biological tissue samples were also tested for comparison. Smooth muscle cells were suspended in pNIPAM-Laponite hydrogel (1C10) (HG) at 4×10^6 cells/ml at 37°C. The hydrogel was absorbed into the scaffold and set by lowering the temperature below 32°C. Scaffolds were cultured in low adhesion plates under standard conditions for up to 6 weeks before histological analysis.

RESULTS: Polyurethane foams were successfully converted to gain auxetic

properties demonstrated by the gaining of a negative Poisson's ratio when compared to the unconverted control. Converted scaffolds containing HG were not auxetic but when compared to the biological tissue sample showed comparable strain distributions. Histology demonstrated the hydrogel was incorporated into the pores of the scaffold. SMCs were suspended, supported by the hydrogel within the pores of the composite scaffold for a period of 6 weeks.

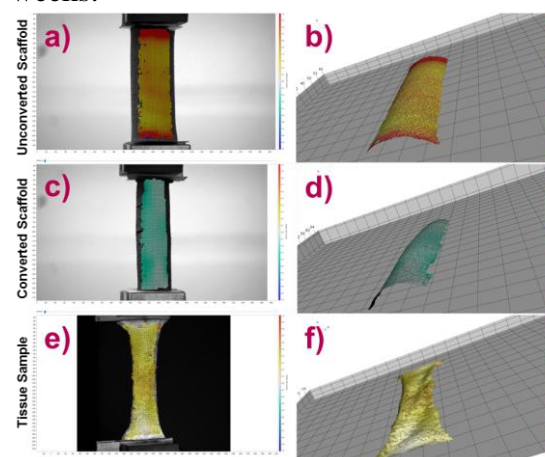


Fig. 1: Digital Image Correlation Images, a,c,e) 2D view contour plot showing Poisson's ratio values at an axial load of 0.1, b,d,f) 3D contour plots of samples showing topology and Poisson's ratio values and distribution across the samples.

DISCUSSION & CONCLUSIONS: 3D DIC has shown that the composite scaffold maintains a similar strain distribution and strain values to that of the biological sample. Therefore this scaffold could recapitulate the natural physical environment of cells from this tissue when under load.

ACKNOWLEDGEMENTS: This work was supported by a grant from Sheffield Hallam University, Pioneer Healthcare and Sheffield Children's NHS Foundation Trust,

Title: Bacterial engineering for the ex-vivo expansion of HSCs

Michaela Petaroudi¹, Aleixandre Rodrigo-Navarro¹, Ewan Ross¹, Matthew Dalby¹, Manuel Salmeron-Sanchez¹

¹Centre for the Cellular Microenvironment, University of Glasgow

Corresponding author: Michaela Petaroudi, 2346155p@student.gla.ac.uk, PhD student – 2nd year

Introduction

Hematopoietic stem cells (HSCs) constitute a rare cellular population residing in the bone marrow (BM) and have recently gained traction in research due to their significant clinical potential. These multipotent, self-renewing cells have the unique capacity to regenerate the whole hematopoietic system in the event of haematological disorders. This particular property has placed HSCs in the spotlight of experimental haematology, making *ex-vivo* HSC expansion a significant challenge for the research community. This unmet challenge would produce clinically relevant numbers from a small sample of cells that could be used for BM transplantation, somatic cell gene therapy as well as differentiation into mature blood cell types.

The complexity of the BM and the variety of signals that support HSC stemness and self-renewal have proven a limiting factor in current approaches to HSC expansion methods. We propose a system focused on engineering a dynamic microenvironment that will provide the signals that HSCs experience in their natural niche, combined with the structural characteristics of the BM. Our approach includes the use of non-pathogenic, genetically-engineered bacterial biofilms (*Lactococcus lactis*), producing key factors (CXCL12, TPO, VCAM-1, FN) that contribute to HSC phenotype maintenance and proliferation. Additionally, the use of hydrogels will mimic the BM architecture. Finally, we aim to incorporate mesenchymal stem cells (MSCs) into the system, to provide a closer representation of the BM.

Materials and Methods

Recombinant proteins (CXCL12, TPO, VCAM1, FN) were cloned in the pT2NX plasmid and the constructs were transformed in *L. lactis* using electroporation. For the CD34+ cell experiments, HSCs were seeded on top of *L. lactis* biofilms developed on Sigmacote-coated coverslips at a density of 50,000 cells/ml. After 5 days of incubation at 37°C, 5% CO₂, the HSCs were collected and phenotyped in a flow cytometer. In parallel, the effect of the biofilms on BM-MSCs were tested. Briefly, cells were seeded at 10,000 cells/cm² and incubated at 37°C, 5% CO₂. MSC spreading and adhesion was evaluated using immunofluorescence and their phenotype was assessed using In Cell Western analysis.

Results and Discussion

We have characterised both protein production and the effect of the cytokines to MSCs and HSCs. Neither cell type seems affected by the presence of bacteria. Furthermore, our results suggest that our system supports HSC phenotype maintenance and can achieve up to 19-fold HSC expansion in 2D experiments. Analysis of the interaction between MSCs and the biofilms has also shown that the MSCs exhibit a niche-like phenotype and could potentially produce more HSC self-renewal factors.

Conclusion

Our data suggests that our system has a promising potential to closely mimic the native BM microenvironment and induce *ex-vivo* HSC expansion.

Bisphosphonate toxicity to the oral mucosa is inhibited *in vitro* by hydroxyapatite granules

G Bullock¹, CA Miller¹, A McKechnie³, V Hearnden²

¹*School of Clinical Dentistry, University of Sheffield, UK.*

²*Kroto Research Institute, Materials Science and Engineering, University of Sheffield, UK.*

³*Faculty of Medicine and Health, University of Leeds, UK.*

INTRODUCTION: Bisphosphonate-related osteonecrosis of the jaw (BRONJ) is a disease found in patients taking bisphosphonates (BPs), a group of drugs used to treat osteoporosis and bone metastases. BRONJ often follows dental surgery, and presents as necrotic sections of the jaw where the overlying soft tissue fails to heal. BPs have a well known binding affinity for calcium, and have previously been demonstrated to bind to calcium phosphate based materials [1]. This study aimed to investigate the potential of hydroxyapatite (HA) to bind BPs and reduce soft tissue toxicity.

METHODS: Pamidronic acid (PA) and zoledronic acid (ZA), two BPs most commonly associated with BRONJ, were used. HA granules or discs were incubated in BP-containing medium for 72 hours. Human oral fibroblasts and keratinocytes were then treated with this medium, and cell viability assessed over 72 hours. BP-containing medium incubated without HA was used as a control. Fibroblasts and keratinocytes were also cultured onto de-cellularised dermis as a 3D oral mucosa model [2], before lifting to air liquid interface and culturing for 7 days to allow epithelial stratification. Models were then treated with control medium or ZA for 7 days, either with or without HA present. Resazurin assays were used to assess the cell viability of the oral mucosa models, with histology used to assess epithelial health.

RESULTS: Both PA and ZA were toxic to fibroblasts and keratinocytes over 72 hours. ZA was toxic to oral mucosa models over 7 days. HA granules inhibited toxicity in both 2D and 3D, while discs had no demonstrable effect. Tissue comparable to native oral mucosa was cultured, with histology showing a stratified squamous epithelium (Fig. 1A). ZA treatment removed this epithelium (Fig. 1B), HA discs had no effect (Fig. 1C), whilst HA granules inhibited this effect (Fig. 1D).

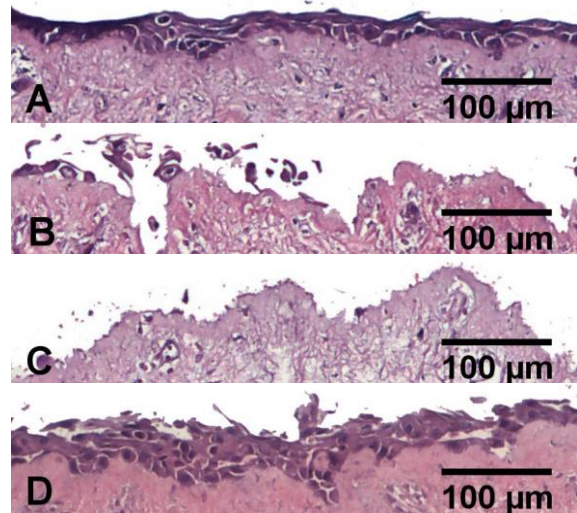


Fig. 1: Haematoxylin and eosin stained sections of oral mucosa model cultured at ALI for 7 days then treated with (A) control medium, (B) 30 μ M zoledronic acid, (C) 30 μ M zoledronic acid in the presence of an HA disc or (D) 30 μ M zoledronic acid in the presence of HA granules, for a further 7 days.

DISCUSSION & CONCLUSIONS: We have demonstrated that HA granules can be used to prevent toxicity to the oral mucosa *in vitro*. Our results indicate a method that may be useful in the prevention of BRONJ or to encourage healing of established lesions. Calcium phosphate materials are already in clinical use, and can be used in the surgeries which precede BRONJ development, following optimisation, which is particularly advantageous. Future work will examine the binding relationship of HA and BPs further.

ACKNOWLEDGEMENTS: The authors would like to thank the EPSRC for funding this research and Ceramisys Ltd for providing the HA granules.

REFERENCES: ¹Bigi & Boanini, (2018) *BJ. Funct. Biomater.*, 9(1), 6, ²Colley, Hearnden, Jones et al. (2011) *Br J Cancer*, 105:1582-92

Clinical Translation of Regenerative Medicines: A Regulatory Primer

A. Wilson^{1,2}

¹*Department of Biology, University of York, York YO10 5DD, UK*

²*CellData Services, York YO43 4TZ, UK*

INTRODUCTION: Efficient translation of regenerative medicines from research into clinical development requires an appreciation of the regulatory environment for tissue engineering and cell-based products. Understanding of regulatory routes and requirements for entry into clinical trials should facilitate the development of effective new therapies.

BACKGROUND: All regenerative medicine products for therapeutic use in Europe will be regulated, generally as either advanced therapy medicinal products (ATMPs) or as medical devices. These two legal frameworks are different in almost all practical respects, including systems for clinical trial approval and authorisation to market the product, requirements for manufacturing, development and control, and data necessary to meet regulatory expectations.

PRESENTATION CONTENT: This talk will outline the principles for classification of regenerative medicine products as medicines or as medical devices, and highlight the importance of correct classification early in product development. Focusing on procedures for initiating a clinical trial, the data requirements, processes and background regulatory framework will be discussed using examples of different tissue engineering and cell-based products.

Development in academic-led groups frequently focuses on generating early evidence of effect and safety. Quality attributes are equally important: mandatory elements such as consistency, identity, purity and potency are highlighted as key aspects of development leading to a successful clinical trial application.

Table 1. Examples of framework differences between cell therapy/tissue engineering products (ATMPs) and medical devices

Aspect	ATMP	Medical Device
Basis of regulation	Pre-market authorisation	Manufacturer declaration
Manufacture	GMP	Quality Systems
Compliance	Guidelines, monographs	International Standards
Clinical Trials start	Early development	Late development
Incentives	CMA ¹ , AA ² , ODD ³ , data exclusivity	Not applicable
Obligations	Paediatric development, sunset clause	Not applicable

¹CMA: conditional marketing authorisation; ²AA: accelerated assessment; ³ODD: orphan drug designation

SUMMARY: Key expectations and minimal data requirements for entry into clinical development will be presented. Common deficiencies and problems with initial submissions will be highlighted, with recommendations on how to avoid rejection of clinical trial applications.

ACKNOWLEDGEMENTS:

REFERENCES:

Decellularisation of Human Femoral Nerves in a Closed System: Towards Introducing a New Nerve Allograft in Healthcare in the UK

V Barrera¹, G Webster², A Joseph¹, P Hogg¹, JN Kearney¹, and P Rooney^{1,2}

¹NHS Blood and Transplant, Tissue and Eye Services R&D, Speke, Liverpool L24 8RB,

²IMBE, University of Leeds, Leeds LS2 9JT

INTRODUCTION: In the UK, there is currently a high medical need for human nerve allografts to treat peripheral nerve regeneration occurring after traumatic injuries. The implantation of an autologous nerve graft, or an imported allograft from the US, both present limitations and a high NHS cost. We aimed to develop a new nerve allograft by decellularising human femoral nerves from deceased donors in the UK, while validating a new closed-system for processing tissue to meet GMP requirements in national tissue banking.

METHODS: Twelve femoral bundles were retrieved from 6 independent donors within 48 hrs of death (age range: 20-66 years old; 1:1 male to female), and 25-30 cm long native nerves were dissected out. One nerve segment (min 6 – max 25 cm) from each donor was decellularised by a series of hypotonic, mild detergent, nuclease and hypertonic steps over a total of 5 days at 37-42°C in a closed system bag (CryoMACS). Histological analyses were performed on native versus decellularised nerve biopsies and included: Van Gieson, Sirius Red, DAPI, Fluoromyelin® and immunohistochemical staining. The absolute amount of residual double stranded DNA was measured by a PicoGreen assay on dried tissue. Biomechanical testing was performed by using a uniaxial pull-to-break assay on a Lloyds universal tester (100N load cell).

RESULTS: Human femoral nerves were successfully decellularised, with minimal residual DNA (mean \pm SD: 2.44 ng/mg \pm 1.62; $p < 0.001$) below the acceptable limit of 50 ng/mg of dry tissue. Histology investigation revealed that nerve fascicle architecture has been preserved during decellularisation. Biomechanical properties of the nerve were not significantly affected (mean load at failure \pm SD: 9.32N \pm 8.7 vs 12.2N \pm 7 in native vs decellularised nerves; $p > 0.05$).



Fig. 1: Human femoral nerve decellularisation in a newly developed closed system.

DISCUSSION & CONCLUSIONS: We successfully decellularised human femoral nerves from cadaveric donors in a sterile closed-system. Future work will include cytotoxicity tests *in vitro* and implantation into an animal model of peripheral nerve injury to prove safety and efficacy of the new graft. This study will ultimately lead onto a clinical evaluation of decellularised human nerves in the UK to repair peripheral nerve injuries.

ACKNOWLEDGEMENTS:

We acknowledge the families of the deceased donors who kindly donated their tissues for research. We thank R Hall and S Wilshaw (University of Leeds) for their clinical input and supervision to G Webster work. This work was funded by NHS Blood and Transplant and a CASE studentship to GW. Work was performed under HTA licences 11018 and 12608.

DEVELOPMENT OF A MULTI-LAYERED CRYOGEL BIOREACTOR WITH OPTIMISED FLUID DYNAMICS FOR BIOARTIFICIAL LIVER APPLICATION

Flavia Bonalumi^{1*}, Cyril Crua², Irina Savina¹, Nathan Davies³, Maurizio Santini⁴, Stephanie Fest-Santini⁵, Susan Sandeman¹

¹ Pharmacy and Biomolecular Sciences, University of Brighton, United Kingdom, ² Advanced Engineering Centre, University of Brighton, United Kingdom, ³ The Institute for Liver and Digestive Health, University College London, United Kingdom, ⁴ Dipartimento di Ingegneria e Scienze Applicate, Università degli Studi di Bergamo, Italy, ⁵ Department of Management, Information and Production Engineering, Università degli Studi di Bergamo, Italy

Corresponding author: f.bonalumi@brighton.ac.uk– PhD student (3rd year)

Introduction: Liver disease is a condition that currently affects 29 million European[1] people and there are still no effective treatments other than liver transplantation [2]. Bioartificial liver devices aim to replace the detoxification and metabolic functions of the liver in people with liver failure. Cryogels are supermacroporous hydrogels which hold potential as cell scaffolds with open porosity, interconnectivity of pores and suitable mechanical properties. Cryogel monolith columns have been used by other groups to support HepG2 cells and fill the bioreactor chamber of a BAL prototype [3, 4]. However, device performance was not maintained for more than a few hours. Shear stress and local velocities created by flow inside porous scaffolds need to be optimised to improve cell viability and avoid inflammation but there are no relevant studies to date. We have previously carried out fluid dynamic measurements using a purpose-built micro-particle image velocimetry (μ PIV) setup with video post-processing in order to extrapolate the effect of flow inside the cryogel matrix to improve cell viability and avoid blood cell activation. Starting from PIV results, a multi-layered bioreactor composed of spaced cryogel discs was developed to maximise blood/hepatocyte mass-exchange. Acrylate-based cryogels were previously used by our group for blood detoxification purpose [5] and were here modified to enhance the non-fouling and cell adhesive properties of the surface. This study aimed to investigate whether these cryogel formulations are suitable for use as cell scaffolds in a perfusion device and to assess whether the multi-layered design possess improved bioreactor performance compared to the column version.

Materials and Methods: p(HEMA-co-MBA) cryogels were synthesised by cryogelation technique. Cryogels were then functionalised with alginate by post-synthesis functionalisation. RGD peptide was synthesised by solid phase method and covalently bounded to the surface through activation of hydroxyl groups with CNBr. Porous structure was analysed with SEM, confocal imaging and micro-computed tomography (μ CT). Porosity and permeability was derived from the μ CT scan. Non-fouling properties were investigated by protein absorption studies. Cell viability was assessed by MTT/ATP activity and live/dead imaging. Hepatocyte functionality in bioreactors was investigated by quantification of albumin and urea production using ELISA and a colorimetric assay, respectively.

Results and Discussion: Synthesised cryogels possessed an open porosity, with pore sizes of up to 100 μ m, and an interconnected network of pores, making them suitable to be used in a perfused system. Alginate limited protein absorption from plasma, which is an important precursor to avoiding blood cell activation and inflammation. RGD peptide enhanced hepatocyte functionality in terms of albumin and urea production. Cryogel-perfused bioreactors maintained hepatocyte viability and functionality for up to 1 week. The multi-layered bioreactor design allowed a significantly higher hepatocyte production of albumin and urea compared to the column version. Also, cell colonization and proliferation through the device were significantly increased.

Conclusions: In this study, RGD-alginate-p(HEMA)-based cryogels with engineered surface and optimised fluid dynamics were successfully synthesised and were able to maintain a high fraction of metabolising hepatocytes over time compared to HEMA alone. Flow was previously characterised using an ad-hoc built μ PIV setup which allows flow visualization inside the cryogel porous structure and extrapolation of local velocities. These measurements led to the development of a new multi-layered design scaffold with improved hepatocyte adhesion and functionality, compared to the column version. The multi-layered scaffold design shows promise for use in a BAL application.

References

1. Blachier, M., *et al.*, Journal of Hepatology. 58(3): p. 593-608, 2013.
2. Kumar, A. *et al.*, The journal of extra-corporeal technology. 43(4): p. 195-206, 2011.
3. Jain, E., *et al.*, Colloids and Surfaces B-Biointerfaces.136: p. 761-771, 2015.
4. Damania, A., *et al.*, Scientific Reports. 7, 2017.
5. Ingavle, G.C., *et al.*, Biomaterials. 50: p. 140-153, 2015.

DEVELOPMENT OF A TOPICAL CELL THERAPY FOR OCULAR SURFACE DISORDERS

L. Beeken¹, C. Alexander², F. Rose³ and L.E. Sidney¹

¹Academic Ophthalmology, Division of Clinical Neuroscience, School of Medicine, University of Nottingham, Nottingham, NG7 2UH. ² School of Pharmacy, Boots Science Building, University Park, Nottingham, NG7 2RD. ³School of Pharmacy, Centre for Biomolecular Sciences, University Park, Nottingham, NG7 2RD.

INTRODUCTION: Following severe mechanical or microbial insult to the ocular surface, the critical and destructive acute inflammatory phase can activate the transformation of keratocytes to scar forming fibroblasts, causing significant corneal opacity. Although blindness can be reversed with corneal transplant, the active inflammation is often too high, leading to surgery waiting times of up to 18 months. Corneal stromal mesenchymal stem cells (CMSCs) have been identified to possess potent immunomodulatory properties [1], and their incorporation into a regenerative medicine therapy could provide a novel and exciting treatment option to combat acute inflammation and reduce the wait for surgery. In addition to CMSC characterisation, here we propose the functionalisation of the well characterised contact lens material, poly(2-hydroxyethyl methacrylate) (PHEMA) with ethylene glycol dimethacrylate (EGDMA) as a crosslinking agent, with peptides to augment cell attachment, and inclusion of a photocleavable group for cell sheet detachment at the ocular surface.

METHODS: CMSCs were isolated from human corneal scleral rims and cultured in stem cell media. Cells were characterised using a variety of methods including flow cytometry and immunocytochemistry for phenotypic analysis, presto blue assays for cell viability, RT-PCR for genotypic assessment and in vitro corneal epithelial injury models to assess therapeutic capacity. Optimisation and functionalisation of the poly-HEMA-co-EGDMA hydrogel contact lens was achieved through investigations into cross linker percentage concentration, free radical initiation methods, water content, contact lens molds, additional monomers and plasma polymerisation. Subsequently, cell attachment, phenotype and genotype of the CMSCs cultured on the hydrogel surface were assessed.

RESULTS: CMSCs maintain a mesenchymal stem cell phenotype from passage 4 through to passage 10, with no significant difference in MSC marker expression, cell viability or cell growth rates. Additionally, CMSCs maintained anti-inflammatory potency over the passages, demonstrated on an in vitro corneal epithelial injury model. This indicates some freedom for choosing optimal passage for the CMSC therapy. Optimal lens quality was achieved with thermal initiation, where the monomers were injected between two glass slides separated with a silicone spacer. Functionalisation of the poly-HEMA-co-EGDMA hydrogel resulted in increased CMSC attachment, with greater cell number increasing the potential anti-inflammatory potency of the therapy. Future work is required to assess the cell sheet technology of the lens, in addition to further in vitro assessment of its therapeutic capacity for ocular surface disorders.

DISCUSSION & CONCLUSIONS: Here we present initial steps into the development of a topical cell therapy for ocular surface disorders, including cell characterisation and functionalised lens development. CMSC sheets cultured on contact lenses for direct application to the corneal surface following trauma could reduce waiting times for corneal transplant, in addition to providing hope of salvaging the ocular surface in severe cases of injury.

ACKNOWLEDGEMENTS: We are grateful to Dr Pratik Grunani for his help throughout this project.

REFERENCES:

Bray LJ *et al.*, *Cytherapy*, 2014; 16:64

Development of topographically controlled electrospun scaffolds to deliver proangiogenic agents for wound healing

D. H. Ramos¹, S. MacNeil², F. Claeysens², I. Ortega¹

¹ *The School of Clinical Dentistry, University of Sheffield, Sheffield, United Kingdom,*

² *Kroto Research Institute, North campus, University of Sheffield, Sheffield, United Kingdom*

INTRODUCTION: Angiogenesis plays a key role in tissue regeneration as part of wound repair. Previous tissue engineered skin constructs fail post transplantation if there is delayed neovascularisation. Our recent studies have shown that 2-deoxy-D-ribose (2dDr) [1] and oestradiol (E2) [2] can both stimulate a proangiogenic response. Another strategy to induce tissue regeneration is the inclusion of topographical cues in skin substitutes to mimic to a certain extent the Rete ridges in the skin. We have shown these have a positive effect on cell proliferation [3]. The aim of this project to produce a poly (lactide-co-glycolic acid) (PLGA) electrospun membrane to stimulate wound healing by (i) releasing pro-angiogenic 2dDr or E2 and (ii) providing topographic guides for skin cells.

METHODS: Electrospun PLGA scaffolds (both 50:50 and 75:25) were fabricated using DMF (dimethylformamide) and DCM (dichloromethane) as solvents. Patterned collectors made with microstereolithography (μ SLA) were used to create electrospun membranes with skin-like features. Exploration of the pro-angiogenic effects of 2dDr was achieved by dissolving 2dDr in DMF, and then adding it to the DCM-PLGA solution. SEM micrographs were used to characterize the morphology of the scaffolds and the release of 2dDr was measured. HDFs (human dermal fibroblasts) were seeded onto the scaffolds to evaluate cell viability and proliferation

RESULTS: Release of 2dDr from PLGA scaffolds (50:50 and 75:25) indicated a burst release during the first 24 hours from 50:50 PLGA with less and slower release from 75:25 PLGA (Fig. 1). Preliminary *in vitro* results indicate that scaffolds loaded with 10% wt. 2dDr or E2 had a negative effect on HDFs metabolic activity, whereas scaffolds with lower concentrations of 2dDr (1% and 5% wt.) showed an increment in metabolic activity. Patterned collectors were fabricated to produce

micro-topographical features in the electrospun scaffolds (Fig 2-a). The inclusion of topographical cues in scaffolds affected HDF morphology and distribution (Fig 2-b).

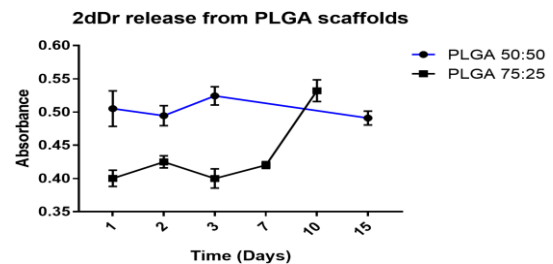


Fig. 1: Release of 2dDr (10% wt.) from PLGA 50:50 and 75:25 scaffolds. ($n=3\pm SD$).

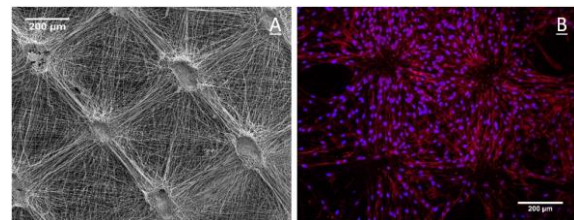


Fig. 2: A) Distribution of PLGA electrospun nanofibers spun on patterned collectors. B) HDFs cultured for 3 days on PLGA 50:50.

DISCUSSION & CONCLUSIONS: PLGA electrospun membranes released 2dDr over 1 (50:50) or several (75:25) days. This shows that the rate of release of 2dDr is tunable depending on the polymer lactide/glycolide composition. The inclusion of topographical cues influenced cell distribution and pilot results show promising results on cell proliferation and viability. This data demonstrates that PLGA electrospun membranes are promising platforms for the delivery of proangiogenic agents and the inclusion of intricate microfeatures to mimic the Rete ridges of skin.

ACKNOWLEDGEMENTS: This project receives financial support from CONACYT.

REFERENCES: [1] Mangir N. et al. European urology focus. 2017. [2] Yar M. et al. Materials Today Communications. 2017;13:295-305. [3] Ortega Asencio I. et al. Journal of Tissue Eng 2018;9:1-8.

Improving stem cell therapies for traumatic brain injury using bioactive ECM scaffolds to attenuate inflammation

C. Lee-Reeves¹, T.J. Keane², J.B. Phillips³, M.M. Stevens²

¹Department of Bioengineering, Imperial College London, UK, ²Department of Materials, Imperial College London, UK, ³School of Pharmacy, University College London, UK.

INTRODUCTION: The brain is limited in its capacity to heal following trauma due to a lack of endogenous stem cell populations and a persistent physical and chemical barrier at the injury site known as the glial scar. The aim of this research is to develop a therapeutic bio-scaffold that may be applied during neurosurgical intervention, to deliver neural stem cells (NSCs) in the early treatment of traumatic brain injury (TBI). Decellularised extracellular matrices (ECMs) possess anti-inflammatory and immune regulating properties that make them ideal candidates as scaffolds for cell delivery and tissue reconstruction. Advanced 3D in vitro tissue models of focal mechanical injury will be utilised to determine the extent to which ECM derived hydrogels from different tissue sources can modulate the characteristic inflammatory responses of astrocytes and the immune response of microglial cells. Characterisation and optimisation of the cellular material will result in pre-clinical testing within an in vivo model of TBI.

METHODS: ECMs derived from porcine brain (WBM) and bladder (UBM) were subject to established mechanical and chemical decellularisation processes^{1,2} and reconstituted as soluble factors and hydrogels. Primary rat astrocytes were isolated and cultured on collagen I coatings with 50, 100 and 200ng soluble UBM in culture media for 72h. These cells were compared to inflammatory astrocytes treated with 10ng/mL TGF- β . Future work will utilise 3D cultures that have been mechanically impacted, as a model system of traumatic injury through which to screen different ECM and NSC compositions.

RESULTS: Decellularised UBM is able to form hydrogels at 37°C at concentrations above 1mg/ml and remains soluble below 500ng/ml. Primary astrocyte cultures display a resting morphology when cultured with UBM compared to an inflammatory morphology when stimulated with TGF- β . Histological characterisation of WBM with Luxol Fast Blue staining of myelin indicates the resulting decellularised material is a preservation of mostly white matter proteins.

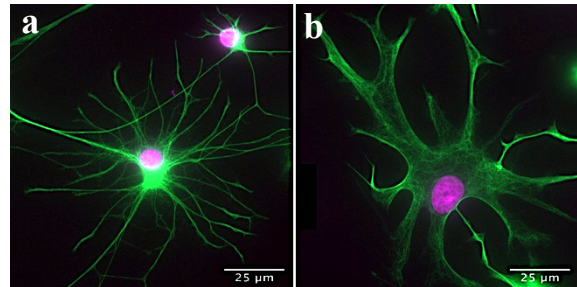


Fig. 1: a) Resting primary astrocyte cultured with 200ng/mL UBM, b) Reactive astrocyte treated with 10ng/mL TGF- β (Green: GFAP, Pink: DAPI, scale bar 25 μ m).

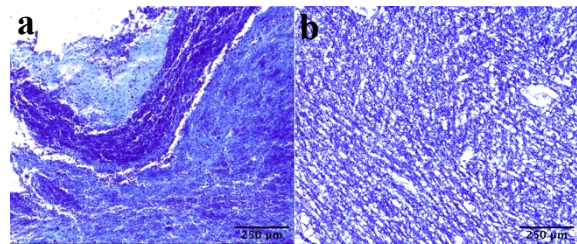


Fig. 2: Luxol Fast Blue staining of a) native brain tissue and b) decellularised brain ECM, scale bar 250 μ m.

DISCUSSION & CONCLUSIONS: Preliminary findings indicate cytocompatibility of UBM gels with glial cells. Optimisation and full characterisation of WBM is ongoing and will be compared with UBM for the ability to deliver NSCs and promote regeneration through modification of the inflammatory injury environment. Additional functionalisation of ECM gels will be investigated for increasing compatibility and efficacy for TBIs, including different methods for gel application to brain tissues.

REFERENCES: ¹D.O. Freytes, et al. (2008) *Biomaterials*. 29(11):1630–1637. ²C.J. Medberry, et al. (2013) *Biomaterials*. 34(4):1033–1040.

Investigating glycosaminoglycans in development and disease using fully defined 3D cell culture environments and human pluripotent stem cells

[J. L. Thompson](#)^{1,2}, [S. Pijuan-Galitó](#)^{1,2}, [J. C. Ashworth](#)^{1,3}, [K.S. Dowding](#)¹, [M.R. Alexander](#)², [C.L.R. Merry](#)¹

¹*Division of Cancer & Stem Cells and* ²*School of Pharmacy, University of Nottingham, UK,*

³*Manchester Cancer Research Centre, Division of Molecular & Clinical Cancer Sciences, University of Manchester, UK*

INTRODUCTION: Glycosaminoglycans (GAGs), including heparan sulphate (HS), are essential components of the extracellular matrix and regulate multiple signalling pathways during development [1]. Mutations in genes for enzymes (e.g. EXT1 and EXT2) in the HS synthetic pathway disrupt normal GAG production, GAG-related signalling and lead to developmental diseases (e.g. Multiple Osteochondromas, MO). We have developed human induced pluripotent stem cell (hiPSC) disease models and optimised a “blank slate” 3D culture environment to investigate how abnormal HS disrupts essential signalling in early development and diseases such as MO.

METHODS: Disease model hiPSCs were generated either by reprogramming MO patient fibroblasts (MO-hiPSCs) or by CRISPR-Cas9 gene editing of wildtype hiPSCs (EXT1^{+/-} and EXT2^{-/-}). Immunocytochemistry, flow cytometry, and AMAC-labelling compositional analysis were used to characterise the GAG profiles of the cell lines. To investigate matrix changes during development, hiPSCs were differentiated in self-assembling peptide hydrogels (FEFEFKFK gelator sequence) [2] under spontaneous or neural induction conditions. Immunostaining and qRT-PCR was used to confirm differentiation in the peptide gels.

RESULTS: MO-hiPSCs stained positive for pluripotency markers and were able to differentiate to all three germ layers. Genotyping confirmed successful knockouts of EXT1 and EXT2 in hiPSCs and analysis of HS produced by these cells under GAG-free culture conditions highlighted differences compared to WT cells. WT hiPSCs were successfully cultured and differentiated in the peptide gels without the need for serum, matrix addition or co-culture (figure 1).

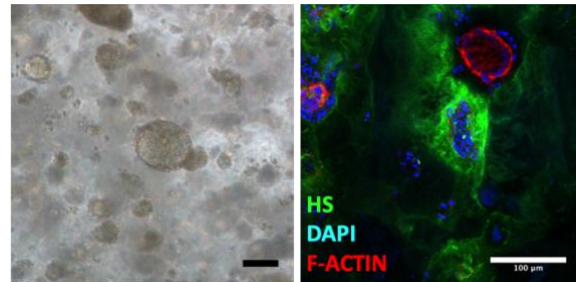


Figure 1. WT hiPSCs cultured for 5 days in unmodified peptide gels, in defined, GAG-free, xeno-free media. The hiPSCs formed round, well-defined colonies. Immunostaining and confocal microscopy were used to detect heparan sulphate (HS) deposition by hiPSCs (right). Scale bars 100 μm.

DISCUSSION & CONCLUSIONS: Here, we demonstrate the use of cellular disease models in combination with a defined, GAG-free 3D system to analyse disease-specific matrix and investigate dysregulated signalling pathways involved in developmental disease. The system can be tuned rheologically or by addition of matrix components to test their impact on cell behaviour, broadening our understanding of cell-matrix interactions.

ACKNOWLEDGEMENTS: This work was supported by the EPSRC grant EP/N006615/1 for the University of Nottingham Next Generation Biomaterials Discovery Programme, the NC3Rs grant NC/N001583/1 and the Swedish Research Council grant 2015-06532.

REFERENCES:

1. Johnson, C.E., et al., *Stem Cells*, 2007. **25**(8): p. 1913-23.
2. Ashworth, J.C., et al., *Matrix Biology* (submitted March 2019)

MAGNETIC HYDROGELS: TISSUE ENGINEERING CONSTRUCTS WITH SWITCHABLE STIFFNESS

J. Roe¹, P. Baynham², G. Guntoli², H. Wilcock¹, P. Roach²

¹Materials department, Loughborough University, Loughborough University, Leicestershire.

²Department of Chemistry, School of Science, Loughborough University, Leicestershire

Introduction

Multiple factors dictate the design process of potential biomaterials. Materials with tuneable and reversible properties offer a desirable advantage over conventional biomaterials, which can be hard to manipulate in a clinical setting. Here we explore the integration of hybridised magnetic nanoparticles into synthetic hydrogels, with the intention to utilise these scaffolds as a cell-seeded regenerative medicine strategy, that has switchable mechanical properties and is non-invasive.

Methods

Hybridised magnetic nanoparticles (HNPs) were synthesised according to previous work.^[1,2] Briefly, gold coated iron oxide nanoparticles containing a poly(ethylenimine) (PEI) intermediate layer (2 mL) were stirred with allyl methyl sulphide (0.5 mL) and sonicated with a pre-polymer solution of poly (ethylene glycol) methyl ether methacrylate (PEGMA) or poly(N-isopropylacrylamide) (PNIPAM). The resultant mixture was degassed using nitrogen and injected into moulds and cured using UV light for 35 minutes. Subsequent hydrogels were swollen in dH₂O, inoculated with 50,000 SH-SY5Y neuroblastoma cells and cultured for 7 days. Samples were processed for live/dead staining and cell viability measurements using Alamar Blue at 3 and 7 days. Samples were analysed using plate-plate rheometry and multi-axial tension testing.

Results

Rheological and strain-tracking tension tests of loaded and unloaded hydrogels reveals tuneable storage moduli dependant upon the attraction of HNP's to a magnetic source and concentration of crosslinker in the pre-polymer solution. Preliminary cell culture experiments indicate the presence of live cells on the surface of the hydrogels.

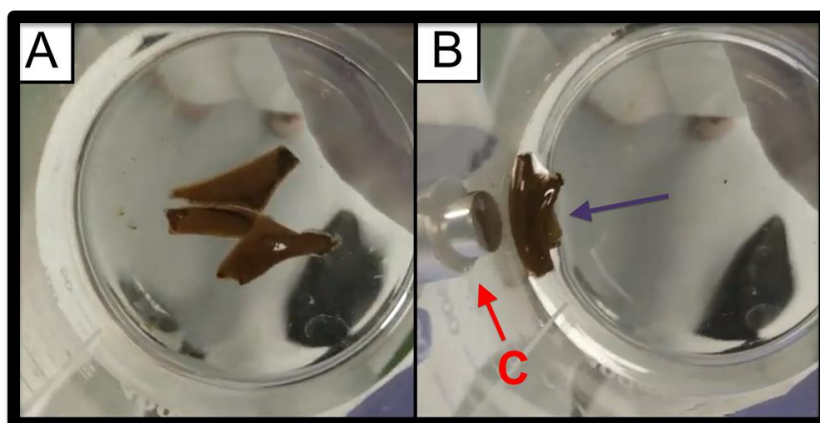


Fig. 1: Swollen PEGMA hydrogels encapsulating HNP's (A) quickly respond to the influence of a neodymium magnet (C).

Discussion & Conclusions

This work presents the possibility of creating new biocompatible smart materials that respond to the influence of magnetic fields. The mechanical properties of the hydrogels themselves may be tailored to suit the target tissue and have been shown to be biocompatible over a 7-day period. Future work will focus on exploring the rheology of such gels under the influence of magnet, as well as further investigations into the cell compatibility of a hydrogel under the influence of a magnet for prolonged periods.

References

- [1] Barnett, C.M. et al., J Nanopart Res, 14:1170–1174, 2012.
 [2] Hoskins, C. et al., J Nanobiotechnology, 10:15, 2012

Acknowledgements

The authors would like to thank the DPT ESPRC funding support of the Brain-on-a-chip mini-CDT, the Loughborough Materials Characterisation Centre (LMCC) for their facilities, Dr Sam Moxon and CellScale for help and guidance with rheometry, and Dr Claire Hoskins of Keele University, for help in synthesising the HNP's.

Modelling and emulating 3D multi-tissue interactions by microfluidic chip technology

S. Bagheri-Hanaei, C.C. Perry, Y. Reinwald, L. Santos.

School of Science and Technology, Nottingham Trent University, Nottingham, GB

INTRODUCTION: Microfluidic chip technology is a powerful platform that can be used to generate 3-dimensional (3D) cell culture systems which more accurately mimic the physiological condition of cells in the body (1, 2). The goal of this study was to develop a bone-on-a-chip (BOC) model in a 3-lane organ-on-a-chip platform (3-lane OrganoPlate, Mimetas) using mouse pre-osteoblasts (MC3T3-E1) and osteocyte-like (MLO-Y4) cell lines. The results generated from this BOC platform can remove the restriction of *in vivo* and 2D *in vitro* systems and has the potential to be applied to complex multicellular interactions for cell and tissue growth with applications in cancer research (3).

METHODS: Osteocytes were encapsulated in 5 mg/ml of type I collagen. Pre-osteoblasts were seeded against the osteocytes in 3D (Fig. 1). The co-culture was incubated for up to 7 days (Fig. 2). In addition, the individual cells in 3D and the co-culture were cultured with the presence of calcitriol in ethanol (treated) or ethanol (untreated control). To characterise the co-culture, the alamar blue, LIVE/DEAD assays and morphological observations by confocal microscopy were performed at days 1, 3 and 7. Figure 3 represents the LIVE/DEAD assay on day 7 while the cells were exposed to 10nM calcitriol.

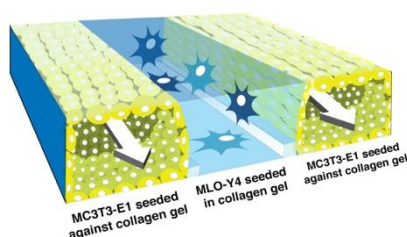


Fig. 1: Schematic diagram of the experimental set-up for MLO-Y4 and MC3T3-E1 cell lines cultivation in the model in the three-lane OrganoPlate platform.

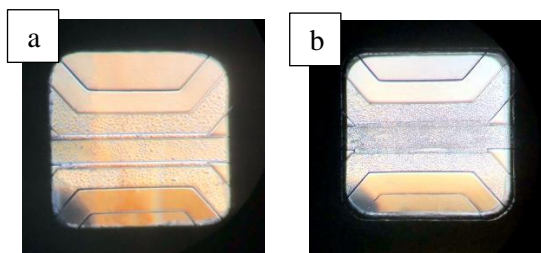


Fig. 2: Phase contrast images of co-culture in the three-lane OrganoPlate, a) day 3 and b) day 7.

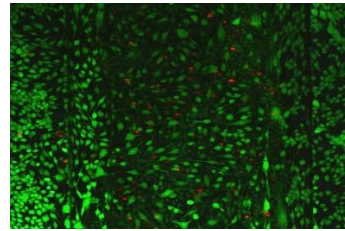


Fig. 3: Viability of MC3T3-E1 and MLO-Y4 cells in 3D co-culture (red: ethidium homodimer; green: calcein-AM dyes).

DISCUSSION & CONCLUSIONS: In the present study we have utilized a 3D co-culture system to mimic bone tissue within a microfluidic chip. As a proof of concept, we developed a BOC platform and observed osteocytes and osteoblasts cells interact in the conditioned media alone and when exposed to calcitriol. The interaction between these two cell lines can provide valuable data for drug discovery and toxicity testing. The results from this research illustrated that there is the capability to design and develop functional tissue models on a chip and also fabricate new chips with novel and advanced features. This BOC model has provided an important step forward in the creation of more physiologically relevant bone tissue models for drug development (4).

ACKNOWLEDGEMENTS: I would like to thank my supervisor Dr Livia Santos, my co-supervisors Professor Carole Perry, Dr Yvonne Reinwald and team members for their assistance and support.

REFERENCES:

1. Lee, H. and Cho, D.W., 2016. One-step fabrication of an organ-on-a-chip with spatial heterogeneity using a 3D bioprinting technology. *Lab on a Chip*, 16(14), pp.2618-2625.
2. Middleton, K., Al-Dujaili, S., Mei, X., Günther, A. and You, L., 2017. Microfluidic co-culture platform for investigating osteocyte-osteoclast signalling during fluid shear stress mechanostimulation. *Journal of biomechanics*, 59, pp.35-42.
3. Jang, M., Kleber, A., Ruckelshausen, T., Betzholz, R. and Manz, A., 2019. Differentiation of the human liver progenitor cell line (HepaRG) on a microfluidic-based biochip. *Journal of tissue engineering and regenerative medicine*, 13, pp.482-494.
4. George, E.L., Truesdell, S.L., York, S.L. and Saunders, M.M., 2018. Lab-on-a-chip platforms for quantification of multicellular interactions in bone remodeling. *Experimental cell research*, 365(1), pp.106-118.

NITRIC OXIDE RELEASING ELECTROSPUN NANOFIBERS FOR ANTIMICROBIAL BONE TISSUE ENGINEERING

Man Li,¹ Jenny Aveyard,¹ Fiona McBride,² Rasmita Raval,² Judith M Curran¹ and Raechelle A. D'Sa¹

¹ Department of Mechanical, Materials and Aerospace Engineering, University of Liverpool, ² Department of Chemistry, University of Liverpool, Liverpool

Corresponding author: Man.Li@liverpool.ac.uk – PhD student (3rd year)

Introduction

Bacterial adhesion and biofilm formation leading to infections is a major reason for failure of guided bone regeneration.¹ Compared to traditional bactericidal agents such as antibiotics, antiseptics and silver, which can lead to drug resistance or high cytotoxicity, nitric oxide (NO) is an attractive antimicrobial as it highly effective without leading to antimicrobial resistance.^{2,3} However as NO is a reactive gas, with a relatively short half-life, delivery of this antimicrobial is challenging. In this study we have synthesized NO releasing coatings on poly(ϵ -caprolactone) (PCL) and gelatin blended nanofibers. The NO donor used is an *N*-diazoniumdiolate which is formed using amino functionalities in the nanofibers. The biofilm inhibition to *Staphylococcus aureus* (*S. aureus*) was employed in evaluating the biological response of NO release nanofibers.

Materials and Methods

Five blends of PCL:gelatin nanofibers were prepared in mass ratios of 100:0, 75:25, 50:50, 25:75 and 0:100. Then samples were placed in a NO reactor to synthesis diazeniumdiolates. Diazoniumdiolates modified samples were analysed using contact angle and XPS. NO release was monitored using a chemiluminescent NO detector. Biofilm CFU assays were performed to determine the inhibition of biofilm formation on NO releasing surfaces after 6h and 24h incubation. In addition, SEM was used to determine *S. aureus* morphology after 6h incubation on NO releasing surfaces.

Results and Discussion

Results have demonstrated that the formation of diazeniumdiolates on nanofibers. The binding energies of N 1s peak at ~401 eV for N⁺ and ~402 eV for N-O were observed from XPS analysis, representing the –(O⁻)N⁺=N(O⁻) group. The kinetics of NO release were dependent on pH, with acidic conditions (pH 4) resulting in the release of higher NO concentrations than pH 7.4 and pH 8.5. The surface releasing the highest concentration of NO showed more than 1 log reduction in *S. aureus* biofilm formation.

Conclusions

Diazoniumdiolates were successfully PCL:gelatin nanofibers. These electrospun membranes have the potential to be use as anti-infectives for guided bone regeneration.

References

1. Zhao L *et al.* J. Biomed. Mater. Res. B. 91(1): 470-480, 2009.
2. Hetrick E. M *et al.* Acs Nano. 2(2): 235-246, 2008.
3. Nablo B. J *et al.* Biomaterials. 26(8): 917-924, 2005.

Optimisation of Microparticle Formulations for Cytokine Delivery for Macrophage Modulation for Potential Application in Spinal Cord Injury

J.Z. Stening¹, F.RAJ Rose¹, L.J. White¹,

¹Regenerative Medicine and Cellular Therapies, School of Pharmacy, University of Nottingham, Nottingham, UK

INTRODUCTION: Currently spinal cord injury (SCI) lacks treatment capable of restoring limb function and sensation. Current strategies focus on alleviating the high inflammatory environment triggered as a result of injury using pharmaceuticals and physiotherapy. Understanding macrophage (MΦ) behavior and the roles of their sub phenotypes in SCI has suggested a method for controlling inflammation by modulation towards a pro-immunoregulatory subgroup (M2) using cytokine IL-4. Microparticles are widely reported as drug delivery methods for controlled and sustained release in pharmaceutical strategies.

METHODS: Particles were manufactured using a double emulsion method (1,2) with 50:50 (lactide:glycolide ratio) PLGA (52kDa). Release kinetics were tailored by incorporation of a PLGA-PEG-PLGA triblock modifier (TB) in different percentages (1). Particles were manufactured using 1g total polymer dissolved in 5ml DCM respectively. Total protein loaded was 10mg/ml for 1g polymer. Particles were characterised using scanning electron microscopy for surface topography and laser diffraction for size distribution. Protein encapsulation efficiencies and release were analysed over 20 days using a micro BCA assay to detect total protein content.

RESULTS: Poly lactic-co-glycolic acid (PLGA) microparticles (20-50 μm) were designed as a drug delivery mechanism for IL-4 using various polymer parameters for controlled release. Protein release kinetics were analysed using lysozyme as a model protein to determine a suitable microparticle delivery system for IL-4 delivery. Release results were reported as μg protein/ mg particles with a maximum of 10 μg/mg encapsulated. In a comparison of triblock percentages for 20% TP 50:50 PLGA, 30% TB showed the fastest release with 10 μg/mg released by day 20. The slowest release was seen for 0% and 20% TB showing a small burst release of 1 μg/mg at day

1 and only reaching 1.5 μg/mg and 3 μg/mg respectively by day 20. 10% TB showed a burst release of 3 μg/mg at day 1 as for 30% TB but showed a promising sustained and continuous release to 6 μg/mg over 20 days.

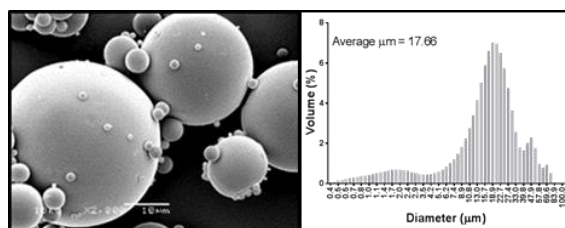


Fig. 1: SEM image (x2000) and size distribution 20% total polymer, 50:50 PLGA, 20% PLGA-PEG-PLGA triblock particles.

DISCUSSION & CONCLUSIONS: Particles made from 50:50 PLGA alone displayed release too slow for IL-4 delivery. Addition of a PLGA-PEG-PLGA triblock enabled release to be controlled with less initial burst release and accelerated overall release. Microparticles fabricated from 50:50 PLGA with 10% TB showed a release profile most suited to 14 days of controlled release.

ACKNOWLEDGEMENTS: Supported by the International Foundation for Research in Paraplegia, Switzerland ‘Combining stem cell and drug delivery to modulate macrophage phenotype toward M2 in spinal cord injury’, grant no. P155.

REFERENCES: ¹ White LJ, *et al.* (2013) Accelerating protein release from microparticles for regenerative medicine applications. *Mater Sci Eng C* **33**(5):2578–83. ² Abu-Awwad HADM, *et al.* (2017) Controlled release of GAG-binding enhanced transduction (GET) peptides for sustained and highly efficient intracellular delivery. *Acta Biomater* **57**:225–37.

PHOSPHATE BASED GLASS COATINGS FOR RAPID Ga^{3+} RELEASE: THE CHALLENGES OF BALANCING CYTOCOMPATIBILITY WITH ANTIMICROBIAL EFFECTS

Kathryn G. Thomas^{*1}, Bryan W. Stuart², Steve Atkinson³, Colin A. Scotchford¹, David M. Grant¹

¹Advanced Materials Research Group, University of Nottingham, ²Department of Materials, University of Oxford, ³Centre for Biomolecular Sciences, University of Nottingham

Corresponding author: kathryn.thomas1@nottingham.ac.uk – PhD student (3rd year)

Introduction

Biofilm infections affect 1-4% of orthopaedic implants, representing cyclical chronic pain for patients and at a cost of \approx £2 billion annually [1]. A successful antibacterial coating must release a dose of a bactericidal agent at the wound site, preventing bacterial adhesion on the implant surface. Human bone cells must later colonise the surface to ensure implant fixation. Ga^{3+} has been reported to be osteogenic at $<100 \mu M$ and antimicrobial against a wide range of pathogens at $<9 mM$ [2][3]. Radio Frequency Magnetron Sputtering can deposit degradable Phosphate based glass (PBG) coatings with excellent substrate conformity and adhesion strengths exceeding the FDA guidelines and Ga_2O_3 can be incorporated into the glass structure. This project's objectives were to produce Ga_2O_3 PBG content coatings for rapid Ga^{3+} release and to determine whether rapid ion release could be tolerated by human osteoblasts. For the first time this was compared to a Ga_2O_3 coating.

Materials and Methods

RF magnetron sputtering of suitable targets deposited coatings on to Ti6Al4V substrates. Ga_2O_3 was incorporated into the coatings in two ways: sputtering from a 10 mol% Ga_2O_3 PBG target and blending from a PBG and Ga_2O_3 target. Coatings compositions and structure were investigated by EDX, XPS, FTIR and RHEED. Degradation and ion release was performed in DMEM and compositional changes were investigated by EDX and XPS. Cytocompatibility testing used MG63 human osteoblast-like cells for Neutral Red and Alamar Blue assays. Bacterial attachment of *Staphylococcus aureus* to the coatings was visualised using confocal microscopy and quantified using COMSTAT 2 ($\mu m^3 / \mu m^2$).

Results and Discussion

Blending Ga_2O_3 with PBG resulted in a 71.9 mol% Ga_2O_3 coating (355nm thick). The glass target gave a 22.4 mol% Ga_2O_3 coating (156 nm thick). XPS confirms that Ga is present as an oxide in all coatings. These coatings are the highest Ga_2O_3 content glass coatings manufactured to date.

Targets used	Coating Ga_2O_3 content (mol%)	Ga^{3+} release at 8 h (ppm)	Ga^{3+} concentration at 8 h (μM)	Ga content 0 h (atomic %)	Ga content 168 h (atomic %)
Gallium doped PBG	22.4	1.9	27	2.6	2.0
PBG and Ga_2O_3	71.9	16.5	237	12.2	8.1
Ga_2O_3	100.0	62.5	897	18.0	0.6

Key findings from the degradation of the coatings in DMEM are summarised in the table above. All coatings were present after 168 h, whereas full degradation was recorded previously in H_2O . We suggest that Ga^{3+} release (which occurs mainly in the first 8 h) from the PBG containing coatings was limited due to Ga being bound into the glass structure, while Ga present in nano-crystallites (as detected by RHEED) was released into DMEM. No coating released enough Ga^{3+} to give antimicrobial mM concentrations, resulting in no difference in biofilm growth across any of the samples. Human cell growth on the coating surfaces is limited in all cases including the PBG control, and significantly so in the 71.9% and 100% Ga_2O_3 coatings. The higher cell growth on the 22.4 mol% samples compared to the higher Ga_2O_3 content coatings suggests that some Ga^{3+} exposure can be tolerated by the cells, as micrographs show healthy cell morphology on the 100% Ga_2O_3 coating after 168 h.

Conclusions

RF Magnetron offers the ability to coat high Ga_2O_3 PBG coatings, which will release Ga^{3+} into DMEM. The degradation of PBG structures in DMEM has not been widely reported and therefore different glass compositions must be investigated to ensure full degradation and Ga^{3+} release. Our results suggest that cells can recover after initial Ga^{3+} exposure and therefore cell response to a Ga^{3+} ion burst must be investigated further to determine if a short lived PBG coating releasing Ga^{3+} could prevent initial bacterial attachment without damage to surrounding tissue.

References

1. Webb J.S. *et al.* NBIC Overview, UKRI. 2019.
2. Strazic G. *et al.* J. Tissue Eng. Regen. Med., 2017
3. Minandri C. *et al.* Future Microbiol., 2014

Acknowledgements

This work was partially funded by Zimmer Biomet Ltd.

Phosphonate-modified graphene–Laponite composites for bone repair

T. Srisubin^{1,2}, J.E. Gough¹, C.F. Blanford^{1,2}

¹*School of Materials, University of Manchester, Manchester, UK*

²*Manchester Institute of Biotechnology, University of Manchester, Manchester, UK*

INTRODUCTION: Interest in materials for bone tissue engineering (BTE) has increased with the increasing need for treatments for bone disorders, especially in ageing populations. This work presents the development of a composite hydrogel containing Laponite nanoclay, graphene and phosphonates for bone repair. Laponite is an osteoinductive synthetic clay that forms injectable hydrogels and degrades into nontoxic products.¹ Phosphonates are organic phosphorous compounds that aim to mimic the function of bone-protecting bisphosphonate drugs.² Graphene is a stiff and readily modifiable form of carbon that can both tune the mechanical properties of composites and serve as a delivery platform for therapeutic agents.³ Therefore, this composite would promote accelerated bone repair and regeneration due to the synergistic effect of all three components.

METHODS: Graphene and graphene oxide (GO) were modified with vinylphosphonic acid (VPA), followed by creating layer-by-layer (LbL) assemblies with poly(ethyleneimine) (PEI). The LbL constructs containing modified graphene derivatives were evaluated by the ability to support primary human osteoblasts (HOBs) *in vitro*. Injectible Laponite-based hydrogels were made and cultured with osteoblast-like cells. Cell adhesion and spreading were investigated by cytoskeletal (phalloidin) staining at 1, 3 and 7 days post-seeding.

RESULTS: An *in vitro* study of HOBs seeded on LbL constructs (Figure 1) showed that PEI/GO assemblies were the most suitable surface for HOBs based on cell adhesion, proliferation and osteoblast mineralisation. Initial results of cell encapsulation in Laponite-based 3D composite hydrogels by cytoskeletal staining (Figure 2) revealed cell morphology and degree of cell spreading within hydrogels.

DISCUSSION & CONCLUSIONS: From 2D culture of HOBs on LbL constructs containing modified graphene derivatives, PEI/GO could

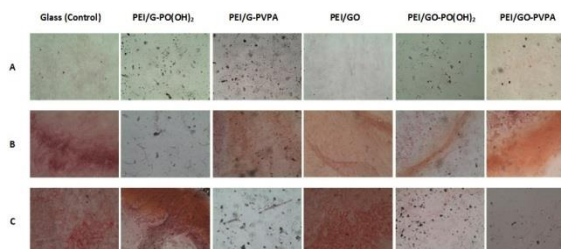


Figure 1. Alizarin Red staining of HOBs on LbL constructs, after incubation with osteogenic media for A) 7 days B) 14 days and C) 21 days. Frame size: 920x690 μm .

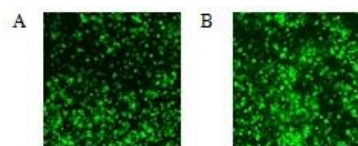


Figure 2. Phalloidin staining of osteoblast-like cells encapsulated in composite hydrogels at 3 days post-seeding. A) Laponite and B) Laponite-GO-PVPA. Frame size: 750x750 μm .

support cell adhesion, proliferation and osteoblast mineralisation while other LbL constructs showed the discrepancy of cell attachment, leading to no proliferating cells and mineralised matrix at some timepoints. Phalloidin staining suggests the restricted cytoskeletal organization of osteoblast-like cell in Laponite-based hydrogels. Cellular function expression and mineralised matrix (e.g. osteocalcin, alkaline phosphatase, collagen I and calcium deposition) will be further investigated to confirm the ability to support bone formation of composites.

ACKNOWLEDGEMENT: The authors would like to acknowledge Jon Dawson (University of Southampton, UK) for providing the Laponite and useful discussions. The authors also thank the Royal Thai Government for the funding.

REFERENCES:

1. Shi, et al. *Advanced healthcare materials* 7.15 (2018), 1800331.
2. Bassi, et al. *Journal of Tissue Engineering and Regenerative Medicine*, 6 (2012), 833-840.
3. Zhang, et al. *Nanoscale*, 4 (2012), 3833-3842.

Stable encapsulation of rifampicin and doxycycline in polymersome nanoparticles for delivery to intracellular bacteria

E. Porges¹, A. De Grazia¹, A. Taylor², D. Jenner², C.A.Rowland², T. A. Newman¹, N. D. Evans¹

¹Bioengineering and Clinical and Experimental Sciences, Faculty of Engineering and the Environment, University of Southampton, UK. ²Defence Science and Technology Laboratory, CBR Division, Porton Down, Salisbury, UK

Presenting author: E.Porges@soton.ac.uk

INTRODUCTION: Intracellular bacterial infections are notoriously difficult to treat, in part due to poor membrane permeability and intracellular bioavailability of antibiotics. They can arise as a result of the implantation of biomaterials [1]. Current treatment options involve high doses of antibiotics for sustained periods of time, therefore contributing to the issues of antibiotic resistance [2]. Antibiotic encapsulation within nanoparticles, such as polymersomes (PMs), may provide an answer to this challenge by promoting intracellular uptake and targeted drug delivery. In this study we tested the hypothesis that polyethylene oxide-polycaprolactone (PEO-PCL) PMs can encapsulate the antibiotic rifampicin, with a view to treating intracellular infections in the future.

METHODS: PMs were prepared by dissolving 6 mg of the amphiphilic di-block copolymer PEO-PCL into 0.4 ml of dimethylformamide (DMF). Polymer solution was then added dropwise into phosphate buffered saline (PBS), under stirring, to facilitate the self-assembly of PMs by nanoprecipitation. Rifampicin and doxycycline were passively incorporated at loading concentrations of 10 mg/ml and 50 mg/ml, respectively. Samples were dialysed, and the resulting PM-antibiotic concentrations determined using UV-vis spectrophotometry. To assess PM-antibiotic stability UV-vis readings were taken at various timepoints across a 14-day dialysis period. For uptake studies, PMs were fluorescently labeled using hydrophobic membrane dye, DiI. PMs were then incubated with RAW 264.7 macrophages for 4 hours before imaging.

RESULTS: Antibiotic release and PM stability studies showed that the PM-rifampicin and PM-doxycycline preparations had 8.5 µg/ml and 15.2 µg/ml retained at Day 14 in bulk suspensions, respectively (Figure 1a). This is equivalent to estimated local nanoparticle concentrations of 5 mg/ml and 10 mg/ml for

rifampicin and doxycycline preparations respectively. The preparations displayed no changes in hydrodynamic radius, as measured by dynamic light scattering, 88.5 nm ± 1.9 for PM-rifampicin, and 102.2 nm ± 2.2 for PM-doxycycline.

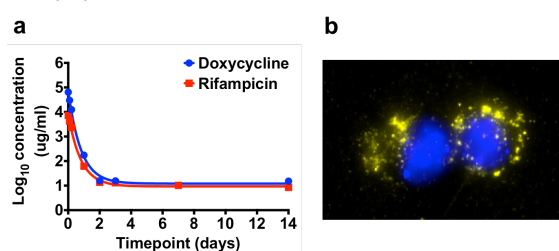


Fig. 1: a) PM-rifampicin and PM-doxycycline preparations retained final concentrations of 8.5 µg/ml ± 2.4, and 15.2 µg/ml ± 2.2, respectively. b) Epifluorescent image of PM-DiI successfully taken up by RAW 264.7 macrophage cells, nuclei stained blue.

Uptake studies indicated that after a 4-hour incubation PM-DiI were successfully taken up into RAW 264.7 macrophages, without penetrating the nuclei (Figure 1b).

DISCUSSION & CONCLUSIONS:

Rifampicin and doxycycline can be successfully encapsulated into PEO-PCL PM nanoparticles, and retained for at least 14 days. We hypothesise this is due to the stabilisation of the antibiotics within the hydrophobic membrane, and/or the entrapment within the hydrophilic core of the PMs. PMs can also successfully be taken up by RAW 264.7 macrophage cells. Future work will assess the efficacy of these nanoparticles on the killing of intracellular *Burkholderia thailandensis*.

ACKNOWLEDGEMENTS: We are grateful to DSTL, EPSRC, and the Institute for Life Sciences, Southampton for funding.

REFERENCES:

- [1] Rochford, E. T. J., Richards, R. G. and Moriarty, T. F. (2012); *Clinical Microbiology and Infection*, 18(12), pp. 1162–1167.
- [2] Ladavière, C. and Gref, R. (2015); *Nanomedicine*, 10(19), pp. 3033–3055.

Use of Antifreeze Proteins to Modify Pores in Directionally Frozen Alginate Sponges for Cartilage Tissue Engineering

A. Sturtivant, A. Callanan

Institute for Bioengineering, School of Engineering, University of Edinburgh, UK

INTRODUCTION: In 2013 8.75 million people over 45 required medical assistance as a result of osteoarthritis in the UK alone¹. This number is on the rise¹, leading to a need for earlier interventions. Tissue Engineering offers the potential to provide such treatments through the combination of novel biomaterials, cells and signalling molecules. This work details the fabrication of cross-linked alginate sponge scaffolds using directional freezing in combination with Antifreeze Protein (AFP). Directional freezing offers the ability to create structures that mimic the anisotropic nature of natural articular cartilage². A number of techniques have been used to control pore size during directional freezing (such as temperature gradients³). Here a protein found in many arctic phyla that can influence ice formation⁴ was added to the precursor solution, in an effort to influence pore structure.

METHODS: A set of AFP free and AFP inclusive Alginate scaffolds were fabricated. This was achieved by directionally freezing a 2% w/v alginic acid sodium salt solution in a mould. The AFP scaffolds were made the same way, but with the addition of 0.1mg/mL of AFP to the solution. Frozen solutions were freeze dried overnight, then crosslinked in 2% w/v of calcium chloride, followed by washing in PBS. Dried sponges were characterised using Scanning Electron Microscopy (SEM) and compression testing. Bovine Chondrocytes were cultured on the scaffold for 24 hours, 3 days and 7 days. Cell viability, biochemical quantification and gene expression were assessed.

RESULTS: Figure 1 shows SEM images of the tops and cross sections of an AFP scaffold and an AFP free scaffold. It shows porosity is higher in the AFP scaffold compared to the AFP free scaffold. Both scaffolds show similar internal morphologies. Table 1 outlines pore size analysis of the tops of the scaffolds, showing average pore size was smaller in the AFP scaffolds. Scaffolds demonstrated an ability to support cell adhesion.

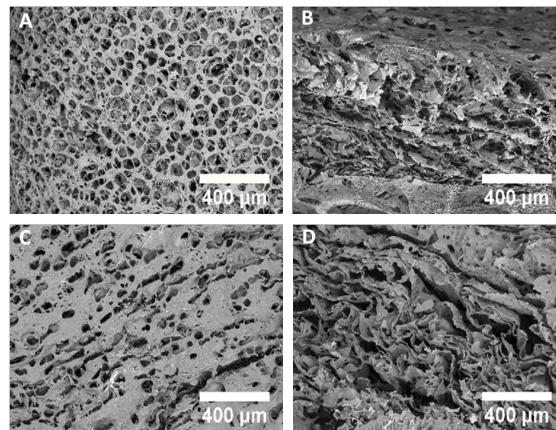


Figure 1 - SEM images of AFP scaffold top (A) and perpendicular cross section (B), and AFP free scaffold top (C) and perpendicular cross section (D).

Table 1- Results from analysis of pores at the top of each scaffold.

Means ± SD	AFP	AFP Free
Pore Area (µm ²)	1071±1621	1259±2136
Min. Diameter (µm)	24±17	22 ± 16
Max Diameter (µm)	39±29	48 ± 52

DISCUSSION & CONCLUSIONS: Directional Freezing offers the potential to produce scaffolds with anisotropic structures that mimic the native extracellular matrix of cartilage. Here it has been shown AFPs can influence the structures produced during directional freezing. Differences in structural and mechanical properties, and cell behaviour were also observed. Further work is needed to refine this process specifically to the application of cartilage tissue engineering.

ACKNOWLEDGEMENTS: EPSRC number: EP/R5132091. UKRMPII grant MR/L022974/1

REFERENCES: 1- Arthritis UK. (2018). 2- Munir & Callanan, Biomed. Mater. (2018) 3- Zhang et al. Sci Rep. (2017). 4- Kim et al. Marine Drugs (2017).

POSTER

3D PRINTED SCAFFOLDS FOR FUNCTIONAL EX VIVO CARDIAC TISSUE MODELS

Aidan Meenagh,¹ Adrian Boyd¹, Brian Meenan¹

¹Ulster University, NIBEC, Shore Road, Newtownabbey, Co. Antrim. BT37 0QB

Corresponding author: meenagh-a2@ulster.ac.uk – PhD student (2nd year)

Introduction

The development of new procedures, interventions and medications for the treatment of cardiovascular disease is dependent on rigorous preclinical and regulatory testing to ensure safety and the efficacy for the patient. A central aspect of this testing is the use of animal models, in particular porcine testing, as an *in vivo* element of the preclinical assessment regime. The provision of improved human based *in vitro* models that can significantly reduce this dependency on animal studies has clear benefits. Approaches using a blend of the knowledge gained from tissue engineering and lab-on-chip technologies are being developed whereby cardiac cells are combined with a 3D scaffold material and integrated with a suitable measurement platform to generate key elements of functional cardiac tissue. These so-called *ex vivo* systems offer a means to attain optimum physical, mechanical, and electrophysiological characteristics in a system designed to replicate the native myocardium. A key consideration of this approach is the ability to mimic the electrical properties of the myocardium in way that will reflect an appropriate respond to various types of treatments, e.g. drug and/or electrostimulation. In this work, the effects of integration of graphene to enhance the electroactive properties of a poly-e-caprolactone 3D scaffold designed to act as a matrix for functional cardiomyocytes is presented.

Materials and Methods

Poly-e-caprolactone (PCL) powder with a relative molecular mass of 50,000 amu (Polysciences Europe, Germany) with a particle size of <600 μm (98%) was used as the base system for 3D printing. Graphene nanoplatelets (2-10 nm) with a molecular weight of 12.01 g/mole (ACS, Pasadena, USA) were added to the PCL to create 0.25%, 0.50%, 0.75%, 1%, 2% and 5% w/w mixtures. Each powder mixture was placed in a hot extrusion cell of a bioplotter (EnvisionTEC, Germany) and used to print a range of 3D honeycomb structures that have been previously shown to promote cardiomyocyte function. The resulting structures and materials have been characterised by SEM, Conductivity measurements and TGA.

Results and Discussion

Figure 1 shows Scanning Electron Microscopy (SEM) images of honeycomb type 3D structures printed from PCL/Graphene w/w mixtures. These data indicate that it is possible to create the required structures with up to 5% graphene thereby resulting in a conductivity of 1×10^{-3} S/m compared to 1×10^{-16} S/m for PCL.

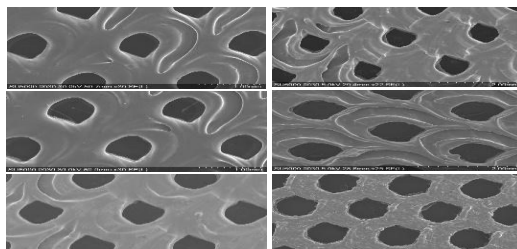


Figure 1: SEM micrographs of PCL 3D structures with (a) 0.25%, (b) 0.5%, (c) 0.75%, (d) 1%, (e) 2%, (f)-5% w/w

Thermogravimetric analysis (TGA) has been used determine the residual Graphene content after thermal degradation of the PCL.

Conclusion

Honeycomb-like 3D structures have been successfully fabricated from PCL/Graphene mixtures in the range 0.1% to 5% w/w. Above 5% Graphene inclusion, it is found that the structures no longer have the required integrity. Conductivity measurements suggest that the 95%PCL/5%Graphene system has electrical properties that may allow for stimulation of cardiomyocytes therein.

Acknowledgements

The authors are pleased to acknowledge financial support from the European Union's INTERREG VA programme, managed by the Special EU Programmes Body (SEUPB) via the ECME Project

References

[1] Hasan *et al*, *Adv. Sci.* 2015, 2

A caprine model of intervertebral disc degeneration: a testing platform for an injectable hydrogel

J Snuggs¹, C Rustenberg², K Emanuel², S Partridge¹, C Sammon¹, T Smit², C Le Maitre¹

¹Biomolecular Sciences Research Centre, Sheffield Hallam University, Sheffield, UK

²VU University Medical Centre, Amsterdam, The Netherlands

INTRODUCTION: Low back pain affects 80% of the population at some point in their lives with 40% of cases attributed to intervertebral disc (IVD) degeneration. There are many animal models to investigate IVD degeneration, such as murine and porcine models. However due to significant differences in physiology between these types of models and humans, such as the preservation of notochordal cells into adulthood, they are not completely representative of the human condition. Therefore, a more representative large animal model for IVD degeneration is needed to mimic human degeneration. Here we investigate a caprine IVD degeneration model for its use in testing our synthetic, Laponite® cross-linked pNIPAM-co-DMAC, injectable hydrogel (NPgel). NPgel has been shown to induce differentiation of human MSCs (hMSCs) towards a nucleus pulposus (NP) cell phenotype without the need for additional growth factors *in vitro* [1]. Through utilising the caprine model of IVD degeneration we aim to validate whether the NPgel retains these characteristics *in vivo*.

METHODS: After three days of culture in a bioreactor under diurnal, simulated-physiological loading (SPL) conditions, 33 healthy lumbar caprine IVDs were degenerated enzymatically by injecting 50 μ L of 1 mg/mL collagenase and 2 U/mL chondroitinase ABC (cABC). After injection, the IVDs were subjected to SPL again after two hours of digestion, for another 10 days. A no-intervention and phosphate buffered saline (PBS) injected group were used as controls. Disc deformation was continuously monitored and changes in disc height recovery behaviour were quantified using stretched-exponential fitting. Histological staining was performed on caprine discs to assess extracellular matrix (ECM) production and immunohistochemistry (IHC) was performed to determine expression of catabolic protein expression. Following establishment of the IVD model, NPgel was injected into goat IVDs and similar tests performed.

RESULTS: The injection of collagenase and cABC had severe effects on the mechanical behavior of the IVDs, especially in time constants and creep behaviour (Figure 1). These changes were progressive over time. Histological staining identified a decrease in ECM components such as collagens and glycosaminoglycans (GAGs) in enzyme injected discs. IHC identified an increase in degradative enzymes such as MMP3, MMP13 and ADAMTS4 and a decrease in aggrecan and collagen II also in enzyme treated discs.

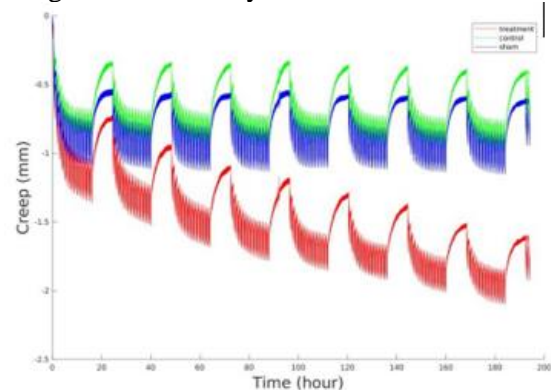


Figure 1: Creep behavior of collagenase/cABC treated (red), PBS-injected sham (blue) and no-injection control (green) caprine discs.

DISCUSSION & CONCLUSIONS: Here we show a novel, reproducible large animal model of IVD degeneration which mimics IVD degeneration. This model allows the testing of biomaterials and other potential treatments of IVD degeneration on a scale more representative of the human disc than more commonly used murine and porcine models.

The development of treatments for IVD degeneration is hindered using models which do not closely represent human IVD degeneration. Here we have established a reproducible, large animal model of IVD degeneration that has the potential for use in the screening of biomaterials and other treatments for IVD degeneration.

REFERENCES: [1] Thorpe AA et al., (2016). Acta Biomater. 36:99-111.

A comparative study to evaluate bioactive surfaces to deliver NGF and BDNF on neuronal cells

AM. Sandoval-Castellanos¹, F. Claeysens¹, JH. Haycock¹

¹Department of Materials Science and Engineering, Faculty of Engineering, The University of Sheffield, United Kingdom.

INTRODUCTION: Peripheral nerve injury is a major cause of disability, affecting 1 in 1000 patients every year in Europe [1]. The gold standard is the use of nerve autografts; however, their performance is limited. Nerve guide conduits are an alternative, but they do not support significant nerve regeneration. Surface functionalisation of biomaterials is a promising approach to encourage neurite outgrowth. This project investigates the effect of neurite formation and elongation when nerve growth factor (NGF) or brain derived neurotrophic factor (BDNF) are delivered using a bioactive surface modification.

METHODS: A bioactive surface was designed using allylamine plasma deposition as a basis to support heparin binding. Concentrations of 1 pg/mL, 1ng/mL, 10ng/mL, 100ng/mL and 1µL of either NGF and BDNF were included in this surface in solution or immobilised. PC12 neuronal cells were cultured *in vitro* on bioactive surfaces for 5 days. DAPI and phalloidin staining was performed to identify nuclei and F-actin filaments to measure neurite length and calculate developed neurites. Metabolic activity was evaluated with MTS assay on day 5.

RESULTS: Bioactive surfaces with immobilised NGF 1pg/mL, 1ng/mL, 10ng/mL, 100ng/mL developed neurites on average 56µm, 42µm, 55µm and 36µm respectively. Bioactive surfaces with immobilised BDNF 1pg/mL, 1ng/mL, 10ng/mL, 100ng/mL, 1µg/mL developed neurites on average 60µm, 37µm, 34µm, 65µm and 51µm respectively. Whereas the negative control developed an averaged neurite length of 23µm (Figure 1). Bioactive surface immobilised with 1 µg/mL of BDNF increased the expression of neurites from 0.5% (negative control) to 15% (Figure 2.B). MTS assay showed no significant differences among the metabolic activity of the bioactive surfaces.

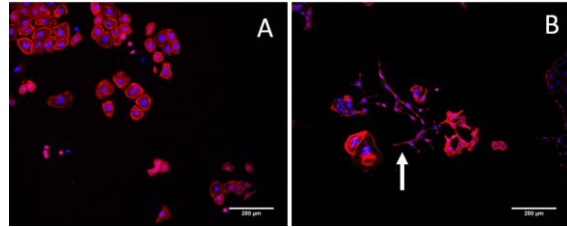


Fig. 1: Bioactive surfaces stimulate neurite length and expression. A) Negative control B) Immobilised BDNF 1µm/mL. Arrow shows neurite development in comparison with the negative control. Scale bar 200 µm.

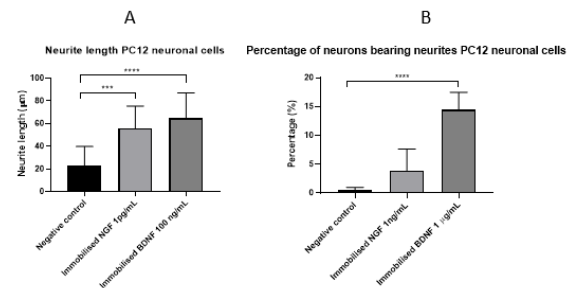


Fig. 2: Effects on A) Neurite length and B) Percentage of neurons bearing neurites for PC12 neuronal cells seeded in immobilised NGF and BDNF bioactive surfaces.

DISCUSSION & CONCLUSIONS: Surface immobilisation of NGF and BDNF stimulates neurite growth by a 143% and 183% respectively when compared to the negative control (Figure 2.A). The results suggested that immobilised concentrations encouraged the rapid assembly of f-actin filaments forming longer neurites. This approach could stimulate neurite outgrowth after injury by delivering NGF and BDNF in a bioactive surface as a novel technology part of the development of nerve guide conduits.

ACKNOWLEDGEMENTS: This project receives financial support from CONACyT.

REFERENCES: [1] Gu, X. et al. Progress in Neurobiology. 2011; 93; 2; 204-230. [2] Crawford-Corrie A, Buttle DJ & Haycock JW. 2017. Medical Implant. WO2017017425A1.

A NEW METHOD TO QUANTIFY BIOFILM FORMATION ON BIOMATERIALS SURFACES

Sophie E Mountcastle^{*1,2}, Nina Vyas², Richard M Shelton², Rachel L Sammons², Sophie C Cox³, Sara Jabbari⁴, A Damien Walmsley², Sarah A Kuehne²

¹EPSRC Centre for Doctoral Training in Physical Sciences for Health, University of Birmingham, ²School of Dentistry, University of Birmingham, ³School of Chemical Engineering, University of Birmingham, ⁴School of Mathematics, University of Birmingham.

Corresponding author: sem093@bham.ac.uk – PhD student (2nd year)

Introduction

There are numerous studies focusing on improving biomaterials to generate antimicrobial properties and reduce rates of implant failure due to infection^{1,2}. Biofilms account for up to 80% of infections, including those related to implantable devices³, and therefore are vital to consider when evaluating antimicrobial activity. However, quantifying biofilm formation on surfaces is challenging as microbiological methods often rely on manual counting, and are laborious and resource-intensive. Confocal imaging is a useful technique as it enables visualisation of biofilm formation in 3D. However, there is little consensus on analysing the resulting images. This work aims to develop a robust image analysis method to enable automated quantification of biofilm formation from confocal micrographs. Ultimately, this will support the development of much needed approaches to prevent and treat costly infections.

Materials and Methods

Streptococcus sanguinis was seeded on coverslips (n=5). Traditional cell counting methods were carried out for comparison with computational analysis. The number of live bacteria at 0, 1, 2, 5 and 7 days was established using CFU-plating. Total bacteria at each time-point were counted using a haemocytometer. Live-dead staining of biofilms at each time-point was imaged using confocal laser scanning microscopy (LSM 700, Zeiss, Germany) using a x40 oil immersion objective. Five random locations were scanned on each biofilm sample. Z-stacks were taken for each time point for 3D visualization. Image analysis was carried out using two software packages, Fiji (ImageJ, v1.52h) and Matlab (v2017b). The percentage of viable and dead bacteria in each image was determined by calculating the number of pixels corresponding to the numbers of dead (red) and live (green) bacteria (Figure 1). A similar methodology was applied to determine cell numbers.

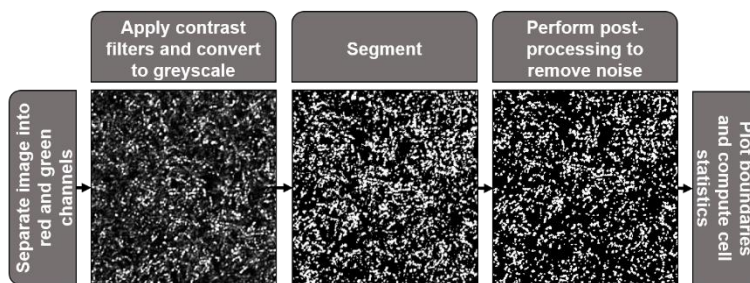


Figure 1: Schematic outlining image processing methods utilised to determine percentage of live cells for single-species biofilms. Images of key stages are presented.

Results and Discussion

Computational image analysis methods were compared with each other, and with standard cell counting techniques. The overall trend in live cell percentage varied between methods. The Matlab script demonstrated a similar trend to the manual counting methods but overestimated the percentage of live cells at all time-points. Calculating cell numbers resulted in a lower estimation of live cells at early time-points, but was more closely aligned to the biological cell count at 5 and 7 days. The reasons for these differences will be explored and further development of the computational analysis techniques will be discussed. Finally, results from the 3D image analysis will also be presented and compared with 2D data.

Conclusions

Computational analysis has advantages by automating the quantification process, whereas traditional methods rely heavily on manual counting. Improving and standardising analysis techniques will enable better comparison of antimicrobial surfaces. The technique developed here can be applied more broadly to the medical implant and biofilm fields.

References

- 1 H. J. Busscher, H. C. Van Der Mei, G. Subbiahdoss, P. C. Jutte, J. J. A. M. Van Den Dungen, S. A. J. Zaat, M. J. Schultz and D. W. Grainger, *Sci. Transl. Med.*, 2012, **4**, 153rv10.
- 2 J. Grischke, J. Eberhard and M. Stiesch, *Dent. Mater. J.*, 2016, **35**, 545–558.
- 3 Z. Khatoun, C. D. McTiernan, E. J. Suuronen, T.-F. Mah and E. I. Alarcon, *Heliyon*, 2018, **4**, e01067.

Acknowledgements

The authors gratefully acknowledge financial support from the EPSRC through a studentship from the Physical Sciences for Health Doctoral Training Centre at the University of Birmingham (EP/L016346/1).

A NOVEL ORGANIC-INORGANIC HYBRID HYDROGEL FOR CELL ENCAPSULATION AND DRUG DELIVERY

Soher Jayash^{1*}, Paul Cooper¹, Richard Shelton¹, Gowsihan Poologasundarampillai¹
¹School of Dentistry, University of Birmingham, 5 Mill Pool Way, Edgbaston, Birmingham, UK
 Corresponding author: s.jayash@bham.ac.uk

Abstract

Introduction: Chitosan is a natural polysaccharide copolymer which is widely used in drug delivery and bone tissue engineering. Thiolated chitosan (TC) has several advantages compared with unmodified chitosan, including significantly improved permeation and mucoadhesive properties arising from thiol groups on side chains. Moreover, soluble TC displays gelling properties that facilitate controlled drug release, cell encapsulation and bioprinting (1). Recent studies in polymer and bioengineering have resulted in developments in hydrogels for therapeutic delivery. In the present study, a novel hydrogel was prepared based on thiolated chitosan (TC) and silica to be used for bone regeneration in future applications.

Materials/methods: A range of novel organic-inorganic hybrid hydrogel composed of a range of ratio TC and silica were prepared. A low molecular weight chitosan (LMWC)/silica hydrogel was prepared for comparison. The chemical structures of the hybrid hydrogels were confirmed using Fourier-transform infrared spectroscopy (FTIR) and nuclear magnetic resonance (NMR) spectroscopy. The fundamental rheological properties of gels were determined using an oscillating rheometer. Hydrogel degradation was examined in phosphate buffer saline (PBS) or PBS containing 1.5 mg/mL lysozyme. The sample solution was extracted at 30 minute, 1 hour, 7 hours and 24 hours and up to 504 hours and replaced by fresh solution. Inductively coupled plasma atomic emission spectroscopy (ICP-AES) was used to obtain the soluble silica release profiles in the degradation solution and high-performance liquid chromatography (HPLC) was used for the quantification of chitosan and glycerol. Moreover, the cytotoxicity of the hybrid hydrogels on osteoblasts (SAOS-2) was evaluated by both direct and indirect contact methods. For the indirect contact method, hydrogels were incubated in McCoys media for 24 hours. The extraction ratio was 0.2 g/mL, according to ISO 10993-12. After seeding cells, cultures were fed with extraction media. For the direct contact method, cells were cultured on the surface of the hydrogel samples in a culture plate. Cell cultures were then incubated for 24, 48 and 72 hours. The viability of cells was determined by using the alamarBlue assay. Cell viability of SAOS-2 cells encapsulated in hydrogels was evaluated using the live/dead assay and confocal microscopy image analysis.

Results: The hybrid spectra of hydrogels synthesised here shown to exhibit characteristic absorption bands which included: Amide II (1570 cm^{-1}), Si-O (924 cm^{-1}) and Si-O-Si (854 cm^{-1}). Also, NMR techniques showed a reaction between the epoxide ring of silica and chitosan. Strain and frequency sweep tests demonstrated a solid-like response of the hydrogel, which increased for the TC/silica hydrogel compared with the LMW/silica hydrogel. Silicon release was more rapid during the first 24 hours of the experiment and subsequently silicon release remained at a relatively slow rate over 21 days. All hydrogels exhibited limited cytotoxicity as viability of osteoblasts seeded on hydrogels remained at >60% over 72 hours culture. Notably the growth of osteoblasts seeded on hydrogels increased gradually as exposure time increased. For the indirect contact method, viability of osteoblasts was greater than 80% over the 72 hour period.

Conclusion: The newly developed TC/silica hydrogel exhibited specific degradation and mechanical properties which showed no significant cytotoxic effects during material-cell contact. Thus, the hybrid hydrogels have potential to be used for cell encapsulation, tissue engineering and intelligent drug delivery.

References:

1. Sreenivas, S. A., & Pai, K. V. Tropical Journal of Pharmaceutical Research, 7, 1077-1088, 2008.

A NOVEL WEIGHT-BEARING ANTIBIOTIC ELUTING TEMPORARY HIP SPACER MANUFACTURED BY SELECTIVE LASER MELTING

Sophie E.T. Louth^{*1}, Parastoo Jamshidi², Neil M. Eisenstein^{1,6}, Mark A. Webber³, Hany Hassanin^{2,7},
 Moataz M. Attallah², Duncan E.T. Shepherd⁴, Owen Addison⁵, Liam M. Grover¹, Kenneth Nai⁸, Sophie C. Cox¹.
¹ School of Chemical Engineering, ² School of Materials and Metallurgy, ³ School of Biosciences, ⁴ Department of Mechanical Engineering, ⁵ School of Dentistry, ¹⁻⁵ University of Birmingham, ⁶ Royal Centre for Defence Medicine
⁷ School of Mechanical and Automotive Engineering, Kingston University, ⁸ Renishaw PLC.
 Corresponding author: sel713@student.bham.ac.uk – EngD student (2nd year)

Introduction

Hip implant failure due to infection is a major problem with over 8000 UK patients receiving a revision due to microbial colonisation in 2017 [1]. The gold standard for revision of an infected prosthetic is a two stage procedure, including thorough debridement of the soft tissue and the use of a temporary spacer that elutes antibiotics [2]. These devices are often made of bone cement and are not fully load bearing leading to extensive periods of bed rest [2]. The focus of this work is to develop a novel hip spacer, to enable patients to load bear during this 6 – 8 week period. Conventional implant manufacturing techniques, such as casting, are unable to create the complex structures required to house an antibiotic eluting biomaterial. Selective laser melting (SLM) is an additive manufacturing technique that enhances design freedom through layer-by-layer manufacture. The novel porous lattice design explored is built from Ti-6Al-4V using SLM. In order to assess the feasibility of the design, four key research areas require exploration. The lattice, which provides the main mechanical support for the spacer as well as controlling drug release. The biomaterial embedded in the lattice that incorporates the antibiotic, in initial experiments this has taken the form of a brushite cement. The channels through which the antibiotic is released, these have been investigated in terms of filling the internal volume and release of the antibiotic. Finally the surface properties can be manipulated to minimise adhesion of both bone cells, as this is a temporary device that needs to be easily removed, and of bacteria to reduce the risk of additional infections.

Materials and Methods

In order to find the optimal lattice design, cylindrical lattices (12 mm diameter, 15 mm height) were generated in Element (nTopology, USA), and built on a Ren AM500M (Renishaw PLC, UK) from gas atomised Ti-6Al-4V powder using optimised in-house parameters, and compression tested in accordance with ISO 13314:2011. The initial biomaterial investigated was dicalcium phosphate dihydrate known as brushite. β -tricalcium phosphate (β -TCP) and monocalcium phosphate monohydrate (MCPM) powders were mixed with deionised water in a powder-to-liquid ratios (PLR) of 2:1 for 30 s. To investigate the best strategy for placement of the channels, three model implants were designed with a 2 mm diameter hole in the top and four 1 mm diameter holes in either the sides horizontally, inclined at 45 degrees, or vertically at the bottom. These were filled using the brushite cements loaded into a 5 mL syringe attached to a 15G needle. Micro-CT was then used to visualise the cement inside the model. To investigate the elution characteristics of a gentamicin loaded brushite cement, the antibiotic was dissolved in deionised water at 100 mg/mL, and then mixed at a PLR of 2:1, resulting in a final concentration of 50 mg per 1 g of cement. Cement cylinders and implant models containing cement were immersed in 10 mL of phosphate buffered saline incubated at 37°C. 10mL samples were withdrawn at intervals over 6 hours. These were tested for gentamicin using a CE 7500 UV-Vis spectrophotometer (Cecil Instruments, UK) and compared to cement without gentamicin.

Results and Discussion

The compression testing found that the BCCZ lattice at 60 % volume fraction had the highest compressive yield strength at 444.3 ± 6.9 MPa, which is around double the strength of bone, while leaving 40 % of the volume for the biomaterial. Micro-CT visualisation of the cement filled model implants found all designs were filled both in the reservoir and channels. However, defects were seen in the cement of all designs, particularly for the vertical channel model. The cumulative release of gentamicin from the cement after 6 hours was greatest from bare cement, with only 28 % release from the vertical channels, 10 % from horizontal, and 5% from inclined, the quantity of defects may have had an influence on this. The minimum inhibitory concentration of gentamicin against *S. epidermis* and *S. aureus* was found to be 1 and 16 μ g/mL. All the model implant designs were shown to elute sufficient concentrations of gentamicin to inhibit the growth of both *S. epidermis* and *S. aureus*.

Conclusions

This work has demonstrated the possibility to exploit additive manufacturing technologies to enhance the value of medical devices. More specifically, the design freedoms of this technique have been exploited to generate load bearing structures for use in two-stage revision of infected hip arthroplasty. Work on the mechanical and chemical interactions between the biomaterials and the lattice structure is on-going. Future work will look at whether the lattice structure can be used to tailor antibiotic release from the device in order to treat the infection quickly using a minimum quantity of the drug and without creating antibiotic resistance.

References

1. Powers-Freeling L, National Joint Registry 15th annual report.
2. Cooper H.J. The Bone & Joint Journal, 95B: 84–87, 2011

A zero-order drug eluting material to improve nerve grafting

H. Gregory, U. Angkawitwong, V. H. Robertson, G. Williams, J. B. Phillips

UCL Centre for Nerve Engineering, UCL School of Pharmacy, University College London, UK

INTRODUCTION: Nerve allografts, or engineered tissues containing allogeneic cells, eliminate the donor site morbidity associated with autografting in the repair of large peripheral nerve gaps but require long-term immunosuppression to prevent rejection. Systemic administration could be avoided using a controlled release implant. Drug-loaded core-shell structured nanofibres can exhibit extended zero-order release *in vitro* [1] and here are developed for tacrolimus-based immunosuppression in allografted nerve repair.

METHODS: Tacrolimus-loaded polycaprolactone (PCL) fibres were produced by coaxial electrospinning of a shell solution of 10% PCL in 90/10 w/v trifluoroethanol: deionised water with a core solution of 133.3 mg/ml tacrolimus in ethanol for two hours. The fibres were analysed using digital microscopy, and fully characterised using scanning electron microscopy (SEM), thermal methods and X-ray diffraction. An *in vitro* release study was performed over a period of 12 days using UV-Vis spectroscopy.

RESULTS: Analysis by SEM indicates cylindrical and largely smooth fibre morphology, with an average fibre diameter of $1.15 \pm 0.92 \mu\text{m}$ (Fig. 1).

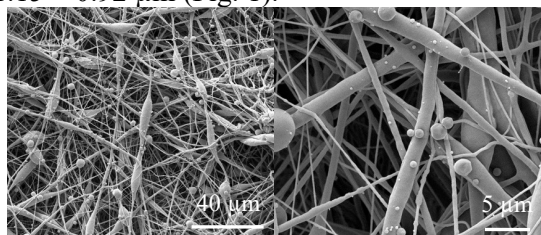


Fig. 1: Scanning electron microscopy images of tacrolimus-loaded fibre mat.

Characterisation by X-ray diffraction and differential scanning calorimetry suggested tacrolimus is present in the fibres in an amorphous state. The fibre mat showed zero-order release of tacrolimus over a period of 12 days (Fig. 2).

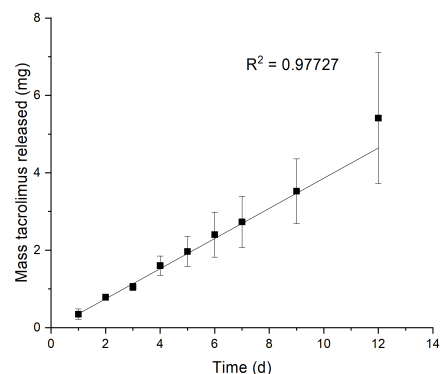


Fig. 2: *In vitro* release data of fibre mat displaying zero-order release characteristics.

DISCUSSION & CONCLUSIONS:

Tacrolimus was successfully incorporated into fibre mats which displayed zero-order release characteristics over a 12-day period. There was no evidence of burst release. The mass of tacrolimus released from the fibre mat samples over time is within an appropriate range to provide a local dose that would potentially be effective in reducing an immune response and promoting nerve regeneration through an allogeneic cell or tissue graft.

ACKNOWLEDGEMENTS: The authors thank the CDT in Advanced Therapeutics and Nanomedicines. This research was funded by the ESPRC, grant EP/L01646X.

REFERENCES: [1] Angkawitwong, U., Awwad, S., Khaw, P.T., Brocchini, S., et al. (2017) *Acta Biomaterialia*. [Online] 64, 126–136.

Accelerating collagen deposition with macromolecular crowding can disrupt collagen fibre alignment

[D.A. O'Loughlin](#)^{1,2}, H.J. Levis¹, V.R. Kearns¹, C. Sheridan¹, [E.G. Canty-Laird](#)²

¹*Department of Eye and Vision Science,* ²*Department of Musculoskeletal Biology I. Institute of Ageing and Chronic Disease, University of Liverpool, UK*

INTRODUCTION: *In vitro* models of the cornea can be used for a variety of applications from drug toxicity and wound healing to investigating the mechanisms of collagen fibril alignment. However, it can typically take months to create a construct that resembles the native corneal stroma with its highly aligned collagen fibrils. One way to reduce culture times is to use macromolecular crowding which has been shown to increase collagen deposition. The aim of this study was to increase collagen deposition using carrageenan as a macromolecular crowder on cells cultured on an aligned nanofibre substrate.

METHODS: Friction transfer was used to coat glass coverslips with aligned polytetrafluoroethylene (PTFE) nanofibres. Human corneal fibroblasts (hCFs) were seeded onto these coverslips and cultured in either complete media or complete media with 75 µg/ml of carrageenan (CAR) for up to 30 days. The collagen deposited by cells was imaged using a collagen probe or using immunocytochemistry for collagen type I. An ImageJ plugin, OrientationJ, was used to analyse the alignment of collagen fibres.

RESULTS: hCFs aligned along the topographical cues provided by the PTFE nanofibres. The collagen probe revealed that the collagen fibres deposited by the hCFs cultured in normal media aligned parallel to the topographical cues. OrientationJ analysis confirmed collagen fibre alignment with 70% of these fibres aligning within 10°. When CAR was added to the media there was an increase in collagen deposited however, the collagen fibres seemed to aggregate as opposed to form fibres. Further analysis with immunocytochemistry confirmed that these aggregates contain collagen type I.

DISCUSSION & CONCLUSIONS: When cultured in normal media the hCFs deposited aligned collagen fibres that mimicked a lamella

within the corneal stroma. Macromolecular crowding with CAR disrupted the fibre deposition and granules of collagen were present instead. Similar work has previously shown that collagen forms granules when dextran sulphate is used as a crowder and this is thought to be a result of the crowder being negatively charged [1]. These results suggest that CAR is probably an unsuitable macromolecular crowder when trying to recapitulate the exquisite structure of the corneal stroma. Alternative methods of reducing culture time to emulate the corneal stroma *in vitro*, such as use of neutral crowders could be considered.

ACKNOWLEDGEMENTS: The authors would like to thank the Crossley Barnes Bequest Studentship for funding and Magnus Höök for providing the plasmid for the collagen binding domain of *S. Aureus*. The use of human tissue was approved by REC 16/EM/0090.

REFERENCES: ¹ R. R. Lareu (2007) *Tissue Eng.* **13**:385-391

ACELULAR GELATINE-ALGINATE SCAFFOLDS FOR DENTINE-PULP REGENERATION

Ignacio Medina-Fernández*, Adam D. Celiz
 Department of Bioengineering, Imperial College, South Kensington, SW7 2AZ, London
 Corresponding author: im1116@ic.ac.uk – PhD student

Introduction

Dental decay and poor long-term outcomes of traditional endodontic treatments have led the search for new dental tissue regeneration strategies. There is a lack of biomaterial approaches that harness the native dental pulp stem cells (DPSCs), which constitute one of the main agents responsible for the intrinsic regenerative capabilities of the pulp. To achieve this, a hybrid gelatine-alginate scaffold crosslinked via tetrazine-norbornene click chemistry incorporating bioceramic particles as an odontogenic moiety is proposed.

MATERIALS & METHODS

Sodium alginate (KIMICA, Japan) was modified with 2-norbornene (Sigma-Aldrich, UK) and gelatine (Nitta Gelatin Inc. Japan) will be functionalised with 5-(4-(1,2,4,5-tetrazin-3-yl)benzylamino)-5-oxopentanoic acid, which is being synthesised using nickel triflate as catalyst as described by Alge et al.¹ Proton Nuclear magnetic resonance (¹H NMR) will be used to characterise the tetrazine and confirm the functionalisation of alginate and gelatine with norbornene and tetrazine, respectively. Biphasic calcium phosphate (BCP), a mixture of hydroxyapatite (HA) and tricalcium phosphate (TCP) was prepared via wet precipitation and calcination at 1000 °C. Bredigite (Ca₇Mg(SiO₄)₄) and β-dicalcium silicate (β-DCS; Ca₂SiO₄) were synthesised via a sol-gel process and calcination at 1150 °C and 800 °C, respectively. X-ray diffraction (XRD) was used to assess the crystallinity and formation of the bioceramics. Extracts of these were prepared via incubation at 37 °C and 5 % CO₂ in DMEM for three days at 200 g/L. DPSCs were cultured in dilutions of the extracts (from 0 to 100 g/L) and MTT assays were performed after 1, 3 and 5 days to assess DPSC proliferation.

RESULTS & DISCUSSION

XRD spectra confirmed the formation of BCP with a high β-TCP/HA ratio (approximately 80/20), pure bredigite and β-DCS after calcination. A more prevalent β-TCP phase is considered desirable as BCPs with higher β-TCP/HA ratios have been described to be more odontogenic, presumably due to the higher bioresorbability of β-TCP.² Ceramic extracts displayed no significant DPSC cytotoxicity against control (media without extract), except for BCP extracts for which DPSC viability greatly decreased at the highest concentrations, (2x and 4x dilutions) but remained high at the lowest concentrations (16x and 64x dilutions). Polymer modification with tetrazine and norbornene moieties allows for bio-orthogonal crosslinking which will enable encapsulation of bioactive molecules such as growth factors and cytokines to engineer endogenous DPSCs.

CONCLUSION

In this work, preparation and characterisation of the main components of an acellular scaffold for dentine-pulp regeneration is presented. The hybrid scaffold combines the tuneable mechanical properties of alginate with the pro-attachment moieties and biodegradability of gelatine. Future work includes optimisation of hybrid scaffold parameters such as porosity and Young's modulus to support DPSCs in-vitro and incorporation of bioceramics and other odontogenic elements for differentiation of endogenous DPSCs.

ACKNOWLEDGEMENTS

We would like to thank the Department of Bioengineering at Imperial College London for providing the funding and resources to carry out this work.

REFERENCES

- 1 Alge, D. L. *et al.*, *Tetrahedron Lett.*, 54:5639–5641, 2013
- 2 AbdulQader, S. T. *et al.*, *Mat. Sci. Eng. C*, 49(1):225–233, 2015.

Airway smooth muscle cell morphology, proliferation, and α -smooth muscle actin is modulated by substrate stiffness

J. Ramis^{1,2}, D. Shaw³, F. Rose¹, L. Buttery¹, and A. Tatler³

¹Division of Regenerative Medicine and Cellular Therapeutics, School of Pharmacy, University of Nottingham, University Park, NG7 Nottingham, United Kingdom

²Department of Chemical Engineering, Technological Institute of the Philippines, Quiapo, Manila 1001, Philippines

³Division of Respiratory Medicine, University of Nottingham, Nottingham City Hospital, Hucknall Road, Nottingham, NG5, United Kingdom

INTRODUCTION: Airway smooth muscle, capable of modulating the bronchomotor tone, has been associated with several life-threatening diseases such as asthma and COPD. These conditions exhibit hyperreactivity in terms of mechanical transduction within the airways. In this study, we have developed a hydrogel-based model to assess the effect of mechanical stiffness to the morphology, proliferation, and expression of α -smooth muscle actin of the primary human airway smooth muscle cells.

METHODS: Primary ASMCs (n=3) were expanded with 10% serum on hydrogels of increasing stiffness (1x, 6x, and 12x physiological stiffness) and assessed for proliferation by metabolic assay. Following serum starvation to induce a contractile phenotype the cell size was assessed using morphometric analysis and flow cytometry. Additionally, cells were immunostained for alpha-smooth muscle actin (α -SMA) expression. Finally, propidium iodide staining was used to determine cell cycle stage.

RESULTS: After 24h of serum starvation the morphology of ASMCs changed significantly as cell area, cell perimeter, and nuclei area increased with increased matrix stiffness ($p < 0.0001$). The aspect ratio and nuclei eccentricity decreased denoting a morphological change from “spindle-like” to a “spread-out” morphology ($p < 0.0001$). The increase in cell size was confirmed using flow cytometry, with increasing forward scatter as the matrix stiffened ($p = 0.0319$). α -SMA expression increased four-fold with increased matrix stiffness ($p < 0.0001$). Furthermore, increased matrix stiffness led to an increase in ASMC proliferation ($p = 0.0047$) and an increase in the percentage of cells in S phase of cell cycle ($p = 0.0125$).

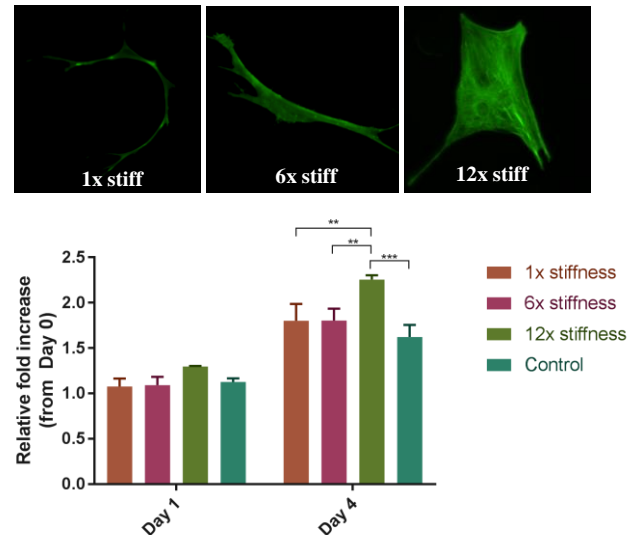


Fig. 1: α -SMA immunofluorescence of ASMCs and proliferation assay

DISCUSSION & CONCLUSIONS: The stiffness of the matrix affects the morphology, proliferation and the α -SMA expression of ASMCs. Together, the results suggest that the airway remodelling/stiffening could contribute to a phenotypic change on resident ASMCs, which occurs in chronic conditions such as asthma

ACKNOWLEDGEMENTS: This work is Funded by the Newton Agham grant from British Council and Department of Science and Technology by the Philippine Government.

REFERENCES:

- Berair, R., Hollins, F. & Brightling, C. Airway smooth muscle hypercontractility in asthma. *Journal of allergy* **2013**, 185971, doi:10.1155/2013/185971 (2013).
- Johnson, P. R. *et al.* Airway smooth muscle cell proliferation is increased in asthma. *Am J Respir Crit Care Med* **164**, 474-477, doi:10.1164/ajrccm.164.3.2010109 (2001).

An ex vivo tissue assay to reduce animal use in advanced genetic therapy testing

L. Smith¹, K. M Shakesheff¹, A Tatler¹, J. E Dixon¹

¹University of Nottingham

INTRODUCTION: There is currently need for development of advanced genetic therapies to treat rare genetic diseases; present animal based models do not provide accurate translation for human treatment, and expensive large and small *in vivo* pre-clinical trials require thousands of animals. Here, we utilise PCLS (Precision Cut Lung Slices) from mouse and patients, and the novel GET peptide delivery system to develop a model for genetic therapy testing, and investigate effects of enhanced vector, dose, and delivery parameters, alongside assessment of viability, transfection efficiency and comparison by weight/protein content. Visual analysis was also carried out, to determine location of expression, viability post transfection, and localisation of DNA. Such a platform to test lung gene delivery will be valuable in comparing new genetic therapies for Cystic Fibrosis (CF) and delivery of CFTR gene corrections, which we intend to investigate further with this model.

METHODS: PCLS were generated by lung perfusion, dissection and slicing on a vibratome, after which they were slow cooled and stored in liquid nitrogen long term. Batches of PCLS were thawed and utilised as needed. Initial viability was determined on Day 3 post thaw with an alamar blue viability assay. PCLS were transfected with pCMV-Glux, pGM206, and pGM206 modified with α SMAR (pGM206SMAR) vectors on Day 5 post thaw. Further viability assays and luciferase reporter assays were carried out at specific time points to determine viability and transfection efficiency over time, post transfection. Samples transfected with pGMZsgreen1 vector were imaged using fluorescence and confocal microscopy, on day of transfection and on days following transfection. Livedead staining was also carried out to determine visual viability.

RESULTS: Vectors, dosage, and delivery parameters: Initial comparison of serial delivery of standard Glux, pGM206, & pGM206SMAR demonstrated each vectors efficiency over time. Higher doses, 2 μ g in

particular, delivered on alternate days (Every two days or every three days) appeared to show the highest levels of transfection. **ZsGreen transfection:** initial fluorescence imaging and initial confocal data highlighted potential expression possibly in specific lung structures, and even individual cells. **Live dead for visual viability:** staining showed transfection did not negatively affect viability of cells within PCLS, regardless of transfection agent used or day imaged post-transfection. The most viable cells in all PCLS appeared to be specific to airway perimeters.

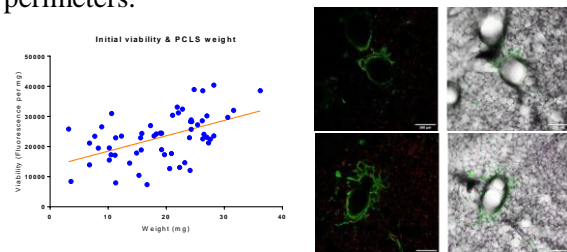


Fig. 1: Viability and weight show some positive correlation (left); and visual viability with Livedead confirmed transfection did not negatively affect cells within tissue (right).

DISCUSSION & CONCLUSIONS: Results demonstrate consistent viability and transfection efficiency of PCLS samples from batch to batch, and begin to identify vector efficiency and the potential delivery and dosage parameters needed. Further work will aim to identify DNA localization and cell types involved in transfection (IHC, fluorescent labelled DNA) and refine model adaptability to Air liquid interface (ALI). Once refined, it can be utilised to deliver CFTR gene corrections and test lung gene delivery, and could prove useful in future investigation of other lung disorders where gene augmentation or correction could be therapeutic.

ACKNOWLEDGEMENTS: EPSRC & MRC Regenerative Medicine CDT, & the RMCT Division at the University of Nottingham.

REFERENCES: G. Osman et al., J. Control. Release, 2018, 285, 35-45. Switalla et al. Tox Let. 2010, 71, 565. Rosner et al. Am J. Resp Sci Mol. Bio. 2014, 50, 876.

Anti-Inflammatory Properties of Corneal Stroma-Derived Stem Cells: Potential as a Topical Therapy for the Ocular Surface

O.D. McIntosh, M.L. Orozco Morales, N.M Marsit, A. Hopkinson, L.E. Sidney

Academic Ophthalmology, Division of Clinical Neuroscience, School of Medicine, University of Nottingham, Nottingham, England, UK

INTRODUCTION: The cornea functions to provide two thirds of the eye's refractive power, as well as being the major barrier to the inner content of the eye. At present, when the cornea is damaged or diseased, transplantation of a donor cornea, known as keratoplasty is the most effective technique to restore vision. However, worldwide 8-10 million individuals have no access to a corneal transplant. Furthermore, patients may suffer from rejection of allogeneic corneal tissue or have to wait for long periods before finding a viable donor graft. For these reasons, corneal research has turned to the use of stem cell-based regenerative therapies for corneal tissue regeneration. Corneal stroma-derived stem cells (CSSC) show potential as a stem cell source for corneal regeneration and wound healing, by acting as bi-directional sensory "factories" that secrete trophic factors in response to an injured microenvironment. Delivering CSSC topically to an injured corneal surface, using a substrate such as amniotic membrane (AM), represents a novel cellular therapy for severe keratitis conditions that can potentially lead to blindness.

METHODS: In this study, we optimised an in vitro inflammation model using human corneal epithelial cells (hCEC) treated with combinations of ethanol, and pro-inflammatory cytokines, interleukin 1- β and tumour necrosis factor- α . The effect of this combined injury was assessed for effect on hCEC viability and proliferation, cytotoxicity, cell lysis, and further expression of pro-inflammatory cytokines. To assess the anti-inflammatory potential of the CSSC, a co-culture system was used, with and without cells seeded on AM. Expression of anti-inflammatory trophic factors by CSSC was analysed using protein arrays and ELISAs.

RESULTS: Co-culture of the optimised hCEC injury model with the CSSC cell therapy led to increased hCEC viability and proliferation, decreased cytotoxicity and cell lysis, and

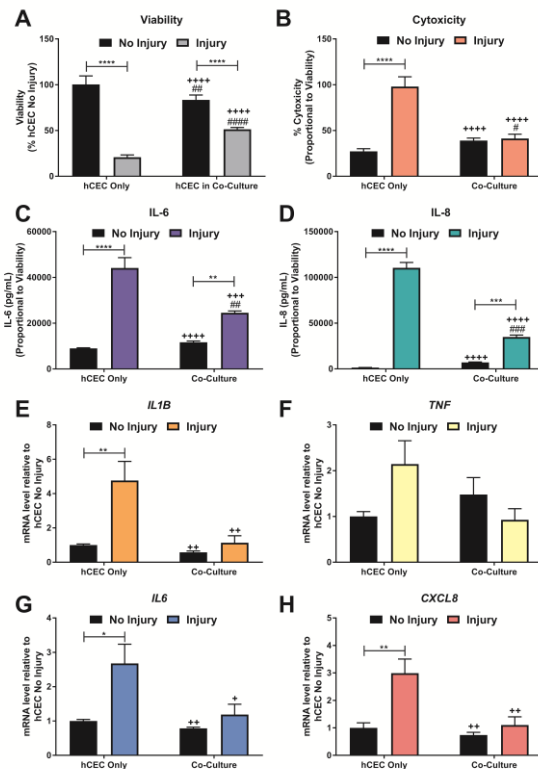


Fig.1 Effect of co-culture with CSSC on hCEC response after injury. hCEC were treated with an injury model consisting of 30s EtOH treatment followed by stimulation with 1 ng/mL IL-1 β for 72 h.

decreased levels of proinflammatory cytokines, when compared to injury alone, demonstrating the anti-inflammatory potential of the CSSC. CSSC could be easily cultured on the AM, establishing a promising method of applying the cells topically to the cornea.

DISCUSSION & CONCLUSIONS: CSSC demonstrate an anti-inflammatory effect with potential to be clinically translated into a topical therapy for the injured ocular surface, using a carrier such as amniotic membrane.

ACKNOWLEDGEMENTS: Funded by Laura Sidney's Anne McLaren Fellowship, Fight for Sight and an EPSRC Impact Acceleration Award.

Antibacterial efficacy of nitric oxide releasing hydrogels on 2D and 3D human skin models

Robert C. Deller¹, Jenny Aveyard¹, Rachel L Williams² and Raechelle A D'Sa^{1*}

¹School of Engineering, University of Liverpool, ²Institute of Ageing and Chronic Disease, University of Liverpool
 Corresponding author: rdsa@liverpool.com

Introduction

The healing of burn wounds are hindered by bacterial infections which can lead to increases in morbidity and mortality rates.[1, 2] This problem is exacerbated by the rise in multidrug resistant bacterial strains that limit the efficacy of antibiotics.[3] Alternative approaches such as nitric oxide have shown promise as potent and broad-spectrum antimicrobial agents which can interact with DNA, lipids and proteins thereby killing the bacteria.[4] Nitric oxide also serves as a signalling molecule that can stimulate the immune response and wound healing processes.[5] Here we investigate the antimicrobial efficacy of nitric oxide releasing materials against *Staphylococcus aureus* and a secreted extracellular protease (V8 protease) capable of disrupting epithelial barrier function.[6, 7]

Materials and Methods

A variety of standardised biophysical techniques and commercially available *in vitro* biochemical assays have been utilised to characterise the physical and chemical properties of our nitric oxide releasing materials (e.g. chemiluminescence) and their efficacy against *S. aureus* (NCTC 13811) and V8 protease. Subsequent impact on cell viability (e.g. alamar blue) and cell functionality (e.g. transepithelial electrical resistance) utilised HaCaT (skin keratinocyte) and WS1 (skin fibroblast) human cell lines co-cultured on 1 µm Polyethylene Terephthalate (PET) membranes.

Results and Discussion

Here we demonstrate a pH mediated burst release of nitric oxide from diazeniumdiolate functionalised hydrogels over a 24 hour period. Diazeniumdiolate functionality was confirmed by FT-IR and pH mediated nitric oxide release via chemiluminescence. The bactericidal efficacy of our nitric oxide releasing materials was assessed directly against *S. aureus* at several initial seeding densities and time points. Activity against the *S. aureus* secreted V8 protease was determined by changes in the rate of proteolytic cleavage of a fluorescently labelled tripeptide and changes in the transepithelial electrical resistance of co-cultured HaCaT and WS1 cells on 1 µm PET membranes. Subsequent viability (e.g. Live/Dead) and barrier functionality (e.g. zonula occludens-1 immunostaining) assessments against co-cultured skin keratinocytes (HaCaT) and skin fibroblasts (WS1) highlight the biocompatibility of our nitric oxide releasing materials. Preliminary work has also explored the utilisation of our nitric oxide releasing materials against a wounded and subsequently *S. aureus* infected 3D human skin equivalent (Labskin^{1.1}). Current work is focussing on the administration of *S. aureus* to our co-cultured systems and subsequent treatment with our nitric oxide releasing materials to assess concurrent antimicrobial and functional activities.

Conclusions

pH responsive nitric oxide releasing materials are capable of acting as a potent antimicrobial agents against *S. aureus* without detrimental impact to the viability and functionality of multiple human skin cell types.

References

- [1] Daum R.S. N. Engl. J. Med., 357: 380-390, 2007.
- [2] Norbury W. *et al.* Surg Infect (Larchmt). 17: 250-255, 2016.
- [3] Foster T J. FEMS Microbiol. Rev. 41: 430-449, 2017.
- [4] Martinez L R *et al.* J. Invest. Dermatol. 129: 2463-2469, 2009.
- [5] Schairer D O *et al.* Virulence. 3: 271-279, 2012.
- [6] Ohnemus U *et al.* J. Invest. Dermatol. 128: 906-916, 2008.
- [7] Murphy J *et al.* Laryngoscope. 128: E8-E15, 2018.

Acknowledgements

All authors acknowledge funding from the engineering and physical sciences research council (EPSRC) UK healthcare impact partnership 2017 grant EP/P023223/1.

Armoured growth factors for tissue engineering

C. Whitty¹, J. Oswald², C. Pernstich¹, P. Baranov², M. Jones¹

¹Cell Guidance Systems Ltd., Babraham Research Campus, Cambridge, UK

²Harvard Medical School, Boston, MA, USA

INTRODUCTION: The inherent instability of recombinant growth factors (GFs), with typical half-lives ranging from minutes to hours, limits their utility in the lab and the clinic. Efficacy may be improved by encapsulation within biomaterials to provide sustained bioavailability over a longer time. However, current delivery systems are limited by protein denaturation and burst release. Refinement of delivery systems to provide sustained release and improved retention may provide therapeutic efficacy at lower doses, improving cost-effectiveness and preventing adverse side effects. PODS (Polyhedrin Delivery System) is a highly durable, crystalline product which encases a GF of interest within polyhedrin protein. The stability of PODS means that crystals degrade slowly, resulting in a steady release of protein over several weeks at physiologically-relevant levels. Here, we show that PODS crystals can functionalise biomaterials for sustained GF release, and that PODS improve 3D retinal ganglion cell (RGC) organoid culture, compared with standard recombinant GFs.

METHODS: For biomaterial functionalisation, PODS were incorporated into electrospun PCL and PLA fabrics, and peptide-based hydrogels. Release of GF over time was measured by ELISA. For organoid formation, mouse embryonic stem cells (mESCs) were cultured in optic vesicle medium, and from Day 9 were transitioned to optic cup medium. PODS GFs factors were introduced to the culture system on Day 20 by a single addition of both PODS BDNF and PODS GDNF crystals. During the 10-day period of PODS treatment, a single half media change was performed. Fluorescence-activated cell sorting (FACS) was utilised to analyse three RGC subtypes by measuring three cellular markers (Brn3a, osteopontin and melanopsin). Quantification of total RGCs was assessed using the neurochemical marker RBPMS.

RESULTS: Bright and fluorescence microscopy indicated that PODS were successfully incorporated into biomaterials.

ELISA data indicated that growth factor was released in a sustained manner over time. FACS data showed that yields of each RGC subtype (and therefore total RGCs) were increased by as much as 2-fold by the addition of PODS GFs (Fig. 1). Organoids incubated with PODS crystals appeared healthier with smoother surfaces. An RGC increase approaching that achieved with PODS could only be attained by supplementing with 250 ng each of recombinant BDNF/GDNF, which was added every two days over the 10-day culture period.

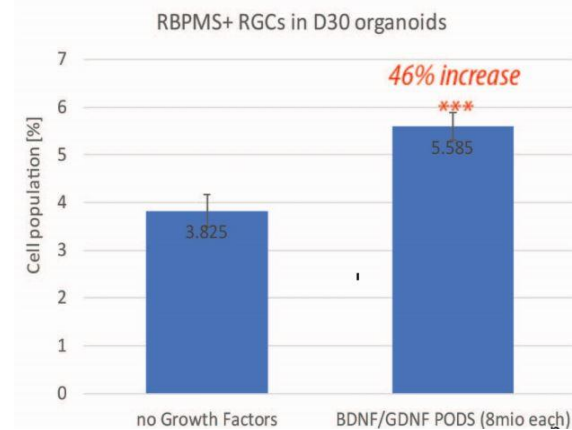


Fig. 1: FACS shows that culturing with PODS BDNF and PODS GDNF increases total RGCs

DISCUSSION & CONCLUSIONS:

Sustained release GFs may provide a solution to the inherent instability of standard recombinant GFs. Improved RGC organoid formation was observed by culturing with PODS GDNF and PODS BDNF compared with standard recombinant GFs. Furthermore, PODS can pattern surfaces or be incorporated into biomaterials to functionalise scaffolds, for a wide range of applications.

ACKNOWLEDGEMENTS: RGC organoid culture and FACS was performed by J. Oswald and P. Baranov. Release assays and biomaterial incorporation was performed by C. Whitty.

Assessing the paracrine effects of fat on dermal fibrosis

S. J. Higginbotham¹, V. L. Workman¹, N. Green¹, D. L. Lambert², V. Hearnden¹

¹ *Department of Materials Science and Engineering, The University of Sheffield, UK.*

² *School of Clinical Dentistry, The University of Sheffield, England, UK.*

INTRODUCTION: Pathological fibrosis results from a lack of myofibroblast apoptosis upon the finalisation of wound healing. After tissue damage Transforming Growth Factor Beta-1 (TGF β -1) causes fibroblast differentiation to myofibroblasts. Subcutaneous injections of lipoaspirate have been shown to inhibit this process¹. Despite this knowledge, little has been done to elucidate the mechanisms behind the regenerative powers of adipose tissue. This project's aims are to test the efficacy of various forms of human adipose tissue at reducing fibrotic markers and their effect on myofibroblast differentiation.

METHODS: Human dermal fibroblasts (HDFs) were differentiated into myofibroblasts using 5ng/ml of TGF β -1. The protein and RNA levels of myofibroblasts markers α -SMA, FN1-EDA, and Col-1 were then assessed using a combination of qPCR, western blotting, and immunofluorescence. Human tissue from NHS liposuction was either left as lipoaspirate, used to isolate Adipose Derived Stem Cells (ADSCs) or processed into Nanofat². We intend to examine how paracrine factors from these forms of adipose tissue effect myofibroblast differentiation. Conditioned medium will be taken from these deposits and HDFs will be cultured with this medium along with TGF β -1. Levels of myofibroblast differentiation will be examined as before to determine the relationship between adipose paracrine factors and fibrosis. Adipose and dermal tissue was taken by informed consent under ethics approval 15/YH/0177.

RESULTS: Incubation with TGF β -1 resulted in increased expression of fibrosis markers. RNA markers FN1-EDA and Col-1 showed increased expression after 72 hours of TGF β -1 treatment (Figure 1). Protein levels of α -SMA were also increased after treatment (Figure 2). Examination of the effects of adipose conditioned medium will be forthcoming.

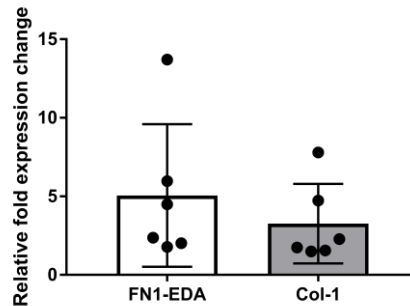


Fig. 1: Change in expression of fibrotic markers FN1-EDA, Col-1(A) compared to housekeeping gene U6.

DISCUSSION & CONCLUSIONS:

Incubation with TGF β -1 was sufficient to induce a myofibroblast phenotype in dermal fibroblasts. Adipose tissue is known to secrete a variety of paracrine factors that may inhibit fibrosis such as Fibroblast Growth Factor³. Our future work will examine whether this can prevent fibroblast to myofibroblast differentiation.

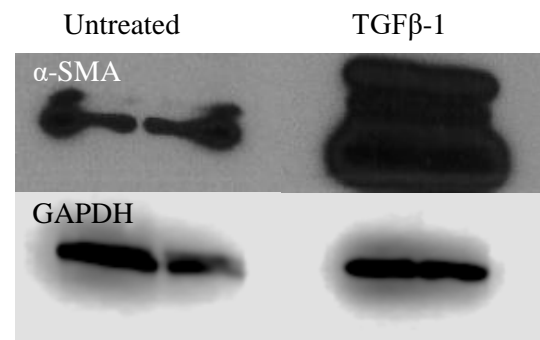


Fig. 2: Protein expression levels of α -SMA compared to housekeeping gene GAPDH in HDFs treated with and without TGF β -1.

ACKNOWLEDGEMENTS: Thanks to ESPRC, Ms Victoria Giblin and the Sheffield Hospital Directorate of Plastic, Reconstructive Hand and Burns Surgery for the patient samples.

REFERENCES: [1] Rigotti *et al.* (2007) *Plast Reconstr Surg.* 119(5): 1409-22. [2] Tonnard *et al.* (2013) *Plast Reconstr Surg.* 132(4): 1017-26. [3] Moon *et al.* (2012) *Int J Mol Sci.* 13(1): 1239-57.

Assessment of lithium exposure in an *ex vivo* chick femur culture model

N. Salam¹, S. Hoppler¹, I. Gibson¹

¹*Institute of Medical Sciences, School of Medicine, Medical Sciences, and Nutrition, University of Aberdeen, UK*

INTRODUCTION: The deficit in translating bone regeneration approaches from *in vitro* to *in vivo* has led to increased adoption of complex culture models to bridge this gap ⁽¹⁾. *Ex vivo* organ culture models offer anatomical preservation without the expense and arduousness of *in vivo* research. In particular, the embryonic chick femur model permits assessment of endochondral ossification in an economical and high-throughput manner ⁽²⁾. Using this model, chemical activators or inhibitors, growth factors, and culture environments, can be studied. Previous research has established the relationship between Wnt signalling and bone biology ⁽³⁾. Hence, the aim of this work is to investigate the effect of lithium, an activator of canonical Wnt signalling, on skeletal tissue.

METHODS: Femurs from E9, E10, and E11 chick embryos were isolated and cultured for 10 days at the gas/liquid interface as depicted in *Fig. 1*. After 24 hours in basal media to allow for acclimatisation, femurs were cultured in basal media or supplemented with lithium chloride at 1, 10, and 25 mM for a further 9 days. At culture endpoint, the morphology of femurs was observed following Alcian blue/Alizarin red whole mount staining, while, ossification markers were assessed *via* histology and immunohistochemistry.

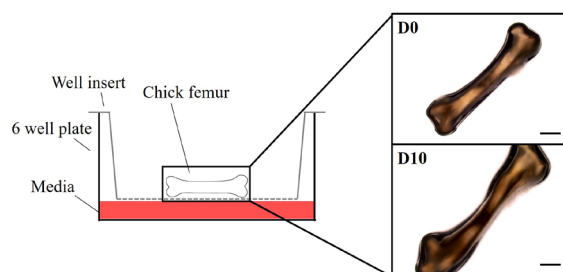


Fig. 1: Culture setup of the embryonic chick femur model. Brightfield images depict E10 femurs in basal media at culture outset and endpoint; scale bar represents 1 mm.

RESULTS: Results demonstrated greater osteogenesis upon lithium exposure with increased osteoid production (collagenous bone matrix), mineralisation, and expression of late-stage endochondral ossification markers. Comparisons between different embryonic stages suggested later stage femurs required a higher lithium concentration. However, high lithium concentrations (25 mM) elicited loss of cartilage, regardless of embryonic stage, as demonstrated with the absence of Alcian blue staining.

DISCUSSION & CONCLUSIONS: Data presented adds to the growing literature on lithium's effect on chondrogenesis and osteogenesis. Exploring the interaction between lithium concentration and cells of different origins and lineage-commitment, furthers our understanding of lithium's potential in fracture repair. Accordingly, these findings have implications on future fabrication of lithium-containing bone scaffolds.

ACKNOWLEDGEMENTS: This work is supported by a doctoral studentship from the Institute of Medical Sciences at the University of Aberdeen.

REFERENCES:

1. G. Hulsart-Billström *et al.*, *Eur. Cell. Mater.* **31**, 312–22 (2016).
2. E. L. Smith, J. M. Kanczler, R. O. C. C. Oreffo, *Eur. Cells Mater.* **26**, 91–106 (2013).
3. R. Baron, M. Kneissel, *Nat. Med.* **19**, 179–192 (2013).

Association of Environmental Cues with Mesenchymal Stem Cell Fate

R Al Hosni, S J Roberts, U Cheema

Department of Materials and Tissue, UCL, London, UK

INTRODUCTION: Tissue engineering and regenerative medicine aims to develop stem cell-based therapies for the treatment of bone fractures. Efforts to deliver mesenchymal stem cells (MSCs) in bio-degradable scaffolds, have illustrated the limitations associated with loss of cell phenotype and/or cell death post-implantation. Thus, it is imperative that an understanding of the interaction between MSCs and their extracellular matrix (ECM) is developed so as to maintain cell viability and potency. A potential solution is to recapitulate the physical niche and microenvironment in which stem cells reside *in situ*, which is known to influence stem cell fate¹. These micro-environmental cues include stiffness, geometry and oxygen tension. This study aims to identify and understand the biophysical components of the bone marrow pericytic niche required to maintain MSC characteristics and to trigger stem cell differentiation.

METHODS: In attempt to replicate the biophysical properties of the MSC niche, a collagen type-1 matrix was utilised. This matrix protein is a prominent ECM component, which is thought to facilitate the ECM-cell interactions required to modulate proliferation, self-renewal and differentiation of skeletal stem cells. Immortalised pericytic MSCs (iMSCs) were cultured in a 2D monolayer or 3D rat-tail collagen type-1 with a density of either 0.2% or 10%, supplemented with conventional growth medium as illustrated in Figure 1A. The cells were cultured in either 20% O₂ or physiological normoxia at 5% O₂. The signalling dynamics in each condition was assessed using qPCR.

RESULTS:

iMSCs cultured in a 0.2% collagen matrix at physiological normoxia for 14 days, displayed significant increases in defined skeletal stem cell markers (*CD164*, *CD73*, *NESTIN*, *PDPN* and *PRX1*) and transcription factors associated with osteogenic (*RUNX2*) and chondrogenic (*SOX9*) lineage commitment, relative to cells cultured in either 2D or a 10% collagen matrix.

As ECM stiffness is known to influence cellular behaviour, a further study was conducted to assess the cell's ability to regain stem-like

characteristics, which were initially lost when cultured in a 10% collagen matrix². A dynamic stiffness culture was prepared by culturing iMSCs in a 10% collagen construct for a period of 7 days and subsequently embedding it in a less dense 0.2% collagen matrix for 14 days under physiological normoxia (Figure 1B). Following 14 days, the iMSCs that previously illustrated minimal stem cell characteristics in the dense collagen scaffold, demonstrated significant increases in all human skeletal stem cell markers upon migration into the less dense environment. Additionally, expression of *RUNX2* and *SOX9* significantly increased.

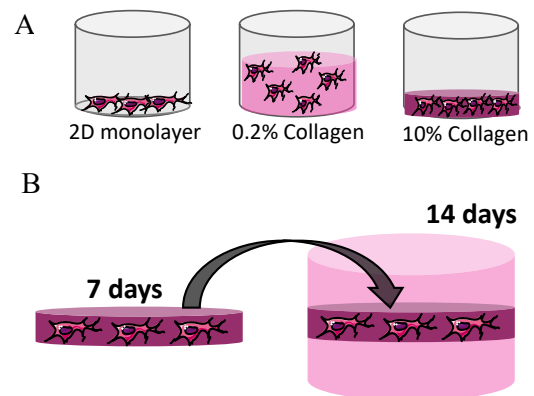


Figure 1: Schematic of the (A) 2D and 3D cultures and (B) dynamic stiffness culture.

DISCUSSION & CONCLUSIONS:

These data indicate the impact that the microenvironment has on stem cells and suggests a biomechanical requirement for stem cell identity. Specifically, this relates to the ability of pericytes to retain their stem cell markers and potentially guide cell fate determination.

The application of an *in vitro* engineered MSC niche allows for the understanding of the role of each ECM component and other biophysical and mechanical factors on directing the resident stem cell behaviour. Synthesizing a well-defined environment as a tissue substitute for implanting stem cells *in vivo* is a promising approach to maintaining stem cell characteristics and prime the bone regeneration cascade.

REFERENCES: (1) Lin, H. et al., 2019. *Biomaterials*, 203, pp.96-110. (2) Guilak, F. et al., 2009. *Cell stem cell*, 5(1), pp.17-26.

Biocompatibility of Graphene for Regenerative Medicine Applications using Dental Pulp Stem Cells

I Slinn¹, C Banks², L. A. Hidalgo-Bastida^{1,2,3}

¹Centre for Biomedicine, ²Centre for Advanced Materials and Surface Engineering, ³Centre for Musculoskeletal Science and Sports Medicine, Manchester Metropolitan University, UK

INTRODUCTION: Dental pulp stem cells (DPSCs) have been shown to be a phenotype of mesenchymal stem cells (MSCs), possessing their pluripotency, but with the benefit of deriving from teeth, thus yielding an abundant source of these cells. DPSCs have shown to proliferate and differentiate faster than regular MSCs, due to this their potential in regenerative medicine is high. Graphene oxide (GO) has rapidly become one of the most researched nanoparticles due to its unique characteristics, the relatively simple method to synthesize and the ability to control its characteristics during synthesis. The difficulty arises when one tries to introduce graphene oxide into the environment of the DPSCs. Due to GOs poor dispersion into growth media at high concentrations, the question stands as to how much of an effect if any does GO have on the proliferation of DPSCs. This work examined whether GO has any effect on the proliferation of DPSCs in a 2-dimensional environment, while determining whether the dispersion and charge of GO in growth media can be improved to provide optimal conditions for the cells to thrive.

METHODS: The characterisation of the graphene oxide (GO) was done through various methods including, Zetasizer (Malvern) to determine the dispersion in growth media, the size of the flakes and the charge of the solution. UV/Vis spectroscopy (UV/Vis agilent 8453) and zetasizer tests were performed to optimise the method of dispersion of GO in growth media, ultra-sonication in a water bath (ultrasonic bath XUBAI) and probe sonication (Vibra cell probe sonicator). SEM images (Zeiss supra 40vp) of GO determined the aggregation and smoothness of the GO flakes. Mesenchymal stem cells and Dental pulp stem cells (Axol) were exposed to GO growth media and incubated (autoflow IR direct heat CO2 incubator) for up to 7 days and tested for viability with cell titer glo (Promega, plate reader Biotek gen5).

RESULTS: GO was characterised when in media physically and for biocompatibility with DPSCs, showing that both the charge and the concentration of GO in media affect the dispersion.

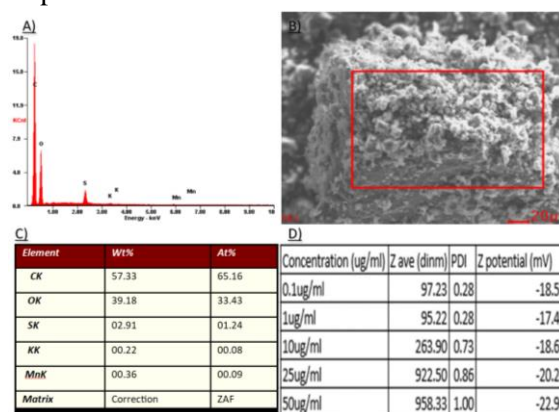


Fig. 1: Graphene oxide characterisation. A) EDX graph of GO, B) SEM image of GO. C) EDX table values of GO, D) Zetasizer results of testing GO dispersion in DMEM 4.5g/L glucose media shown in the zeta average (size of flakes), PDI (dispersion value) and zeta potential (charge of the liquid sample).

DISCUSSION & CONCLUSIONS: The net charge of the cell culture growth media with GO was not favourable (-22mV) as the net charge of the nanoparticle determines how it will be taken up into the cell. The optimal value found was ~ +40mV as the positive charge exhibits superior internalisation levels due to the electrostatic interaction between the nanoparticle and the negatively charged cell membrane causing an increased cellular uptake of the nanoparticle.

ACKNOWLEDGEMENTS: We thank the technical staff of the School of Healthcare Sc and the School of Sc and Environment (MMU) for all the technical support.

BIOENGINEERING 3D MICROENVIRONMENTS TO STUDY MECHANOTRANSDUCTION AND VASCULARIZATION IN BONE REGENERATION

Sofia Perea-Ruiz, T. Hodgkinson, M. J. Dalby and M. Salmerón-Sánchez
 Centre for the Cellular Microenvironment (CeMi), University of Glasgow, Scotland, UK
 Corresponding author: speruiz@gmail.com – PhD student (2nd year)

Introduction

Bone is a high vascularized tissue so engineering successful novel bone biomaterials must involve not only the formation of new bone tissue but also promote the creation of a microvascular environment resembling the uninjured tissue. In the present work, VEGF is presented tethered to poly-ethyl acrylate (PEA) to induce vascularization. This polymer has been shown to allow solid-phase presentation of GFs through material surface-binding mimicking the stem cell microenvironment and allowing low and controlled dose administration of signals¹. In addition, the current work is focused in the application of nanovibrational stimulation or 'nanokicking' (NK) in order to study stretch-activated ion channels, gated specifically by mechanical force in mesenchymal stem cells (MSCs). This mechanical stimulation have shown a strong osteogenic response in two-dimensional (2D) and three-dimensional (3D) conditions^{2,3}.

Materials and methods

Fibrin gel in vitro angiogenesis assay was used to evaluate tube formation of HUVECs in 24-well plates. Briefly, after FN (20 µg/ml) and VEGF (25 ng/ml) coatings, cells were seeded at a density of 10,000 cells/cm² complete endothelial cell medium and left at 37 °C overnight. Then, fibrinogen and thrombin were added to the plates which were placed in CO₂ incubator at 37 °C for 1 hour to polymerize. After clotting, fibrin matrix was covered with endothelial complete growth medium that was changed every 48 hours. Plates were nanostimulated during this period by a bioreactor at 1000 Hz and 30nm. After this, immunostaining was carried out for CD31 and phalloidin to evaluate protein expression and tubular formation.

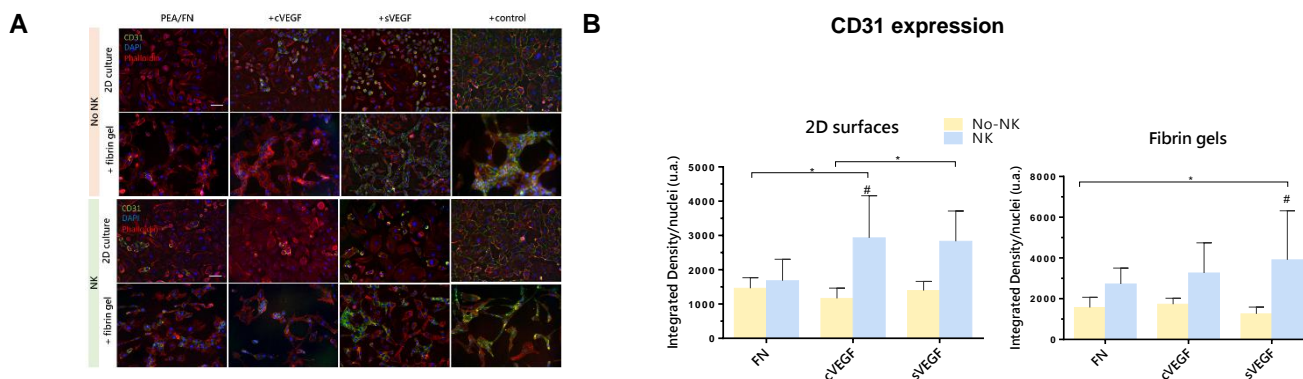


Figure 1. **A-** Immunofluorescence images of ECs monocultures after 7 days under stimulated (NK) or unstimulated (No-NK) conditions. Scale bar: 100 µm. cVEGF = Surface VEGF-coated; sVEGF = soluble VEGF in media. **B-** Quantification of CD31 expression of image A. Statistical significances attributes to values $p < 0.05$ as determined by two-way ANOVA with Tukey's multiple comparisons test (* p-value between groups; # p-value within the same group).

Results and Discussion

CD31, an adhesion molecule that is expressed in intracellular EC junctions, plays a crucial role in the formation and maintenance of vessels as well as in forces transduction. In 2D conditions, ECs do not form any tubular-like structure and expression of CD31 is only significantly higher between stimulated and unstimulated groups in coated-VEGF surfaces. When fibrin gels are present, only soluble VEGF showed statistical differences, although an increased general trend is noticeable for NK samples.

Conclusion

The material-based system allows engineering a model for angiogenic and osteogenic growth factors binding. With an in vitro angiogenesis assay, CD31 analysis suggests that nanovibrations themselves do not seem to induce tubule formation but does it appear to increase CD31 expression. We could propose that this will make the cells more receptive to MSCs, but not affecting vasculature formation per se. Thus, co-cultures with MSCs are being carried out in order to further investigate this concept.

References

- Llopis-Hernández, V. *et al. Sci. Adv.* **2**, e1600188 (2016).
- Tsimbouri, P. M. *et al. Nat. Biomed. Eng.* (2017).
- Childs, P. G. *et al. Acta Biomater.* **34**, 159–168 (2016).

Bioengineering Dual Gradient Platforms for the Control of Cell Behaviour and Differentiation

Laurissa Havins,¹ Mark Lewis,² Steve Cristie,¹ Paul Roach¹

¹Department of Chemistry, Loughborough University ²School of Sport and Exercise Medicine/Loughborough University
 Corresponding author: L.Havins@lboro.ac.uk – PhD student (1st year)

Introduction

In an aging population, diseases targeting neuron subsets in the brain are becoming more prevalent. In the UK, approximately 270,000 people in the UK suffer with Parkinson's disease which is poorly treated and understood. Treatments available currently depend on delaying progression rather than prevention or cure and therefore it is crucial that new methods of treatment become available. Generation of mature and functional neurons as a clinical therapy for a therapeutic benefit is one possible avenue.

Neuron development *in vivo* is reliant on the surrounding environment for signalling cues, morphogen gradients and extracellular matrix (ECM) support (1). These factors play an important role in deciding neural progenitor fate. In a tightly controlled, specific environment, biological proteins provide a concentration gradient, driving progenitors through differentiation (2). The ability to harness these distinct characteristics for *in vitro* work may enable the differentiation of neuron subtypes, which could ultimately be used within the clinic.

The aim of this work is to drive work towards recapitulating a controlled biochemical gradient environment. Cell attachment is tightly regulated through the use of a cell-phobic poly(potassium 3-sulfopropyl methacrylate) (PKSPMA) polymer brush layer. The polymer brush surface is designed as a dual gradient, whereby the a density gradient is presented orthogonally to a polymer chain-length gradient, thus allowing fine control over biochemical attachment and exhibition. Biological proteins are attached to the ends of the polymer brush, creating a change in protein concentration across the gradient surface. Our hypothesis is that this surface environment will affect attachment and subsequent behaviour of cells.

Materials and Methods

Borosilicate glass coverslips are chemically modified by a polymer brush using a surface initiated atom transfer radical polymerisation methodology. After immersion in 2-bromoisobutyryl bromide- acetonitrile (BIBB-ACN) solution for 1hr, initiator prepared coverslips are then immersed in pKSPMA solution and polymer is grown for 1hr. NHS-ester functionalisation is carried out in two stages, first using tris(2-aminoethyl)amine in DMF for 48 hrs under nitrogen at 65 °C. This is followed by immersion in DCM with DMSO and DMAP for 18 hrs under nitrogen. FITC staining was carried out and imaged using fluorescence microscopy. Cell culture was carried out using SH-SY5Y neuroblastoma cells seeded at 200,000 per well in a six well plate. Cells were fixed with formaldehyde and stained with DAPI and F-Actin after two days. Plates were imaged using fluorescence microscopy. Analysis was carried out on chemistry treated slides using x-ray photoelectron spectroscopy (XPS), fourier- transform infrared spectroscopy (FTIR) and drop shape analysis (DSA).

Results and Discussion

A BIBB-ACN initiator gradient was analysed and confirmed through DSA, with a clear contact angle gradient. The pKSPMA polymer brush treated coverslips were analysed using XPS, FTIR and DSA to discern whether the chemistry had been deposited correctly. Results confirmed chemical modification of the surface. SH-SY5Y seeding on half-treated polymer surfaces showed a preference of attachment on the clean glass rather than the polymer. FITC binding after the NHS-ester functionalisation step showed fluorescence on the polymer half of the coverslips only, confirming again that the functionalisation chemistry had worked. The results show clearly that polymer brush chemistry has been deposited on the surface, and acts as a 'cell-phobic' zone for cells seeded onto the surface. This allows us to manipulate cell attachment on the surface in a highly controlled way, especially when a gradient is employed.

Conclusions

With this biomaterial interface, the ability to control and manipulate cell growth is optimised. The dual gradient system allows for two variables to be introduced in a controlled manner, without the need for complex or messy experiment set ups. The addition of a biological gradient reflects the signalling system seen within the brain during development and neurogenesis, which is an important aspect when attempting to derive mature neurons. Whilst in its early stages, this work lays the foundation for designing a high-throughput system of generating neurons in a controlled manner, in an environment reflecting *in vivo* ECM like support.

References

1) Chen L *et al.* J. Materials Today. 21: 38-59, 2018. 2) Sansom S *et al.* J. Csh Perspect Biol. 1:a002519,2009.

Acknowledgements: We acknowledge support from EPSRC CDT in Regenerative Medicine and Lboro School of Science for funding.

Bioresponsive hydrogels for on-demand modulation of elastase activity

R. Obenza-Otero^{1*}, E. Russo¹, D. Clements², S. Johnson², M. Ashford³, P. Gellert³, W. Chan, G¹. Mantovani¹, M. Zelzer¹.

¹School of Pharmacy, University of Nottingham, UK. ²School of Medicine, University of Nottingham, UK. ³AstraZeneca, Charter Way, Silk Road Business Park, Macclesfield, UK.

*rebeca.obenzaotero@nottingham.ac.uk

INTRODUCTION: Bioresponsive materials able to release their cargoes in response to disease-specific cues are of great interest for targeted therapeutics due to their potential to limit drug release to its site of action, minimising side effects¹. The use of proteases as triggers for biomaterial response is particularly attractive as upregulated protease activity, such as elastase, is related to several pathological states like tissue destruction associated with chronic wounds and respiratory diseases¹⁻³. As elastase also possesses important functions crucial for maintaining a healthy status, full enzyme suppression is not desirable. Instead modulation of elastase activity to restore the natural protease/inhibitor balance that favours tissue integrity restoration would be advantageous. Feedback-controlled modulation of elastase in response to the actual enzyme activity can be achieved by incorporating inhibitors and elastase-sensitive components in the material. For this reason we aimed to develop peptide-crosslinked PEG hydrogels able to release the elastase inhibitor α -1-antitrypsin in response to the level of elastase in its environment, mimicking the body's natural strategy for balancing proteases levels for restoring tissue integrity (Fig.1).

METHODS: Thiol-reactive poly(ethyleneglycol) (PEG) was crosslinked with elastase-sensitive peptides⁴. Physicochemical properties of hydrogels were characterised by NMR and rheology. Macromolecule encapsulation and elastase-responsive properties of the hydrogels were assessed by encapsulation and release of fluorescently labelled dextrans (Mw 40kDa and 70 kDa). The elastase inhibitor α -1-antitrypsin (AAT) was encapsulated and its release in presence and absence of elastase characterised. Elastase was externally supplemented to A549 cells to reproduce detrimental effects of elastase on epithelial cells. Effect of hydrogels, elastase, and AAT in cell viability and migration on epithelial cells was assessed by the PrestoBlue and scratch assays, respectively.

RESULTS: Hydrogels showed strong mechanical properties (G' in the kPa range) and mesh sizes in the nanometer range. Encapsulated dextrans

followed a sustained release profile after an initial burst release. Higher release of dextrans upon incubation with elastase confirmed the elastase-controlled release mechanism of the hydrogels. Hydrogels did not affect cell viability. Elastase decreased epithelial cell viability and migration in a concentration-dependant manner with significantly lower metabolic activity and slower migrations from 10 nM. Administration of AAT lead to recovery of the cell migration and metabolic activity.

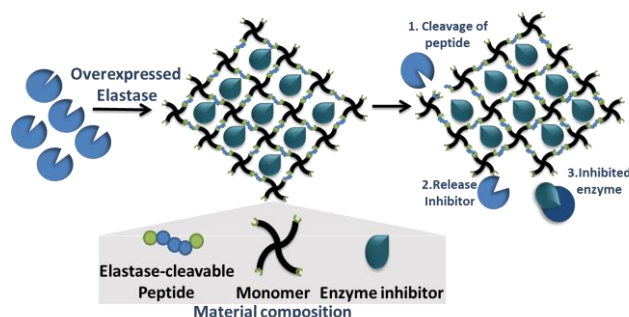


Fig. 1: Preparation and mechanism of protease-modulation from elastase-responsive hydrogels.

DISCUSSION & CONCLUSIONS:

Functionalised polymeric hydrogels successfully encapsulated model macromolecules and α -1-antitrypsin and they showed to be biocompatible. Elastase-controlled release of hydrogels was demonstrated, highlighting their potential as elastase-responsive delivery systems. The detrimental effects of overexpression of elastase in epithelial cell viability and repair function were successfully reversed after administration of AAT elastase inhibitor, showing promising applications for this therapy.

ACKNOWLEDGEMENTS: EPSRC grant number EP/L01646X. B Coyle is acknowledged for the valuable scientific discussions about materials testing.

REFERENCES: ¹R. Chandrawati. *Exp Biol Med.* 2016. 972-979. ²W.L. Lee, G.P. Downey. *Am J Respir Crit Care Med.* 2001. 896-904. ³T. E. Serena, B. M. Cullen, S. W. Bayliff, *et al.*, *Wound Repair Regen.* 2016. 589-595. ⁴A. A. Aimetti, A. J. Machen, K. S. Anseth. *Biomaterials.* 2009. 6048-6054.

Blended PCL/PLA/GO grooved nerve guide conduit for the treatment of peripheral nerve injury

Y. Lu¹, C.F. Blanford^{1,2}, A.J. Reid³, J.E. Gough¹

¹School of Materials, University of Manchester, UK, ²Manchester Institute of Biotechnology, University of Manchester, UK, ³Division of Cell Matrix Biology & Regenerative Medicine, School of Biological Sciences, University of Manchester, UK

INTRODUCTION: Peripheral nerve injury can be treated by autograft, however this has many disadvantages. Synthetic and natural nerve guide conduits can be used as a bioengineering solution [1]. One advantage of this technique over the traditional autograft is that various defect sizes and lengths depending on individual patients can be achieved without secondary surgical harvest. Development of off-the-shelf conduits requires extensive materials development and characterisation. Mechanical properties and adequate shelf life post-sterilisation are key factors for success [2]. This study investigates the effects of the addition of graphene oxide (GO) on conduit properties, due to the intrinsic physical and biological properties of graphene-family nanomaterials.

METHODS: PCL/PLA/GO films were fabricated by blending PCL/PLA and graphene oxide nanoparticles using solvent casting within an environmental chamber. In order to investigate the influence of sterilization on fabricated films, we initially applied ultraviolet sterilization on both PCL/PLA films and modified PCL/PLA/GO films.

RESULTS: Homogeneous PCL/PLA/GO films were fabricated successfully, with integrated grooved pattern (Fig.1). *In vitro* study of adipose derived stem cells differentiated toward a Schwann cell-like phenotype (dASC), indicated positive results on modified films (Fig.2). In terms of thermal properties, DSC results indicated that the addition of GO can improve T_g of materials from -33.86°C (PCL/PLA) to -27.49°C (PCL/PLA/GO).

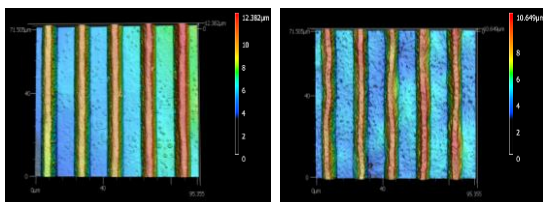


Fig. 1: Surface morphology of fabricated films: PCL/PLA (left) vs. PCL/PLA/GO (right).

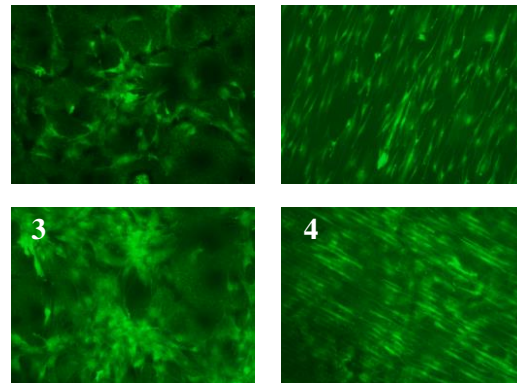


Fig. 2: Effect of addition of GO on dASC cell morphology and viability: Flat PCL/PLA (1), Grooved PCL/PLA (2), Flat PCL/PLA/GO (3) and Grooved PCL/PLA/GO.

DISCUSSION & CONCLUSIONS: The addition of GO resulted in maintenance of the integrity of the grooved pattern with better surface wettability and surface roughness. Initial results suggest improved responses by adipose derived stem cells differentiated to a Schwann cell phenotype. Modified films were able to keep their macro-structure without the evidence of loss of mechanical properties.

ACKNOWLEDGEMENTS: The authors would like to gratefully acknowledge the China Scholarship Council (CSC) for financial support of the project.

REFERENCES:

- [1] Muheremu A, Ao Q. Past, present, and future of nerve conduits in the treatment of peripheral nerve injury. *BioMed research international*. 2015.
- [2] Hukins DW, Mahomed A, Kukureka SN. Accelerated aging for testing polymeric biomaterials and medical devices. *Medical engineering & physics*. 2008 Dec 1;30(10):1270-4

Can We Fine-tune Mesenchymal Stem Cells for Therapeutic Angiogenesis? – Preliminary Study on the use of Hypoxic Pre-conditioned Cells

J. Ho¹, U. Cheema¹, M. Lowdell¹, P. De Coppi¹, M. Birchall¹

¹University College London

INTRODUCTION: Mesenchymal stem cells (MSCs) have the most established track record for translational use, but how to fine-tune its cellular function and behaviour for specific *in vivo* use is still not fully understood. In particular, MSCs have been indicated in their therapeutic benefits in wound healing, regenerative potential, and hence its concurrent use in transplantation into tissue-engineered product. Therapeutic angiogenesis is desirable especially from the tissue engineering perspective. Enhancing neovascularisation of implanted scaffold can help increase survivability of transplanted cellular material *in vivo*. Our aim is to determine the exact *in vitro* oxygenation conditions which can help potentiate and enhance angiogenic pathway to aid its therapeutic purpose *in vivo*.

METHODS: MSCs were isolated from human bone marrow. During sub-culturing, the cells were pre-conditioned in either normoxic and hypoxic levels and subsequently seeded into Type I collagen hydrogels in 24 well plates. These cell-loaded 3D hydrogels were subjected to three different oxygen conditions (<1%, 5% and 21%). Media from different time points were collected and analysed for VEGF levels. Viability and proliferative capacity were also determined.

RESULTS: Cells pre-conditioned in 2D in hypoxia (5% O₂) prior to being seeded did not exhibit any benefit in increased VEGF production when compared to cells pre-conditioned in normoxic (21% O₂) conditions. Cell viability between cells grown in 21% and 5% were not significantly different, but proliferative ability decreased when cells were cultured in <1% O₂. Normoxically pre-conditioned cells produced more angiogenic factors when subsequently placed in 3D hypoxic conditions (5% and <1%) than if they were hypoxically pre-conditioned and then cultured in 3D hypoxia. In all 3D cultured conditions, angiogenic factor release appear to peak at 48 hours of incubation.

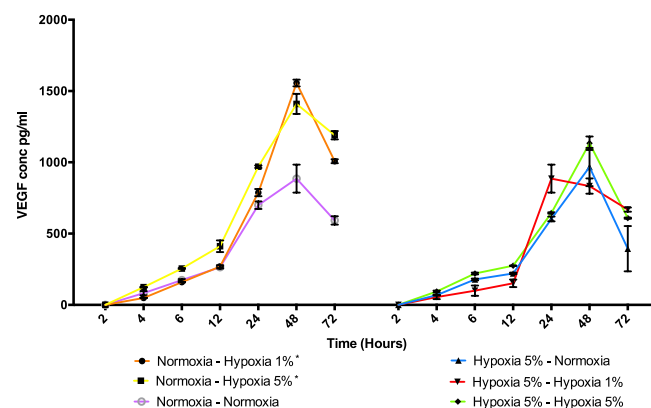


Figure 1: VEGF concentration in media collected from MSCs seeded in 3D hydrogels. * = P < 0.0001.

DISCUSSION & CONCLUSIONS: These early preliminary results offer an indication to how cells would behave when transferred from a place of higher oxygenation to one of poor oxygenation in a 3D setting, perhaps mimicking what would happen in an *in vivo* setting after transplantation on a tissue engineered scaffold. The results above also call in the question the effects of chronic hypoxia on mesenchymal stem cells and the effects of changes in oxidative stress on the cells and their angiogenic pathways. Further work could be performed on the use of conditioned media to incubate cells in 3D scaffold in the initial periods to assess for effect on subsequent angiogenic factor release as well as the upregulation of HIF1a gene response to hypoxia. Whether such enhancement in angiogenic factor production would translate into improved neoangiogenesis *in vivo* is still uncertain. Further research into optimising the stem cell niche for therapeutic purposes will have huge impact on future cell therapy uses in regenerative medicine, such as wound healing and tissue engineering.

ACKNOWLEDGEMENTS: This study is funded by the MRC and Rosetrees Trust.

Characterization of a low-cost synthetic mesh for abdominal wall repair

A. Grillo¹, V. Mudera¹, A. Kureshi¹

¹Division of Surgery & Interventional Science, University College London, London, UK

INTRODUCTION: Every year almost 20 million hernia surgeries are performed worldwide [1]. These utilize expensive surgical meshes which are not affordable to healthcare systems or patients in the developing world. For this reason, surgeons operating in those areas of the world have tried to find a more affordable alternative, using mosquito nets. Sorensen and Rosenberg [2] reviewed different studies involving implantation of mosquito nets in humans and found that, overall, the rate of short-term complications was similar to that associated with commercial meshes and the cost was much lower. However, these materials are not characterized. This study aims to characterize the mechanical properties and ultrastructure of a low-cost synthetic meshes.

METHODS: Micrographs of the meshes (Mountain Warehouse, UK; Purple Turtle, UK) (Figure 1) were taken with the Scanning Electron Microscope (SEM) (FEI XL30 FEGSEM, FEI UK, UK). Mechanical properties of the nylon fabrics were tested with a uniaxial tensile system (BT1-FR5.0TN, Zwick Roell Group, Ulm, Germany) where the samples (N=8) were held to a 0.5 kN loading cell in position controlled mode.

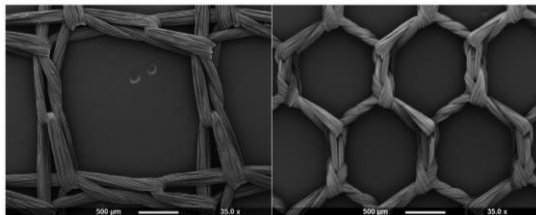


Figure 1. Micrographs of large pores (left) and small pores (right) meshes (35x).

RESULTS: Figure 1 shows the micrographs of the large and small pores meshes which have a pore size of 2.52 ± 0.048 mm and 1.160 ± 0.069 mm respectively, considering the longest distance between two opposite angles of a pore. Figure 2 (left) shows the average break stress between large and small pore meshes, 13.78 ± 1.09 MPa and 17.22 ± 2.19 MPa respectively, indicating that the small pore mesh has greater tensile strength than the large pore mesh. Average break strain (Figure 2, right) for the

large pores mesh was 130.49 ± 16.56 %, demonstrating greater extensibility than the small pores mesh at 110.26 ± 8.87 %.

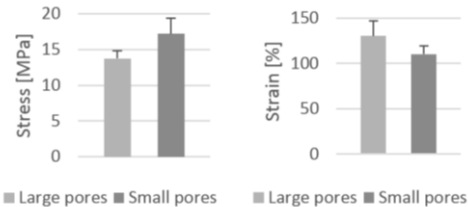


Figure 2. Average break stress (left) and strain (right) of large and small pores nylon meshes.

DISCUSSION & CONCLUSIONS: The large pores mesh appears to be the more appropriate for abdominal wall repair since it has mechanical properties, in particular break stress, closer to that of the rectus sheath, the abdominal wall layer mostly involved in hernia formation [3]. This characteristic may provide better integration and compatibility with the host tissue because its structure would allow improved cell infiltration, thereby reducing complications after implantation [4]. Future works will involve biocompatibility tests of the mesh with human dermal fibroblasts (HDF).

ACKNOWLEDGEMENTS: Thanks to Dr Nicola Mordan for her support during SEM analysis and to Jacob Salmonsmith for his help with mechanical tests.

REFERENCES:

1. Kingsnorth, A. and K. LeBlanc, *Hernias: inguinal and incisional*. Lancet, 2003. **362**(9395): p. 1561-71.
2. Sorensen, C.G. and J. Rosenberg, *The use of sterilized mosquito nets for hernioplasty: a systematic review*. Hernia, 2012. **16**(6): p. 621-5.
3. Hollinsky, C. and S. Sandberg, *Measurement of the tensile strength of the ventral abdominal wall in comparison with scar tissue*. Clinical Biomechanics, 2007. **22**(1): p. 88-92.
4. Klosterhalfen, B., K. Junge, and U. Klinge, *The lightweight and large porous mesh concept for hernia repair*. Expert Rev Med Devices, 2005. **2**(1): p. 103-17.

Characterization of Detachable Gelatin/Chitosan Hydrogels for Tissue Engineering Applications

Kayla Kret*,¹ Alastair Campbell Ritchie,¹ Colin Scotchford²

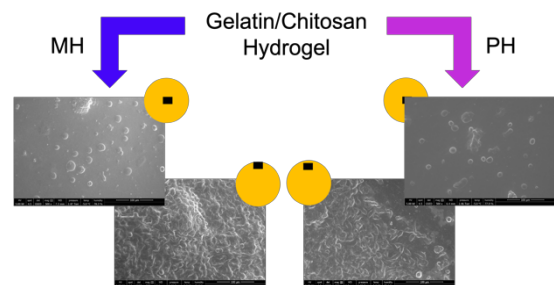
¹Bioengineering Research Group, ²Advanced Materials Research Group, University of Nottingham

*Corresponding author: Kayla.Kret@nottingham.ac.uk – PhD student (3rd year)

Introduction: Hydrogels are becoming an increasingly popular biomaterial for scaffolds within tissue engineering. In this research, gelatin and chitosan are used as the core materials due to their abundance, low cost, and cytocompatibility. These materials interact strongly with the substrate material, which then results in the inability to produce isolated hydrogels. In order to form freestanding hydrogels using these materials, an intermediate layer was utilized that enabled complete detachment of the hydrogels after gelation. In this research, the hydrogel discs will be characterized to determine their practicality for tissue engineering applications. In future research, these freestanding, detached hydrogels will be further developed and adapted to create a hybrid tissue engineered ligament.

Methods: A mixture of 3% chitosan and gelatin was combined at 37°C with a 2% solution of proanthocyanidin as a binding agent to form the hydrogel. Three hydrogel samples were created: hydrogel cast into a well plate as a control (NH), hydrogel cast onto an intermediate layer of cell culture medium (MH), and hydrogel cast onto an intermediate layer of PBS (PH). Cytotoxicity assays were performed on the hydrogel samples using NIH-3T3 cell line, including an elution assay from the intermediate layer. ESEM images were taken of the samples before cell culture and after 5 days of cell culture at a low seeding density. The surface chemistry of the samples was analysed using Near Ambient Pressure XPS. The hydrogel was formed into rectangles to allow for MicroTensile testing to determine their applicability in a tissue engineered ligament application.

Results and Discussion: By casting the hydrogel onto an intermediate layer, the hydrogel samples, MH and PH, become fully detached after gelation and removal of the liquid. The freestanding discs maintained their integrity throughout cell culturing, imaging, and tensile testing. The hydrogel was successfully cast into discs for cell culture and a variety of rectangular shapes for tensile testing. The cytotoxicity assay showed the high cytocompatibility of the hydrogel composition. At day 3 of cell culture, the assay showed significant difference between both MH and PH to NH. Although by day 7, there was no significant difference between MH and NH. The ESEM images after cell seeding show the cell morphology on the NH samples is typical of fibroblasts on a relatively stiff surface, spread and elongated with very few rounded cells. The cells on the MH and PH samples showed a rounded morphology near the center of the hydrogel disc. Nearer the edge, the cells began to elongate and are more numerous. The surface chemistry revealed that there were no deposits of Na and Cl, concluding that the intermediate layer does not have a unfavourable effect on the surface of the hydrogel. The MicroTensile testing showed that MH was significantly stiffer than PH.



It is well documented that fibroblasts will attach and elongate on a perceived stiffer surface (1,2), the NH sample in this case. Both the MH and PH samples are lacking the substrate tension that fibroblasts prefer to become elongated and proliferate. This can be attributed to the lack of anchorage of the hydrogel sample to a substrate. This may be the cause of the lower proliferation at early time points on MH and PH. At the longer timepoints, it is believed that the cells have adapted to the surface and have begun to sense the other cells on the surface, seen in the monolayer near the edge. The cell growth can be optimised through the anchoring of the detached hydrogel in application. The hydrogel composition shows high cytocompatibility, a necessary characteristic of scaffolds for tissue engineering. The durability of the scaffolds, ease of creation, and manipulation of size and shape shows promise for this method of creating isolated hydrogels to be used for a variety of different applications.

Conclusions: The hydrogel composition shows high cytocompatibility. The cytocompatibility is maintained after casting the hydrogel onto the intermediate layers. The freestanding hydrogel discs are durable in handling, a positive sign for tissue engineering applications. The intermediate layer did not leave any residue on the surface of the hydrogel that diminishes cellular activity. Although, the PH elutant treatment had significantly lower cell viability than that of the MH treatment and control treatment. The freestanding hydrogel was successfully cast into a rectangular shape for tensile testing, a similar shape when used for tissue engineered ligaments. Overall, the MH samples had higher cellular viability and was stiffer in tension than PH.

References:

1. Eastwood M. Proc Instn Mech Engrs 1998:85-92.
2. Handorf A.M. et al. Organogenesis 2015:1-25.

Combined bio-ink and supportive bath strategies for bio-mimetic 3 dimensional printing

Zhuoran Jiang, Zhanfeng Cui & Julian Dye

Institute of Biomedical Engineering, Department of Engineering Science, University of Oxford, Oxford, United Kingdom

INTRODUCTION: *In vitro* models of angiogenic vascular networks for tissue engineering can be formed by extrusion-based three-dimensional (3D) printing of hydrogel (bio-ink) encapsulated living cells. This requires shear thinning, self-spanning rheology¹. The novel strategy of printing within a supportive bath gel enables free design of complex bio-mimetic constructs. Granulized biocompatible polymers used as supportive materials with further crosslinking strategies enable support of as-printed structures.^{2,3} Here, we report the use of cellulose derivatives as rheologically effective and versatile supporting bath materials for 3D bio-printing with various bio-inks, through study of the rheological properties, responsive mechanisms and crosslinking strategies.

METHODS: Methylcellulose (MC), and Hydroxypropyl Methylcellulose (HPMC) (1.0, 2.5, 5.0 and 7.5%) were prepared as supportive materials by dispersing in 80°C DI water & hydrating (> 12h, 4°C). Calcium chloride, α -Cyclodextrin and Cucurbit[6]uril were utilized to influence the ionic and thermal rheology behaviour of cellulose derivatives. Sodium Alginate, Xanthan gum, κ -Carrageenan and Gelatin were used as bio-inks. All materials were from Sigma-Aldrich, UK. Sodium alginate (6%) was crosslinked with 0.1M CaCl₂ in the supportive bath. Optimum viscosities of Xanthan gum & κ -Carrageenan for post extrusion fidelity of shape retention were (4% & 2%) respectively. 8% Gelatin was extrudable with room temperature gelation.

RESULTS: The viscosity, gelation temperature, and gel strength of MC and HPMC are known to be controllable by concentration, molecular weight, degree of substitution and additives.⁴ Figure 1 shows system assessment by initial manual extrusion of bio-inks into a supportive bath. This demonstrates the feasibility of utilizing 6% sodium alginate or 4% xanthan gum as bio-inks and 5% MC or HPMC as supportive material for potential bioprinting of *in vitro* 3D angiogenic networks.. Table 1 shows results of

trialling potential crosslinking and removal strategies of supportive materials.

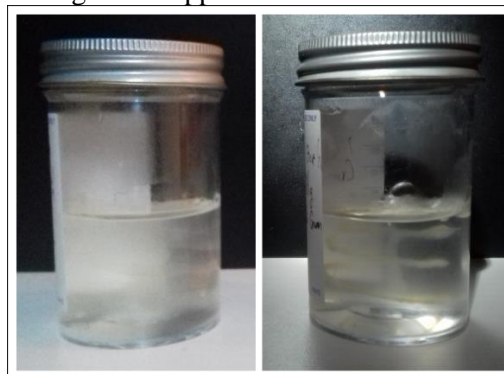


Figure 1. Assessment of bio-ink/ supportive bath systems: Uncrosslinked sodium alginate and xanthan gum (L). Cross-linked sodium alginate and xanthan gum, (R).

	CaCl ₂	β -CD	C[6]U
MC	Partially crosslinked	Dissolved	Partially dissolved
HPMC	Partially crosslinked	Dissolved	Undissolved

Table 1. Summary of potential crosslinking and removal methods for supportive materials

DISCUSSION & CONCLUSIONS: We demonstrate the use of shear thinning rheology cellulose derivatives as suitable supportive bath materials for extrusion-based 3D bio-printing with various gellable bioinks. These combinations provide stable support of 3D shapes, suitable for printing. Viability and proliferation studies of endothelial and fibroblast cells will be needed to use these systems for *in vitro* angiogenesis models.

ACKNOWLEDGEMENTS: JZ is supported by the Jardine Foundation and Oxford IBME.

REFERENCES:

1. Wu, W., Deconinck, A., & Lewis, J. A. (n.d.). *Omnidirectional Printing of 3D Microvascular Networks*.
2. Hinton, T. J., et al (2015) *Science Advances*, 1(9), e1500758.
3. Bhattacharjee, T. et al (n.d.). *Writing in the granular gel medium*.
4. Sarkar, N. (1979). *J Applied Pol Sci*, 24(4), 1073–1087.

Control of Topographical Features on PCL Electrospun Nanofibre Scaffolds for Liver Tissue Engineering

Y.Gao, A. Callanan

Institute for Bioengineering, School of Engineering, University of Edinburgh, United Kingdom

INTRODUCTION: At present, liver tissue engineering shows promise for the treatment of liver disease¹. Nanofiber scaffolds produced via electrospinning have shown good compatibility and mechanical properties for support of liver cells. The morphology of fibres significantly effects cell growth². Here, we intend to investigate the effect of fibre topography on the phenotype of liver hepatocellular carcinoma (HepG2) cells.

METHODS: The surface was modified by using different solvent systems; adding non-solvent to polymer solution can induce phase separation resulting in topographical changes³. Dimethyl sulfoxide (DMSO) is useful for depression formation on Polycaprolactone (PCL) scaffolds, which was added to initiate phase separation. Solvent and non-solvent combine in the ratio of 9:1. The test groups were 14% w/v PCL/Chloroform (CFM)/ DMSO (small surface depression) and 16% w/v PCL/(5:1) CFM/Methanol/DMSO (large surface depression), and the control group was 16% w/v PCL/(5:1) CFM/Methanol (PCL control). Scaffold morphologies were assessed by scanning electron microscopy (SEM). HepG2 liver cells were seeded onto the scaffolds cultured for 24h, 7days and 14days. Biochemical quantification and gene expression were performed at various time points.

RESULTS: Three electrospun fibre samples with different surface morphologies were successfully fabricated. Solution A has small depressions on the fibre surface; solution B has larger and round depressions; control group (A) has a smooth fibre surface (Fig.1). The diameters of these groups are similar at roughly 3µm (Table.1).

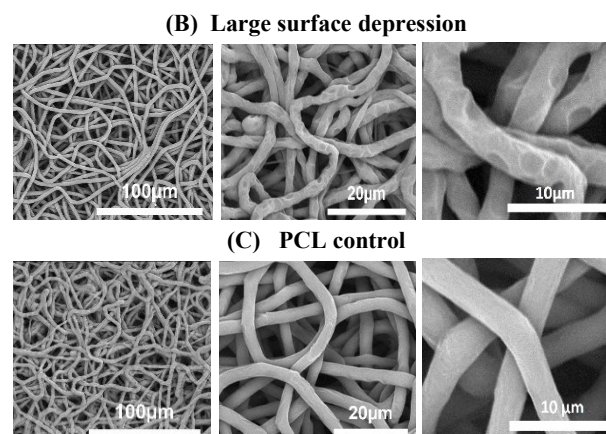


Fig. 1: SEM images of different fibre surface morphologies. (A) Small depression. (B) Large depression. (C) PCL control.

Table. 1 Average fibre properties of each sample (mean ± SD)

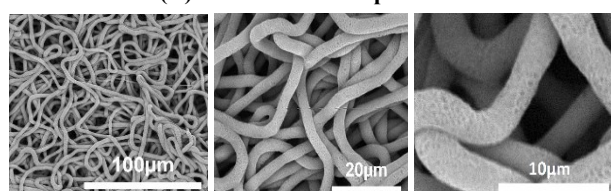
Sample	PCL control	Small surface depression	Large surface depression
Fibre Diameter (µm)	3.14 ±0.28	3.10 ±0.29	3.03 ±0.32
Pore Diameter (µm)	-	0.37 ±0.10	2.14 ±0.62

DISCUSSION & CONCLUSION: Non-solvent induced phase separation results in the formation of depressions. Because non-solvent DMSO has a much higher boiling point than CFM and Methanol, thus DMSO evaporates much slower than CFM, which produces an unstable solvent system allowing phase separation to occur. This study shows the ability to control depression formation on PCL scaffold, and cell attachment and viability was shown in all scaffolds.

ACKNOWLEDGE: MRC grant MR/L012766/1.

REFERENCES: ¹Grant, R et al. (2018). Biomed. Phys. Eng. Express 4.065015. ² Burton, T et al. (2017). Biomed. Mater. 13.015006. ³ Huang, C et al. (2018) Eur. Polym. J. 99, 464–476

(A) Small surface depression



Controllable dehydration of cell-seeded type I collagen hydrogels using sodium polyacrylate.

LM. Beattie¹, CJ. Henderson¹, SP. MacKay², PE. Riches¹, [MH. Grant](#)¹.

¹Biomedical Engineering, University of Strathclyde, Glasgow.

²SIPBS, University of Strathclyde, Glasgow.

INTRODUCTION: Collagen hydrogels are an ideal biomaterial for cell and tissue engineering applications; however they are inherently mechanically weak¹. Plastic compression was developed by Brown et al.² to increase the collagen concentration and strength of collagen hydrogels. The aim of our research was to develop a controllable method, with a readily available superabsorber, which increased the concentration of collagen and mechanical strength of cell-seeded collagen hydrogels whilst maintaining their ability to support cells.

METHODS: 0.3% Collagen gels embedded with human dermal fibroblasts (HDFs) were prepared by mixing: Collagen; 1/1000 acetic acid; and 2:1 10xDMEM: 0.4M NaOH. The pH was adjusted with 1M NaOH to pH 8-8.5. HDFs (3×10^4 cells/cm²) were added to the collagen gel before allowing it to set for 90 minutes in 35 mm tissue culture plates at 37°C. The gels were weighed, then complete DMEM added to complete polymerisation for 30 minutes. The DMEM was removed before dehydration took place. Sodium polyacrylate (SP; 10% (w/w) of the gel wet weight.) was chosen as the superabsorber. For plastic compression, a layer of 100 micron nylon mesh, then filter paper followed by SP was placed on the surface of the gel for a set time. The mesh, filter paper and SP were removed and the gels reweighed to calculate collagen concentration. The cell-seeded gels were maintained in complete DMEM for upto 4 weeks and an MTT assay completed at the endpoint to measure viable cell number. A Pro-collagen ELISA (AbCam) was also completed on cell media to measure new collagen synthesis.

RESULTS: Plastic compression using SP gave a controllable dehydration with time (Figure 1). These results show a 43 fold increase in collagen concentration from 0.3% to 12.8% during the 60 minute dehydration. The gels lose 96% of their initial weight in the first 10 minutes of dehydration. The dehydration process became more consistent when carried out for longer (SEM data not shown).

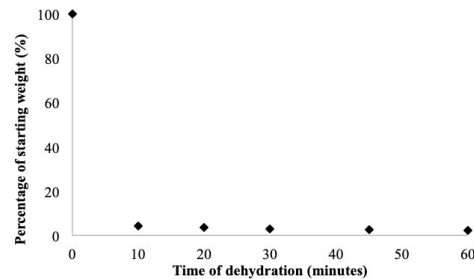


Figure 1: Percentage of starting weight of gel after dehydration. $n=4$, mean + SEM.

The MTT assay results (Table 1) showed viable metabolising cells after 1 and 4 weeks in both hydrated and dehydrated gels. Viable cell number increased significantly ($p < 0.05$) from 1 week to 4 weeks, increasing 1.36 and 1.6 times in hydrated and dehydrated gels respectively, suggesting cell division took place. ELISA of pro-collagen, showed de novo synthesis in hydrated and dehydrated gels over 4 weeks (Table 1). After 4 weeks, synthesis increased significantly ($p < 0.01$) in dehydrated gels. There was no significant difference in hydrated gels over the same period ($p = 0.13$).

Table 1: Cell number and pro-collagen measured by MTT and ELISA respectively. $n=4$, mean \pm SEM.

	1 week		4 weeks	
	Hydrated	Dehydrated	Hydrated	Dehydrated
Cell number (cells/cm ²)	82,681 $\pm 2,584$	61,390 ± 307	112,842 $\pm 4,606$	98,649 $\pm 12,030$
Pro-collagen (ng/ml)	92.35 ± 0.43	91.09 ± 0.23	79.93 ± 7.81	115.89 ± 6.29

DISCUSSION & CONCLUSIONS: This method produced quick and consistent results showing a dramatic increase in collagen concentration. A novel superabsorber, sodium polyacrylate, which is more commonly used as artificial snow was employed and no further expensive reagents or equipment were required. This produces layers of mechanically stable, highly concentrated collagen embedded with viable cells, useful for many cell or tissue engineering applications.

ACKNOWLEDGEMENTS: The authors thank funders Medical Research Scotland and Collagen Solutions Plc.

REFERENCES: ¹Busby GA, Grant MH, MacKay SP, Riches PE (2013) Confined compression of collagen hydrogels. *Journal of Biomechanics* **46**: 837–840. doi:[10.1016/j.jbiomech.2012.11.048](#). ²Brown RA, Wiseman M, Chuo C-B, Cheema U, Nazhat SN (2005) Ultrarapid Engineering of Biomimetic Materials and Tissues: Fabrication of Nano- and Microstructures by Plastic Compression. *Advanced Functional Materials* **15**: 1762–1770. doi:[10.1002/adfm.200500042](#).

Cross-linking of bone derived extracellular matrix hydrogels to alter mechanical properties

J. Jones¹, S. Kellaway², L.J. White¹

¹ School of Pharmacy, University of Nottingham, Nottingham, GB, ² Centre for Nerve Engineering, University College London, London, GB

INTRODUCTION: Decellularised tissues can be digested and solubilised to allow the generation of extracellular matrix (ECM) derived hydrogels, many of which are undergoing research for a multitude of clinical applications¹. Whilst the amorphous nature of hydrogels benefits some use, their lack of mechanical strength hinders their utility in some forms of medical implantations, particularly in areas such as orthopaedics. The use of chemical cross-linking agents induce physical cross-links within a gel to improve strength and resilience, with glutaraldehyde (GA) and carbodiimide (EDC) being commonly used agents². In this study the effects of GA and EDC on the mechanical properties of bone ECM based hydrogels have been assessed through rheometry.

METHODS: Bovine tibiae were subjected to an established decellularisation technique³, yielding bone derived ECM (bECM) material which was digested and solubilised. Neutralisation at 37°C resulted in the formation of a bECM hydrogel, which were created at a concentration of 8mg/ml. Glutaraldehyde (0.625%) or EDC (10mM) were added to the formed hydrogels and reacted at room temperature for 2 hours. Once the time point was complete gels underwent four, 30 minutes wash stages (two 1x PBS, two pure water washes). Rheology was performed immediately using the Physica MCR 301 rheometer (Anton Paar, Hertford, UK). Amplitude sweep testing was conducted in the range of 0.1-200% strain with a constant angular frequency of 1 rad/s.

RESULTS: Treatment with glutaraldehyde resulted in a significantly ($p < 0.0001$) increased gel strength compared to untreated gels, with storage moduli of 2600Pa and 160Pa respectively, however the strain value decreased (7.5% and 21% respectively). There was no significant difference in the gels treated with 10mM EDC, which exhibited the same storage modulus as untreated gels.

Table 1. Relative allocation and amount of resources in research.

	Maximum Load (G')	Maximum Strain
Untreated	160 Pa	21%
GA cross-link	2600 Pa	7.5%
EDC cross-link	160 Pa	25%

DISCUSSION & CONCLUSIONS:

Treatment with GA successfully increases the maximum load that a bECM hydrogel can withstand, effectively increasing its strength. This, however, comes at a detrimental cost to the maximum strain that the cross-linked gel can withstand meaning that gels become stronger, but more brittle and can break easier under certain angular stresses. The results obtained for EDC cross-linking is contradictory to the published literature, however this is believed to be due to the methodology used in this project. Many studies employ the use of *N*-hydroxysuccinimide (NHS) to facilitate EDC cross-linking, but no NHS was used in this project due to time constraints. This work is being evaluated further and changes to the methodology shall be made which will rectify this.

ACKNOWLEDGEMENTS: The author would like to thank the EPSRC for their funding of the project.

REFERENCES: 1.L.T. Saldin, M.C. Cramer, S.S. Velankar, L.J. White, S.F. Badylak, *Acta Biomater.* 2017, 49, 1-15. 2.A. Oryan, A. Kamalia, A. Moshiri, H. Baharvand, H. Daemie, *Int. J. Biol. Macromol.* 2018, 107, 678-688. 3.M.J. Sawkins, W. Bowen, P. Dhadda, H. Markides, L.E. Sidney, A.J. Taylor, F.R.A.J. Rose, S.F. Badylak, K.M. Shakesheff, L.J. White, *Acta Biomater.* 2015, 9, 7865-7873.

Decellularized materials support Schwann cell growth and alignment in engineered neural tissue

SC. Kellaway^{1,2}, LJ. White², JB. Phillips¹

¹*Centre for Nerve Engineering, University College London, England, GB*, ²*Division of Regenerative Medicines and Cell Therapies, University of Nottingham, England, GB*

INTRODUCTION: Engineered neural tissue (EngNT) made using aligned cellular collagen promotes axonal regeneration across critical sized defects [1]. We present alternative hydrogel materials that are suitable for use in EngNT and may improve its regenerative capacity.

METHODS: Decellularization protocols for a range of tissues were adapted [2-3]. dsDNA and glycosaminoglycan (GAG) contents were quantified, and hydrogels were formed. Mechanical properties were characterized using a rheometer (Anton Paar, Hertford, UK). Viability of Schwann cells (SC) incorporated within gels was assessed using the Cell Titer-Glo assay (Promega, Southampton, UK). SC were seeded at 0.5, 1, 2 and 4 x 10⁶ cells/ml to produce contraction profiles and cellular alignment was visualized via immunofluorescence microscopy.

RESULTS: Extracellular matrix (ECM) derived from bone (B-ECM) possessed the lowest dsDNA content (27.4 ± 5.3 ng/mg) whilst small intestinal submucosa ECM (SIS-ECM) had the highest (424.4 ± 4.0 ng/mg). Similarly, B-ECM had the lowest GAG content at 1.9 ± 0.8 µg/mg, compared to the highest of 5.6 ± 0.9 µg/mg for SIS-ECM. The B-ECM gel displayed the fastest gelation and exhibited a sigmoidal gelation profile. The liver ECM (L-ECM) gel was the stiffest at 453 ± 9 Pa, whilst the urinary bladder ECM (UBM-ECM) was the softest at 61 ± 8 Pa. Additionally, all materials displayed strain stiffening responses.

SC viability was higher for 6 mg/ml compared to 4 mg/ml gels and was highest for B-ECM and lowest for SIS-ECM. Contraction was dependent on both gel and cell concentrations; higher cell concentrations and lower gel concentrations produced the most contraction (Figure 1E). Adequate SC alignment was seen in 4 and 6 mg/ml B-ECM (Figure 1F) and SIS-

ECM gels however, no alignment was observed in L-ECM or UBM-ECM gels.

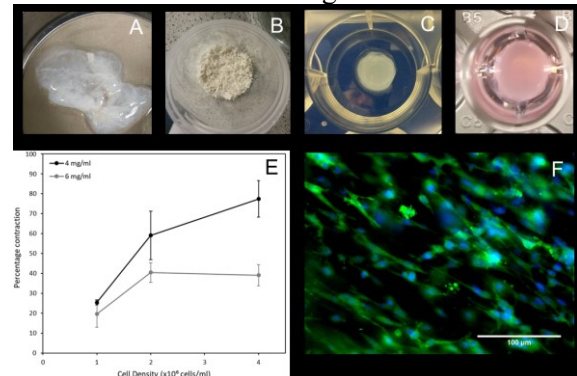


Figure 1: L-ECM [A], B-ECM [B]. Acellular [C] and SC seeded [D] B-ECM hydrogels. SC contraction profile [E] and alignment [F] in B-ECM hydrogel.

DISCUSSION & CONCLUSIONS: Biochemical and mechanical properties affect SC viability. B-ECM and SIS-ECM are further suitable for use in EngNT. Future work will involve co-cultures of neurons to assess axonal regeneration.

ACKNOWLEDGEMENTS: EPSRC grant EP/L01646X

REFERENCES

- [1] Georgiou M et al. *Biomaterials* 2014; 34(30): 7335-7343.
- [2] Sawkins M et al. *Acta Biomaterialia* 2013; 9(8): 7865-7873
- [3] Crapo P et al. *Biomaterials*. 2011;32(12): 3233-3243

Design of nerve repair conduits with the aid of an *in silico* model

S Laranjeira^{1,3}, KS Bhangra^{2,3}, JB Phillips^{2,3} and RJ Shipley^{1,3}

¹ UCL Mechanical Engineering, London, UK, ² Department of Pharmacology, UCL School of Pharmacy, London, UK., ³ UCL Centre for Nerve Engineering, UK.

INTRODUCTION: Peripheral nerve injury (PNI) affects 1M people in Europe and the USA p.a.¹ Patients experience debilitating symptoms resulting in loss of end-organ function and morbidity.¹ The current gold standard aims at establishing a connection between proximal and distal nerve stumps through microsurgical autografts.¹ However, the clinical outcomes are still poor as only 50% of patients experience functional recovery.¹

Engineered Neural Tissue (EngNT), an anisotropic cellular hydrogel nerve conduit, has been developed as an engineered alternative to tissue grafts and is showing significant promise.² Here we seek to inform the design of EngNT by developing computational models of neurite growth in order to identify spatial arrangements of biomaterial within a conduit, as seen in Fig. 1, that maximise the rate of regeneration. Neurites respond to a suite of physical cues, and this provides an opportunity to arrange these cues spatially to promote neurite growth. We present a new computational model that predicts neurite growth in response to the mechanical environment, and combine it with *in vitro* and *in vivo* data to inform conduit design.

METHODS: Neurite growth is described through a 3D latticed-based random walk. At each time step (Δt), the stochastic movement of a neurite (Δx) is calculated following a Euler approximation of an overdamped Langevin equation, which relates the movement of cells to the forces acting on them.³ Here three forces are considered: 1. the mechanical resistance of cells to a change in direction, $M(N)$, modelled as $\mathcal{N}(0, \sigma^2)$ dependent on the angle made between the current and any future direction the neurite may take (θ_N); 2. a forward bias representative of the chemotactic cues between the distal and proximal ends of a repair site ($B(N)$); 3. a durotactic bias along a stiffness gradient ($D(N)$):

$$\Delta x = \frac{1}{\beta} [M(N) + B(N) + D(N)] \Delta t, \quad (1)$$

where β is the kinetic friction.

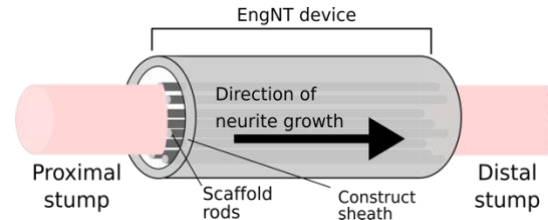


Fig. 1: Schematic presenting the design for an EngNT nerve repair constructs with embedded rods.

The $M(N)$ and $B(N)$ functions and parameters were determined by fitting to *in vivo* neurite counts within EngNT and to mimic neurite orientation data using a particle swarm algorithm.^{1,4} Additionally $D(N)$ parameters were chosen to ensure bias movement towards larger stiffness. The model was run for thousands of neurites on a 3D cylindrical geometry to mimic a preclinical nerve injury scenario.

RESULTS: The particle swarm fitting approach demonstrated good agreement with experimental data. Performing a sensitivity analysis where simulations with $\pm 10\%$ difference in parameter values compared to the data resulted in a mean error of 2%. The parameterised model was used to explore the spatial arrangement of biomaterial in a conduit, and identify new candidate conduit designs for future preclinical testing.

DISCUSSION & CONCLUSIONS: An *in silico* model of PNI was developed and tested within a multidisciplinary framework. This is the first parameterised model for PNI repair, which can now be taken forward to inform the optimal spatial arrangement of materials to promote neuronal regeneration following injury.

REFERENCES: 1. Grinsell, D. & Keating, C. P. *BioMed Research International* (2014). 2. O'Rourke, C. *et al. Sci. Rep.* 8, 2951 (2018). 3. Zubler, F. & Douglas, R. *Front. Comput. Neurosci.* 3, (2009). 4. Vaz, A. I. F. & Vicente, L. N.. *J. Glob. Optim.* 39, 197–219 (2007).

DESIGNING AN ANGLED INTERFACE FOR AN IN VITRO FLEXOR DIGITORUM PROFUNDUS ENTHESIS MODEL THROUGH HUMAN HISTOLOGICAL INVESTIGATION

Jeremy W Mortimer*¹, Subashan Vadibeler¹, Mario Macia¹, Miriam Graute¹, Philippa A Rust², Jennifer Z Paxton¹
¹Deanery of Biomedical Sciences, University of Edinburgh, UK, ²Department of Plastic Surgery, St. John's Hospital, Livingston, UK

*Corresponding author: j.w.mortimer@sms.ed.ac.uk – PhD student (3rd year)

Introduction

Interfacial tissue engineering (ITE) endeavours to reproduce the soft-hard tissue interface for potential implantation in diseased or traumatised tendon/ligament-bone regions. ITE primarily targets commonly injured large joints, such as the rotator cuff or anterior cruciate ligament,¹ with native morphological replication of models overlooked in favour of cellular or materials research. Trauma at the flexor digitorum profundus (FDP) insertion onto the distal phalanx (DP) in the hand, the most frequent closed flexor tendon injury,² shares similar treatment challenges as large joint entheses injuries, and our group is designing an *in vitro* ITE model particular to this anatomical region. Since the angle of tendon fibres at the tendon-bone entheses are an important mechanical consideration in physiological function and pathogenesis,³ we have investigated FDP entheses tendon fibre angle histologically, aiming to design and produce a more morphologically accurate *in vitro* model.

Materials and Methods

48 fresh frozen human cadaveric fingers from 6 body donations to The University of Edinburgh Medical School were dissected to obtain isolated samples of the FDP attachment to the DP. 10µm mid-sagittal sections through the entheses were prepared by wax histology, stained with toluidine blue, and digital scans analysed with ImageJ software for the tendon fibre angle at the mineralised-unmineralised interface (tidemark). Inter-observer reliability was assessed. An angled culture shelf and separate mold were designed with Tinkercad software and 3D printed to create this angle at the tendon-bone interface in an *in vitro* model using a rat fibroblast-seeded fibrin tendon analogue and a brushite bone anchor. Early investigations are underway on the feasibility and reproducibility of the novel model.

Results and Discussion

The mean tendon fibre angle (\pm SEM) for all fingers (3 male, 3 female; mean age 79.3, range 73-91) at the mineralised-unmineralised interface was 30.08° (\pm 0.64°). Cronbach's α for reliability between 2 observers was high at 0.91. A 30° angled culture shelf for a 6-well plate created a cured silicone base layer in the wells at a reciprocal 30° to the plate, but allowed the forming tendon analogues to be cultured horizontally without gravity or slippage effects. The specially designed mold produced the negative space in the silicone layer for the brushite anchor to be positioned at 30° to the horizontal tendon analogue while encompassing a larger circular area for contraction of the fibroblast-seeded fibrin gel. Careful mutual design of the size and shape of the bone anchor through similar Tinkercad mold creation and 3D printing is essential for the anchor to be held firmly at the correct angle whilst preventing the tendon analogue attaching to unintentionally exposed surfaces.

Conclusions

Through quantitative morphometric analysis of tendon fibres at the human FDP entheses, we have designed and created an *in vitro* tendon-bone model with enhanced anatomical characteristics. This anatomical approach to ITE design could improve the clinical applicability of *in vitro* models of any entheses region.

References

1. Patel S *et al.* J Orthop Res. 36: 1069-1077, 2018.
2. Freilich A. Clin Sports Med. 34: 151-166, 2015.
3. Benjamin M & Ralphs J. J Anat. 193: 481-494, 1998.

Acknowledgements

Orthopaedic Research UK: grant 528.

Special acknowledgement to the body donors of The University of Edinburgh Medical School.

Developing a human blood-brain barrier model using 3D-biomaterials and iPSC derived brain microvascular endothelial cells

[G Potjewyd](#)¹⁻³, [W Zhang](#)², [S Moxon](#)¹, [K Fisher](#)¹, [T Wang](#)², [M Domingos](#)³, [N Hooper](#)¹

¹Division of Neuroscience and Experimental Psychology, ²Division of Evolution and Genomic Sciences, ³School of Mechanical, Aerospace and Civil Engineering, The University of Manchester, Manchester, UK.

INTRODUCTION: The blood-brain barrier (BBB) is a key interface between the neural and vascular components of the neurovascular unit (NVU). Selective permeability to drugs and circulatory compounds is crucial to healthy BBB function. Dysfunction of the BBB precedes and exacerbates many different neurological diseases, including Alzheimer's disease (1), and further investigation of this is crucial to understanding disease pathogenesis. *In vitro* BBB models enable drug testing and disease research, without the need for animal models. In this study, tissue engineering of a human BBB-model was optimised through use of human induced pluripotent stem cell (iPSC) derived brain microvascular endothelial cells (BMECs), seeded onto different protein and polysaccharide based hydrogels that replicate aspects of the BBB-extracellular matrix (ECM).

METHODS: OX1-19-iPSCs were differentiated into BMECs using a previously published protocol (2). The BMECs were then evaluated for BBB phenotype using immunostaining for tight junction (TJ) (ZO-1, occludin and claudin-5) and glucose transporter 1 expression (GLUT1), and permeability measurements through using trans-endothelial electrical resistance (TEER) and sodium fluorescein assays. Alginate-collagen (alg-col) blend or collagen hydrogels were tested using oscillatory rheology to determine appropriate shear modulus for BBB tissue. Shear modulus was measured using a 20 mm parallel plate under 1 Hz (60 BPM) strain – replicating stresses that occur at the BBB. ECM based protein coating of tissue culture surfaces was optimised for BBB phenotype using collagen IV and fibronectin (Col-Fn) and Matrigel, with and without ROCK inhibitor (3). After ECM coating of hydrogels, BMECs were seeded and cultured for 3-4 days until a functional BBB-BMEC phenotype was recorded. Hydrogel based BBB-BMEC monolayer functionality was determined using TEER and sodium

fluorescein permeability assays, along with immunostaining for TJ proteins and GLUT1.

RESULTS: BMECs produced from the differentiation protocol expressed both brain endothelial TJ proteins and GLUT1. Comparison of BMECs grown on Col-Fn or Matrigel showed no significant difference in permeability, TJ protein or GLUT1 localisation and expression, exhibiting a strong BBB phenotype. Addition of ROCK inhibitor to newly seeded BMEC monolayers (24 h) improved their permeability. BBB-BMEC monolayers failed to form on alg-col, with stiffness independent (0.5-2.5 kPa) low functional permeability values and poor adherence to the hydrogel surface. However, collagen hydrogels (900 Pa) facilitated BMEC adhesion, monolayer formation, higher permeability values, and TJ protein and GLUT1 expression.

DISCUSSION & CONCLUSIONS: The developed human BBB-BMEC model allows for the testing of drug or potentially toxic compound permeability to the brain parenchyma. In addition, the model serves as a platform for the introduction of supporting cell types (astrocytes, pericytes and neurons) to both improve BBB phenotype and enable investigation of NVU inter-cellular interactions in disease pathogenesis.

ACKNOWLEDGEMENTS: MRC and EPSRC for funding the research. Grant reference number: EP/L014904/1

- REFERENCES:** 1. Nation, D. A. *et al.* *Nat. Med.* **25**, (2019).
2. Stebbins, M. J. *et al.* *Methods* **101**, 93–102 (2016).
3. Katt, M. E., Linville, R. M., Mayo, L. N., Xu, Z. S. & Searson, P. C. *Fluids Barriers CNS* **15**, 7 (2018).

Developing an Oral Insulin Delivery System using GET-peptide-mediated transcytosis

S. Rehmani, KM. Shakesheff and JE. Dixon

Wolfson Centre for Stem Cells, Tissue Engineering, and Modelling (STEM), Centre of Biomolecular Sciences, School of Pharmacy, University of Nottingham, Nottingham, NG7 2RD, UK.

INTRODUCTION: Designing systems for oral insulin delivery (OID) with adequate bioavailability will revolutionize diabetes management. Development of an oral insulin system represents overpowering challenge, here we describe the use of a novel fusion peptide system to minimize these limitations, termed Glycosaminoglycan-binding-Enhanced Transduction (GET) system. This novel peptide system is being exploited for numerous drug delivery application particularly nucleic acids (plasmid DNA, RNA) and protein delivery.¹ During last few decades, Cell-penetrating-peptides (CPPs) have arose as potential trans-epithelial delivery vectors for intracellular delivery of therapeutic proteins including anti-diabetic agents e.g. insulin, GLP-1, and exendin-4. This project is aimed at exploiting the potential of GET system (named PLR) and derivative peptides in efficiently enhancing the intracellular transduction of insulin and its successive release into the systemic circulation.

METHODS: Fluorescent labelling of insulin with NHS-fluorescein was followed by complexation with GET peptide to get insulin-GET nanocomplexes (Ins-GET-NCs). These Ins-GET-NCs were evaluated for their potential for transepithelial insulin delivery and stability using model Caco-2 cells cultured on transwell. Recycling of these NCs was studied using different regulators for cell secretion and serial multiple drug delivery. These NCs were characterized for their size and surface charge using dynamic light scattering, additionally confocal microscopy was used to visualize intracellular distribution of insulin and Ins-GET-NCs on cell monolayers. The functional activity of these NCs was also assessed using insulin-reporter-DT-40 cells.

RESULTS: GET system efficiently promotes insulin transport across Caco-2 cell monolayers, resulting in greater >22 folds translocation efficiency compared to naive insulin. The post-transfection insulin release from cell-monolayers provided insight for insulin recycling, additionally, cellular accumulation resulting from multiple delivery allowed cells to act as depot for sustained release. The Ins-GET-NCs were positively charged (+27.10) with average particle size of 140nm. CLSM images also confirmed greater intracellular insulin accumulation with GET peptide. Furthermore, both GET peptide and Ins-GET-NCs were stable to degradation by proteolytic enzymes and stayed intact post-translocation inside the cells. This peptide-modified-insulin was found to be sufficiently biologically active thorough functional activity assay.

DISCUSSION & CONCLUSIONS: This study demonstrated that insulin/GET complexation greatly enhances the insulin absorption, thereby making this combination a potential system for OID. GET-peptide based systems are promising tools for overcoming problems of low permeability; formulation of these particles aiding protection from the harsh GI environment through use of enteric based systems and ultimately enhancing insulin bioavailability are now under investigation.

REFERENCES: ¹Dixon et al (2016) Highly efficient delivery of functional proteins by the synergistic effect of GAG binding motifs and cell-penetrating peptides. PNAS **113**: E291-9.

ACKNOWLEDGEMENTS: Authors are highly thankful to PEEF, Pakistan for funding Ph.D. and University of Nottingham for the research grant.

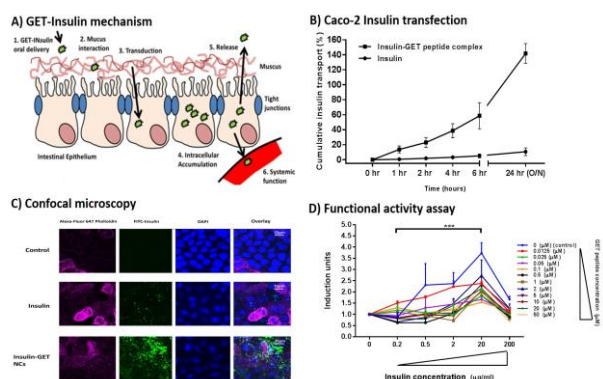


Fig. 1: The GET-Insulin oral Insulin delivery system. A) Schematic of GET-Insulin mechanism of oral insulin delivery by loading intestinal epithelial cells with insulin with systemic release and function. B) GET-Insulin (P21-LK15-8R; PLR) loads intestinal epithelial barriers with Insulin (this is beyond naive insulin delivery). C) CLSM images of distribution of F-insulin and F-insulin-GET peptide complex on Caco-2 cell monolayer transfected for 5hr. D) Functional assay at varying final insulin concentration showing that insulin (negative control) caused 4 folds induction of DT-40 cells, while progressively increasing concentration of GET peptide caused slight reduction in induction.

Development of 3D Tumour Models for Ameloblastoma

Bakkalci. D¹, Fedele. S¹, Jell. G¹, Cheema. U¹

¹Division of Surgery and Interventional Science, University College London (UCL), UK

INTRODUCTION: Ameloblastoma (AM) is a rare odontogenic neoplasm. Its main mode of action is bone resorption of the jaw bones^{1,2}. The underlying mechanisms are not well defined. Although growing cancer cells in two-dimensional (2D) monolayers is crucial to understand the pathology of diseases, it may not represent the actual tumour microenvironment³. This project aims to develop a 3D tumour model for the two most common types of AM, plexiform and follicular. The main goal is to recreate parameters of the physical microenvironment to mimic the tumour environment *in situ*.

METHODS: AM cells (AM-1 (plexiform) and AM-3 (follicular) cells) and osteosarcoma cells (MG-63) were cultured using the RAFT™ 3D Cell Culture system. 50 000 cells for each cell line were seeded per artificial cancer mass (ACM). The gels were compressed via RAFT absorbers to remove excess fluid. Invasion was determined by measuring cancer cell invasion into the surrounding stroma from within the cancer mass.

RESULTS: MG-63 and AM-1 invaded as cell sheet pattern, whereas AM-3 cells form bud-shape cell aggregates around ACM and invades into stroma by maintenance of bud-like aggregates for 21 days. When invasion distances of AM cells and MG-63 cells were compared over 21 days, AM-1 and MG-63 cells can invade greater distances than AM-3.

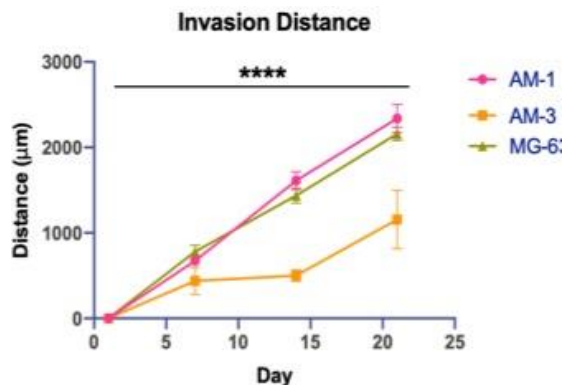


Figure 1: Invasion distances of AM-1, AM-3 and MG-63 cells at day 1, 7, 14 and 21. (n=3, ordinary two-way ANOVA, ***p<0.0001).

DISCUSSION & CONCLUSIONS: 3D tumour models enable the us to investigate characteristics of different cell lines based on their invasion patterns. Previously, it was reported that highly metastatic cancers invade into the surrounding stroma within tumoroids as cell sheets³. A previous study showed that, a highly metastatic colorectal cancer cell line HCT116 was found to invade as cell sheets³. AM-1 and MG-63 cells also showed the similar sheet pattern during invasion. Exclusive invasion of MG-63 can be due to the fact that its association with poor prognosis upon metastasis and recurrence of the disease⁴.

AM-3 invades shorter distance than AM-1 and MG-63. This might be due to cell sheet invasion pattern as both AM-1 and MG-63 cells have the same pattern of cell sheets, whereas AM-3 has the bud-like shape. This mimics the known invasion pattern *in situ* for the follicular and plexiform subtypes of AM.

Future works will focus on the direct and indirect mechanisms of bone resorption induced by AM cells by looking at bone resorptive proteins such as matrix metalloproteinases (MMPs) and receptor activator of nuclear kappa B (RANK).

REFERENCES:

1. Becelli R, Carboni A, Cerulli G, Perugini M, Iannetti G. Mandibular ameloblastoma: analysis of surgical treatment carried out in 60 patients between 1977 and 1998. *J Craniofac Surg.* 2002;13(3):395-400; discussion
2. Siar CH, Tsujigiwa H, Ishak I, Hussin NM, Nagatsuka H, Ng KH. RANK, RANKL, and OPG in recurrent solid/multicystic ameloblastoma: their distribution patterns and biologic significance. *Oral Surg Oral Med Oral Pathol Oral Radiol.* 2015;119(1):83-91.
3. Magdeldin T, Lopez-Davila V, Pape J, Cameron GW, Emberton M, Loizidou M, et al. Engineering a vascularised 3D in vitro model of cancer progression. *Scientific reports.* 2017;7:44045.
4. Lindsey BA, Markel JE, Kleinerman ES. Osteosarcoma Overview. *Rheumatology and therapy.* 2016;4(1):25-43.

DEVELOPMENT OF A BIOPROCESS FOR THE EXPANSION AND DIFFERENTIATION OF IPSCS

Fritz de la Raga,¹ Eric Hill¹, Christopher J Hewitt¹, Mariana Petronela Hanga¹

¹Life and Health Sciences, Aston University, Birmingham, B4 7ET, UK

Corresponding author: delarafa@aston.ac.uk – PhD Student (2nd year)

INTRODUCTION:

Neural precursor cells (NPCs), derived from human induced pluripotent stem cells (hiPSCs), are a promising cell source which offer unprecedented opportunities for personalised drug screening, disease modelling and regenerative medicine applications.^{1,2} However, the avenue towards the sustainable commercial use of hiPSC derived NPCs is hindered by the lack of robust and reliable large-scale bioprocess designs. Therefore, here we aim to develop a bioprocess integrating the expansion and differentiation of hiPSCs into NPCs, whilst employing bioreactor platforms to reduce the cost and labour investment compared to the conventional planar approach.

MATERIALS AND METHODS:

In order to determine the optimal seeding density, hiPSCs were seeded on vitronectin coated plates at various seeding densities ranging from 2×10^4 to 6×10^4 cells/cm². Growth kinetics and glucose profiles were recorded over 5 days. hiPSCs, were then differentiated to NPCs as monolayers. Cell morphology and glucose consumption were monitored. Furthermore, since hiPSCs are adherent cells, 8 commercially available microcarriers without additional coating were screened for their ability to support cell attachment and expansion.

RESULTS AND DISCUSSION:

Cells achieved 80% confluency after 3 days in mTeSR Plus when seeded at 4×10^4 and 6×10^4 cells/cm², whilst the lower cell density of 2×10^4 cells/cm² required 4 days. Cell survival indicated by cell viability at day 1 after single cell passaging, was higher when cells were seeded at 4×10^4 and 6×10^4 cells/cm² compared to the lower seeding density. Nonetheless, after day 2 in culture, the specific growth rates of cells at all seeding densities were similar. On the other hand, the differentiation of hiPSCs and the emergence of NPC populations were indicated by the formation of neural rosettes after 9 days in neural induction medium. hiPSCs were also shown to have successfully adhered onto Cytodex 3 and Cytodex 1 (GE Healthcare), Cultispher G and Cultispher S (Sigma) and Collagen (SoloHill PALL) microcarriers by live-dead staining and phase contrast imaging.

CONCLUSION

The optimal seeding density was found to be 4×10^4 cells/cm². Neural rosettes formed within 9 days in neural induction medium (Stem Cell Technologies). Additionally, only certain microcarriers were found to support the attachment of hiPSCs. Further work will be conducted to investigate growth profiles of hiPSCs on the different microcarriers, followed by the development of a one-step bioprocess for the production of NPCs from hiPSCs.

REFERENCES

1. Yap, M. S. *et al.* Neural Differentiation of Human Pluripotent Stem Cells for Nontherapeutic Applications: Toxicology, Pharmacology, and In Vitro Disease Modeling. *Stem Cells Int.* **2015**, 1–11 (2015).
2. Nagoshi, N. & Okano, H. iPSC-derived neural precursor cells: potential for cell transplantation therapy in spinal cord injury. *Cell. Mol. Life Sci.* **75**, 989–1000 (2018).

Development of a composite hydrogel-decellularised scaffold intervention for chondrocyte implantation

P. Statham¹, L. Jennings¹, E. Jones², J. Warren¹, M. Izon³, H. Fermor¹

¹ Institute of Medical and Biological Engineering, University of Leeds, Leeds ² St. James University Hospital, Leeds ³ Tissue Regenix PLC, Leeds

INTRODUCTION: Autologous chondrocyte implantation has emerged as a promising regenerative approach to cartilage repair, and has recently been recommended by NICE for lesions >2cm². However, prior to regeneration the cell/matrix graft has limited mechanical strength or function, and has complications such as cell leakage². We propose the use of cell seeded decellularised grafts as a novel treatment for cartilage lesions. This study details development and assessment of a decellularised scaffold of dimensions appropriate for large shallow lesions, as well initial viability results of cells encapsulated in a self-assembling peptide (SAP) cell delivery system.

METHODS: Porcine legs were obtained from a local abattoir and femoral condyles were extracted. These were subsequently shaped to dimension of 2(w) x 2(l) x 0.5(d), and were subject to the Leeds decellularisation process. Following this, the decellularised scaffolds were assayed for DNA content, and for cytotoxicity of scaffold and extract. For the SAP experiment, cells were seeded at 4x10⁵ cells/cm² in SAP/CS and assayed with LIVE/DEAD reagents at Day 7 and 14.

RESULTS: Whilst members of our group have previously demonstrated decellularisation of osteochondral pins, this is yet to be confirmed for the new scaffold dimensions. Figures 1 & 2 demonstrate successful decellularisation of the scaffold, as well as its cytocompatibility.

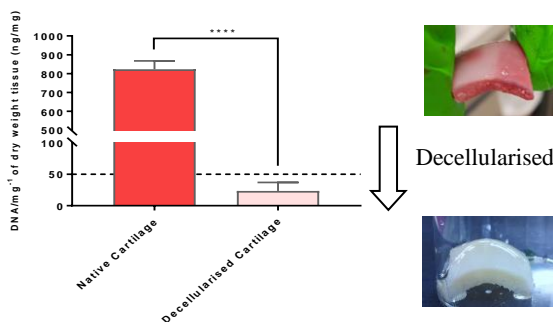


Fig.1: Assay comparing DNA content in native cartilage versus decellularised cartilage sheets (**** = p<0.0001). Images indicated scaffolds before and after decellularisation.

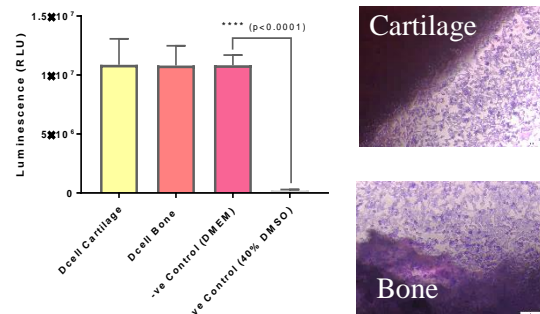


Fig.2: Extract (left) and contact (right) cytotoxicity assay of decellularised osteochondral scaffolds with BHK cells (**** = p<0.0001)

Before generating and testing the composite scaffold we deemed it important to investigate the ability of the hydrogel system to support cell delivery and proliferation. We conducted a 2-week time course study and assayed for cell viability using LIVE/DEAD staining. Despite the qualitative nature of this result, this data provides promising indications that over 14 days, our hydrogel can support cell survival.

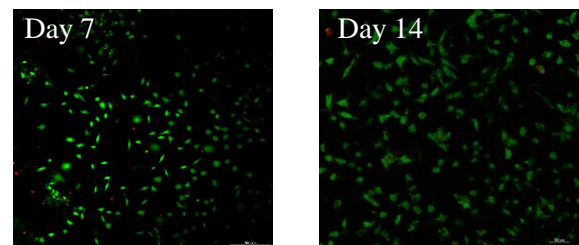


Fig.3: LIVE/DEAD assay of L929s encapsulated in P11-8/CS at Day 7 & 14

DISCUSSION & CONCLUSIONS: This data provides indications to pursue development of this technology towards the composite scaffold system of cells, scaffold and hydrogel. Once cell viability has been determined over time, investigations into the biomechanical function of these scaffolds will be conducted.

REFERENCES: ¹ NICE (2017) Autologous chondrocyte implantation for treating symptomatic articular defects of the knee. www.nice.org.uk ² Lee WY-w, Wang B. 2017, Cartilage repair by mesenchymal stem cells: Clinical trial update and perspectives, *Journal of Orthopaedic Translation*, **9**: 76-88.

Michael Moore, Elena Mancuso, George Burke, Brian J. Meenan

Nanotechnology and Integrated Bioengineering Centre (NIBEC), Ulster University,
Shore Road, Newtownabbey BT37 0QB, UK

Corresponding Author: moore-m23@ulster.ac.uk – (PhD Student 2nd Year)

Introduction: Additive manufacturing (AM) technologies provide a promising strategy for fabricating custom made and patient specific scaffolds for bone tissue engineering (BTE) (1). Whereas, the development of polymeric filaments and inks for use in 3D printing is advancing rapidly, the same cannot be said for ceramics. The majority of the literature reporting the use of calcium phosphate AM inks revolves around complex mixtures of aqueous-based slurries. Such mixtures are difficult to prepare and must undergo controlled dehydration to form a green structure before sintering. Also, most of them require the use of solvents and binders which may lead to harmful residues along with un-intended chemical interactions such as oxidation or crystallisation (2). The research presented here investigates the use of solvent-free hydroxyapatite-derived inks, based on the use of triglycerides, in order to enable the 3D printing of ceramic-based bespoke substitutes for BTE.

Material & Methods: A pre-sintered grade of hydroxyapatite (HA, Plasma Biotral, UK) was mixed with the triglyceride linoleic acid (TLA, Sigma Aldrich, UK) to form an ink with varying weight to weight ratios. Subsequently, 3D scaffolds were manufactured using a 3D Bioplotter (EnvisionTEC, Germany). SolidEdge CAD software was used to design the required scaffold structures and exported as an STL file to the Bioplotter RP software. A low-temperature extrusion head was employed with the ink HA-TLA ink maintained at 22°C during the printing process. The fabricated scaffolds are then sintered to 1200°C for 3 hours in a Carbolite furnace at a ramp rate of 5°C/min. The resulting scaffolds and inks were characterised in terms of their physical and chemical properties (SEM, micro-CT and TGA).

Results & Discussion. Integral 3D scaffolds were produced using the HA-TLA ink system developed here. A range of scaffolds with various layer geometry and orientation were successfully fabricated. Micro CT analysis of the 3D structures is provided in Figure 1 for a 3D scaffold designed to have a 1mm spacing and a 0-90° layer configuration giving an indicative porosity in the range of 40% with interconnectivity of 98%, which is similar to that of human cancellous bone. These data confirm that the internal structure and associated key parameters, such as porosity, pore interconnectivity and surface area, are all fully representative of the CAD design files employed. SEM analysis was used to evaluate the surface topography and pore size of the constructs. Figure 2(a) shows a typical scaffold has an average macro pore size of 502 µm and a strut diameter of 698 µm. Figure 2(b), illustrates the presence of micro pore of 126 µm on the surface of the sintered HA struts.

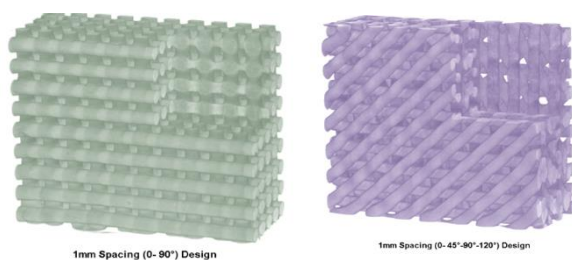


Figure 1. Micro-CT reconstructions of HA-TLA scaffolds.

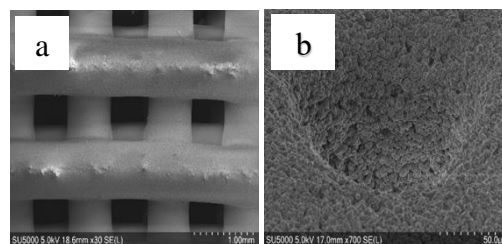


Figure 2. SEM Images of (a) macro-structure and (b) micro-porosity of HA-TLA scaffolds.

Conclusion: A solvent-free ink based on various w/w ratios of hydroxyapatite and triglyceride linoleic acid has been demonstrated to be capable of forming advanced and complex anisotropic 3D structures, via additive manufacturing technology. The system lends itself to the development of custom-made calcium phosphate-based scaffolds to treat complex critical sized bone defects within orthopaedic surgery

References

1. S. Bose, M. Roy, A. Bandyopadhyay, Recent advances in bone tissue engineering scaffolds, Trends Biotechnol. 30 (10) (2012) 546–554.
2. C. Slots *et al* Simple additive manufacturing of an osteoconductive ceramic using suspension melt extrusion- (2017) 198-208

Discovering novel immune-modulatory monosaccharides using high-throughput screening strategies

M Alobaid¹, S-J Richards², M.I Gibson², M Alexander³, A Ghaemmaghmi¹,
1Immunology School of life science University of Nottingham..2Department of Chemistry and Medical school, University of Warwick 3School of Pharmacy, University of Nottingham

INTRODUCTION: Dendritic cells (DCs) are immune sentinels that sense the surrounding environment using pathogen recognition receptors (PRRs such as the membrane bound c-type lectins (CTLs). Different CTLs have affinities for different sugars and upon interaction will determine the response of DCs and ultimately determines the fate of T cells through production of different cytokines and expression of surface markers^{1,2}. In this project we applied high throughput screening strategies to investigate immune modulatory properties of a combinatorial library of synthetic monosaccharide with a particular focus on the ability of different monosaccharides in modulating key functional properties of human Dendritic cells (DCs)³. We hypothesised that monosaccharides with distinct structures are able to promote generation of immune stimulatory or regulatory DCs with the ability to initiate or suppress immune responses. Herein we studied the immunomodulatory effects of a combinatorial library of sugars consisting of mannose, galactose and fucose in two isoforms in a plate bound format on LPS stimulated DC. DCs immunogenicity was assessed using Indoleamine 2,3-dioxygenase (IDO) enzymatic activity surface marker studies and cytokine profile as primary readouts.

METHODS: Dendritic cells were differentiated from CD14 isolated monocytes in the presence of GM-CSF and IL4. These cells were incubated with immobilised sugars in different concentrations in the presence or absence of a TLR4 ligand (LPS) for 24hrs. Cells were collected for flow cytometry to analyse surface marker expression while supernatant was assessed for cytokine profile. Co-cultures were performed between autologous T-cells and DCs where DCs were initially cultured with the sugars in the presence LPS. Supernatant was collected for cytokine analysis.

RESULTS: DCs treated with Immobilised sugars had a lower expression of CD40 and a varying levels of CD86 compared to LPS alone while no changes were observed in PD-L1 expression which suggests a modulation of DC phenotype is caused by the immobilized sugars. These findings go along the decrease in IDO activity, interleukin (IL)-12 and the increase in IL10 production for fucose and galactose combinations favouring an anti-inflammatory phenotype. Conversely, mannose combinations treated DC showed some decrease in IDO activity while having an increase in IL12 favouring a pro-inflammatory phenotype. This is further consolidated with the DC/T-cell co-cultures showing increase in T-regulatory cells in the presence of galactose combinations and Th1 protective phenotype. Interestingly, sugars have shown to have an increase in IL17 where pure galactose in isoforms while a decrease is seen if mannose is associated with galactose.

DISCUSSION & CONCLUSIONS: Collectively these observations show the potential immunomodulatory effects of monosaccharides in priming DCs and skewing immune responses towards different functional phenotypes. Optimised combination of monosaccharides could provide a powerful tool for immune modulation with potential applications in vaccination, cancer therapy and managing a host of inflammatory diseases.

REFERENCES

1. Van der Leek, A. P.; et al., *Frontiers in immunology* 2017, 8.
2. Rabinovich, G. A et al. *Annals of the New York* 2012, 1253.
3. Salazar, F.; Ghaemmaghmi, A. M., *Frontiers in immunology* 2013, 4, 356.

Effect of conditioned media from adipose-derived stromal cells, adipose tissue and emulsified fat on endothelial cells

A. Penuelas Alvarez¹, J. Shepherd², V. Hearnden¹

¹ Department of Material Science and Engineering, The University of Sheffield, United Kingdom.

² School of Clinical Dentistry, The University of Sheffield, United Kingdom

INTRODUCTION: Although different skin engineering strategies have been developed to promote wound healing, crucial obstacles such as vascularization have yet to be overcome. Fat-derived stromal cells have been shown to aid in wound healing through their ability to drive angiogenesis, increase protein production, and reduce inflammation. In addition, data suggest that the regenerative potential from adipose tissue and its stromal cells come from their derived secreted products. In this work, we tested and compared the pro-vascularization properties of conditioned media of human adipose tissue, emulsified fat, and cultured adipose-derived stromal cells.

METHODS: Adipose-derived stromal cells (ADSC) were isolated using enzymatic digestion and adherence culture. Emulsified-fat was produced passing minced adipose tissue between two syringes 100 times. Conditioned media from adipose tissue, emulsified-fat and cultured ADSC were obtained after 3 days of culture. Human microvascular endothelial cells (HMEC-1) and human dermal microvascular endothelial cells (HDMEC) were used to analyze the pro-vascularisation properties of the conditioned media. The cell viability assay using MTT reduction to formazan by viable cells was performed to test if the conditioned media promoted cell proliferation; while a migration assay was used to study if conditioned media also was able to stimulate cell migration.

RESULTS: Conditioned media from the different studied groups did not increase the metabolic activity or migration on HMEC-1 (Figure 1). In addition, vascular endothelial growth factor (VEGF), and fibroblast growth factor (FGF) did not significantly increase metabolism or migration of the cells indicating that this cell line is hard to stimulate. However, the conditioned media from adipose tissue and ADSC significantly increased HDMEC migration compared to control (Figure 2B). The conditioned media did not, however, affect the metabolic activity of these primary cells (Figure 2A). These results indicate that the growth

factors in the conditioned media promote endothelial cell migration.

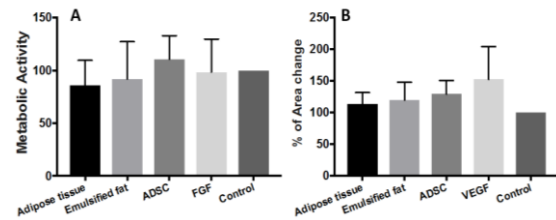


Figure 1. Metabolic activity (1A), and migration stimulation (1B) of HMEC-1 using conditioned media of adipose tissue, emulsified fat, and ADSC. VEGF and FGF were used as positive controls and normal media as negative control. N=3, n=3. Error bars indicate SD±.

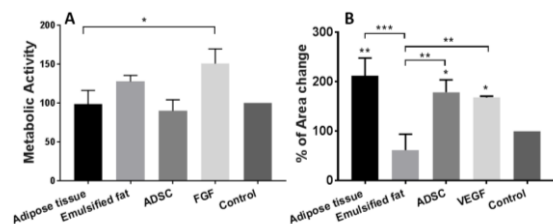


Figure 2. Metabolic activity (2A), and migration stimulation (2B) of HDMEC using conditioned media of adipose tissue, emulsified fat, and ADSC. VEGF and FGF were used as positive controls and normal media as negative control. N=1, n=3. Error bars indicate SD±. *p<0.05, **p<0.01, ***p<0.001.

DISCUSSION & CONCLUSIONS: ADSCs have previously been shown to be a promising tool for regenerative medicine since they enhance wound healing, however there are relatively few *in vitro* studies investigating whole fat. Conditioned media from adipose tissue and ADSC had a stimulatory effect on HDMEC migration suggesting that its pro-angiogenic properties come from promoting endothelial cell migration. Further investigation is needed to analyse the pro-vascularisation factors released in the conditioned media.

ACKNOWLEDGEMENTS: This work is supported by Consejo Nacional de Ciencia y Tecnología (CONACYT), and The University of Sheffield. The patient samples were made available through the Sheffield Hospital Directorate of Plastic, Reconstructive Hand and Burns Surgery under research ethics number 15/YH/0177.

EMBEDDED BIOPRINTING AN *IN VITRO* COCHLEA MODEL FOR STUDYING COCHLEAR IMPLANTS

Iek Man Lei¹ (PhD student - 2nd year), Chen Jiang², Manohar Bance² and Yan Yan Shery Huang^{1*}

¹Department of Engineering, University of Cambridge

²Department of Medicine, University of Cambridge

*Corresponding author: yysh2@cam.ac.uk

Introduction

Since the mid-1980s, cochlear implants have been used to treat severe hearing loss, remarkably improved patients' quality of life¹. Though its successful clinical outcome, several issues of the current cochlear implants, such as the distortion problem caused by the uncontrolled current spread within cochleae, enormous individual differences in outcomes and the lack of pre-implant predictor of outcomes, have yet to be addressed^{2,3}. In addition, the absence of predictive models for cochlear implant studies is an obstacle to improving the current implants. Animal models have been extensively used in the preclinical hearing research, however these models fail to represent the anatomical features and variability of human cochleae. In an effort to reduce *in vivo* approaches and to develop a personalised approach for cochlear implant testing, this work aims to develop an *in vitro* cochlea model as a tool for cochlear implant research. Here, we demonstrate a novel technique to fabricate a cochlea model by embedded printing a fugitive ink inside a bone-mimetic matrix.

Materials and Methods

All experiments in this work were performed with a custom-built 3D bioprinting system. The 3D fugitive template of human anatomical cochlea structure was printed inside a bath of polysaccharide-hydroxyapatite composite matrix. After printing, the matrix was crosslinked and subsequently the fugitive ink was removed, leaving a hollow structure of cochlea inside a bone-mimetic matrix. To optimise the matrix formulations, rheological and swelling properties of the matrix material were assessed. Electric field imaging (EFI) profiles measured in patients and the bioprinted models were compared to evaluate the potential of the model as a tool for cochlear implant studies.

Results and Discussion

We show a novel embedded bioprinting approach to fabricate a freestanding hollow structure of cochlea inside a bone-mimetic matrix. Our bioprinted model closely mimics the anatomical feature of human cochlea, and the matrix formulation has been tailored to mimic the biochemical composition of cortical bones. The EFI measurements show similarities between patients and the bioprinted model.

Conclusions

In this work, we have fabricated an *in vitro* cochlea model by embedded printing a fugitive cochlea structure inside a bone-mimetic matrix. The geometry of the model and the matrix composition closely mimic native cochleae. We anticipate that our biomimetic model can accelerate the advancement of cochlear implants and possibly advance the development of a personalised model for testing cochlear implants.

References

1. Hainarosie, M., Zainea, V. & Hainarosie, R. *J. Med. Life* (2014).
2. Pisoni, D. B., Kronenberger, W. G., Harris, M. S. & Moberly, A. C. *World J. Otorhinolaryngol. - Head Neck Surg.* (2017).
3. Ballesterio, J. *et al. Trends Hear.* (2015).

Acknowledgements

The authors would like to thank the European Research Council, the W D Armstrong Trust, the Evelyn Trust and the Wellcome Trust for their funding and Advanced Bionics Corporation for providing cochlear implants and software on this research.

Engineering the Liver Using Self-assembled Peptide Hydrogels

Y. Xin¹, A. Saiani^{1,2}, A. F. Miller^{2,3}, J. E. Gough¹

¹School of Materials, University of Manchester, Manchester, UK, ²Manchester Institute of Biotechnology, University of Manchester, Manchester, UK, ³School of Chemical Engineering & Analytical Science, University of Manchester, Manchester, UK

INTRODUCTION: Liver diseases are becoming a significant public medical burden[1]. To overcome the lack of donor livers and high cost of therapy, this project aims to exploit a long-term culture system that maintains hepatocyte specific functions [2] and cell viability for liver regeneration using self-assembled peptide hydrogels to mimic the normal hepatic extracellular matrix (ECM). Previous work [3] proved that a three dimensional cell culture environment could keep differentiated hepatocytes compared with *in vitro* cell culture on a flat surface.

METHODS: All tested self-assembled peptide hydrogels, PeptiGel® Alpha1, Alpha2, Alpha3 and Alpha4, were purchased from MANCHESTER BIOGEL. HepG2 cells (2×10^6) were suspended in 166 μ l fresh media then encapsulated within 1ml peptide hydrogel to get an homogeneous cell-gel mixture. 100 μ l of cell-gel mixture were placed into 24-well inserts, with fresh media added to surround each insert and on top of the sample. Cell viability at days 1, 4, 7 and 14 was investigated using LIVE/DEAD® cell viability assay with confocal microscopy (Leica SP5). The viscoelastic properties of peptide hydrogels and the porcine liver tissue were measured using rheometry (DHR-2, TA Instruments). The secondary structure of peptide hydrogels was analysed using FTIR and nano-structure was analysed using AFM microscopy (Multimode 8, Bruker).

RESULTS: The theoretical net charge of peptide hydrogels and mechanical stiffness of hydrogels and porcine liver tissue were investigated. At pH 7, Alpha1 and Gamma1 were at neutral charge, Alpha2 had one positive charge, Alpha4 and Gamma4 had two positive charges. As illustrated in Fig.1, at 1 Hz, the G' of collagen type I was 256.51 ± 19.47 Pa, Alpha2 peptide hydrogel was 12.01 ± 1.9 kPa and porcine liver tissue sample was 64.49 ± 11.84 kPa. A cell viability assay showed that over 14 days *in vitro* culture, HepG2 cells

proliferated within Alpha1 and Gamma1 and would survive within Alpha2 and Alpha3.

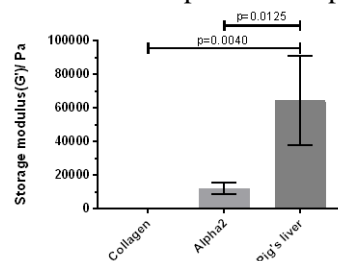


Fig. 1: The average storage modulus (G') of collagen, Alpha2 and porcine liver tissue samples at 1 Hz, results were recorded at 37°C.

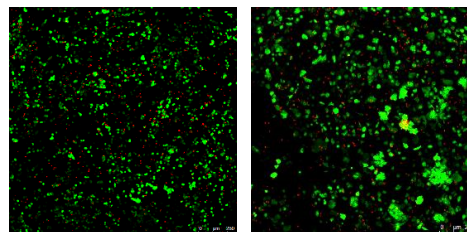


Fig. 2: Live/Dead assays of HepG2 cells encapsulated in PeptiGel® Alpha1 at Day1 (left) and Day3 (right). Scale bar=250 μ m.

DISCUSSION & CONCLUSIONS:

These initial results show maintenance of hepatocyte viability within peptide hydrogels warranting further investigation into functional behaviour. The cell spheroid pattern (Fig.2) suggested HepG2 cells may maintain hepatic functions and further investigations are underway[4].

ACKNOWLEDGEMENTS: Thanks for the guidance and support from my supervisors Prof. Julie Gough, Prof. Alberto Saiani and Prof. Aline Miller.

REFERENCES:

- [1] L. Rolfe *et al.*, *Lancet*, vol. 391, no. 10125, pp. 1097–1107, 2017.
- [2] O. Ogoke, J. Oluwole, and N. Parashurama, *Journal of Biological Engineering*, vol. 11, no. 1. 2017.
- [3] C. T. Nicolas *et al.*, *Stem Cells*, vol. 35, no. 1, pp. 42–50, 2017.
- [4] M. Bokhari *et al.*, *J. Anat.*, vol. 211, no. 4, pp. 567–576, 2007.

Enhanced proliferation and osteogenic differentiation of MC3T3-E1 cells on piezoelectric polymeric scaffolds

B.Tandon^{1,2}, J J Blaker^{1,2*}, Sarah H Cartmell^{1*}

¹School of Materials, The University of Manchester, Manchester, UK, ²Bio-Active Materials group, School of Materials, The University of Manchester, Manchester, UK.

INTRODUCTION: Piezoelectric materials are receiving attention in bone tissue regeneration, are capable of delivering electrical cues to cells, and can influence their differentiation [1]. In this study, polyvinylidene fluoride (PVDF) fibres were fabricated and the response of MC3T3-E1 cells on PVDF films and fibres was analysed.

METHODS: Solution blow spinning (SBS) and electrospinning (ES) were utilised to fabricate PVDF micron and sub-micron fibres to study the effect of processing on production rate, fibre diameter distribution, piezoelectric characteristics, and bone like cell response. Scanning electron microscopy, Fourier-transform infrared spectroscopy, differential scanning calorimetry and X-ray diffraction measurements were performed on fibres.

Cellular metabolic activity, cell number and alkaline phosphatase (ALP) activity of MC3T3-E1 cells on fibres was investigated and compared to commercially available poled and non-poled PVDF films. Poly(ϵ -caprolactone) (PCL) fibres were used as control fibres in all the studies.

RESULTS: PVDF fibre membranes with different fibre diameter distributions were produced (400 ± 140 nm for SBS, and two batches of ES fibres at 550 ± 320 nm and 2.54 ± 1.1 μ m). SBS enabled fibre production rates three times higher than ES. Quantification of electroactive β -phase showed higher content in the SBS fibre membranes, over ES fibrous membranes, with SBS fibre membranes β -phase content comparable to that of the poled films. Batch-to-batch comparison of the β -phase content revealed lower variability in the fibres fabricated using ES (n=3).

Cell metabolic activity (day 7) and ALP activity showed no significance difference among the fibre groups, and found similar to non-piezoelectric (non-polarised) PVDF films. The positive and negative surfaces of piezoelectric PVDF films (polarised) were both

found to have higher metabolic activity, cell number and ALP activity than PVDF sub-micron fibres.

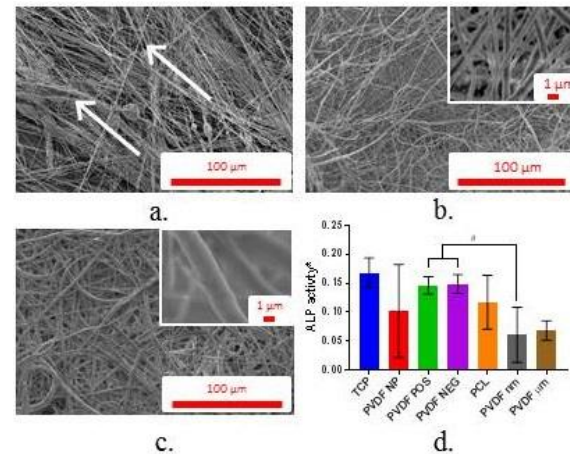


Figure 1 SEM images of fibres obtained from SBS (a) and ES (b. sub-micron (nm) and c. micron (μ m)), ALP activity observed on day 10 on different materials; # represents $p < 0.05$ using one way ANOVA analysis; *normalized to cell number.

DISCUSSION & CONCLUSIONS: The batch-to-batch variation in SBS could be attributed to compressed air temperature and solution temperature, which can affect the solvent evaporation and consequently the formation of phases [1]. Enhanced cellular response on charged surfaces has been shown to arise from attraction of ions towards the charged surfaces, which has been shown to have direct effect on proliferation and differentiation of cells [2]. The polarised films showed higher ALP activity and cell number when compared to that of fibrous membranes. The involvement of specific pathways (ERK and p38) in altering cellular response is currently under investigation.

ACKNOWLEDGEMENTS: BT would like to thank the Commonwealth Scholarship Commission (CSC) for funding this PhD.

REFERENCES: [1] Tandon B et al, Acta Biomaterialia, 2018, 73(1). [2] Kumar D et al, Acta Biomaterialia, 2010, 6(1549-1554).

EXAMINATION OF THE SUITABILITY OF LIPIODOL AS A CONTRAST AGENT FOR POLYETHYLENE BIOMATERIALS

Fedra Zaribaf¹, Harinderjit Gill, Elise Pegg

¹Department of Mechanical Engineering, University of Bath, Bath, UK

Corresponding author: PHZZ20@bath.ac.uk – PhD student (3rd year)

Introduction

Ultra-high molecular weight polyethylene (UHMWPE) is a bearing material used for almost all joint replacement designs. However, UHMWPE has a limited X-ray attenuation, which means early diagnosis of failures such as dislocation, bearing fracture and wear can be challenging because the position of the part cannot be identified (Figure 1). The presence of the polyethylene bearing can be confirmed using embedded metallic radiographic markers; but it has been shown that the radiographic markers can increase the risk of fracture and failure¹. We have used a novel method to enhance the radiopacity of polyethylene by diffusing an FDA-approved contrast agent into the surface of the polymer. The aim of this study is to find an optimal radiopacity level, where the part can be identified in a radiograph while retaining the static material properties.

Materials and Methods

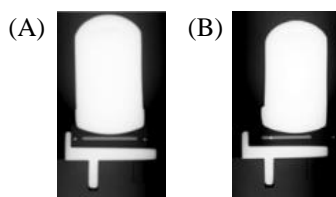


Figure 1. Position (A) and issues like overhanging (B) are difficult to diagnosed of polyethylene bearing cannot be identified using X-ray imaging due to the low X-ray visibility

Un-irradiated medical grade 4 mm thick UHMWPE sheet (GUR1050, Celanese, Oberhausen, Germany) was machined into tensile test samples in accordance with ISO-572 Annex A. An elevated temperature was applied to facilitate the diffusion (85°C, 105°C, 125°C) for 12 h, 18 h and 24 h to achieve a range of radiopacities. The melting point and crystallinity of the samples were quantified using DSC (TA instrument, DSC 250, 20°C-200°C, heat rate= 10 °C/min). Each sample was imaged using a μ CT scanner (X Tec, XT H 225 ST, Nikon Metrology UK Ltd, Derby, UK, 162 kV, resolution 0.2 mm) to quantify the radiopacity. Analysis of the CT data was performed using Simpleware ScanIP (Synopsys, Inc., Exeter, UK (release version 2017)). Water, air and untreated polyethylene were used to convert the CT- grayscale to Hounsfield Unit (HU). Tensile tests were conducted at

room temperature in accordance with ISO-527 using an electromechanical test machine (Instron 5965) at a rate of 50 mm/min, on; virgin UHMWPE, thermally treated UHMWPE and Lipiodol treated UHMWPE. Five specimens per condition were tested to obtain tensile modulus (E), 0.2% yield strain, ultimate tensile strength (UTS), toughness and elongation at failure.

Results and Discussion

The results of our study (Figure 2) confirmed that treating polyethylene with Lipiodol does not alter the crystallinity of the polymer ($p=0.56$) while it enhances the X-ray visibility of the samples (from 110 HU to 1200 HU). In terms of mechanical properties, there was no significant alteration in the yield strength ($p=0.07$) and ultimate tensile strength ($p=0.3$) of the Lipiodol treated, thermal treatment and virgin UHMWPE samples provided the treatment temperature was less than 125 °C. However, there was a slight increase (2%) elongation at failure ($p=0.049$) of the samples. It has been shown that other clinically available oil-infused UHMWPE (e.g. vitamin-E) has a similar plasticising effect on polyethylene, but the effect can be mitigated through irradiation-induced crosslinking³.

Conclusions

The aim of this study was to identify the optimal level of radiopacity. Based on the current result the optimal radiopacity can be achieved at by treatment at 105 °C for 24 h (approx. 400 HU). Under these conditions the contrast agent (Lipiodol) does not alter the crystallinity or the tensile properties of the samples, and are comparable with untreated polyethylene. Radiopaque UHMWPE is a promising material for medical use; however, the differences observed in the toughness and ductility will be investigated further as part of future work to assess the safety of the material.

References

Pegg *et al*, EFORT, 2016

Sobieraj *et al*, J Mech Behav Biomed Mater 2009

Oral *et al*, ORS, 2006

Acknowledgement: Celanese for providing medical grade UHMWPE

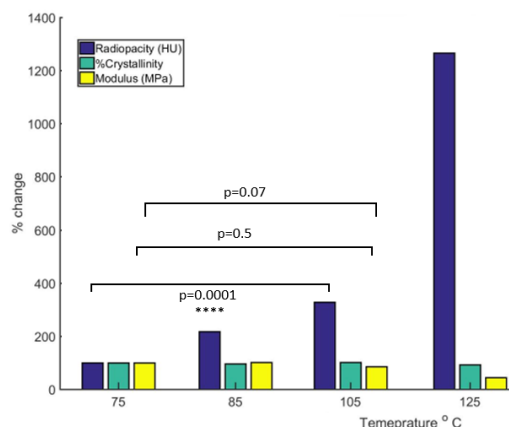


Figure 2. The radiopacity, crystallinity, and elastic modulus of the untreated polyethylene samples compared to those treated with Lipiodol under varying conditions.

Experimental investigation on the impact of an Engineered Bioactive Microenvironment using Growth factors on PEEK Osteoinduction

N. Alotaibi^{1,2}, K. Naudi¹, M. Salmeron-Sanchez², M. J Dalby², Ashraf Ayoub¹

¹ Glasgow Dental Hospital & School, ² Centre for Cellular Microenvironment, University of Glasgow, Glasgow, Scotland

INTRODUCTION: Applied regenerative medicine has become the future of medicine. This study focused on the implementation of a material based system via engineered synthetic microenvironments to potentiate osseointegration. This is based on the ability of plasma polymerised ethyl acrylate (p-PEA) to facilitate the fibrillogenesis of fibronectin (FN) which exposes integrin and growth factor (GF) binding domains (1). The system allows a synergistic interaction of the integrin/growth factor receptors.

Polyetheretherketone (PEEK) is a thermoplastic polymer introduced as an alternative for metal implants. It overcomes the limitations of titanium implants which support its potential utilisation as an implant, but PEEK's inertness does not encourage osseointegration which is required in this particular application. Therefore, this project tested the efficacy of biologically activated PEEK on mesenchymal stem cells (MSCs) as a substrate to stimulate osteogenic differentiation. This can have major clinical implications with the production of PEEK implants that can be used to replace extracted teeth.

METHODS: We investigated the application of p-PEA coated with fibronectin followed by the loading of a low dose of BMP-2 [100ng/ml] on the surface of the PEEK (Figure 1). Coating optimisation was assessed by WCA, AFM, FN and BMP-2 adsorption. The coating thickness was measured by the Scratch test. The availability of GF and integrin domains was tested using ELISA. The BMP-2 release over 14 days was quantified via ELISA. The tensile test was assessed to check the adhesion force of the coating. Cell adhesion using MSCs was determined after three hours culture by SEM. The short- and long-term osteogenic differentiation of the cells was evaluated using alkaline phosphatase activity assay at 14 days and ALP staining at 28 days.

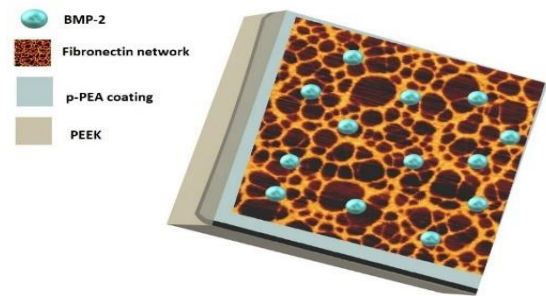


Fig. 1: Illustration of the engineered bioactive system. p-PEA: plasma polymerised poly (ethyl acrylate), PEEK: polyetheretherketone, BMP-2: bone morphogenic protein 2.

RESULTS: The thickness of the deposited p-PEA coatings was (≈ 344 nm). The engineered bioactive microenvironment was able to deliver less than 10% of bound BMP-2 over 14 days. The adhesion strength between the p-PEA and the surfaces (PEEK & Glass) was 5.1 ± 1.6 MPa and 5.5 ± 0.5 MPa, respectively. The SEM showed more cell adhesion and spreading on the coated PEEK surface in comparison to the uncoated ones. Both short- and long-term differentiation studies confirmed the potential of the engineered bioactive coating to create a more favourable and controlled microenvironment for implant osseointegration.

DISCUSSION & CONCLUSIONS: This in-vitro study confirms the efficiency of the engineered bioactive microenvironment using an ultra-low BMP-2 dose. The ability of the controlled release of BMP-2 allowed the osteogenic differentiation of undifferentiated MSCs and promoted osteogenesis on PEEK. An in-vivo study is underway before clinical trials.

REFERENCES: 1. Cheng, Zhe A., et al. "Nanoscale Coatings for Ultralow Dose BMP-2-Driven Regeneration of Critical-Sized Bone Defects." *Advanced Science* 6.2 (2019): 1800361.

Feeder-free Culture of Naïve Human Pluripotent Stem Cells in Normoxic Conditions

S. Pijuan-Galito^{1,2}, J.L. Thompson^{1,2}, L.C. Lewis¹, C. Tamm³, M.R. Alexander², C. Denning¹, C. Annerén³ and C.L.R. Merry¹

¹Division of Cancer & Stem Cells and ²School of Pharmacy, University of Nottingham, UK.

³Dept. of Medical Biochemistry & Microbiology, Uppsala University, Uppsala, Sweden.

INTRODUCTION: The naïve pluripotent stem cell (PSCs) is a recently discovered human PSC state that relates to an earlier embryonic stage. The naïve PSC state has the potential to improve current stem cell therapies, as naïve PSCs have no differentiation bias (seen in traditional stem cell lines), can be clonally expanded and are not growth factor dependent. However, human PSCs have shown resistance towards reversion to the naïve state, with protocols requiring feeder cells and hypoxic conditions, and a selection step being required before any analytical technique can be performed. We have previously shown that a human serum-derived protein, Inter-alpha inhibitor (IαI), supports human PSCs as a media additive (coating-free conditions) on tissue culture plastic, for long-term culture without loss of pluripotency(1). Here, we present successful generation and culture of human naïve PSCs in coating-free, feeder-free and normoxic conditions compatible with biomaterial studies by using the addition of IαI to the medium. Two different strategies were used, RSeT (StemCell Technologies) or 2iGö chemical resetting (2). The cells were then characterised and found to show typical naïve colony morphology, clonal capability and overall DNA hypomethylation.

METHODS: Four human PSC lines were reverted to naïve pluripotency by using RSeT or 2iGöY protocols in normoxic conditions on non-coated tissue-culture treated plastic with IαI as a media additive. After several passages, the cells are assessed for colony morphology, overall DNA methylation status using High-Resolution Confocal microscopy and a specific 5-methylcytosine antibody (C15200081, Diagenode), and naïve marker expression (*data not shown*).

RESULTS: After more than 5 passages in modified, feeder-free resetting conditions the human PSC line AT-1 shows change from flat large colonies to smaller, dome-like 3D colonies typical of naïve pluripotency (Fig. 1). Moreover, after twenty passages in feeder-free, RSeT medium supplemented with IαI, the human PSC

line HUES7 shows significant overall DNA hypomethylation (Fig. 2).

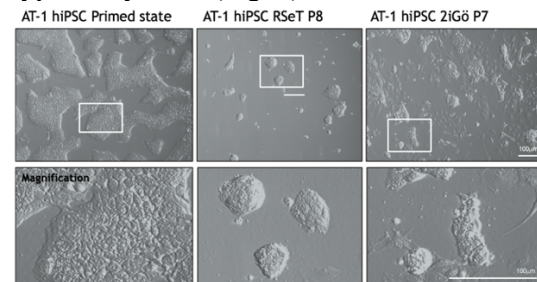


Fig. 1: Brightfield images of human PSC line AT-1 grown in traditional conditions (left), RSeT (middle) and 2iGö chemical resetting (right) (scale bar shows 100μm).

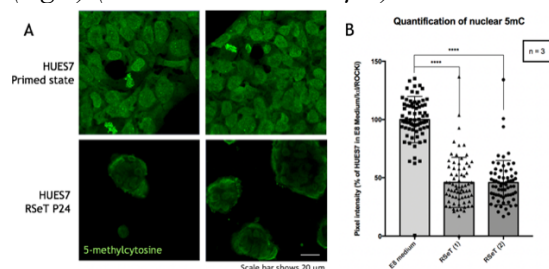


Fig. 2. DNA Methylation shown by 5-methylcytosine nuclear staining (A) images and (B) quantification of confocal image intensity of 5-methylcytosine nuclear staining of primed HUES7 human PSC line and HUES7 after 24 passages in feeder-free RSeT culture (Statistical analysis shows **** = $p < 0.001$).

DISCUSSION & CONCLUSIONS: In this study we have optimised human PSC resetting to naïve pluripotency, making it simpler and more time-efficient. This platform now has the flexibility to allow the use of naïve human PSCs in conjunction with a wide range of biomaterials.

ACKNOWLEDGEMENTS: This work is supported by the Wellcome Trust (Sir Henry Wellcome Fellowship, 201457/Z/16/Z) and the Swedish Research Council (2015-06532).

REFERENCES: (1) Pijuan-Galito S. et al. Nat Comms. 12170, 2016. (2) Guo G et al. Development 144:2748-63, 2017.

GELATIN MICROPARTICLES AS CARRIERS FOR THE DELIVERY OF ANTIMICROBIAL PEPTIDES

Kiran Mann,¹ Jenny Aveyard¹, Graeme Pitt¹ and Raechelle A. D'Sa*¹
² Centre of Materials and Structures School Of Engineering, University of Liverpool,
 Corresponding author: r.dsa@liverpool.ac.uk – PhD student (1st year)

Introduction

Antimicrobial peptides (AMPs) are naturally occurring macromolecules that demonstrate a potent antimicrobial activity against a broad range of microbes, including viruses, bacteria, and fungi. AMPs are part of every organism's innate immune response and act as a first line of defence against infection. The mechanism of action of AMPs is dissimilar to that of current clinically used antimicrobial agent and therefore, they are not susceptible to developing resistance and hence there is interest in the development of AMPs for as therapeutics for multidrug-resistant infections. While the use of AMPs for infection control shows significant promise, efficacy can be hampered owing to proteolytic degradation and low bioavailability. Entrapment of AMPs into drug delivery vehicles can significantly increase the therapeutic index of AMPs by stabilising the peptide, increasing the residence time and potentially targeting it to the site of action.

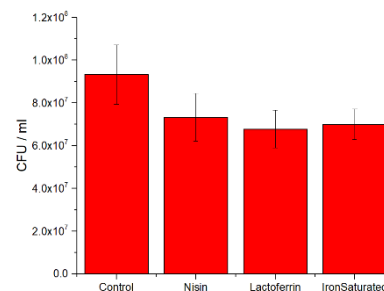
This study investigates two potent and FDA approved AMPs (nisin and lactoferrin (LF)) encapsulated in gelatin microparticles in a facile one-pot synthesis for the treatment of infections. Nisin is a versatile AMP due to its diverse applications in many fields from medicine to the food industry. It is a cationic amphiphilic peptide consisting of 34 amino acids with a cluster of hydrophobic residues at the N-terminus and hydrophilic residues at the C-terminus¹. Lactoferrin (LF) is a glycoprotein produced in various mammalian species, which is found in bodily secretions, including tears, saliva, bile, gastrointestinal fluids, urine, milk and colostrum. LF displays strong antimicrobial activity against a broad spectrum of bacteria, fungi, yeasts and viruses and in addition displays anti-inflammatory and anti-carcinogenic properties¹. The influence of the choice of AMP, particle size, zeta potential value, drug loading and in vitro drug release was studied.

Materials and Methods

Gelatin microparticles were prepared using an oil in water (O/W) emulsion technique. An aqueous solution of gelatin was added to corn oil to form the O/W emulsion, which was subsequently precipitated using acetone. A solution of nisin or LF was then left to incubate with the gelatin microparticles for 24 hrs to entrap the AMPs onto the microparticles. The microparticles were characterized with Fourier-transform infrared spectroscopy (FTIR), Zeta potential, particle size analysis and Scanning electron microscopy (SEM). The antimicrobial efficacy were tested against *Staphylococcus aureus* *S.aureus* using the spread plate technique and the colony forming units (CFU) were measured at 4 and 24 hr time points.

Results and Discussion

The influence of a number of experimental variables of microparticle synthesis and AMP used was investigated. The control particles sizes varied from 148.7 d.nm to 4893 d.nm, with a zeta potential of 3.34. After entrapment of the AMPs the particles sizes there was an increase in size and zeta potential. The antimicrobial efficacy of the AMP-loaded microparticles was tested against *S. aureus* and shown in figure 1. There was a 1-log reduction in the nisin and lactoferrin loaded microparticles compared with the control gelatin.



Conclusion

In this study we have developed a procedure to entrap antimicrobial peptides gelatin microcapsules using an oil-in-water emulsion method. Characterisation of the particles was performed using Zeta potential, particle size analysis FTIR and scanning electron microscopy. The AMP-loaded microparticles showed promise as a drug delivery vehicle to improve the delivery of the active agent for the treatment of infections.

References

1. J Aveyard, *et al.* J. Mater. Chem. B, 2017, 5, 2500-2510

Acknowledgements

This work was supported by EPSRC Centre of Doctoral Training (CDT) in Risk and Uncertainty (EP/L015927/1).

Generating Intrafusal Skeletal Muscle Fibres *In-Vitro*

P. Barrett¹, V. Mudera¹ and D. J. Player¹.

¹*Division of Surgery and Interventional Science, Faculty of Medical Sciences, University College London, UK*

INTRODUCTION: Muscle spindles (MS) are described as sensory organs, that detect and mediate static and dynamic information about skeletal muscle fibre length and stretch (proprioception). MS are embedded within skeletal muscle, running parallel and surrounded by regular, force producing fibres (extrafusal fibres). They consist of an encapsulated bundle of intrafusal muscle fibres, innervated by afferent sensory and efferent γ -motor neurons. There are three types of intrafusal fibres, categorised based upon their multinucleate morphology; nuclear bag1, bag2 and chain. (Banks, 1994). Impairment of proprioception is associated with many diseases including multiple sclerosis and motor neuron disease, as well as spinal cord and peripheral nerve injury. These patients display various difficulties in controlling the speed and magnitude of their limbs, which will affect various basic motor skills (Guo et al., 2017). While the use of human samples is ideal, the type of studies that can be performed are limited by tissue availability and ethical considerations. We aim to produce an *in vitro* 3D biomimetic system composed of the intrafusal fibres, this will facilitate novel studies of the molecular and cellular mechanisms regulating their phenotype, in a defined, controlled system. Neuregulin isoform 1 (NRG-1) is well documented to induce muscle progenitor cell intrafusal differentiation and therefore is a suitable candidate for use in the proposed model.

METHODS: C2C12 myoblasts were grown to confluence in growth media consisting of DMEM (SH30022.01, Hyclone), 20% FBS (SV30160.03, Hyclone) and 1% antibiotic solution (SV30079.01, Hyclone) at 37°C, 5% CO₂. To induce myotube formation the serum media concentration was reduced to 2% horse serum (HS, H0146, Sigma). To induce intrafusal specific differentiation media was supplemented with NRG-1 in a time-course and dose dependent manner. Immunofluorescence microscopy was used alongside morphological assessment to define the extent of intrafusal differentiation.

RESULTS: It is evident that standard differentiation methods, produce myotubes with heterogeneous morphologies (Fig 1.), which currently are not identified as either extra- or intrafusal. Intrafusal fibre formation and specific morphological parameters are under characterization.

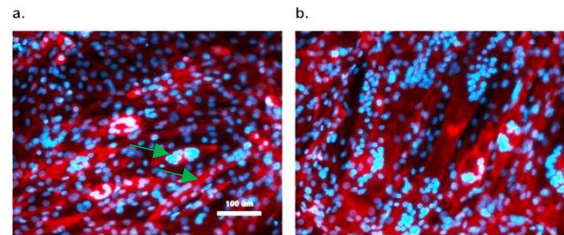


Fig 1: C2C12 myoblast differentiation generates heterogeneous morphologies. A: Early (3 days) myotubes, B: late (5 days) myotubes. Red = Phalloidin, Blue = DAPI. Arrows show heterogenous morphologies.

DISCUSSION & CONCLUSIONS: We are developing a 3D biomimetic model with intrafusal fibres generated *in-vitro*. Experiments are currently ongoing with respect to the time-course and dose response relationship of NRG-1 induction of intrafusal fibre differentiation of myoblasts. Future work will seek to adopt a tissue engineering approach to generate a reproducible and testable 3D model of the MS. Furthermore, we would like to test using relevant clinical samples obtained from innervated and denervated tissue, to explore the basic biology of intrafusal regeneration.

ACKNOWLEDGEMENTS: PB is in receipt of a John Scales Studentship.

REFERENCES: Banks, R. W. The motor innervation of mammalian muscle spindles. *Prog. Neurobiol.* 43, 323–362 (1994).

Guo, X. et al. Tissue engineering the mechanosensory circuit of the stretch reflex arc with human stem cells: Sensory neuron innervation of intrafusal muscle fibers. *Biomaterials* 122, 179–187 (2017).

Kucera, J., Walro, J. M. & Gorza, L. The Jourd of Histochemistry and Cytwhemistry I Expression of Type-specific MHC Isoforms in Rat Intrafusal Muscle Fibers'. **40**, (1992).

Human Extracellular Matrix Powder Hydrogels: Development of a New Human Tissue-Specific Product in NHSBT

Rathbone S¹, Barrera V¹, Ingham E², Kearney JN¹ and Rooney P¹

¹NHS Blood and Transplant, Tissue and Eye Services R&D, Speke, Liverpool L24 8RB,
²IMBE, University of Leeds, Leeds LS2 9JT.

INTRODUCTION: NHS Blood and Transplant have developed methodologies for the decellularisation of various tissue types (amnion, bone, dermal tissue, heart valves, tendon, nerves) as allografts for clinical use. The demand for hydrogels containing human tissue extracellular matrix (ECM) components is increasing, to provide a tuneable scaffold for expansion and differentiation of human cells *in vitro*. We aim to use human decellularised tissue as a starting material to develop a wide range of human tissue-specific ECM hydrogels.

METHODS: ECM powder was obtained from three different types of human tissue - cryopreserved human skin and bone from deceased donors and amniotic membrane from living donors. Skin and amnion were decellularised using a mild detergent (0.01-0.05% w/v SDS)¹ frozen and ground. Bone decellularisation was achieved by a combination of sonication, warm water washes and centrifugation followed by demineralisation and grinding (Eagle 2014)². Histology and Quant-iT PicoGreen dsDNA kit were used to assess tissue architecture and measure DNA quantity in tissue samples respectively. All tissue ECM powders were solubilised using porcine pepsin, following the protocol of Badylak S *et al.* (2007)³. The final tissue concentration in the hydrogels varied between approximately 8-22mg/ml. ECM hydrogels were assessed for biocompatibility by culturing human cells appropriate to the tissue type (human amnion cells, human dermal fibroblasts and MG63 an osteosarcoma cell line) for up to 7 days before performing live/dead staining and proliferation assays. Cells were either 1) added to gels in solution and the temperature was increased to allow gels to set; or 2) inoculated on top of pre-set gels. In vitro contact cytotoxicity assays were also performed on gels alone with appropriate cells.

RESULTS:

Histological analysis of decellularised tissues showed complete removal of cellular

components, and the histoarchitecture remained intact. When the temperature was increased to physiological temperature, all gels set within 35 minutes. No ECM hydrogels were cytotoxic and set gels allowed cells to survive, attach and proliferate both inside (Fig. 1A) and on top of gels (Fig.1B-C) up to 1.5-1.9 fold increase.

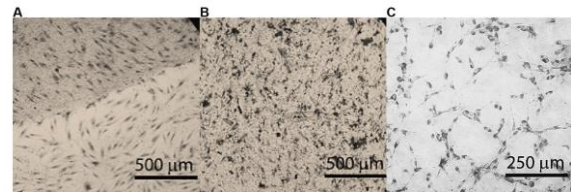


Fig. 1: Human fibroblasts (A-B) and amnion (C) cells growing inside and on top of ECM-derived hydrogels.

DISCUSSION & CONCLUSIONS: Human tissue-specific ECM hydrogels may represent a new formulation of human allograft delivery, which can be used in translational research in academia or clinical evaluations. Generating a liquid ECM which can be administered by injection provides a minimally invasive procedure to deliver the tissue graft and treat certain conditions for which a whole allograft is not needed or is characterized by challenging surgical procedures (i.e. spinal cord injuries).

ACKNOWLEDGEMENTS:

We are grateful for the generosity of donors/donor families who kindly donated the tissues for research. This work was funded by NHS Blood and Transplant and performed under HTA licences 11018 and 12608.

REFERENCES:

1. Hogg P *et al.* (2013) Development of Decellularised Dermis. *Cell Tissue Bank* 14, 465.
2. Eagle M *et al.* (2014) Production of an Osteoinductive Demineralised Bone Matrix Powder without the use of organic solvents. *Cell Tissue Bank*.
3. Badylak S (2007) The Extracellular Matrix as a Biologic Scaffold Material. *Biomaterials* 28(25:3587).

IDENTIFICATION OF SCALABLE POLYMERS CAPABLE OF MODULATING MACROPHAGE POLARISATION

Chidimma Mbadugha,¹ Morgan R. Alexander², Amir Ghaemmaghani¹

¹Division of Immunology and immuno-bioengineering, School of Life Sciences, University of Nottingham, ²Laboratory of Biophysics and Surface Analysis, School of Pharmacy, University of Nottingham
 Corresponding author: chidimma.mbadugha@nottingham.ac.uk – PhD student (4th year)

Introduction

Host immune responses to biomaterials play a critical role in clinical success or failure of medical devices¹. Adverse immune responses elicited by macrophages against biomedical implants has been a long standing issue in the field of biomedical engineering. A potential approach to limit these reactions is developing biomaterials with immunomodulatory abilities. These materials could direct macrophage polarisation away from a pro-inflammatory phenotype and towards pro-healing phenotype, thereby accelerating healing while reducing tissue damage and fibrosis². Biomaterials surface chemistry has been shown to influence functions of different cell types, including macrophages³. In this study, using a high throughput screening strategy, we sought to identify immune-instructive polymers with the ability to induce macrophage polarisation towards pro or anti-inflammatory phenotypes.

Materials and Methods

Using a high-throughput micro-array screening approach, we investigated the immunomodulatory effects of 283 acrylate or acrylamide polymers, on the polarisation of primary human monocyte-derived macrophages. Screening was carried out by quantifying expression of pro-inflammatory (M1) and anti-inflammatory (M2) markers, calprotectin and mannose receptor respectively, expressed by cells on different polymers. Polymers observed to impact macrophage polarisation were scaled up. Subsequently, the impact of these scaled-up polymers on cell viability, cytokine production, gene expression and phagocytic ability was assessed.

Results and Discussion

The development of biomaterial design principles that will enhance the generation of favourable cell-material interaction has been the focus of various studies. Polymer micro-array strategy employed in this study presents a time and cost efficient approach, for screening a wide range of materials for desired responses. From the initial screen, polymers which influenced macrophage polarisation were identified. Following polymer scale-up, we observed a differential expression of M1 and M2 associated cytokines and transcription factors by macrophages grown on different polymer materials, with some polymers inducing a highly polarised M1 or M2 phenotype. Furthermore, polymers were seen to have varying effects on macrophage phagocytic ability.

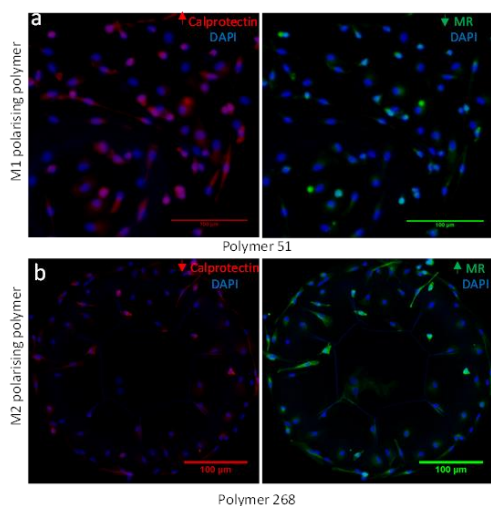


Figure 1: Immunofluorescence images of macrophages on different polymer spots. Images show differential expression of calprotectin and mannose receptor by cells on M1 and M2 polarising polymers. A) polymer 51 B) polymer 268. Representative images are shown from n=3 biological replicates.

Conclusion

Our findings show that polymer choice influence macrophage behaviour. Future work will focus on investigating the molecular basis of material-induced macrophage polarisation.

References

1. Brown B. N. et al. Biomaterials 33: 3792-3802, 2012
2. Franz S. et al. Biomaterials 32: 6692-6709, 2011
3. Rostam H. et al. Immunobiology 221(11): 1237-1246, 201

Immune Instructive Polymers for Dendritic Cell Modulation

L. Kämmerling¹, M. R. Alexander², Amir M. Ghaemmaghami¹

¹*School of Life Sciences, University of Nottingham, UK,* ²*School of Pharmacy, University of Nottingham, UK*

INTRODUCTION: Frequently the immune system does not respond appropriately to cues and misguides its responses (e.g. allergies). The redirection of these responses is therefore an indispensable tool to overcome any misguidance of the immune system. Dendritic cells (DC) are known as the bridge between the innate and the adaptive arm of the immune system, as such, they are quintessential in the facilitation and regulation of an adaptive immune response due to their capability to interact with T cells. DC phenotype (particularly their maturation level) effect differential adaptive immune responses (e.g. T cell activation and polarization) and can be modulated¹. In order to fine tune immune responses, research has shifted to engineer more effective materials for this task. Identifying polymers that are changing DC phenotype and function - and understanding how - will hence not only lead to greater understanding on how to modulate the adaptive immune response but also lead to novel immune instructive polymers for clinical applications.

METHODS: Monocytes were isolated from human blood donations and differentiated with IL-4 and GM-CSF supplementation into DCs. DCs were then cultured on different UV-polymerized acrylate and methacrylate coatings². DCs were harvested after 24 hours and were screened by either viability assays, flow cytometry, ELISA or proliferation assay analysis.

RESULTS: Here, we screened a library starting with 222 different polymers and present hit polymers 1) that are inducing an activated DC state (similar to LPS stimulation) or 2) prevent the development of an activated state (even in presence of LPS). These hit polymers show significant modulations of surface marker phenotype, cytokine secretion profile, uptake abilities and as well as on the induction of memory T lymphocyte proliferation.

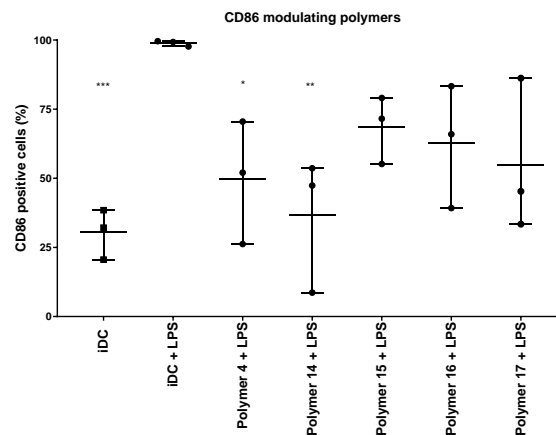


*Fig. 1: Effect of polymers on the upregulation of costimulatory surface marker CD83 as DC phenotype. Cells were stained and analysed by flow cytometry; data are percentage of positive cells and presented as mean \pm SD. For statistical tests: ONE-way ANOVA with Bonferroni multiple comparisons test; * <0.0332 ; ** $<.0021$; *** <0.0002 ; (n=3).*

DISCUSSION & CONCLUSIONS: To our knowledge, this represents the first large scale screen of synthetic polymers on their effects on DC phenotype and function. Immunomodulation of DCs by synthetic polymers discovered in this study may prove to be relevant for translation into future biomaterial design, as modulation of the immune response is an important focus of 'bio-instructive' material research and modulation of DCs has not been achieved by only materials so far.

REFERENCES:

1. Kou, P. M., Schwartz, Z., Boyan, B. D. & Babensee, J. E. Dendritic cell responses to surface properties of clinical titanium surfaces. *Acta Biomater.* **7**, 1354–1363 (2011).
2. Hook, A. L. *et al.* High throughput methods applied in biomaterial development and discovery. *Biomaterials* **31**, 187–198 (2010).

***In vivo*-like ramified morphologies are induced in neural immune cells (microglia) when cultured in 3D collagen hydrogels**

J.J. Goldfinch¹, B. Kabiri², K. Storey¹, [S.I. Jenkins](#)^{1,2}

¹[Neural Tissue Engineering Group](#), Institute for Science and Technology in Medicine (ISTM), Keele University, GB, ²School of Medicine, Keele University, GB

INTRODUCTION: Microglia, the principal immunocompetent cells of the brain and spinal cord (central nervous system, CNS) are critical to the resolution of neurological injury/disease. They switch between various activation states, displaying pro-/anti-inflammatory and pro-repair behaviours. But, inappropriate activation is increasingly implicated in exacerbating, or even causing, neurodegeneration. Studying this phenotype-switching is critical to understanding pathologies and may provide opportunities to harness pro-repair functions through immunomodulatory therapies.

However, typical *in vitro* microglial cultures fail to replicate the morphological and behavioural features of microglia *in vivo*. This is likely due to such systems using hard, flat surfaces (glass, plastic), without extracellular matrix (ECM) and with serum-supplemented media. These conditions do not mimic the soft, 3D milieu of the CNS, where the blood-brain barrier excludes serum. These differences likely contribute to the unramified/amoeboid microglial morphologies reported for *in vitro* culture, which more closely resemble pro-inflammatory microglia *in vivo* and in histology. Indeed, many studies suggest typical *in vitro* culture conditions always generate pro-inflammatory microglia.

To facilitate more accurate study of microglial phenotype-switching, we have developed a neuromimetic 3D, serum-free microglial culture system, using hydrogels.

METHODS: High purity microglial fractions (~98% Iba1⁺) were derived from primary rat cerebral cortices. Microglia were seeded in collagen I hydrogels (~800 µm depth), with control cultures on coverslips. Serum-free medium was compared to serum-supplemented medium. Time-lapse microscopy was used to examine microglial morphologies, process extension/retraction, and migration. Live/dead staining was used to assess culture viability. Immunocytochemistry was used to confirm microglial identity and assess activation status, with z stack fluorescence microscopy.

RESULTS: Microglial in hydrogels exhibited far greater ramifications than in 2D (Fig. 1), while also expressing typical microglial markers (Iba1, Cd11b, CD68, iNos, Arg1).

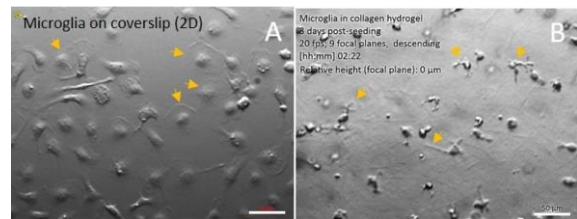


Fig. 1: Microglia cultured in collagen hydrogels exhibited highly ramified morphologies, including secondary branching. Ramified morphologies were rarely observed in 2D (coverslip) cultures, with a 'fried egg' morphology predominating.

DISCUSSION & CONCLUSIONS: The highly ramified morphologies that predominated when microglia were cultured in 3D hydrogels closely resemble the morphologies reported *in vivo* and in histological analyses. Therefore, this system may be useful for generating genuinely unactivated microglia *in vitro* (not typically possible under standard culture conditions). This may provide baseline conditions more closely matching those in healthy CNS tissue.

Further work is underway, stimulating microglia in hydrogels to study phenotype-switching.

Identifying/developing 3D biomaterial constructs which support microglial culture without pro-inflammatory activation would be of great benefit to neuroimmunological researchers, and would suggest potential for material implantation into the CNS without adverse immune responses, possibly facilitating drug/cell delivery for therapeutics.

ACKNOWLEDGEMENTS: BK's work was supported by a Biomedical Vacation Scholarship (Wellcome Trust, 2018).

Incorporation of antioxidant into structurally organised PCL scaffolds for cartilage tissue engineering

N. Munir, A. McDonald, A. Callanan

Institute for Bioengineering, School of Engineering, University of Edinburgh, United Kingdom

INTRODUCTION: The prevalence of osteoarthritis is on the rise and effective treatments for cartilage defects are still being sought¹. Cartilage tissue *in vivo* encompasses complex structures and composition, both of which influence cells and many properties of the native cartilage. The extracellular matrix structure and components provide both morphological cues and the necessary signals to promote cellular functions². Moreover, the accumulation of reactive oxidative species (ROS) has been linked to the pathogenesis of osteoarthritis³. Thus, the aim of this study was to produce scaffolds which mimic the complex structure of the cartilage and scaffolds which encompass antioxidant properties to reduce oxidative stress.

METHODS: Multizone scaffolds consist of three different zones (Fig 1A). The deep zone scaffold was fabricated by cryo-printing of an 8% w/v PCL/1, 4-Dioxane solution. The middle and superficial electrospun layers are composed of randomly orientated and aligned electrospun fibers, respectively (8% w/v PCL and HFIP). Multizone scaffolds were seeded with primary human chondrocytes and cultured for 24 hrs, 1, 3 and 5 weeks. Antioxidant incorporation was assessed in the directionally frozen zone of the multizone scaffold. Antioxidant scaffolds were fabricated using directional freezing of 8% w/v PCL/acetic acid. Scaffolds at various antioxidant concentrations were seeded with bovine chondrocytes for 24hrs, 3 and 6 days.

RESULTS: Multizone scaffolds successfully mimic the collagen fibre orientation and compressive properties of the native cartilage. Moreover, chondrocyte seeded multizone scaffolds demonstrated the ability to support long-term chondrocyte attachment and survival over a 5 week culture period. Furthermore, chondrocyte seeded multizone scaffolds were found to regulate expression of key genes in comparison to the controls (Fig 1B), as well as allowing the production of glycosaminoglycans. All Antioxidant scaffolds display a fibrous architecture which allowed cell attachment and

viability. Antioxidant scaffolds exhibited antioxidant capabilities which were noted through the reduction of hydrogen peroxide (Fig 1C, D).

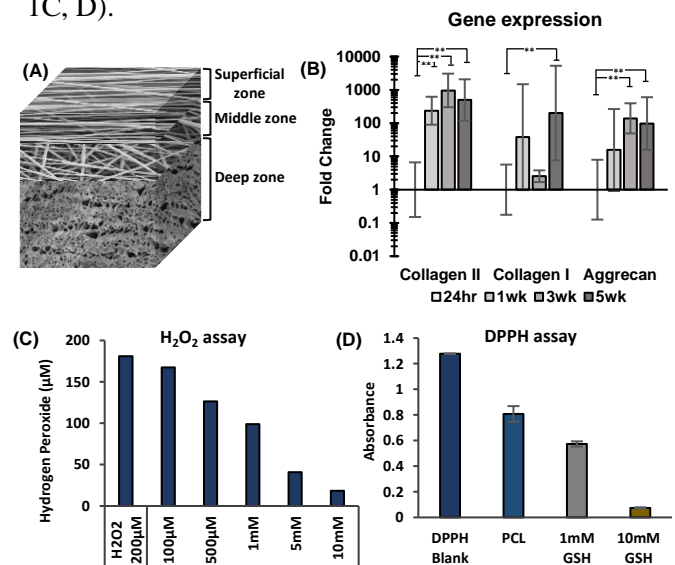


Fig. 1: (A) Illustration of the various layers of the multizone scaffold. (B) Gene expression in multizone scaffolds. Antioxidant capabilities of scaffolds noted through the reduction of (C) hydrogen peroxide after 24 hours and (D) 2,2-diphenyl-1-picrylhydrazyl (DPPH). Error bars=SE. * $p < 0.05$, ** $p < 0.01$; one-way ANOVA.

DISCUSSION & CONCLUSIONS: Multizone scaffolds provide a viable initial platform that captures the complex structure and compressive properties of the native cartilage. Moreover, they maintain chondrocyte phenotype and function, highlighting its potential in cartilage tissue engineering applications. Hybrid PCL and antioxidant scaffolds allowed for cell attachment and survival. These scaffolds also successfully displayed antioxidant capabilities.

ACKNOWLEDGEMENTS: EPSRC (EP/N509644/1) and MRC (MR/L012766/1).

REFERENCES: ¹ T. Lu et al (2013) *International Journal of Nanomedicine*. **8**: 337-350. ² K. Yudoh et al (2005) *Arthritis Research & Therapy*. **7**: 380-391. ³ F. Bhatti et al. (2013) *Inflammation Research*. **62**: 781-789.

Incorporation of Laminin into Polymeric Scaffolds for Kidney Tissue Engineering

B. Baskapan, A. Callanan

Institute for Bioengineering, School of Engineering, University of Edinburgh, UK

INTRODUCTION: Kidney disease is a worldwide public health problem that affects 10% of the world population.¹ Since current treatment options for renal failure are incapable of meeting the need, tissue engineering is seen as a promising approach to generate alternative renal models for regenerative treatment. Incorporation of natural extracellular matrix (ECM) protein into the synthetic polymer has been shown to enhance biocompatible properties of polymeric scaffolds.² Laminin, one of the major components of ECM is known to control the cellular activities in the basement membrane of kidneys.³ However, there is a paucity of data on the impact of laminin in kidney tissue engineering. Therefore, in this study, the effect of incorporating laminin into polycaprolactone (PCL) via different electrospinning techniques was investigated.

METHODS: Scaffolds were produced using three different electrospinning techniques containing PCL and laminin. For blend electrospinning laminin was mixed with 10% w/v PCL in HFIP. For emulsion electrospinning an aqueous solution of 30% w/v laminin in water was mixed with oil phase consisting of Span80 as a surfactant in a 14% w/v PCL solution at 1:60 v/v ratio. 10% PCL only was used as a control scaffold, and laminin amount was kept at 5 µg/ml for both blend and emulsion solutions. Morphology of the scaffolds was observed using Scanning Electron Microscopy (SEM). Mechanical properties of scaffolds and biochemical quantification of kidney cells (RC-124) on different scaffolds were analysed.

RESULTS: As seen in Figure 1 laminin incorporated PCL scaffolds with similar fibre sizes were successfully produced via different electrospinning methods. Table 1 shows the effect of laminin on fibre diameter and the tensile strength of blend and emulsion scaffolds. Cell viability studies also show that combinations of laminin with synthetic scaffolds provide good attachment of kidney cells onto scaffolds.

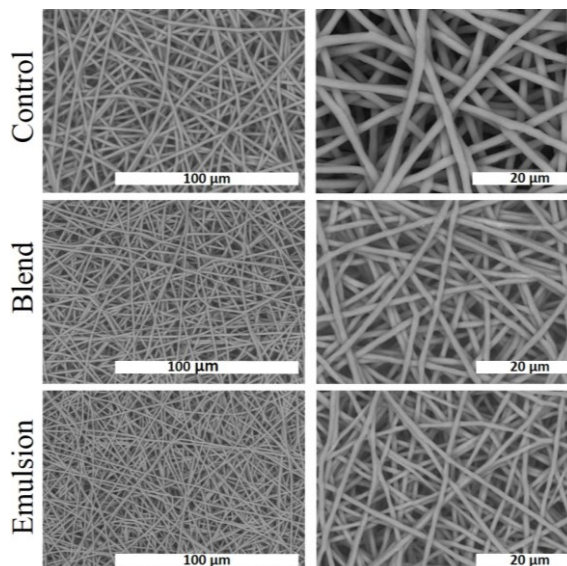


Fig. 1: SEM images of control, blend and emulsion scaffolds at different magnification.

Table 1. Fibre diameter and tensile strength of different scaffolds.

	Control	Blend	Emulsion
Fibre diameter (µm)	2.83±0.21	2.16±0.57	1.81±0.24
Tensile strength (MPa)	0.32±0.15	0.34±0.06	0.31±0.11

DISCUSSION & CONCLUSIONS: Results show that incorporation of natural ECM protein into PCL influences kidney cell behaviour on polymeric scaffolds. These first findings highlight the importance of further investigation of laminin in kidney tissue engineering to improve both understanding and treatment of renal diseases.

ACKNOWLEDGEMENTS: This work is funded by a Turkish Ministry of National Education studentship and MRC grant MR/L012766/1.

REFERENCES: ¹Bulletin of the World Health Organization. 2018. 96:414-422. ²Chevtchik N.V. et.al. 2018. J Tissue Eng Regen Med. 12:1670–1678. ³van Genderen A.M et.al. 2018. Adv. Healthcare Mater. 2018. 1800529.

INVESTIGATIONS INTO NOVEL TITANATE CONVERSION OF DC MAGNETRON SPUTTERED TITANIUM THIN FILMS FOR BIOMEDICAL APPLICATIONS

Matthew D. Wadge*¹, Burhan Turgut¹, Reda M. Felfel¹, Ifty Ahmed¹, David M. Grant¹

¹Department of Mechanical, Materials and Manufacturing Engineering, University of Nottingham, UK

Corresponding author: matthew.wadge@nottingham.ac.uk – PhD student (2nd year)

Introduction

The current process for improving implant surfaces to be bioactive, therefore, providing a more natural fixation, is reliant on high temperature (>1500 K⁽¹⁾) plasma spraying of hydroxyapatite (HA). However, these surfaces have been shown to spall due to their brittle nature, high internal stresses, and weak mechanical adhesion⁽²⁾. Titanate surfaces have been developed as an alternative since the mid-1990s by Kokubo *et al.*⁽³⁾, however, their applicability have been limited to titanium (Ti) and its alloys only *via* chemical conversion routes. The authors propose a novel method for generating nanoporous titanate surfaces on non-Ti biomedical materials through conversion of DC magnetron sputtered Ti films.

Materials and Methods

Commercially pure polished 10 mm 316L S.S. discs were subjected to DC magnetron sputtering using a cp-Ti (Miba Coatings; 99.5% purity) target (1.56 kW/cm² power density; optional 0 to -100 V substrate bias and up to 300 °C substrate heating). The produced *ca.* 4 μm films were then treated in NaOH (5 M; 60 °C; 24 h) to assess the effect of sputtering parameters on titanate conversion. The samples have been labelled according to the following convention: negative substrate bias (V)/applied substrate temperature (°C), e.g. 100V/150°C for -100 V bias and 150 °C applied temperature. Characterisation using SEM, EDX, XPS, Raman, FTIR, XRD, and texture coefficient analysis was conducted.

Results and Discussion

SEM micrographs (*Figure 1A-D*) demonstrated 3.89 ± 0.04, 3.90 ± 0.03, 3.71 ± 0.04 and 3.68 ± 0.02 μm thick Ti coatings for the 0V, 100V, 100V/150°C and 100V/300°C samples, respectively. Through application of a substrate bias, and bias in conjunction with substrate heating, the density of the films increased (reduction in coating thickness and surface voids). Furthermore, texture coefficient analysis of measured XRD spectra (*Figure 1E-F*) using the Harris equation⁽⁴⁾, exhibited a shift from columnar (preferred orientation in the Ti HCP (002) plane (PDF 00-044-1294); Texture coefficient ($T_{c(002)} = 3.39$) in the 0V sample, to more equiaxed ($T_{c(002)} = 1.54$; for pure equiaxed, $T_c = 1$) in the 100V/300°C sample. Subsequent titanate conversion of the above samples produced 1.12 ± 0.04, 1.20 ± 0.02, 1.20 ± 0.03, and 1.63 ± 0.06 μm thick titanate layers for the 0V, 100V, 100V/150°C, and 100V/300°C samples, respectively. Despite the proposed hypothesis that increased porosity would allow better NaOH penetration, therefore, increasing titanate conversion, this was not observed in the samples tested. EDX, XPS and Raman analysis, showed incorporation of 7.6 ± 0.1, 8.9 ± 0.1, 11.5 ± 1.8, and 7.6 ± 0.1 at.% of Na in the 0V, 100V, 100V/150°C, and 100V/300°C samples, respectively.

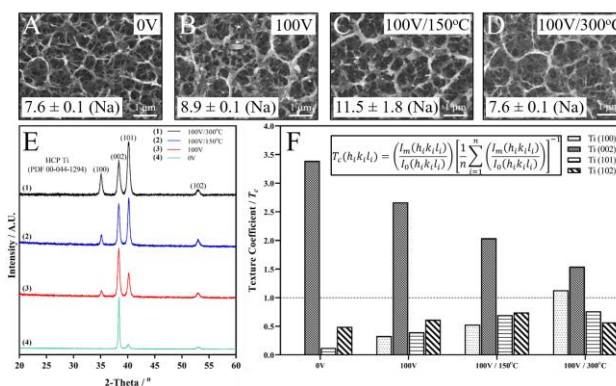


Figure 1. A-D) SEM micrographs and Na EDX inclusion (Insert) in titanate converted samples. E) XRD spectra and F) Texture coefficient calculations (Harris equation; Insert) of pre-converted samples.

Conclusions

Overall, the data presented demonstrates the successful conversion of DC magnetron sputtered Ti coatings into titanate structures, with increased Na inclusion for the unbiased (7.6 at.%), biased (8.9 at.%), and biased/heater runs (11.5 at.% & 7.6 at.%), respectively. The hypothesis that increased penetration in the more porous unbiased film was not evidenced, however, clear structural differences in the film produced have an effect on Na inclusion and titanate morphology of the conversion layer.

References

- [1] Y. C. Tsui *et al.*, *Biomaterials*, vol. 19, no. 22, pp. 2015-29, Nov 1998.
- [2] K. De Groot *et al.*, *Journal of Biomedical Materials Research Part A*, vol. 21, no. 12, pp. 1375-1381, 1987.
- [3] T. Kokubo *et al.*, *The Open Biomedical Engineering Journal*, vol. 9, no. 1, 2015.
- [4] G. Harris, *The London, Edinburgh, and Dublin Philosophical Magazine and Journal of Science*, vol. 43, no. 336, pp. 113-123, 1952.

Mathematical modelling informing tissue engineering protocols for a microcarrier bone culture

I.D. Burova¹, I.B. Wall^{2,3}, R.J. Shipley¹

¹Department of Mechanical Engineering, UCL, UK, ²Aston Medical Research Institute and School of Life and Health Sciences, Aston University, UK, ³Institute of Tissue Regeneration Engineering (ITREN), Dankook University, Republic of Korea

INTRODUCTION: Bone tissue engineering is a promising treatment for bone injury when self-regeneration is impaired due to extensive trauma or compromised by diabetes or osteoporosis¹. Regenerative bone cell therapies have the potential to deliver clinically-relevant cell numbers without the drawbacks of current treatments. Seeding osteoprogenitors on microcarriers in a bioreactor is a promising bottom-up tissue engineering technique which preserves cell phenotype by providing 3D cell-to-cell interaction and supplies sufficient nutrients and mechanical stimulation. Mathematical modelling can aid the translation of engineered bone tissues to the clinic by characterising the fluid flow, shear force and nutrient concentration required to produce functional grafts with uniformly-spread, clinically-relevant cell numbers.

METHODS: Building on our previous mathematical model of a microcarrier culture in static conditions², here we present a CFD model capturing the flow induced by an orbital shaker. The aim is to parameterise the simulations to experimental data on cell number at different rotation speeds to obtain a cell growth function dependent on shear stress. A centrifugal volume force is applied to the culture domain to represent the movement of the shaker platform. The Navier-Stokes equations for incompressible laminar flow alongside the level set two-phase flow method are adopted to track the free surface developed due to the shaking. Advection-reaction-diffusion equations model mass transport of oxygen, glucose and lactate in the system. A modified logistic growth law models cell number as a function of local oxygen concentration and shear force. The model is solved using finite-element methods in COMSOL Multiphysics.

RESULTS: The CFD model is first validated against PIV experiments published in literature³ (Fig.1), showing a good agreement for the free

surface position at all points during the orbital period. The method is then applied to the culture set-up under investigation to evaluate mass transport of the nutrients and the wall shear stress exerted at the bottom of the well (acting on the microcarrier-seeded cells).

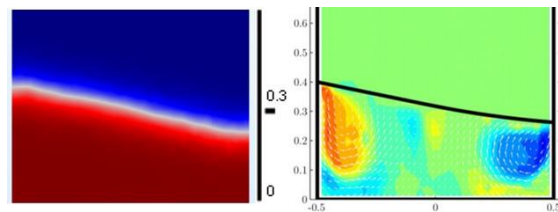


Fig. 1: Simulation results (left) and PIV experimental results (right)³ of free surface position in equivalent instance of rotation.

DISCUSSION & CONCLUSIONS: By developing this model and parameterising it to experimental data we aim to obtain a cell-specific shear stress-dependent growth function. This would enable the model to predict flow settings which maximise cell yield by improving nutrient availability at non-damaging stress levels in a time and cost-efficient manner.

ACKNOWLEDGEMENTS: IDB thanks the Rosetrees Trust for kindly funding this work.

REFERENCES: 1.Burova, I., et al., 2019. Mathematical and computational models for bone tissue engineering in bioreactor systems. *J.TissueEng.*, 10,p.204173141982792
2. Burova, I., et al., 2019. A parameterised mathematical model to elucidate osteoblast cell growth in a phosphate-glass microcarrier culture. *J.TissueEng.*, 10,p.2041731419830264.
3.De Silva Thompson, D., et al., 2019. Assessing behaviour of osteoblastic cells in dynamic culture conditions using titanium-doped phosphate glass microcarriers. *J.TissueEng.*,10,p.2041731419825772.
4.Weheliye, W., et al., 2013. On the fluid dynamics of shaken bioreactors—flow characterization and transition. *AIChE Journal*, 59(1), pp.334-344.

Mechanical loading attenuates atrophy in tissue engineered skeletal muscle.

[K Aguilar-Agon¹](#), [A Capel¹](#), [N Martin¹](#), [D Player²](#), [MP Lewis¹](#)

¹[School of Sport, Exercise and Health Sciences](#), Loughborough University, Loughborough ²[Institute of Orthopedics and Musculoskeletal Science](#), University of College London, Stanmore.

INTRODUCTION: Skeletal muscle exhibits a high degree of plasticity. Thus, mechanical loading of skeletal muscle results in molecular and phenotypic adaptations characterized by enhanced muscle size. However, dexamethasone (DEX) a type of glucocorticoid (GC) drug, is known to induce muscle atrophy both *in vitro* [1] and *in vivo*, as a side effect of GC treatment for conditions such as arthritis, asthma and chronic obstructive pulmonary disease (COPD) [2]. Muscle atrophy in severe cases leads to muscle weakness, fatigue and delayed ambulation. Hence, understanding the contracting mechanisms of GC-induced atrophy are of great clinical importance. In this investigation 3D skeletal muscle was tissue engineered (TE) utilizing the murine cell line C2C12, which bears likeness to native tissue (e.g. parallel, highly differentiated and functional myotubes) and benefits from the advantages of traditional *in vitro* experiments (e.g. high levels of control). The work aimed to determine if mechanical loading would protect and attenuate the effects of DEX administration to engineered skeletal muscle.

METHODS: Cells at a density of $1 \times 10^6/\text{mL}$ were pipetted into a Collagen/Matrigel™ (65%, 20%) solution and set in 3D printed molds. Following 14 days of culture, engineered muscles were administered 40 μM DEX over 24 hours, during which engineered muscles were floated in differentiation media and loaded using a mechanical stimulation bioreactor (MSB), or *vice versa*. Engineered muscles were homogenized or fixed for either RNA extraction or immunohistochemical staining.

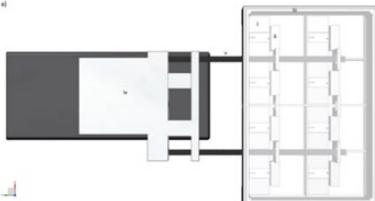


Fig 1: CAD model of the MSB used for mechanical overload.

RESULTS: We investigated candidate atrophic gene expression, along with myotube growth/loss and tissue function. Mechanical loading significantly decreased the upregulation of both ubiquitin ligases MAFbx and MuRF-1 post DEX administration. Furthermore, mechanical loading had a protective effect on atrophic genes prior to DEX administration. Positively, we observed hypertrophy of the myotubes both post and prior to DEX administration within the engineered muscle.

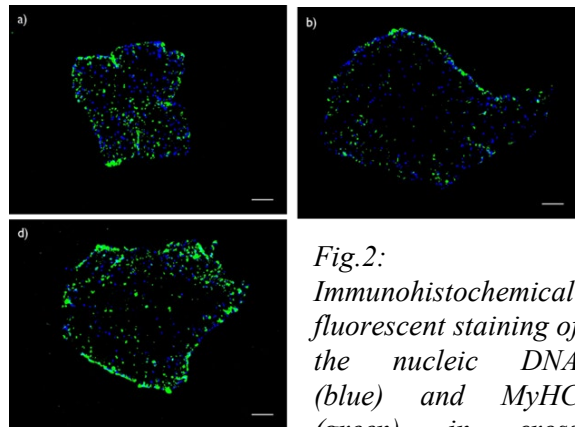


Fig.2: Immunohistochemical fluorescent staining of the nucleic DNA (blue) and MyHC (green) in cross sections of engineered muscles ($\times 10$ magnification) (a) CON (no DEX administration), (b) DEX administration, (d) DEX administration over 24 hours replaced with differentiation media and mechanically loaded for 3 hours and sampled after 48 hours.

DISCUSSION & CONCLUSIONS: We have described the molecular, morphological and functional adaptations to mechanical loading in mature TE skeletal muscle following a bout of acute atrophy succeeding/preceding DEX administration.

ACKNOWLEDGEMENTS: EPSRC/MRC CDT in Regenerative Medicine.

REFERENCES: ¹ Shimizu, K. *et al.*, (2017). *Bioengineering*, 4(2), 1–11. ² Schakman, O. *et al.*, (2013). *The International Journal of Biochemistry & Cell Biology*, 45(10), 2163–2172.

Micro-computed tomography as a predictive tool in the cell-sieving capabilities of structurally graded lyophilised collagen scaffolds

J.H. Shepherd^{1,2}, D. Howard³, C. Ghevaert³, S.M. Best², R.E. Cameron²

¹Department of Engineering, University of Leicester, ²Cambridge Centre for Medical Materials, Department of Materials Science and Metallurgy, University of Cambridge.

³Division of Transfusion Medicine, Department of Haematology, University of Cambridge

INTRODUCTION: Platelet transfusions are an essential part of treatment for a range of conditions including bone marrow failure, inherited platelet disorders and cancer. Unlike red blood cells, the storage and supply of platelets is challenging and there is demand for a clinically viable system for the *ex vivo* generation of donor independent platelets. Here we have considered a structurally graduated scaffold within a bioreactor to support human pluripotent derived megakaryocytes (MKs). The scaffold structure should act as a bone marrow analogue, supporting the MKs, offering sieving capability and shear flow over the cell surfaces to enhance platelet output.

A structurally graduated pore structure is desired such that the larger megakaryocytes are distributed through the scaffold, whilst only platelets are released into the flow. We employed micro-computed tomography (μ CT) in combination with micro-particle filtration for investigation of cellular separation in these graduated scaffolds.

METHODS: Scaffolds with a graduated pore structure (large on the top surface, reducing in size towards the lower surface) were produced through a two-stage lyophilisation process¹. Accessible pathways for platelets and MKs were predicted using interconnectivity analysis from μ CT and filtration capabilities analysed with synthetic micro-particle cell analogues.

μ CT was carried out on 5mm diameter samples with a scan pixel size of 1.5 μ m (Skyscan 1272, Bruker). Volumes of interest were selected and porosity and directional interconnectivity analysis carried out. The cellular filtration set-up was replicated with 10 and 20 μ m particles (analogues for platelets and MKs respectively). Particle distribution was analysed using μ CT.

RESULTS: Interconnectivity analysis predicted a highly accessible pore structure for MK cells. Micro-particle filtration experiments suggested a greater degree of 'cell' selection with on average 60% of the 10 μ m platelet

simulating particles counted in the outlet flow and almost none of the MK analogues. Micro-CT post-filtration demonstrated a uniform distribution of 20 μ m particles throughout the structure.

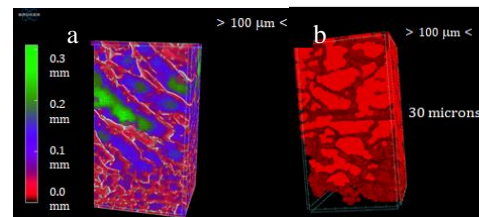


Figure 1a. Volume rendered model with structural graduation highlighted. b. predicted accessible pathways for MK sized particles.

DISCUSSION & CONCLUSIONS: In this work we successfully distinguished micro-particles from the scaffold struts, supporting the application of μ CT as a tool for the imaging of cellular infiltration². Subsequent analysis with platelets and megakaryocytes suggested micro-particle filtration to be a good predictor of cell behaviour in the context discussed here. Whilst the interconnectivity analysis did not prove a direct predictor of cellular filtration μ CT provides a body of scaffold data unobtainable from other methods. The theoretical analysis did not consider cell-substrate interactions, cell rheology, cell clusters, the blocking of pathways or cell generated ECM.

ACKNOWLEDGEMENTS: The work was supported by the European Research Council (ERC Advanced Grant 320598 3D-E), EPSRC grant E P/N019938/1 and grants from NHS Blood and Transplant, the Medical Research Council (MR/L022982/1) and the European Union (Silk Fusion: AMD-767309-3)

REFERENCES:

1. Shepherd, J.H. Howard, D. *et al.* *Biomaterials* **182** (2018), 135-144.
2. Shepherd, D.V. Shepherd, J.H. *et al.* *J. Mater. Sci. Mater. Med.* **29** (2018), 86

Microvessel-on-chip model.

Jenny O'Dowd¹, Magda Gerigk¹, Yan Yan Shery Huang¹

¹*Nanoscience Centre, Department of Engineering, University of Cambridge, GB*

INTRODUCTION: Metastasis is responsible for over 90% of cancer-related deaths[1], so it is crucial to develop tools to help better understand the processes, right down to the single-cell level. Metastatic cells intravasate into blood vessels and use them to travel within the body to new locations where they can extravasate and colonise the new site. Currently a lot of testing of potential drugs involves using 2D cells cultures but these often lack key features present in vivo which can lead to different responses to drugs. Therefore, we need to develop 3D, physiologically-relevant, validated models to study the interactions between cancer cells and blood vessels. There are several categories of approach for creating 3D models one of which is microfluidics. Here a PDMS-glass microfluidic device is seeded with Human Umbilical Vein Endothelial Cells (HUVECs) to form a microvessel-on-chip model compatible with high-resolution imaging.

METHODS: A master was created using soft lithography. Polydimethylsiloxane (PDMS) was poured onto the master, degassed and cured. Holes were punched for the inlet and outlet and the devices were soaked in ethanol overnight. The devices were dried before being air-plasma treated alongside 22mm glass cover slips which were then bonded to the devices, sealing them and forming the base. Whilst still hydrophilic from the air-plasma treatment, the channels were coated with poly-d-lysine (PDL). The devices were washed with DIW and left at 50°C for 18-24hrs. The channels were coated with collagen IV to facilitate adhesion of the cells and then later washed with cell culture medium (EGM-2 with 2% fetal bovine serum (FBS)) to remove excess collagen, submerged in medium and left in an incubator (5% CO₂ at 37 °C) overnight. HUVECs were inserted into the channel by pipette. Two hours later the devices were flipped 180° and seeded with cells again. Two hours after that the devices were flipped back and the media was replenished. The cells were fixed with 4% para-formaldehyde (PFA), stained with Phalloidin 488 (1:400) and CD31 (1:200) and imaged using confocal microscopy.

RESULTS: A microfluidic device was created in PDMS with a glass base (Fig. 1a). HUVECs were then seeded inside the channel of the device where they formed a microvessel. Devices were fixed and stained at four different time points (3, 6, 24 and 48h) and the growth of the microvessel was characterised by confocal microscopy. At three hours, cells had attached primarily to the bottom surface and had not yet formed a layer or any tight junctions. By six hours the cells had started to form a confluent layer on one surface of the microfluidic channel and were starting to form junctions. By 24 hours a vessel had formed with confluent layers on both the top and bottom of the devices. The CD31 staining showed that the cells had formed tight junctions (Fig. 1b). The HUVECs successfully formed a vessel with a lumen however the cross-section was rectangular. In the 48 hour samples, the vessel still had many tight junctions but there were noticeably more gaps present than at 24 hours.

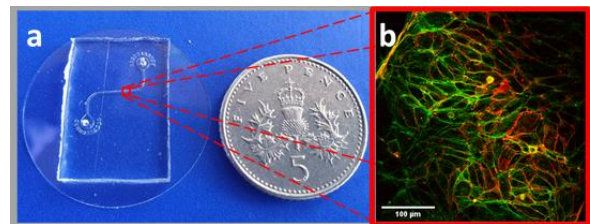


Fig. 1: (a) The PDMS-glass microfluidic device. (b) HUVECs in the channel, fixed at 24 hours and stained for tight junctions (CD31, red) and F-actin (Phalloidin, green).

DISCUSSION & CONCLUSIONS: A three-dimensional vessel was created by seeding HUVECs into a PDMS-glass microfluidic device. The device was created with a glass coverslip forming the bottom to allow for better imaging. A vessel with tight junctions and a lumen was formed by 24 hours from the second cell seeding. However, the wide design of the channel meant that the cross-section was rectangular rather than circular. By decreasing the width of the channel and therefore lowering the aspect ratio a cylindrical vessel may be formed.

REFERENCES: [1] Gupta, G.P. and Massagué, J. (2006). *Cell* 127 (4) 679-695

Modulating fibroblast behaviour using microparticle systems

Arsalan Latif¹, Adam Dundas², Valentina Cuzzucoli Crucitti², Ricky Wildman², Derek Irvine², Morgan R. Alexander³, Amir Ghaemmaghami¹

¹*School of life sciences, University of Nottingham, United Kingdom* ²*Department of chemical and environmental engineering, University of Nottingham, United Kingdom* ³*School of pharmacy, University of Nottingham, United Kingdom*

INTRODUCTION: The implantation of foreign materials into a host body, as used in medical devices, is known to induce an immune response. This immune response, known as the foreign body response, dictates whether biomaterial implantation leads to successful material integration and healing or towards encapsulation of material with extracellular matrix components, leading to fibrosis and rejection¹.

Fibroblasts have been shown to play an important role in both healing process and fibrotic capsule formation (as part of the foreign body response) depending on the nature of biochemical stimuli, e.g. from immune cells such as macrophages, and the physicochemical characteristics of the materials. Conversion of fibroblasts to myofibroblasts is the hallmark of fibrosis² and is associated with enhanced ECM secretion and could lead to fibrotic capsule formation if not regulated. Regulation of fibroblast to myofibroblast differentiation using biomaterial surface characteristics such as surface chemistry to control fibrosis is the goal of this work. High throughput screening of homo-polymers from the acrylate and methacrylate family, identified materials which either promoted or suppressed fibrotic behaviour of fibroblasts. To study these materials in 3-dimensions and in a clinically relevant format, they were fabricated into microparticles.

METHODS: Microparticles were fabricated using a droplet microfluidic technique forming Oil-in-Water (O/W) emulsions; having a dispersed phase containing UV photoinitiator and surfactant consisting of the desired chemistry. The emulsions were then solidified by UV curing (365nm) to form solid microparticles. Human skin fibroblasts (BJ cell line) were seeded onto these microparticles. Cells were then assessed for attachment, proliferation and the following cytokines: Fibroblast Growth Factor (bFGF), Interleukin - 1 β (IL-1 β) and Hepatic growth factor (HGF).

RESULTS: Our data clearly show that the microparticles fabricated using 'hit' polymers from the high throughput screen are able modulate (i.e. suppress or accelerate) fibroblast response as evidenced by changes in cell proliferation and secreted cytokines, figure 1.

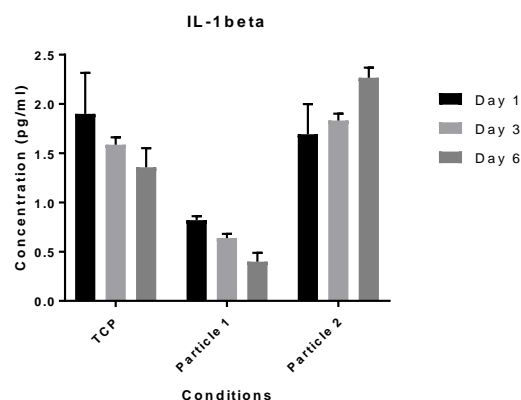


Fig. 1: Fibroblast secretion of pro-inflammatory cytokine IL-1 β on TCP and microparticles.

DISCUSSION & CONCLUSIONS: Studying fibroblast – microparticle interactions provides a base to influence fibrotic tissue microenvironments. In this study we assessed the ability of microparticles in modulating fibrotic responses in human skin fibroblasts. Inclusion of these microparticles in fibrotic microenvironments may provide a means for modulating deleterious fibrotic responses by directly influencing fibroblast proliferation and phenotype. Future work will focus on investigating microparticle effect on macrophages and the cross-talk between fibroblasts and macrophages in these microparticle systems

ACKNOWLEDGEMENTS:

Authors acknowledge EPSRC for grant funding (EP/N006615/1), and the School of Life Sciences Imaging Centre (SLIM) for use of their imaging facility.

REFERENCES:

1. Vishwakarma, A. et al. Engineering Immunomodulatory Biomaterials To Tune the Inflammatory Response. *Trends Biotechnol.* **34**, 470–482 (2016).
2. Jones, K. *Fibrotic Response to Biomaterials and all Associated Sequence of Fibrosis. Host Response to Biomaterials* (Elsevier Inc., 2015). doi:10.1016/B978-0-12-800196-7.00009-8

Morphological control of liver ECM-PCL electrospun scaffolds

TSR. Bate¹, SJ. Forbes², A. Callanan¹

¹*Institute for Bioengineering, School of Engineering, The University of Edinburgh, UK*

²*MRC Centre for Regenerative Medicine, The University of Edinburgh, Edinburgh BioQuarter, UK*

INTRODUCTION: Global mortality rates linked to liver disease have exhibited an upward trend since the 1970s, contrary to downward trends observed in other leading causes of death^{1,2}. *In-vitro* drug development methods are unable to provide effective and efficient routes in which new treatments can be achieved³. More relevant *in-vitro* models are required in order for drug development to progress. Electrospun scaffolds have been a subject of interest for *in-vitro* research due to the ability to mimic Extracellular Matrix (ECM) structures with biocompatible polymers and the potential of incorporating natural ECM to provide relevant biochemical cues. This study has explored the potential of the defined morphology of electrospun polycaprolactone (PCL) fibres combined with liver derived ECM (LECM) for controlled and reproducible 3D *in-vitro* liver tissue cultures.

METHODS: PCL scaffolds were electrospun with three varied architectures and two fibre sizes. LECM-PCL fibres were manufactured using decellularised rat livers. Briefly, whole rat livers were isolated and decellularised by perfusion with 0.25w/v% Sodium Dodecyl Sulphate (SDS) solution. These were subsequently washed and lyophilised then powdered using a planetary ball mill. The powder was dissolved with PCL in HFIP and electrospun into fibres. Fibres were characterized using SEM imaging, mechanical analyses and FTIR Spectroscopy. Scaffolds were seeded with HepG2 cells and cell viability, DNA quantitation, IHC staining and RT-qPCR Gene analysis were conducted at 24hr, 7 day and 14 day timepoints.

RESULTS: Larger fibres observed higher rates of proliferation than small fibres, with porous cryogenic scaffolds showing the highest rates for both small and large fibres. The morphology also influenced the structure of cell clusters. Maintenance of key liver function genes was observed on PCL scaffolds with a relative reduction in interstitial ECM genes. The presence and bioactivity of electrospun rat liver ECM is preserved with higher cell viability

observed on ECM scaffolds. LECM scaffolds influence gene expression in HepG2.

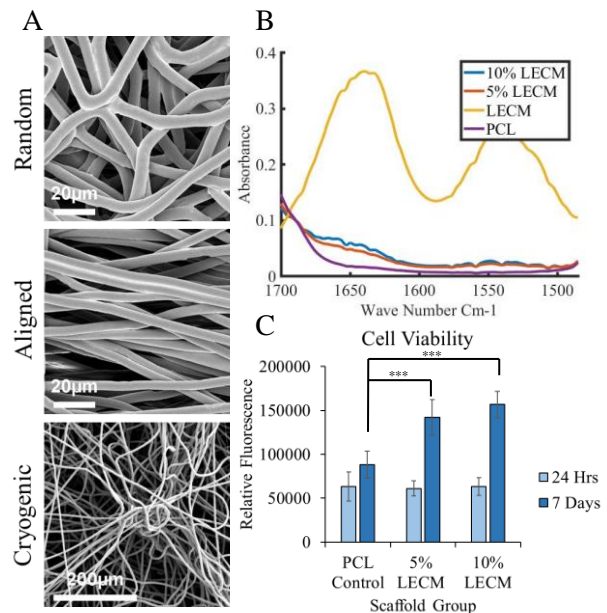


Figure 1: A) SEM images showing PCL fibres. B) FTIR spectrum confirming the presence of ECM moieties within ECM-PCL electrospun scaffolds. C) Cell viability of HepG2 cells on ECM-PCL scaffolds. $N=5$, One-way ANOVA, Tukey's analysis, *** = $p < 0.001$, error bars: $\pm SD$

DISCUSSION & CONCLUSIONS: Scaffold morphology has a measurable influence on HepG2 cultures. The incorporation of rat liver ECM into electrospun PCL scaffolds is capable of inducing altered biochemical responses in HepG2 cells, indicating that bioactive elements within the electrospun ECM are retained. Further investigation should confirm the degree to which bioactive ECM can be preserved within electrospun PCL scaffolds whilst maintaining tractable morphology.

ACKNOWLEDGEMENTS: EPSRC grant EP/N509644/1 and MRC grant MR/L012766/1.

REFERENCES: ¹Tapper, E. B. *BMJ* **362**, k2817 (2018). ²Williams, J. *Hepatology* **63**, 297–299 (2015). ³Hay, M., *Nat. Biotechnol.* **32**, 40–51 (2014).

MULTICELLULAR AGGREGATES GENERATED USING DROPLET MICROFLUIDICS FOR CARTILAGE TISSUE ENGINEERING

Juan Aviles Milan^{1,2}, J. West², X. Niu², Rahul S. Tare^{1,2}, Jonathan I. Dawson¹

Presenting Author: Juan Aviles Milan, J.Aviles-Milan@soton.ac.uk

¹Bone and Joint Research Group, Centre for Human Development, Stem Cells & Regeneration, University of Southampton, SO16 6YD, UK; ²Engineering and the Environment and Institute for Life Sciences, University of Southampton, SO17 1BJ, UK

INTRODUCTION: Musculoskeletal disorders cause severe impacts on the ageing global population and a large number of them require articular cartilage repair [1]. Human bone marrow stromal stem cells (hBMSCs) are a promising cell source but they pose a crucial limitation: subpopulation heterogeneity [2]. Hereby, we present a proof of concept for high-throughput cell aggregation in microdroplets simulating early chondrogenic condensation. This opens up the possibility of enriching hBMSC chondroprogenitor subpopulations on the basis of functional, condensation-dependent markers such as SOX9.

METHODS: qPCR and immunofluorescence (IF) were conducted to study *in vitro* SOX9 expression in hBMSCs for various cell numbers at the gene and protein level, respectively, as an early chondrogenic functional marker. Alcian Blue/Sirius Red and Safranin O stainings were also employed to assess the histological structure of the spheroids. Human articular chondrocytes (HACs) were included as a clinically relevant positive control. ATDC5 chondroprogenitor cells in chondrogenic differentiation medium were used for on-chip optimisation purposes, together with hBMSCs and HACs. Cells were harvested and injected through the inlets of a PDMS chip with continuous gentle stirring. QX200™ generation oil (Bio-Rad) was used for droplet stabilisation. Droplets were imaged onto a haemocytometer after 6, 24, 48 and 72 h to visualise cell aggregation and viability.

RESULTS: IF and qPCR ($p < 0.001$) confirmed SOX9 expression at early time points (day 1, 3 and 7) following hBMSC aggregation even at low cell number aggregates (500 and 5000; $n = 3$). Heterogeneous SOX9 expression was observed in hBMSCs from day 7 to day 21 for all cell numbers, whereas HACs maintained SOX9 protein expression. Alcian Blue/Sirius Red and Safranin O stainings

further highlighted the marked difference between unselected HBMSCs and HACs, the latter of which yielded a more uniform cartilage-like histological structure.

The droplets generated on the microfluidic platform had volumes ranging from 0.5 to 4 nL and had a highly monodisperse distribution ($COV < 0.5\%$). All three cell types formed aggregates 24 h following encapsulation that remained viable over 72 h of incubation, suggesting the stability of the culture system for early SOX9 screening.

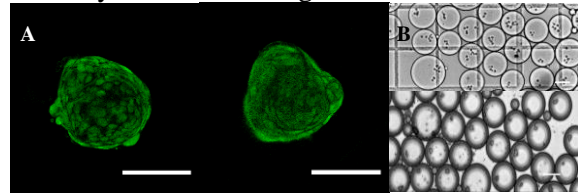


Fig. 1: (A) SOX9 IF distribution in 500 HAC (left) and HBMSC aggregates (right) on day 7; (B) cells in microdroplets after recovery (top); cell aggregates in microdroplets (bottom). Scale bar = 100 μ m.

DISCUSSION & CONCLUSIONS: This work illustrates the high-throughput potential of droplet microfluidics to yield stable aggregates. Early stage in SOX9 expression up to one week after aggregation at low cell numbers and the droplet volumes attainable suggest the suitability of this approach for enriching the hBMSC chondroprogenitor stem cell fraction.

ACKNOWLEDGEMENTS: This research project has received financial support from Versus Arthritis as part of a PhD Studentship for Juan Aviles Milan.

REFERENCES:

- [1] Briggs A et al. *Gerontologist*. 2016; 56(2):243-55
- [2] Bianco P et al. *Stem Cells*. 2001; 19(3):180-92

Musculoskeletal Tissue Interface Development

W. Balestri¹, R. Morris¹, J. A. Hunt¹, Y. Reinwald¹

¹Nottingham Trent University, School of Science and Technology, Nottingham, GB

INTRODUCTION: Tissue interfaces are present in all parts of the body. They are transition zones placed, which transfer load between different tissues. Interfaces have properties that belong to both tissues they connect ¹. Recently, the interest in their study has grown, because they are unable to regenerate after damage or deterioration. This deficiency can lead to organ malfunction and graft instability ².

Many *in vitro* three-dimensional (3D) tissue models have been developed in the last years. Biomaterial must be biocompatible, biodegradable and sterilisable. It can have natural or synthetic origin. By choosing the right combination of material and technique, it is possible to get a model that mimics the physical properties of the native tissue.

Several studies have been performed to study tissue interfaces. The additional tasks with interface models are the interaction among different cell types and different compositions and features ³.

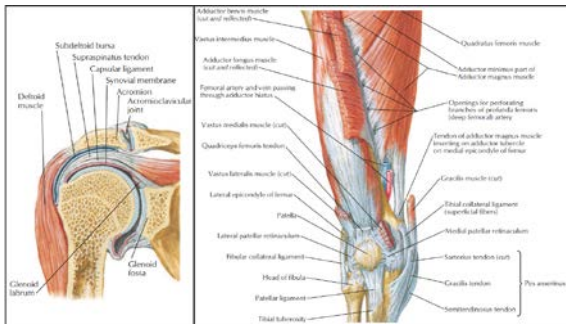


Figure 1: Joints in the human body. The rotator cuff (a) and synovial joint (b). In both images, it is possible to see the interface between the different tissues. Figures adapted from *Atlas of Human Anatomy*, seventh edition, 2019, F.H. Netter ⁴

AIM: The aim of this project is to develop a model of bone, tendon and muscle to study the interfaces among these tissues. Research will focus on the regeneration of interfaces and the behaviour of the different cells present in these tissues.

METHODS: A 3D model of bone, tendon and muscle was created. It was composed of smart biomaterials and fabricated with 3D printer techniques.



Figure 2: Cellink Bio X 3D printer

The response of human osteoblast-like cells, fibroblasts and muscle cells seeded onto this scaffold was studied and the development of the interface investigated. The study was conducted in a growth chamber developed specifically to keep tissues separated, but at the same time allowed cellular communication of the interface development.

REFERENCES:

1. Yang PJ, Temenoff JS. Engineering Orthopedic Tissue Interfaces. *Tissue Eng Part B Rev.* 2009;15(2):127-141. doi:10.1089/ten.teb.2008.0371
2. Lu HH, Subramony SD, Boushell MK, Zhang X. Tissue engineering strategies for the regeneration of orthopedic interfaces. *Ann Biomed Eng.* 2010;38(6):2142-2154. doi:10.1007/s10439-010-0046-y
3. Chang H-I, Wang Y. Cell Responses to Surface and Architecture of Tissue Engineering Scaffolds. In: *Regenerative Medicine and Tissue Engineering - Cells and Biomaterials*. InTech; 2011. doi:10.5772/21983
4. Netter FH (Frank H, Machado CAG, Hansen JT, Benninger B, Brueckner JK, Preceded by: Netter FH (Frank H. *Atlas of Human Anatomy*.

NANOCOMPOSITE HYDROGEL SYSTEM FOR BIOMEDICAL APPLICATIONS

Nathalie Sällström¹, Andrew Capel², Mark Lewis², Daniel Engstrom³, Simon Martin¹

¹Department of Materials, Loughborough University, ²School of Sport, Exercise and Health Sciences, Loughborough University, ³Wolfson School of Mechanical, Electrical and Manufacturing Engineering, Loughborough University
 Corresponding author: S.M.N.Sallstrom@lboro.ac.uk – PhD student (Final year)

Introduction

Hydrogels are insoluble polymeric networks which can contain large quantities of water. Since hydrogels contains a lot of water, they mimic the soft natural tissues and thus are of interest in tissue engineering. One of the main issues of hydrogels are their poor mechanical properties which limit their practical use. There are various methods to improve mechanical properties, and in this work nano-clay is used as a crosslinker which can attach to several polymer chains and thus reinforcing the hydrogel. The monomer used is a zwitterionic sulfobetaine monomer which was selected due to its non-adhesive potential as well as its potential non-cytotoxic nature.

Materials and Methods

Hydrogel preparation: Laponite XLG (4-10wt%) was dispersed in deoxygenated deionised water, then the monomer N-(3-Sulfopropyl)-N-methacroyloxyethyl- N,N-dimethylammonium betaine (SPE) (10-50wt%) and a photoinitiator Irgracure 2959 (0.5wt%) were added and the suspension was placed in moulds and UV-cured for 1hr.

Mechanical testing: Uniaxial tensile and compressive properties of the hydrogels were evaluated using universal testing machine (Instron 5944) fitted with a 2kN load cell. Hysteresis tests were also performed.

Additive manufacturing: Syringe based extrusion printing was used to create structures using the Biplotter (envisionTEC) by using a printing then curing approach.

Cell culture: SH-SY5Y neuroblastoma cell line was used to evaluate cellular response to the hydrogels. Three different conditions were tested; control, indirect and direct. Alamar blue assay was performed to evaluate cell viability and fluorescent staining used to evaluate cell count and neurite length of the different conditions.

Result and discussion

A soft hydrogel system with very high elongation abilities (~1200%) was developed. The hydrogels could also recover well from compression forces and did not break after 90% compression. The hydrogels also displayed self-healing abilities which is caused by the ionic interactions between the polymer and the clay platelets. Furthermore, due to the shear thinning properties of the pre-hydrogel solution, the material could be extruded successfully and since the material quickly recovered its original properties, a structure could be fully printed before curing was required.

The cell culture work showed that hydrogels did not cause cytotoxic responses to the neuroblastoma cell line used, there was no difference in cell viability between the different conditions. Cells were also shown to grow on top of the hydrogel surface which could potentially be caused by the clay providing anchoring points for the cells to attach to.

Conclusion

SPE successfully formed mechanically robust hydrogels with clay as a crosslinker. The material could be extruded with a printed then curing approach due to its shear thinning behaviours. The hydrogels did not have any negative effects on the cell viability and cells were shown to grow on the hydrogel surface.

Acknowledgements

The author would like to thank EPSRC (EP/L01534X/1) for providing financial support to this project.

NANOPOROUS ENTEROSORBENT YAQ001 AS AN ORAL TREATMENT FOR LIVER DISEASE THROUGH ENDOTOXIN ADSORPTION AND MODERATION OF IMMUNE DYSREGULATION

Tochukwu Ozulumba^{1*}, Ganesh Ingavle^{1,2}, Jane Macnaughtan³, Nathan Davies³, Rajiv Jalan³, Susan Sandeman¹
¹Pharmacy and Biomolecular Sciences, University of Brighton, United Kingdom, ²Symbiosis Centre for Stem Cell Research, Symbiosis International University, India, ³Institute for Liver and Digestive Health, UCL, United Kingdom
 Corresponding author: t.ozulumba@brighton.ac.uk – PhD student (4th year)

Introduction: Disruption of gut barrier function and passage of bacterial endotoxin and other inflammatory products to extra intestinal sites exacerbates immune dysregulation to instigate potentially lethal sepsis in liver cirrhosis. No treatments beyond antibiotics exist to suppress the mechanisms by which bacterial translocation occurs and antibiotics raise issues of resistance and increased gut microbiome disruption. Enteric adsorption may be used to remove bacterial endotoxin, cytokines and other inflammatory products in order to limit translocation into the mesenteric lymph nodes, portal vein and systemic circulation. However, significant adsorption is challenging to achieve because of the large size of key inflammatory molecules which must be removed and the complex nature of the enteric environment. We have investigated the repression of endotoxin mediated inflammatory stimulus by a nanoporous adsorbent, Yaq001, using a THP-1 monocyte cell model. The aim was to investigate adsorptive capacity and mechanism of effect in order to potentially modulate immune dysregulation through physical adsorption of gut derived inflammatory products in the treatment of liver cirrhosis.

Materials and Methods: Phenolic resin derived activated carbon beads (Yaqrit Ltd) were characterised by mercury and gas nitrogen porosimetry, scanning electron microscopy and energy dispersive X-ray analysis. Bead adsorption of molecular weight marker molecules, albumin, myoglobin and caffeine were measured by UV/Vis spectroscopy. Endotoxin adsorption was measured using a chromogenic LAL assay. Impact on *S. aureus* and *E. coli* bacterial growth kinetics was measured by optical density analysis. Production of cytokines IL-8, IL-6 and TNF by THP-1 monocytes stimulated with endotoxin and impact of incubation with Yaq001 was measured using ELISA.

Results and Discussion: Physical characterisation of the beads indicated a nanoporous structure with a high surface area and bimodal pore size distribution in the microporous (<2 nm) and macroporous (50-150 nm) range. The beads removed small, middle and high molecular weight marker molecules in comparison to micropore only controls which were unable to remove significant amounts of high molecular weight albumin. Significant endotoxin adsorption was observed by Yaq001 from simulated intestinal fluid but not by the microporous control. No disruption to bacterial growth kinetics was observed. Significant adsorption of cytokines IL-8, IL-6 and TNF occurred in contrast to microporous controls where TNF adsorption was half that of the test samples. This was mirrored in the THP-1 results where repression of LPS stimulated TNF production by the cells at the 4-hour time point was almost complete for Yaq001 but not for the microporous control. Endotoxin stimulated THP-1 cytokine production was significantly reduced by bead incubation suggesting a disruptive mechanism which removes both bacterial toxin stimulus and excessive cytokine response.

Conclusions: Enterosorbent Yaq001 provides adsorptive surface area and internal nanoporosity enabling bound bacterial endotoxin removal and subsequent repression of primed inflammatory THP-1 cytokine production. In the gut, removal of key bacterial and inflammatory products could moderate the negative impact of disrupted gut barrier function and impaired immunity in liver disease.

NANOVIBRATION INDUCED MESENCHYMAL STEM CELLS FOR 3D OSTEOGENESIS IN FREEZE DRIED COLLAGEN SPONGE-HYDROGELS COMPOSITE FOR BONE TISSUE ENGINEERING

W. Orapiriyakul^{1,7}, PM. Tsimbouri¹, P. Childs², RMD. Meek³, KE. Tanner⁴, M. Salmerón-Sánchez², ROC. Oreffo⁵, S. Reid⁶, MJ. Dalby¹

¹IMCSB, University of Glasgow, UK, ²School of Engineering, University of Glasgow, UK, ³Southern General Hospital, Glasgow, UK, ⁴School of Engineering and Material Science, Queen Mary University of London, UK, ⁵IDS, University of Southampton, UK, ⁶Department of Biomedical Engineering, Strathclyde University, UK, ⁷Department of Orthopedics, Faculty of medicine, Prince of Songkla University, Thailand

INTRODUCTION: Nanovibrational stimulation (NS) can enhance osteogenesis of human mesenchymal stem cells (MSCs) (1,2). We are developing MSC-seeded biphasic scaffolds comprising collagen hydrogels (in which the cells grow) and freeze dried collagen sponges (to provide rigidity) to allow long term 3D culture within the nanokick bioreactor aimed at generating viable bone graft.

METHODS: Stro1-selected human MSCs were seeded in 1.8 mg/ml rat tail collagen type I hydrogels. 5% freeze dried collagen sponges were produced and integrated into MSC-seeded gels making gel-sponge composites. The properties of the scaffolds were tested by rheology, compression testing, SEM and nanodisplacement measurement. The biological response testing including viability, qPCR, western blot, metabolomics, mitochondrial activity measurement, protein arrays and pathway inhibition testing.

RESULTS: In the gels, NS amplitudes were consistent (~90nm) measured by interferometry at 1000Hz. At day 9, significant osteogenic gene up-regulation (RUNX2, osteonectin, osterix, osteopontin and osteocalcin) was observed. Western blotting showed pRUNX2/totalRUNX2 up-regulation. Protein arrays showed collagen and integrin up-regulation. The NS effect involved lipid metabolism, increased mitochondrial activity, produced low-level controllable reactive oxygen species (ROS) and inflammatory cytokines (IL-6, TNF α), and involved MAPK pathways tested by protein inhibition as is seen in physiological bone healing. Again, corresponding to the normal bone healing process, inflammation was suppressed at 2-3 weeks. In the biphasic scaffold, microscopy

showed MSCs migrating from the gel into the sponge. Cells experiencing NS in the scaffolds were viable and temporal gene analysis (days 7-21) showed osteogenic gene upregulation (RUNX2, osterix, osteonectin and osteopontin).

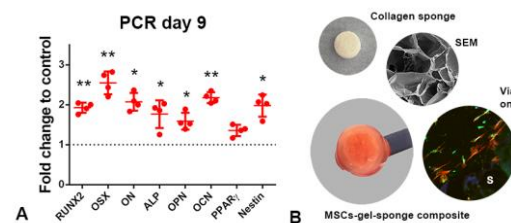


Fig. 1: 3D osteogenesis in gel-sponge composite. A. NS can induce osteogenic gene expression. B. MSCs-gel-sponge composite is safe and possible for clinical use.

Table 1. NS optimisation for gel-sponge composite.

Validation	Tests	Gel	Gel-sponge
Mechanical	Rheology/compression	161.3 Pa	137.3 MPa
	Interferometry	-90 nm	-90 nm
Viability	Alamar blue	Safe	Safe
Phenotype	RT-PCR	Osteo	Osteo
	Western blot	pRUNX2	OPN
Inflammation/Stress	IL-6/ROS	controllable	controllable

DISCUSSION & CONCLUSIONS: NS induced controllable inflammation and ROS promoting 3D osteogenesis. Biphasic collagen scaffolds allowed NS transmission inducing osteogenesis and improved composite handleability for potential clinical use.

ACKNOWLEDGEMENTS: The authors thank the Royal Thai Government, Find A Better Way, BBSRC (BB/N012690/1), EPSRC (EP/N013905/1) and Mrs Carol-Anne Smith for technical support.

REFERENCES:1. Nikukar H et al., ACS Nano 7, 2758, 2013. 2. Tsimbouri MP et al., Nature Biomedical Engineering 1, 758, 2017.

Novel approach for wound healing processes

Abed F. Ali*, Yvonne Reinwald

Department of Engineering, School of Science and Technology, Nottingham Trent University

*abed.ali@ntu.ac.uk

INTRODUCTION: Wound healing is one of the major therapeutic and economic issues in medicine¹. Understanding the healing process and nutritional influences are critical to achieve success in wound management. Protein deficient diet, vitamins, or minerals delay wound healing. DL-Methionine known as an antioxidant, acts as an originator amino acid for important antioxidant molecules such as glutathione, cysteine, and taurine that protect the cells from oxidative damage and play a vital role in detoxification. This study aided the identification of suitable DL-Methionine concentrations to enhance cell growth in two-dimensional cell culture.

METHODS: Primary human keratinocytes (hKC), human dermal fibroblasts (hDFB) and human mesenchymal stem cells (hMSC) were cultured until 70% confluent. Then DL-Methionine was added as a medium supplement at concentrations ranging from 0-4.5 mg/ml. Cell proliferation, cell morphology, and metabolic activity were assessed. Live cell images (IncuCyte S3 Live Cell Imaging System) were acquired via the IncuCyte analyzer at 3-h intervals over 3 days to provide real-time cellular confluence and eccentricity data based on segmentation of high-definition phase-contrast images. Cell proliferation is expressed increase in confluency (%) and eccentricity (%) for change in cell morphology. In addition, the expression of fibroblast maker CD90 and keratinocyte markers K10 (differentiation, migration) and K16 (proliferation) were investigated. Data were statistical analysis by one-way ANOVA in SPSS.

RESULTS: The results illustrate that DL-Methionine treatment enhanced cell metabolic activities. (Figure 1 A). DNA content was significantly different between the control, and the treated medium at high concentration (Figure 1B). Eccentricity analysis showed unchanged cell morphology except in hKC control and medium concentration (Figure 1 C). Confluency (%) appeared significantly increased in cell proliferation between day 1 and 3.

Immunocytochemistry staining showed DL-Methionine did not affect cells phenotype, except hKC (Figure 2).

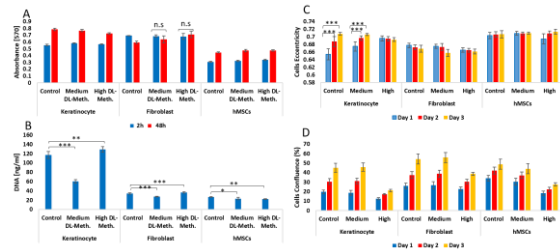


Figure 1: Three cell types in different concentration. Cell viability by alamar blue (A), DNA content by PicoGreen assay (B), eccentricity (%) (C) and confluency (%) (E) * denotes $p \leq 0.1$, ** $p \leq 0.01$ *** $p \leq 0.001$. Values are mean \pm S.D (n = 4).

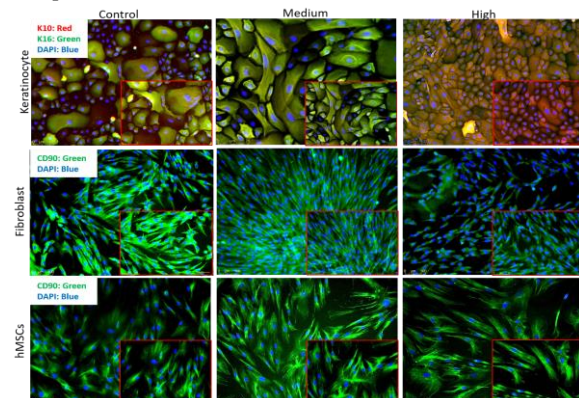


Figure 2: Immunocytochemistry staining of cells cultured in DL-Methionine. Magnification X10 & X20.

DISCUSSION & CONCLUSIONS: MSCs, KC and DFB in normal skin play a critical role in the inflammatory, proliferative, and remodelling phases of wound healing². The key findings include that both concentration increased proliferation of hKC and hDFB. Here, we demonstrated that DL-Methionine influences the proliferation of skin cells and plays a crucial role in the maintenance of cells phenotype⁽³⁾. However, increased hKC and hDFB proliferation will enhance the wound healing.

REFERENCES:

1. Guest, J.F., *et al.*, (2016). Int. Wound J., doi: 10.1111/iwj.12603;2.
2. Hocking, A.M., Gibran, N.S., 2010. Exp Cell Res. 316.3.
3. Martínez, Y. *et al.*, (2017). Amino Acids, 49:2091–8, DOI 10.1007/s00726-017-2494-2.

NOVEL POROUS STRUCTURES FOR ENHANCED OSTEOINTEGRATION IN ORTHOPAEDIC DEVICES

Ian PF Richards^{1*}, Christopher J Sutcliffe², Judith M Curran², Simon R Tew¹

¹Institute of Ageing and Chronic Disease, University of Liverpool. ²School of Engineering, University of Liverpool.

*Corresponding author: ian.richards@liverpool.ac.uk – PhD student (3rd year)

Introduction

Initial fixation is a key factor that determines the long-term success of implantable orthopaedic devices. To improve initial fixation, and reduce the prevalence of aseptic loosening, a method for optimising the surfaces of orthopaedic devices to enhance osteointegration has been developed. This is achieved via production of porous titanium wireframe structures using Selective Laser Melting (SLM) technology. Accelerated bone ingrowth, enabled by interactions between the surface and the surrounding tissue, allows for mechanical interlocking of the device. Previous work introduced a software algorithm that allowed the surface of structures to be roughened, which increased the coefficient of friction between the surface and bone tissue. Here, we have further developed this algorithm to allow for directionally biased surface roughening. This could allow for easier device insertion and decrease micro motion, while still supporting cell adhesion and promoting osteogenesis.

Materials and Methods

Test specimens with an array of surface features (Fig. 1a) were produced using SLM. Specimens were inserted axially into synthetic bone material (*SawBones*) at a rate of 1mm/s, and then pulled out at the same rate. Maximum push-in and pull-out force (N) was recorded. Specimens were rotated using a custom-built rig. Maximum torque force (Ncm) was recorded. Specimens were seeded with 2.5, 5, 7.5 and 10x10⁵ Green Fluorescent Protein-transfected Mg-63 Osteosarcoma cells and incubated at 37°C for 4h. Cell adhesion and distribution were observed using confocal microscopy (Fig.1b).

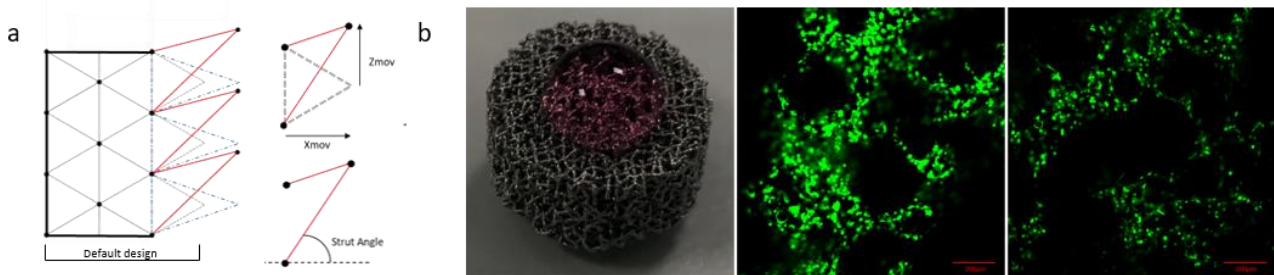


Figure 1: a. Schematic representation of surface manipulation. b. Ø10x5mm specimen seeded with media containing cells (left) and confocal microscopy images showing adhered cells (middle, right). Scale: 200µm. 10x magnification.

Results and Discussion

Data obtained demonstrates that maximum force required for axial push-in, pull-out and torque is largely dictated by interference. As interference increases, the force required becomes greater in response. Specimens with a Z movement of 0.4 and 0.5mm required greater force during push-in despite their increased lower strut angles. This may be explained by the fact that struts do not appear to deflect upon insertion (not expected) but rather cut through the synthetic bone material. Lower struts with smaller angles receive greater support from upper struts and aid cutting. This cutting phenomenon also explains the markedly reduced forces required to pull-out specimens. When push-in and pull-out data are displayed alongside lower strut angle there is no obvious trend, although when push-in/pull-out are considered as a ratio (i.e. easiest to push-in and hardest to pull-out), an angle of 48° (Z0.2, X0.15) is the optimum variable in this regard. Confocal microscopy has shown that the surface supports initial cell adhesion and validates our seeding method for use in future *in vitro* experiments.

Conclusions

We have developed a method for producing novel, reproducible surface features to increase mechanical fixation in porous orthopaedic medical devices. Initial data has shown mechanical interference to be a key factor in device fixation, although the effects of directional bias are less clear. We have also shown that the surface supports initial cell adhesion. Future work will further investigate the osteoconductive potential of this novel surface design.

Acknowledgements

The authors wish to acknowledge EPSRC for their ongoing financial support.

Optimisation of Cell Ratio and Medium composition for the tri-culture of cells in wound-healing

Vinuri Abeygunawardana, Abed F. Ali, Yvonne Reinwald

Department of Engineering, School of Science and Technology, Nottingham Trent University
School of Medical Science, Griffith University

INTRODUCTION: The global impact of wounds has prompted insightful research, which has largely relied upon the use of models to simulate wound-healing. Wound-healing is a highly complex process that aims to restore barrier breach, consisting of four sequential yet overlapping phases: hemostasis, inflammation, proliferation and maturation¹. Several cell types are involved in the wound-healing process, but keratinocytes, fibroblasts and mesenchymal stem cells predominate². Co-cultures of the two cell types have been a focus of recent research, but a tri-culture model with all three cell types remains undeveloped despite its clinical potential. The aim of this project is to optimise the cell ratio and growth medium for a tri-culture of keratinocytes, fibroblasts and mesenchymal stem cells, and thus support the production of a physiologically-relevant three-dimensional model for wound healing.

METHODS: Two methodologies were followed to optimise cell ratio. For both, primary cell human keratinocytes (hKCs), human dermal fibroblasts (hDFBs) and human mesenchymal stem cells (hMSCs) were seeded sequentially at 24-hour intervals. The first methodology used a mixed growth medium with the ratio of 1:0.5:1 (keratinocyte medium: fibroblast medium: DMEM). The second methodology ‘cycled’ the three mediums: hMSCs were first seeded and, after 24 hours, DMEM medium was removed and replaced with fibroblast medium; after 48 hours, fibroblast medium was removed and replaced with keratinocyte medium. Live cell images were acquired at 24-hour intervals using an Incucyte S3 Live Cell Imaging System to provide real-time cellular confluence (expressed as an increase in percentage) and eccentricity data. For growth medium optimisation, hKCs, hDFBs and hMSCs were seeded simultaneously in 24-well plates and cultured under different conditions: these comprised a fixed medium (DMEM/F12 3:1 media, supplemented with 5 µg/mL insulin, 0.4 µg/mL hydrocortisone and 1% penicillin-streptomycin), EGF (2.5-10 ng/mL), PBS (0-2%) and L-glutamine (1-3%). Statistical analysis of data was via one-way ANOVA in SPSS.

RESULTS: The results indicate a cell ratio of 1:0.5:1 (hKCs:hDFBs:hMSCs) can be successfully tri-cultured. Confluence analysis of live cell images showed increased cell proliferation in mixed medium over six days, when compared with keratinocyte medium (Figure 1A). Cell eccentricity, which delineates changes to cell morphology, was constant in mixed medium. Confluence analysis of live cell images showed no significant cell proliferation in keratinocyte medium from day four to six (Figure 1B). This was supported by Incucyte live images (Figure 2A).

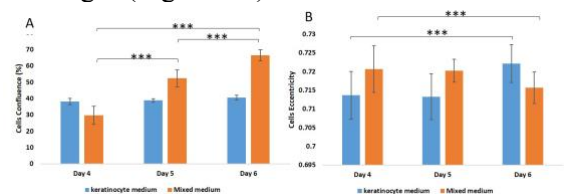


Fig. 1: Cell confluency (A) and eccentricity (B) for tri-culture in mixed medium and keratinocyte medium. *** $p \leq 0.001$. Values are mean \pm S.D. $n = 8$.

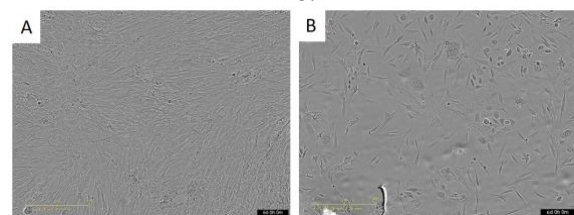


Fig. 2: Tri-culture of hMSCs, hDFBs and hKCs after six days in mixed medium (A) and keratinocyte medium (B).

DISCUSSION & CONCLUSIONS: A basic tri-culture of hKCs, hDFBs and hMSCs was successfully established within a mixed medium. A tri-culture in keratinocyte medium was found to be unsustainable in the long-term as it lacks FBS, an essential growth factor for hDFBs and hMSCs. Further medium optimisation is required to create a stable, long-term tri-culture model.

REFERENCES:

- ¹Wilhelm, K., Wilhelm, D. & Bielfeldt, S., 2016. *Skin Research and Technology*, 23 (1), 3–12.
- ²Walter, M., Wright, K., Fuller, H., Macneil, S., and Johnson, W., 2010. *Experimental Cell Research*, 316 (7), 1271–128.

Optimisation of Microfabricated Devices for Human Neuronal Modelling

Sophie Oakley,¹ Dr Mark Lewis,² Dr Paul Roach¹

¹Department of Chemistry, School of Science, Loughborough University, UK, ²School of Sports, Exercise and Health Sciences, Loughborough University, UK

INTRODUCTION:

In a society with an ever-increasing aging population the direct link between age and neurological diseases predicts a significant burden economically and societally in the near future. Microfabricated devices have facilitated the development of highly controlled neuronal models using primary tissue sources for investigating both disease and pharmaceutical approaches. Concerns regarding the validity and reliability of animal sources drives the need for an effective model using human sources. These cell sources, however, require additional support to survive and grow within the conditions of microfluidic devices.

METHODS:

Microfabricated devices were created by photolithographic patterning of SU8 on a silicon wafer and treated in hexamethyldisilane (HDMS). Poly(dimethylsiloxane) (PDMS) was poured onto the silicon wafer and inverse replication of the pattern produced the devices. PDMS devices and glass slides were solvent cleaned then adhered by oxygen plasma bonding or polyethylenimine (PEI).

SH-SY5Y neuroblastoma cells were seeded into devices at 200,000 cells and 6 well plates at 12500 cells. Cells were maintained in growth media: Dulbecco's modified Eagle's medium (DMEM) supplemented with 1% penicillin-streptomycin (PS) (Thermoscientific) and 10% Fetal bovine serum (FBS) (Thermoscientific), standard media and incubated at 37 °C / 5% CO₂. Differentiation media then was added for 10 days. Cells were fixed with 4% PFA. Florescent and phase contrast microscopy were used to analyse staging, maturity and neurite length.

RESULTS SH-SY5Y differentiation can be manipulated by altering the differentiation media content to promote neurite growth, branching and maturity. Lowering serum levels early in the differentiation period of the protocol led to smaller populations of neuron with slightly higher expression of the mature neuronal marker MAP2.

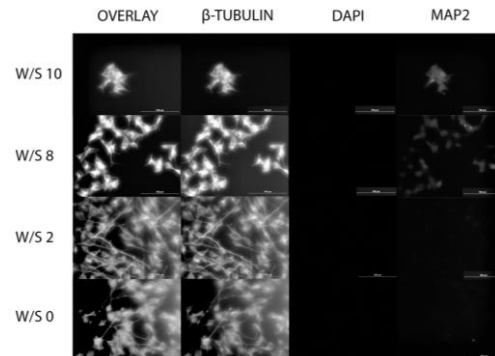


Fig. 1: Effect of serum on differentiation and maturity of SH-SY5Y cells: serum was removed from differentiation media at different time points over the 12 day protocol, days without serum (W/S).

DISCUSSION & CONCLUSIONS:

Microfabricated devices although a key tool in the development of new neuronal models if not controlled correctly offer a harsher environment than standard 2D culture due to shear flow and osmotic stresses in the system [1]. To counter this additional growth factors, chemically modified surfaces and techniques are required to promote survivability and the desired phenotype. SH-SY5Y cells are widely used in the neurodegenerative disease literature however the inconsistency between protocols and resulting cell phenotypes is well documented [2]. By manipulating these factors neuronal branching, length and survivability can be altered to produce a phenotype appropriate for the model.

ACKNOWLEDGEMENTS

We thank EPSRC DPT funding in support of the Brain-on-a-chip MiniCDT.

REFERENCES:

- [1] Goyal, G. and Nam, Y. Biomedical Engineering Letters. Korean Society of Medical and Biological Engineering, 1(2), pp. 89–98, 2011.
- [2] Xicoy, H., Wieringa, B., & Martens, G. J. M. Molecular Neurodegeneration, 12(1), 10, 2017

Optimising a Method to Study the effect of Autologous Fat on Skin Graft Contraction

VL.Workman¹, N.Green¹, S.MacNeil¹, V.Hearnden¹

¹*Kroto Research Institute, Materials Science and Engineering, University of Sheffield, UK.*

INTRODUCTION: If healing from burns injuries is delayed, impaired or requires skin grafts the scar tissue formed contracts, often becoming tight, painful and unsightly. Current treatments are only minimally effective and have not changed for decades. Observations by clinicians have shown that injection of adipose tissue (fat) underneath scarred and contracted skin may reduce stiffness and improve skin quality and pliability. There is a lack of strong scientific evidence to explain how this benefit is achieved and the mechanisms behind it.

Using a tissue engineered (TE) skin model^[1,2] in combination with adipose tissue from clinical samples we hope to establish a strong understanding of how adipose tissue can repair or reverse contracted tissues.

METHODS: TE skin models were fabricated as previously described^[1,2], using decellularised dermis (DED) or cadaveric skin obtained from a European Skin Bank. As TE models are cultured at an air-liquid interface (ALI) on stainless steel grids (Fig. 1a) there was concern that cells from lipoaspirate may escape between the holes in the grid. To prevent this cell escape two different membranes (0.45 μ m (Merck) and 40 μ m (Falcon) pore size) were investigated. Membranes were placed between the grid and the TE model (Fig. 1b). Images of the models were taken roughly every 2-3 days and their areas estimated using ImageJ.

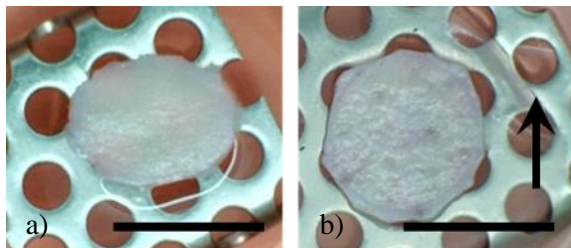


Fig. 1: TE model (day 0) on stainless steel grid used for ALI culture (a), model on 0.45 μ m membrane (edge highlighted) in (b). Scale bar = 1cm

RESULTS: TE skin models in all investigated conditions were observed to contract over time. Models cultured on 40 μ m membranes were observed to contract less, adhere to the

membrane and resulted in less reproducible data. In addition more cells were observed to have escaped from these models than others cultured in the alternative conditions. In contrast, models cultured on 0.45 μ m membranes were observed to contract as much as models on grids. In addition, models cultured on these membranes did not adhere to them, whereas models cultured in both other conditions adhered to the substrate. More rapid contraction that ceased earlier was observed with DED models compared with cadaveric skin models

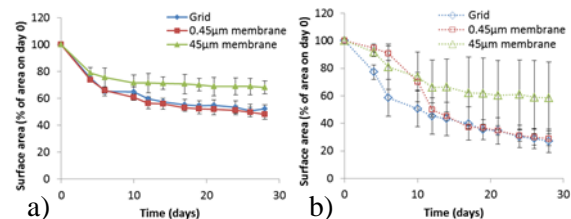


Fig. 2: Area covered by model compared to day 0. Models composed of DED (a) compared with cadaveric skin (b).

DISCUSSION & CONCLUSIONS: By using a hydrophobic membrane with small pores (0.45 μ m) it was possible to culture TE skin models over 28 days. In addition, we were able to observe contraction comparable to control conditions. This adaptation will allow adipose tissue to be placed underneath the skin model and facilitate further studies.

ACKNOWLEDGEMENTS: This study has been made possible thanks to funding from the Peter Sowerby Foundation and Sheffield Hospitals Charity. The patient samples were made available through the Sheffield Hospital Directorate of Plastic, Reconstructive Hand and Burns Surgery under research ethics number 15/YH/0177.

REFERENCES: ^[1] Harrison *et al.* Tissue Engineering. 2006;12(11):3119-33. ^[2] Thornton *et al.* Journal of Burn Care & Research. 2008;29(2):369-377.

PCL and PGS Scaffolds for Osteochondral Tissue Engineering

M.F. Velazquez¹, G.C. Reilly² and F. Claeysens¹

¹Kroto Research Institute, The University of Sheffield, Sheffield, UK; ²INSIGNEO Institute for In Silico Medicine, The University of Sheffield, UK

INTRODUCTION: Biodegradable synthetic polymeric materials are highly suitable as scaffold materials in tissue engineering¹. These materials can also be easily manufactured in custom made shapes with controllable porosities via conventional structuring processes producing foams and novel additive manufacturing processes. A reasonably accessible process to produce foams is emulsion templating where a High Internal Phase Emulsion (HIPE) is used to produce polyHIPE scaffolds. In this project we present the production of Polycaprolactone (PCL) and poly-glycerolsebacate (PGS) polyHIPEs as scaffolds for osteochondral defects².

METHODS: *PCL-M synthesis.* E-caprolactone (Sigma Aldrich) is functionalized with pentaerythritol through a ROP reaction to obtain 4-arm PCL. Methacrylic groups are added to obtain photocurable materials with a degree of methacrylation of approximately 40% and 60%. *PGS-M synthesis.* Sebacic acid and glycerol (Sigma Aldrich) are used in a condensation reaction to obtain PGS. The scaffolds are methacrylated to obtain 50% and 80% degree of methacrylation. Both polymers are characterised using H¹ NMR and DSC. *Mechanical tests.* Compression tests were developed for both PCL-M and PGS-M under standard ASTM D1621-10. *PolyHIPE disks.* PGSM and PCLM are functionalized using a photoinitiator and cast into moulds under UV light to create disks of 0.7 mm diameter and 0.3 mm height. *Cell Proliferation.* Bovine Articular Chondrocytes (BACs) and hES-MPs (human Embryonic Stem Cell-derived Mesodermal Progenitor) are seeded on the scaffolds. DMEM and α MEM media are used as expansion media, enriched with HEPES, Glu, NEAA; and BGP, AA₂P, Dex to BACs and hESMPs respectively. Proliferation is tested by Resazurin assays after 21 days.

RESULTS: *PCLM & PGSM disks.* Poly HIPE disks show average pores of 100-250 μ m diameter, where PGSM disks have a higher porosity than PCLM ones. *Mechanical Tests.*

Compressive strength for PCLM and PGSM ranges in host natural values (in process). *Cell Proliferation.* Cells seeded at a concentration of 50,000 cells per scaffold showed a day 1 attachment efficiency of higher than 50%.

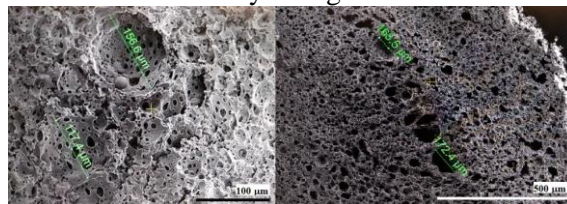


Fig. 1: SEM of PCL-M and PGS-M polyHIPEs.



Fig. 2: PCL-M (top) and PGS-M (bottom) scaffolds after natural shrinkage in methanol solution.

Table 1. Compressive strength results between PCL-M 40%* and 50%** and PGS-M 50%* and 80%**.

Methacrylation	PGS-M	PCL-M
Low*	0.5 – 5 MPa	20-40 MPa
High**	5–10 MPa	30 – 60 MPa

DISCUSSION & CONCLUSIONS: PCL-M and PGS-M disks possess a porous structure that mimic the host tissue and exhibit good propensity for cell ingrowth. Their mechanical properties place them within the range of their respective host tissues. Further work includes tailoring specific mechanical properties for single polymer or co-polymer biphasic disks, successful differentiation of multipotent cells and co-seeding and co-culturing strategies.

ACKNOWLEDGEMENTS: MFV thanks CONACYT for her PhD studentship.

REFERENCES: [1] (2001) Busby, W. *Emulsion-derived foams (PolyHIPEs) containing Poly(ϵ -caprolactone) as Matrixes for Tissue Engineering*. Biomacromolecules, No. 2. Page 154-164. [2] (2006) Kelly, D. & Prendergast, P. *Prediction of the Optimal Mechanical Properties for a Scaffold Used in Osteochondral Defect Repair*. Tissue Engineering, Volume 12, Number 9.

PEG-based hydrogels for minimally invasive cartilage therapies

R. J. A. Moakes¹, N. C. Foster¹, A. J. El Haj¹, L. M. Grover¹

¹*School of Chemical Engineering, University of Birmingham, Birmingham, UK,*

INTRODUCTION: The symptoms arising from osteoarthritis (OA) are what cause it to be one of the leading disabilities within the adult population.¹ Osteoarthritis is brought on through general wear and tear of the hyaline cartilage; naturally present to prevent direct contact between hard tissues within diarthrodial joints. Commonly, small focal defects in the soft tissue become aggravated by mechanical stress, leading to accelerated OA and secondary more complex trauma.² This is further exacerbated, as the avascular structure of cartilage limits its ability to rejuvenate, requiring exogenous intervention. Currently, three main treatments are available: microfracture, mosaicplasty and autologous chondrocyte implantation.³ However, such treatments are faced with a spectrum of drawbacks including invasive surgery, time and costs. As such, this has highlighted a need for therapies which require minimal intervention, which can be applied in the early stages of OA progression.

METHODS: Synthetic MicroGel suspensions (SyMGels) were prepared using a UV photocuring process under shear conditions. In brief, stock solutions containing 3% (v/v) PEGDA in PBS with Omnirad 1173 (0.1% (v/v)) was irradiated with UV light (unfiltered) whilst mixing at speeds between 300 and 700 rpm. Material properties were studied using a rotational rheometer in both linear and non-linear modes. Cytotoxicity was undertaken using P3 sheep chondrocytes by placing the gels directly onto the pre-seeded and attached cells. Metabolic activity was determined using a Presto Blue assay and cell morphology examined under light microscopy.

RESULTS: Shear applied throughout the photo crosslinking of PEGDA resulted in the production of microgel suspensions with the formation of discrete particles (Fig. 1). Analysis of the material behaviours, determined using rheology, highlighted mechanical responses indicative of typical fluid gels; pseudo-solid at rest, but flow under larger deformations (Fig. 1). SyMGels supported cell viability, as a function of the applied mixing during formation, with

increased mixing resulting in lower metabolic responses.

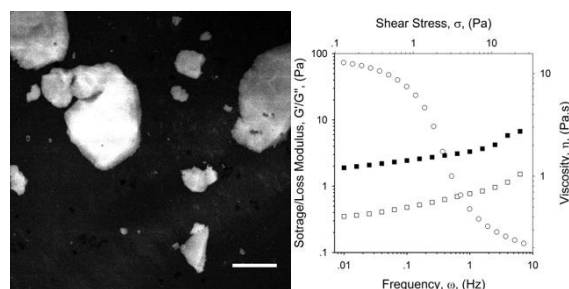


Fig. 1: Typical SyMGel material properties: CLSM image of particle formed at 300 rpm (left) typical fluid gel responses for the same system showing gel-like behaviour at rest (■/□, G' and G'' respectively) and the ability to flow at higher stresses (○) (right).

Table 1. P3 sheep chondrocyte metabolic response to SyMGels as determined using Presto Blue assay.

	Fluorescence (A.U)	95% Confidence
Control	50264	±2221
700 rpm	34577	±3550
300 rpm	47030	±4057
Blank	7763	±208

DISCUSSION & CONCLUSIONS: this study has shown that pre-approved materials in regenerative medicine (PEG) can be restructured in a way to inject into defect sites, whilst retaining its biocompatibility. Therefore, it shows promise as a new carrier device in cartilage regeneration.

ACKNOWLEDGEMENTS: Birmingham Healthcare Technologies Institute (HTI).

REFERENCES:

1. WHO. Osteoarthritis. in *World Health* **12**, 6–8 (2013).
2. Peña, E., *et al.*, *Comput. Biol. Med.* **37**, 376–387 (2007).
3. Bhosale, *et al.*, *Br. Med. Bull.* **87**, 77–95 (2008).

POROUS POLY- ϵ -LYSINE FOR AN ARTIFICIAL CORNEA APPLICATION

Georgia Duffy^{1A,B}, Don Wellings², Kate Black^{1B}, Rachel Williams^{1A}

^{1A}Department of Eye and Vision Science, ^{1B}Department of Engineering, University of Liverpool, UK

²SpheriTech LTD, The Heath, Business & Technology Park, Runcorn, UK

Corresponding author: G.L.Duffy@liverpool.ac.uk – PhD student (1st year)

Introduction

The cornea is an integral part to the functioning of the eye, as it is the most important refractive layer and acts to focus light onto the retina¹. It is made up of three main layers: a stratified epithelium, the stroma, and a single layered endothelium. These three layers maintain the transparency of the cornea via various mechanisms. If the cornea becomes damaged, these mechanisms will be compromised and the cornea will become opaque. Corneal opacities account for 5 % of blindness worldwide², with the leading treatment being the replacement with a cadaveric donor cornea. This treatment has several limitations, such as low availability, tissue rejection and a high cost³, which introduces the need for a more suitable alternative. This research aims to produce an artificial cornea made of a porous poly- ϵ -lysine hydrogel. A preliminary gel has been produced and tested for its porosity, transparency and cytotoxicity *in vitro*.

Materials and Methods

Gel chemistry: Poly- ϵ -lysine (P ϵ K) hydrogels were manufactured using 1-ethyl-3-(3-dimethylaminopropyl) (EDC1) and N-hydroxysuccinimide (NHS) as activators to cross-link P ϵ K with octanedioic acid (Su). These gels were made with varying percentage cross-linking.

Gel preparation: The four reagents were dissolved in water and added to a beaker contained within a stirrer device (Fig. 1), which fragmented the gels during polymerisation. After 20 minutes, the fragments were removed from the stirrer device. They were left to set between two glass plates, pressed with a spacer of 0.5 mm. The fragments then set together as a thin porous sheet.

Percentage light transmittance: The gels were cut and placed into a 96-well plate with 100 μ l of water, which was inserted into a spectrophotometer and read at 486 nm with an emission filter of 520 nm. The resulting absorbance values were converted into percentage light transmittance using the equation: $\text{Transmittance (\%)} = (10^{(-1 \cdot \text{Abs})}) \cdot 100$.

Cell viability: Human corneal epithelial cells (HCE-Ts) were seeded onto the gel. A solution containing reagents for a Live-Dead assay, calcein AM and ethidium homodimer (EthD-1), was added to each well containing cells. The wells were imaged on a fluorescence microscope and a percentage cell viability was calculated.

SEM: Prior to imaging, the samples were freeze-dried and loaded onto a carbon strip on the SEM mount with both the top surface and the cross section visible. All SEM images were taken on a Tabletop SEM TM3030 according to the manufacturer's protocol.

Results and Discussion

Percentage light transmission: The percentage light transmission was measured for gels with two different cross-linking amounts, 30 % and 45 %. Su 30 % 0.0714 g/ml had the highest light transmittance of 75 % compared to 15 % for Su 45% 0.0714 g/ml. This is approaching the value of 90 % observed by the human cornea.

Cell viability: A percentage viability was calculated for the cells on the Su 30 % 0.0714 g/ml fragments after 24 hours then again after 7 days. The hydrogel had a cell viability of 91 % after 24 hours and 80 % after 7 days, compared with a tissue culture plastic (TCP) control that had a cell viability of 98 % after 24 hours and 93 % after 7 days. Despite being lower than TCP on both time points it is more than 75 % cell viability, which deems the Su 30 14 fragments non-cytotoxic to HCETs.

SEM: The images taken show that the gel has a porosity both throughout its cross-section and on its surface. The pores range from 100-200 μ m in size and appear to be interconnected throughout the gel (Fig. 2)

Conclusions

In conclusion, a porous hydrogel has been produced with 30 % cross-linking and 0.0714 g/ml polymer density, which demonstrates a modest transparency and was not cytotoxic to HCET cells. Future work will include conducting mechanical testing on the gels to establish their tensile and compressive strength and seeding stromal fibroblast cells onto the gels to mimic a stromal graft.

References

1. Bakhshandeh, H. et al. *Int J Nanomedicine*. 6: 1509-1515, 2011; 2. Van den Bogerd, B. et al. *J Tissue Eng Regen Med*. 12(4): 2020-2028, 2018; 3. Brunette, I. et al. *Prog Retin Eye Res*. 59: 97-130, 2017

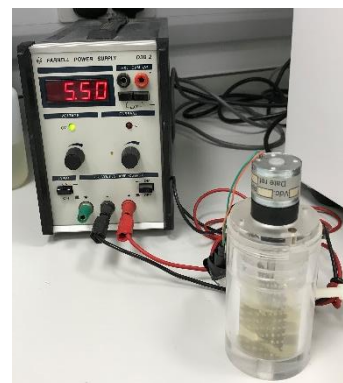


Figure 1: Photo of stirrer device

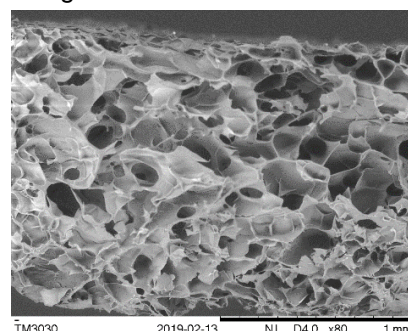


Figure 2: SEM of cross section of Su 30% 0.0714 g/ml fragmented gel

REGULATION OF THE HIF PATHWAY FOR CONTROLLED BONE REMODELLING IN PATIENTS WITH IMPAIRED FRACTURE REPAIR

Yutong Amy Li¹, Adriana-Monica Radu¹, Joel Turner¹, Azadeh Rezaei¹, and Gavin Jell^{1*}

¹Division of Surgery and Interventional Sciences, UCL

Corresponding author: g.jell@ucl.ac.uk

Introduction

Diabetic and elderly patients have a lower rate of bone remodelling, more crystalline bone, together with increased risk of fracture and delayed fracture repair [1]. A decrease in osteoclastogenesis and osteoclast activity in these patients may be partly responsible for such pathologies [2]. Novel approaches are needed to encourage healthy bone regeneration in these patients. The cellular response to changes in oxygen pressure (regulated by Hypoxia Inducible Factor 1 α , HIF-1 α) has been identified as an important upstream regulator of bone tissue regeneration and a regulator of osteoblast-osteoclast cross-talk [3]. Diabetic patients have also been shown to have a decreased response to changes in oxygen pressure due to the inhibition of the HIF pathway in bone cells [4]. Targeting the HIF pathway through the release of HIF mimetics from bioactive glasses may offer a new approach to regulate bone repair in these patients. Here we investigate if three known HIF mimetics (cobalt, DFO and DMOG) can regulate osteoclastogenesis using quantitative in vitro models. These studies will be used to develop new materials that can regulate bone remodelling.

Materials and Methods

An osteoclastic RAW 264.7 sub-clone cell line was generated and cultured in Dulbecco's Modified Eagle Medium (DMEM) GlutaMAX™, supplemented with 10% (v/v) foetal bovine serum (FBS) and 1% (v/v) penicillin streptomycin (P/S), seeded at 3x10³/cm² and a passage number <20. Cells were cultured with 3ng/ml of RANKL for experimental treatments with the HIF mimetics (Co, DMOG and DFO), a positive control (20ng/ml RANKL) and negative control (0 ng/ml RANKL) were included. The effect of HIF mimetics on osteoclast metabolic activity and proliferation was determined with Alamar® Blue and Total DNA assays. Osteoclastogenesis was determined with TRAP-5b staining and resorption of dentin discs (quantified by coherence scanning interferometry). Echinomycin was used to inhibit the HIF pathway.

Results and Discussion

The HIF mimetics Co (12.5-200 μ M), DFO (25-100 μ M) and DMOG (100-400 μ M) increased osteoclastogenesis as determined by the expression of the osteoclast specific TRAP-5b factor (p<0.001). The HIF inhibitor echinomycin, decreased TRAP-5b expression (Fig.1B p<0.001) confirming the role of the HIF pathway. Quantification of osteoclast activity on dentine discs could provide evidence of bone resorption enhancement by HIF mimetics.

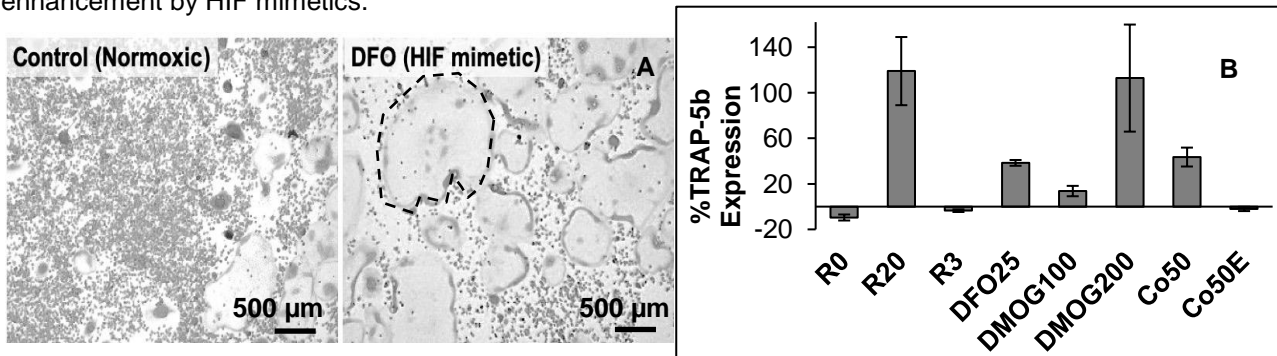


Figure 1. Osteoclast formation determined by HIF mimetics. (A) TRAP staining of osteoclast RAW 264.7 subclone with DFO (HIF mimetic) vs control (3ng/ml RANKL). An osteoclast is indicated by the dashed shape. (B) %TRAP-5b expression control (0ng/ml, 20ng/ml, 3ng/ml RANKL and 50 μ M Co + 2nM echinomycin) vs HIF mimetics (25 μ M DFO, 100 μ M and 200 μ M DMOG and 50 μ M Co). ***p<0.001, n=6 for

Conclusions

The release of HIF mimetics (Co DFO and DMOG) increased osteoclastogenesis and the rate of bone resorption. The next generation of bone repair biomaterials can take advantage of this by regulating both bone remodelling (osteoclasts) and bone formation (osteoblasts).

References

1. Manavalan J.S. *et al.* J Clin Endocrinol Metab. 9:3240–50, 2012.
2. Hu Z. *et al.* Acta Biomater. 84:402–413, 2019.
3. Kang H. *et al.* Front Immunol. 8:1312, 2017.
4. Thangarajah H. *et al.* Cell Cycle.1:75-9, 2010.

Serum-free cryopreservation of engineered neural tissue

KS Bhangra^{1,2,3}, JC Knowles¹, RJ Shipley^{3,4}, D Choi⁵ and JB Phillips^{1,2,3}

¹Biomaterials & Tissue Engineering, UCL Eastman Dental Institute, ²Pharmacology, UCL School of Pharmacy, ³UCL Centre for Nerve Engineering, ⁴Mechanical Engineering, UCL Engineering, ⁵Brain repair and Rehabilitation, UCL Institute of Neurology

INTRODUCTION: Serum is a commonly used supplement in tissue culture that provides a broad spectrum of proteins, hormones and growth factors that enrich the *in vitro* microenvironment (Gstraunthaler, 2003). Despite its prevalent use, it remains largely ill-defined, carries biosafety concerns and from an ethical standpoint its use remains unaligned with the 3R's theme (Gstraunthaler et al., 2013). This work builds on previously published work whereby foetal bovine serum (FBS) was an integral component of a cryopreservation media for the storage and preservation of engineered neural tissue (EngNT) (Day et al., 2017). Herein we explore the use of a novel cryopreservation media to replace the requirement of FBS for the cryopreservation of EngNT.

METHODS: Cellular collagen constructs were made in 24-well plates using filter paper absorbers to stabilise 2 mg/ml bovine collagen hydrogels containing 1 million SCL 4.1/F7 cells/ml. Following hydrogel stabilisation, the cellular collagen constructs were placed into 4 different cryopreservation media. Cryogenic conditions involved controlled-rate cooling and storage at -80°C for 24 h followed by 24 h in liquid nitrogen in; (1) 2.5 M Poly(propylene glycol) (PPG); (2) 2.5 M PPG + 10% dimethylsulfoxide (DMSO); (3) Polyvinylpyrrolidone (PVP); (4) PVP + 10% DMSO. A 60% Media, 30% FBS and 10% DMSO cryopreservation media was used as a positive control. Samples were thawed after 24 h cryopreservation in a water bath at 37°C, cell viability was assessed in relation to the metabolic activity, determined by the 3D CellTiter-Glo assay.

RESULTS: Constructs preserved in PPG + 10% DMSO exhibited the highest metabolic activity that exceeded the positive control (Fig 1). Of the cryopreservation conditions, the second highest metabolic activity was found in those preserved in PPG alone. Constructs preserved in PVP had approximately half the

number of metabolically active cells than the positive control. The addition of DMSO to PVP was seen to slightly increase the number of viable cells but not as much as seen in the PPG condition.

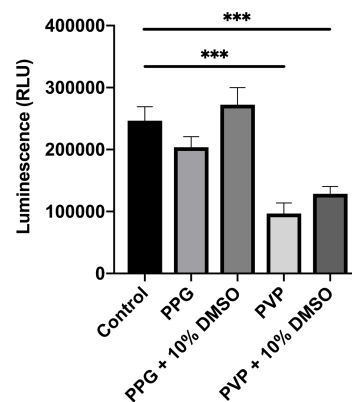


Fig 1: Metabolic activity of SCL 4.1/F7 cells in stabilised bovine collagen hydrogels after 24 h in cryogenic preservation conditions ($n=4$, where the control represents samples cryogenically stored in 60% Media-30% FBS and 10% DMSO. Post-hoc Tukey test, $***P<0.01$. Data are means \pm SEM)

DISCUSSION & CONCLUSIONS: This study demonstrates that EngNT can be cryogenically stored in a serum-free media with comparable metabolic activity to control media contained FBS. There was no statistical significance between the positive control and samples stored in PPG (with or without DMSO). PVP is a non-penetrating cryoprotective agent hence its use in preserving artificial tissue is limited despite its success in preserving cells. PPG with the addition of DMSO provided a powerful penetrating cryogenic media that led to the successful serum-free preservation of EngNT. Further research is required to understand the effects of this cryopreservation media on the efficacy of EngNT following long-term storage.

REFERENCES:

- Day, A. G. E., et al. 2017. *Tissue Eng Part C Methods*, 23, 575-582.
 Gstraunthaler, G. 2003. *ALTEX*, 20, 275-281.
 Gstraunthaler, G., Lindl, T. & van der Valk, J. 2013. *Cytotechnology*, 65, 791-793.

Short-time oxygen plasma treatment of a polyethylene terephthalate anterior cruciate ligament graft.

T. Choreño Machain¹, S. Konan^{1,2}, U. Cheema¹

¹Institute of Orthopaedics and Musculoskeletal Science, Division of Surgery & Interventional Science, University College London, London, GB, ²University College Hospital NHS-Trust (UCLH), 235 Euston Rd, Bloomsbury, London, GB

INTRODUCTION: Anterior cruciate ligament (ACL) injuries represent 40% of all sports injuries in the United Kingdom (1). Since a complete rupture does not heal on its own, the treatment of choice is the reconstruction with a tendon autograft, leaving a second damaged site. Given the need for new solutions as the number of ACL injuries continues to increase, a biocompatible synthetic graft could overcome this challenge. Short-time exposure to O₂ plasma was used to modify a polyethylene terephthalate (PET) scaffold aiming to improve the polymer's biocompatibility.

METHODS: PET scaffolds were modified using a low-pressure plasma system at 100 W to treat with O₂ plasma for 0, 0.5, 1, 2.5, 5 and 10 minutes, at 40 kHz with a gas flow rate of 0.4 mbar. Surface characterization was done by SEM imaging, AFM, and water contact angle. Biocompatibility was tested by seeding immortalized mesenchymal stem cells (iMSCs) onto the scaffolds and testing metabolic activity by means of a Presto Blue assay and DNA content using a Pico Green assay. DMEM-low glucose media supplemented with 50µg/mL ascorbic acid was used throughout all experiments. For all tests, tissue culture plastic was used as positive control and unseeded PET scaffolds as negative control.

RESULTS: Topographically, the PET surface significantly changed in an exposure time-dependent manner as shown in Fig.1A and B. The average roughness (Fig.1C) showed a statistically significant difference for the 2.5, 5 and 10 minutes treated scaffolds when compared to the baseline ($p < 0.001$). Fig.5C shows no statistically significant difference in the effect of O₂ plasma treatment on the micro mechanical properties ($p > 0.05$). Hydrophilicity of untreated PET scaffolds increased significantly ($p < 0.01$) in a time-exposure dependent manner.

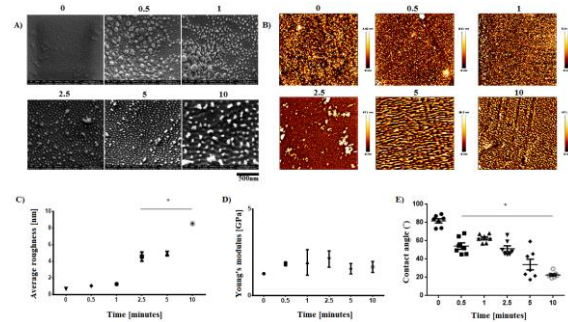


Fig. 1: Time-dependent effect in minutes of oxygen plasma exposure on PET surface. A) SEM and B) AFM surface topography. C) Average roughness, D) Young's modulus, and E) Water contact angle. Error bars represent standard error of the mean ($n=3$). $=p < 0.05$.*

For the biological interactions, there was a consistent increase in metabolic by DNA content activity for all O₂ plasma exposure times in all time points, but there was only a significant increase ($p < 0.001$) from days 7 to 14. At day 14, the metabolic activity by DNA content was significantly higher ($p < 0.02$) for the PET treated scaffold 0.5 when compared to the 1, 2.5 and 5 minutes O₂ plasma exposed scaffolds.

DISCUSSION & CONCLUSIONS:

Short-time exposure to O₂ plasma effectively modifies the hydrophobic and smooth PET surface. The treatment supports cellular growth but does not significantly enhance it. Short-time plasma treatment of PET offers a fast straight forward method as an interfacial bonding layer for the subsequent coating addition to increase the polymer's biocompatibility.

ACKNOWLEDGEMENTS: Work has been funded by the National Council of Science and Technology (CONACyT)-University College London (UCL) Graduate Fellowship.

REFERENCES: NHS. Hospital Accident and Emergency Activity - 2015-16. . in Secondary Care Analysis ND. (ed. charts., E.t.a.).

STRUCTURAL AND MECHANICAL CHANGES IN PLLA-BASED POLYMER BLENDS DURING HYDROLYTIC DEGRADATION

Reece N. Oosterbeek,^{1*} Patrick Duffy,² Sean McMahon,² Xiang C. Zhang,³ Serena M. Best,¹ Ruth E. Cameron¹
¹Cambridge Centre for Medical Materials, Department of Materials Science and Metallurgy, University of Cambridge,
²Ashland Specialties Ireland Ltd, Synergy Centre, TUD Tallaght, Dublin, Ireland, ³Lucideon Ltd, United Kingdom
 Corresponding author: mo23@cam.ac.uk – PhD student (3rd year)

Introduction

Poly-L-lactide (PLLA) is an appealing biomedical implant material, however for certain load-bearing applications such as cardiac stents it suffers several limitations. Among these are its slow degradation time, poor stiffness and strength (requiring PLLA stents to have thicker struts than conventional metallic stents), and tendency for embrittlement during degradation¹. Here we demonstrate how polyethylene glycol functionalised poly-lactide-co-caprolactone (PLCL-PEG) can be blended with PLLA, in order to control both the degradation timescale, and the structural and mechanical changes undergone during degradation.

Materials and Methods

Polymer blends were made using solvent casting and injection moulding, with mechanical testing carried out immersed in deionised water at 37°C. Degradation behaviour was measured in phosphate-buffered saline at 37°C by pH monitoring. Polymer blends were characterised before and after degradation by Differential Scanning Calorimetry (DSC), X-ray Diffraction (XRD), and Gel Permeation Chromatography (GPC).

Results and Discussion

Long-term degradation tests show strong dependence of degradation time on blend composition, demonstrating the ability to controllably accelerate PLLA degradation via blending. The two blend components (PLLA and PLCL-PEG) do not simply degrade independently of each other, but rather the degradation products released by the fast degrading polymer (PLCL-PEG) catalyse and accelerate the degradation of the slower degrading PLLA component. This is shown by the molecular weight distributions (Fig. 1), where the measured blend degradation is greater than would be expected for independently degrading components.

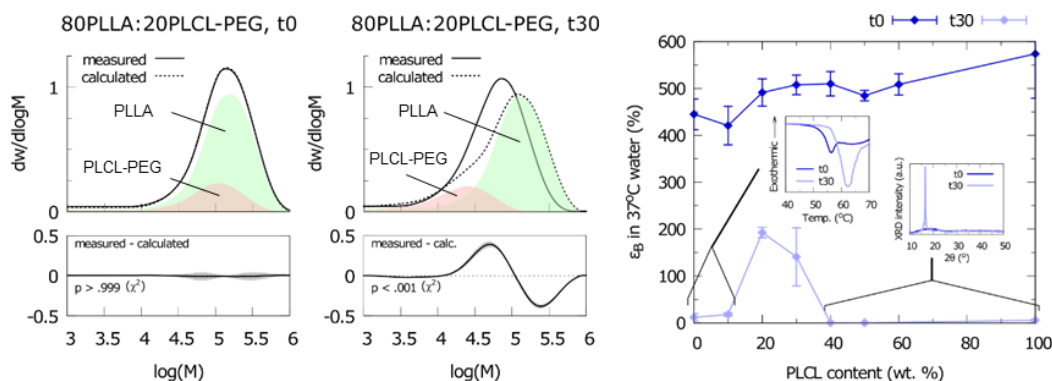


Fig. 1: Molecular weight distributions for PLLA:PLCL-PEG blends before and after 30 days degradation (left and middle). Calculated curves based on linear combination of individual components before and after degradation. Elongation at break (in 37°C water) for PLLA:PLCL-PEG blends before and after 30 days degradation, with DSC and XRD plots inset (right).

Important changes in the mechanical properties during degradation are also observed (Fig. 1). The large initial ductility is lost after 30 days degradation for most blend compositions. For blends with low PLCL-PEG content this occurs due to aging (shown by increased T_g and larger associated endothermic peak in DSC) as the relatively homogeneous composition provides little barrier to rearrangement. For high PLCL-PEG content, molecular weight degradation has shortened chain length sufficiently to allow significant rearrangement i.e. crystallisation (shown by XRD), also resulting in embrittlement. These two effects result in a “sweet spot” of moderate PLCL-PEG content that is high enough to prevent aging, but not so high as to cause degradation-induced crystallisation, leading to delayed structural relaxation and embrittlement for these compositions.

Conclusions

Blending PLCL-PEG with PLLA controllably accelerates hydrolytic degradation. In large amounts this leads to crystallisation and embrittlement, however in smaller amounts PLCL-PEG balances faster degradation and resistance to the structural relaxations (aging, crystallisation) that cause embrittlement. These results pave the way towards achieving bioresorbable materials that have (and retain) favourable mechanical properties along a suitable degradation timescale.

References

- Wayangankar, S. A., & Ellis, S. G. Prog. Cardiovasc. Dis., 58(3): 342-355, 2015

Structure –Function Correlation and Precision Bio-Manipulation of Leukaemic Cell-Matrix Interactions

J. R. James^{1,2}, J. C. Ashworth¹, D. Murukesan¹, K. Arkill¹, C. L. R. Merry¹, A. Wright², A. Thompson¹

¹Faculty of Medicine and Health Sciences, University of Nottingham, Nottingham, UK.

²Faculty of Engineering, University of Nottingham, Nottingham, UK.

INTRODUCTION: The bone marrow niche is a three-dimensional (3D) microenvironment consisting of cells, extracellular matrix (ECM), and soluble biomolecules that together provide the mechanical, biochemical and biophysical signals that regulate both normal haematopoietic stem cell (HSC) and leukaemic stem cell (LSC) behaviour. However, the highly complex matrix and multi-cellular nature of the bone marrow makes it challenging to identify and interpret the cues that drive HSC/LSC fate decisions. We present a synthetic, tuneable peptide gel used to model the 3D structure of the bone marrow, combined with optical trapping to interrogate the biomechanical properties of single cells and the niche at nanometre resolution.

METHODS: Fully-defined peptide gels (FEFEFKFK) were used to culture human leukaemic cell lines and primary mouse MLL-AF9 cells within a matrix-free 3D environment. 1064 nm optical tweezers were used to accurately and non-invasively manipulate single cells within the peptide gels to probe cell viability and functionality. Beads were seeded within the gels pre- and post-gelation and micro-rheological data was collected by observation of the Brownian motion. In addition, the effect of FDA-approved drugs on the viability of encapsulated leukaemic cells was quantified using luminescence.

RESULTS: All cell types investigated proliferated within matrix-free peptide gels demonstrated by cluster formation using live cell imaging and confocal microscopy (Fig.1).

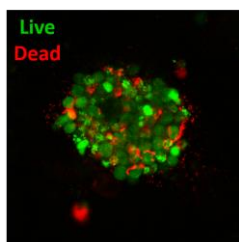


Fig. 1: Primary mouse MLL-AF9 cells in peptide gel imaged with confocal microscopy.

Optical trapping was used to manipulate cells within the peptide gels whilst maintaining

viability and functionality (Fig.2). Bead-seeded peptide gels were successfully used to perform microrheology, allowing for investigation of the local variations in stiffness at the single cell scale^[1]. Drug treatments of encapsulated leukaemic cells is ongoing and will be presented at the conference.

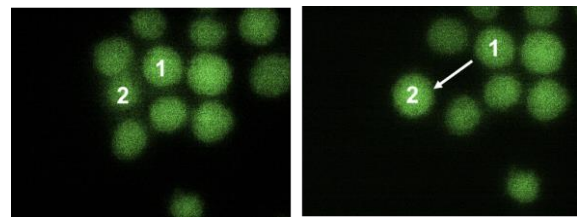


Fig. 2: Before (left) and after (right) images of optical manipulation of a U937 cell away from a cell cluster. Cells stained with calcein AM.

DISCUSSION & CONCLUSIONS:

Accumulating data supports the need to quantify and potentially control biological, chemical and physical stimuli to better understand cell behaviour. HSCs and LSCs have been known and analysed for over 50 years. However, their biophysical properties and the potential role of these in cell function remain to be elucidated. Here we have produced a 3D model allowing independent control of biological, chemical and physical stimuli. This model has been used to assess cell viability, functionality and response to drug treatment. In combination with our ability to physically manipulate relevant cell types within the peptide gels, we intend to obtain an improved mechanistic understanding of cell-cell and cell-niche interactions, with future work aimed at comparative analyses of HSC and LSC interaction with the bone marrow niche.

ACKNOWLEDGEMENTS: Research funding gratefully received from the EPSRC via the Centre of Doctoral Training.

REFERENCES: [1] J.C. Ashworth, J.L. Thompson, J.R. James. *et al.* (in press), *Matrix Biology*, 2019.

Substrate mechanical properties modify bone marrow stem cell behaviour

M. L. Hernandez¹, B.G. Sengers², N.D. Evans^{1,2}

¹Centre for Human Development, Stem Cells and Regeneration, Human Development and Health, Institute of Developmental Sciences, ²Mechanical Engineering, University of Southampton, Southampton, United Kingdom.

INTRODUCTION: Cells interact with their microenvironment by receiving mechanical cues that modify their behaviour. For instance, the stiffness of the extracellular matrix has been widely reported to have an impact on cell spreading, proliferation and differentiation. In addition, factors such as material heterogeneity and thickness need to be understood when designing scaffolds for tissue repair. A material must have the appropriate stiffness to resist cell-applied force of cell groups or cell layers, to maintain tissue integrity and function. This is dependent upon not only the material elastic modulus, but also thickness and dimensions.

METHODS: To test the hypothesis that substrate stiffness and thickness affects spreading of bone marrow stromal cells (BMSCs), we fabricated polyacrylamide hydrogel matrices of different stiffness ranging from 1 to 40 kPa. We also modified the 1KPa hydrogels by varying the polyacrylamide mixture volume (5 - 100 μ L). Hydrogel thickness was measured by light and confocal microscopy (Leica SP5 microscope). Type I (atelo-) collagen at a concentration of 0.1 mg/cm² was covalently linked to the hydrogels. BMSCs were seeded at various densities to evaluate the effect of stiffness or thickness. Cells were then stained with DiD and imaged using a Ti-Eclipse Nikon inverted microscope and single cell spreading area was measured. Osteogenic differentiation was assessed in cells grown (10,000 cells/cm²) for 7 days in α MEM, with or without ascorbate, betaglycerophosphate and dexamethasone. Cells were stained with Fast Violet (Sigma) for alkaline phosphatase (ALP) activity and separately, the absorbance was quantified in a Glomax reader at 405nm. ALP activity was normalised with the DNA concentration obtained by a PicoGreen Assay.

RESULTS: BMSCs were found to spread more on stiff compared to soft hydrogels and thin compared to thick hydrogels. In addition, ALPase activity and DNA synthesis was greater

in cells grown on 40 kPa compared to 1 kPa, but this difference was not statistically significant. 1 kPa hydrogels were thicker than 40 kPa. (~1200 μ m and ~623 μ m respectively for a polyacrylamide volume of 100 μ L). Cells grown on thin 1 kPa gels (~47 μ m) spread to a lesser extent than those on thick gels (1200 μ m) with a mean cell area of 2600 \pm 79 for the former and 5600 \pm 990 μ m² for the latter (Figure 1).

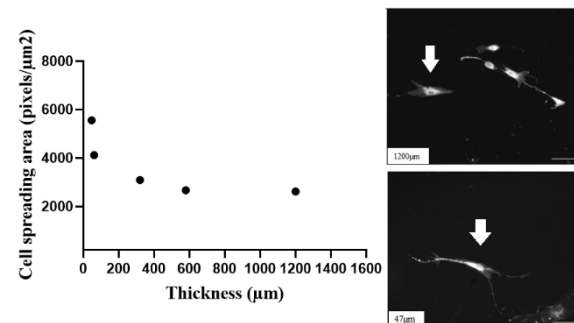


Figure 1. (Left) Substrate thickness decreases cell spreading (Right) BMSCs morphology on thick (above) and thin (below) polyacrylamide hydrogel.

DISCUSSION & CONCLUSIONS: The observation that stiffer and thinner hydrogels promoted cell spreading suggests that these gels are more resistant to cell-applied tension than thick or soft gels. The observation that cells spread to a greater degree on thin gels, regardless of their low modulus (1 kPa) suggested that the cells 'feel through' the soft gel to the underlying glass substrate. This may suggest that by modifying the substrate thickness it would be possible to modify cell morphology and consequently promote differentiation for tissue repair.

ACKNOWLEDGEMENTS: CONACyT (Mexico), FoM, University of Southampton.

REFERENCES: (1) Engler, A. J. *et al.* (2006) 'Matrix Elasticity Directs Stem Cell Lineage Specification', *Cell*, 126(4), pp. 677-689.

(2) Tusan *et al.*, 2018. Collective cell behavior in mechanosensing of substrate thickness, *Biophysical journal*. 114, pp. 2743-2755.

Surface modification and functionalisation of electrically conductive electrospun PLCL/PANI biomaterials using atmospheric dielectric barrier plasma discharge (DBD) for tissue engineering applications

GC Menagh¹, D Dixon¹, G Burke¹

¹ NIBEC, Ulster University, Belfast, Northern Ireland.

INTRODUCTION: Synthetic biomaterials are inherently hydrophobic and lack surface chemical and topographical features to make them ideal candidates for in vitro studies. Plasma surface treatments such as DBD are routinely used to enhance cellular attachment and differentiation in tissue engineering.[1-3] Electrically conductive polymers have become increasingly important as a method of promoting cellular response and monitoring real time cell culture in vitro.[4] Here we investigate the effects of increasing DBD plasma processing on the surface physical, mechanical and chemical properties of electrospun PLCL/PANi an electrically conductive polymer.

METHODS: PLCL/PANi polymers were added to a Chloroform/DMF solvent mixture before being electrospun at 15 cm distance and 18kV to produce a onto a rotating mandrel. This was exposed to increasing dosages of DBD plasma up to 20 J/cm² under atmospheric conditions. After a 48-hour resting period the samples were characterised using wettability analysis, SEM, Tensile Testing AFM, FTiR and XPS.

RESULTS: Randomly aligned, electroconductive electrospun PLCL/PANi matrices 22.86µm (4.47) of thickness, with an average fibre diameter of 0.8µm (0.28) were manufactured. The effect of the increasing DBD treatment caused a dose dependent statistically significant enhancement in their wettability until the point where surface melting was observed. SEM revealed a dose dependent beneficial change in fibre morphology and topography at low DBD dosages up to 10 J/cm². However, higher dosages above this caused polymer fibre fractures and surface melting changes to be observed. FTiR analysis following DBD plasma treatment showed no chemical changes to the bulk properties of the polymer. AFM showed alterations in the topography of the individual surface fibres. Chemical XPS analysis showed an increase of 7% in the oxygen carbon ratio primarily consisting of an increase in C-O bonding formed from free radical formation on the polymer surface during

DBD treatment. Tensile testing was used in this study to firstly assess the effect of adding PANi to PLCL. Adding PANi causes a significant increase in Young's modulus and strength ($P < 0.05$) with no significant difference between the maximum load potentials between the two groups. Increasing plasma dosages on PLCL/PANi was also mechanically tested. A significant decrease Young's modulus and strength was noted on all DBD treated samples ($P < 0.05$), the samples also showed an increased maximal extension following DBD treatment.

DISCUSSION & CONCLUSIONS: The research presented here clearly shows that atmospheric DBD plasma treatment alters the surface topography to improve surface wettability. Atmospheric DBD also oxygenates the surface of the treated polymer which is known to enhance cellular attachment and proliferation. Despite DBD being a cold plasma technology thermal damage to the individual fibres was observed at higher DBD dosages. This is also due in some part to the chain scission on the surface of the fibres causing point defects which can propagate easily into fibre fractures. Tensile testing showed that any level of DBD treatment causes PLCL/PANi fibres to become more pliable at the cost of overall fibre strength. On the balance of all of the available physical, mechanical and chemical analysis 10 J/cm² DBD treatment is the optimal DBD dosage to surface modify electrospun PLCL/PANi matrices balancing the need for improved surface wettability against polymer degradation.

REFERENCES ¹.Sorkio A, Porter PJ et al (2015) *Tissue Engineering Part A* 21:2301-14. ². D'Sa RA (2015) *J Mater Sci Mater Med* 26:260. ³ Wang M, Favi P, Cheng X, et al (2016) *Acta Biomater* 46:256-65. ⁴ Balint R, Cartmell SH. (2014). *Acta Biomater* 10:2341-53.

ACKNOWLEDGEMENTS: PhD Funding from Department for the Economy (DfE) Studentship (Northern Ireland)

SUSPENDED LAYER ADDITIVE MANUFACTURE OF A TRI-LAYER SKIN MODEL

Jessica J. Senior and Alan M. Smith

Department of Pharmacy, University of Huddersfield, UK.

Corresponding author: Jessica.senior@hud.ac.uk – PhD student (3rd year)

Introduction

The treatment of skin defects caused by illness or trauma remains a major healthcare problem - particularly in chronic non-healing wounds. The current gold standard in chronic wound management is the split-thickness autograft. Split-thickness autografting, however, is not suitable for the treatment of wounds which compromise the subcutaneous layer and can lead to contraction and scarring at the wound site following transplantation. Due to the shortcomings of current wound care treatments along with limited donor availability, there is a clinical need for an alternative wound therapy. The use of biologic scaffolds loaded with spatially allocated cells offers a potential solution to these problems by preventing tissue contraction and scar formation. Using suspended layer additive manufacture, whereby 3D scaffolds are printed layer upon layer within a supporting agarose fluid gel ^{1,2}, it is possible to fabricate full thickness tri-layer skin models *in vitro*. These scaffolds feature physiochemically and mechanically defined layers which replicate the epidermis, dermis and hypodermis *in vivo* and have the potential to overcome the issues that we currently face in the treatment of chronic wounds.

Materials and Methods

Agarose fluid gels were prepared by shear cooling agarose solutions (0.5% w/v) and loading into deep petri dishes. Primary human epidermal keratinocytes (HEK), human dermal fibroblasts (HDF) and stromal vascular fractions (SVF) were isolated from an abdominoplasty approximately four hours after excision and cultured to confluency prior to use. The heterogenous SVF population was cultured in order to isolate a homogenous population of adipose derived mesenchymal stem cells (ADSC). SVF heterogeneity and ADSC homogeneity was quantified by flow cytometry. ADSCs were then cultured for a further three weeks for the differentiation of adipocytes as indicated by staining with Oil red O solution. Using a 3D bioprinter (INKREDIBLE[®]), ADSC loaded pectin / collagen blends (ratio 2:1) were printed to form the hypodermis layer. Subsequent layers of HDF loaded pectin / collagen blends (ratio 1:1) to form the dermal skin regions were printed atop the subcutaneous layer and surface seeded HEKs formed the epidermal region (**Fig 1A**). Once printed, the constructs were crosslinked (thermally for collagen and ionically for pectin) prior to removal from the supporting bed. Cell viability and morphology was assessed using confocal microscopy and the microstructure evaluated using scanning electron microscopy.

Results and Discussion

Cells were successfully isolated from the human abdominoplasty and SVF populations were homogenised giving rise to ADSCs (**Fig 1B**). 3D printed skin models exhibited structural integrity throughout the complete part of neighbouring skin regions (**Fig 1C**) and the successful cultivation of spatially allocated cells was achieved. Scanning electron microscopy showed the material microstructure that was comparable to that of native skin (**Fig 1D**).

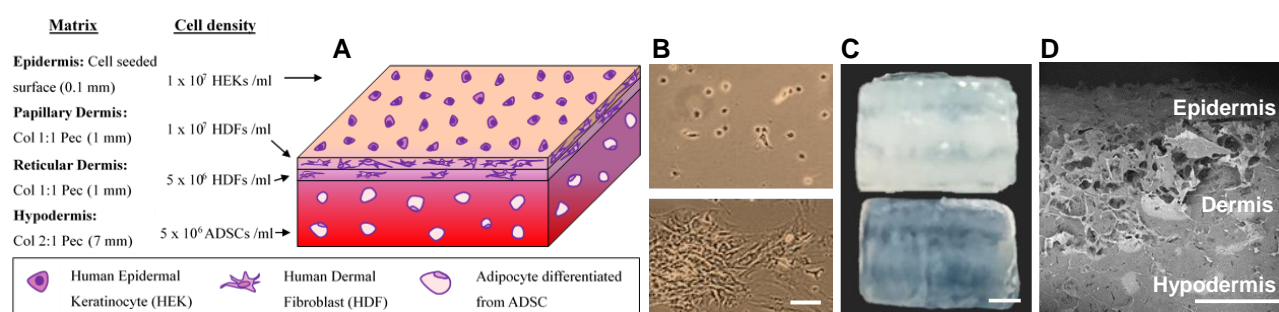


Figure 1 | Design and fabrication of a tri-layer skin model using suspended manufacturing methods. **A**) Design of a tri-layer skin model (15.0 x 15.0 x 9.1 mm) featuring a hypodermis, dual compartment dermis and epidermis. **B**) Culture of cells isolated from the stromal vascular fraction (SVF) at day 1 (upper) and homogenized into ADSCs at day 7 (lower) (scale bar = 100 μ m). **C**) 3D printed tri-layer scaffold (upper) and cross section (lower) displaying a gradient in material matrix (scale bar = 3 mm). **D**) Scanning electron micrograph of a 3D printed tri-layer scaffold displaying a gradient in material matrix at the micron scale (scale bar = 1 mm).

Conclusions

These results demonstrate that tri-layer skin models can be intelligently designed and fabricated using low viscosity collagen and pectin blends in order to manufacture a final construct that contains physiochemical gradients similar to the gradients present within skin tissue.

References

1. Moxon S *et al.* Adv. Mater. 29, 2017
2. Cooke M *et al.* Adv. Mater. 30, 2018

Synthesis of various calcium phosphate nanoparticles from a magnesium-free simulated body fluid.

Ting Yan Ng,¹ Jan Skakle¹, Iain R. Gibson^{1,2}

¹ Department of Chemistry, School of Natural and Computing Sciences / University of Aberdeen, ²Institute of Medical Sciences / University of Aberdeen

Corresponding author: tyn16@abdn.ac.uk – PhD student (3rd year)

Introduction

Hydroxyapatite (HAp) [idealized formula $\text{Ca}_{10}(\text{PO}_4)_6(\text{OH})_2$] is chemically and structurally similar to the main inorganic component in bone and teeth. Although it has been the focus of much research as a bone replacement material, the ability to synthesise it as nanoparticles has led to applications such as a drug delivery system and for use in cell transfection as an alternative to viral systems [1]. Here, the aim of the study was to synthesise nanoparticles of calcium phosphate (CaP) using a biomimetic inspired approach. Thus, a simulated body fluid (SBF), a solution containing similar inorganic ion concentrations to those of human plasma, was used for HAp synthesis. Appropriate cues, such as small increases in calcium and phosphate ion concentration or the presence of nucleation sites can facilitate spontaneous nucleation and HAp crystal growth from SBF at physiological pH (7.4) and body temperature (37°C) [2]. In this study a modified SBF composition, through the removal of magnesium ions, was used to prepare various CaP nanoparticles by adjusting the pH.

Materials and Methods

Mg-free SBF solution was prepared by dissolving reactants in deionised water, adapting the method described by Kokubo *et al.* [2]. The pH value of the solution was measured throughout the experiments. Aliquots of Mg-free SBF were then warmed to 37°C and the pH was adjusted from 7.40 to values between 7.75 and 9.15 by the addition of small volumes of 1M NaOH (aq). After an hour, precipitates were collected from the SBF, dried, then analysed using X-ray powder diffraction (XRD), Fourier transform infrared spectroscopy (FTIR). Dispersed nanoparticles were imaged using transmission electron microscopy (TEM).

Results and Discussion

The XRD patterns of precipitates obtained from Mg-free SBF by adjusting pH to values from 7.75 up to 8.75 resulted in a HAp phase, with broad diffraction peaks consistent with nano-scale crystallites of apatite. In contrast, precipitates formed from Mg-free SBF at pH values of 8.90 up to 9.15 resulted in the formation of an amorphous calcium phosphate (ACP) phase, with no resolved diffraction peaks appearing and a characteristic 'amorphous' pattern observed. The formation of a crystalline apatite or an amorphous calcium phosphate phase was also confirmed by FTIR analysis; the former produced a doublet in the $\sim 550\text{-}600\text{ cm}^{-1}$ region of the IR spectrum, while for the latter a single broad peak was observed. The morphologies of the apatite and ACP nanoparticles were also studied using TEM analysis. Needle and ribbon like crystals (Fig 1a) were observed with the apatite phase and low aspect ratio nanoparticles (Fig 1b) were observed for the ACP phase.

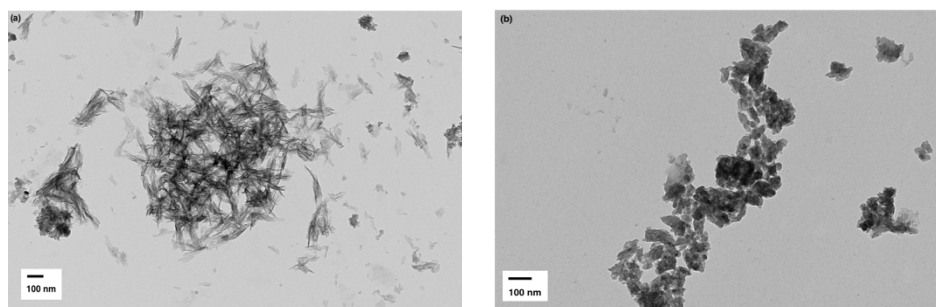


Figure 1. Images of (a) the needle and ribbon shaped crystals precipitated from a Mg-free SBF solution at pH 8 (20000x); (b) low aspect ratio nanoparticles precipitated from a Mg-free SBF solution at pH 9 (30000x).

Conclusion

This study shows that by careful control of synthesis conditions, different calcium phosphate phases can be produced: HAp nanoparticles can be synthesised by using Mg-free SBF solution and different calcium phosphate phases can be synthesised under different pH values of the Mg-free SBF solution. These may behave differently in terms of how they may be internalised by cells and therefore behave as gene delivery systems.

References

1. Shubhra QTH *et al.* *Biomat. Sci.* 5: 972-981, 2017.
2. Kokubo T *et al.* *Biomat.* 27: 2907-2915, 2006.

THE APPLICATION OF COLD ATMOSPHERIC PLASMA GAS TO DIRECT WOUND HEALING IN EQUINES

L. M. Bowker¹, C. Hall¹, J. Kemp-Symonds¹, P. K. Mastalerz, D. O'Sullivan, J. A. Hunt¹

1. Medical Technologies and Advanced Materials - Nottingham Trent University

2. Theradep, Questum Enterprise Centre, Clonmel, Co. Tipperary, Ireland

Corresponding author: laura.bowker2018@my.ntu.ac.uk – PhD student (1st year)

Introduction

Equines are, generally, excellent wound healers, as they are capable of repairing huge skin and muscle traumas. However, in some cases the healing process becomes compromised which can lead to the wound becoming infected. The typical treatment of equine wounds is through cleaning, debridement and bandaging, but wounds can still become infected. More than 90% of chronic wounds contain biofilms which are resistant to treatments. Our research is centred using cold atmospheric plasma to improve the efficacy of wound healing in equines. The emergence of plasma medicine has provided some hope for advancement in wound closure rates for patients with chronic wounds and some positive clinical results have already been observed. However, the potential to combine antimicrobials with plasma medicine has not yet been widely explored and this study outlines one potential way to combine such therapies.

Materials and Methods

Collagen with and without antimicrobials, was introduced into the discharge of cold atmospheric plasma and the activated materials were deposited onto surfaces to produce a dry and adherent coating. The plasma device was then used to deliver the collagen and antimicrobials into bacterial and eukaryotic cultures and the antimicrobial, cytotoxic and wound healing effects were compared to untreated and plasma only treated reference controls.

Results

Surface analysis using FTIR showed that the plasma deposit retained the chemical features of the dissolved protein and antimicrobials. The plasma deposited collagen was shown to effectively promote re-epithelialisation compared to the control. Although plasma treatment alone enhanced re-epithelialisation, the collagen treatment produced a statistically significant ($p < 0.05$) improvement in the rate of angiogenesis and re-epithelialisation. Plasma deposited antimicrobials showed an increased effect in bactericidal activity when compared with plasma treatment alone. The antimicrobials showed cytotoxic activity to eukaryotic cells at high concentrations, however, this was not seen at low concentrations.

Discussion

High energy plasma devices have been shown to kill cells, cauterize flesh and fragment chemical precursors. The data in this research demonstrated that using the above setup, the plasma-modified collagen formed a surface layer which largely retained the chemical properties of the starting material. Treatment with plasma alone showed a beneficial effect for wound healing, while, higher levels of re-epithelialisation and angiogenesis were demonstrated using collagen. From this research, it can be deduced that exposing fibroblasts to cold atmospheric plasma can induce wound healing factors and these can be improved further by plasma deposited collagen. It has been known for a number of decades that certain naturally forming elements have antimicrobial activity; this has also been shown by cold atmospheric plasma. There has, however, been little research in the combination of plasma and other antimicrobials. These investigations showed that plasma treatment alone had bactericidal effects and this effect was further improved by the deposition of antimicrobials via the plasma.

Conclusions

The aim of this study was to determine the antimicrobial and wound healing effect of plasma deposited materials which had not been explored in depth previously. We determined that combining both an antimicrobial and biological therapy with a plasma treatment showed promising results in the treatment of chronic wounds and demonstrated the potential in combining biological therapies with plasma deposition for targeted delivery and enhanced healing.

The Interaction between Cancer and the Stroma within a Tumouroid

Judith Pape¹, Mark Emberton², Umber Cheema¹

¹Division of Surgery, UCL, London, UK, ²Faculty of Medical Sciences, UCL, London, UK

INTRODUCTION: Most research into cancer cell behaviour and pathology relies heavily on 2-dimensional (2D) monolayers of immortalised cancer cell lines. This however, does not recapitulate the complex cell-to-cell communication of cancer and stromal cells, the influence of extracellular matrix components and the spatial configuration that promotes cancer growth and metastasis. Increasingly, the focus has now been to mimic the cancer micro- and macro-environment to better understand tumour growth. This is done through utilising novel 3D models, which provide an extracellular matrix, stromal cells and established chemical gradients essential for cancer progress¹. We have developed complex 3D tumouroids and tested the effects of an acellular stroma, a ‘normal’ cellular stroma and a cancer-associated stroma, to test the effect on cancer invasion.

METHODS: Complex tumouroids were constructed by utilising monomeric collagen type I and RAFTTM plastic compression. Artificial cancer masses (ACMs) containing either highly invasive HCT116, less-invasive HT29 or normal CCD841 CoN cells were implanted into a stromal compartment. The stroma was either acellular, normal or cancer associated containing HUVECs, HDFs or six patient-specific cancer associated fibroblasts (CAFs) and laminin². Finally, CAFs were also added to an established endothelial network to measure angiogenesis- like remodelling caused.

RESULTS: The biomimicry of the tumouroid model was validated through histology and compared to patient samples (*Figure 1 A&B*). The “invasion” of cancer cells into the stromal compartment was exclusively observed in cancer type cells. Rate of invasion was greater for HCT116 compared to HT29 cells due to upregulation of *EGFR* whilst endothelial networks formed were less extensive due to lower expression of VE-Cadherin active protein. Phenotypically, the formation of spheroids within the original cancer mass was due to an upregulation in *EpCAM* and the outgrowth as cell clusters (*Figure 1 C&D*) was driven by the upregulation of *MACC1*, *MMP7* and *HPSE*. CCD841 CoN colon normal cells migrated as single cells and did not form budding cell

clusters detaching from the original mass. The addition of CAFs into the stromal compartment increased invasion significantly (>10 fold) due to upregulation of *TIMP1* and *HGF* but decreased or diminished the development of endothelial networks within the tumouroid models in line with higher *VEGFA* expression but lower *CDH5*.

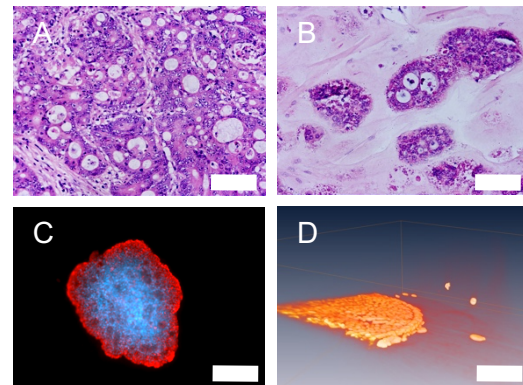


Figure 1: Histology of patient samples (A) compared to HT29 tumouroid (B). Example of invasive body (C) and OPT image of a tumouroid (D). Scale bar= 50 µm for A,B & C and 3 mm for D.

DISCUSSION & CONCLUSIONS: The results indicate that the tissue-engineered colorectal tumouroid model can be utilized as a novel platform to study cancer invasion patterns, vasculogenesis and angiogenesis by comparing to healthy colon cells and looking at specific invasive angiogenic disease markers. Developing a more biomimetic model by incorporating patient-specific CAF samples, allows for the investigation of molecular pathways involved in direct invasion and vasculogenesis. This indicates that CAFs play an essential role in invasiveness, additionally to the formation and remodelling of local blood vessels.

ACKNOWLEDGEMENTS: The EPSRC for funding. Dr. Agata Nyga and Dr. Katerina Stamati for CAF tissues.

REFERENCES:

1. Magdeldin, T. *et al.*. *Sci. Rep.* **7**, 1–9 (2017).
2. Stamati, K., Priestley, J. V., Mudera, V. & Cheema, U. *Exp. Cell Res.* **327**, 68–77 (2014).

Thermosetting decellularised nerve hydrogels for spinal cord injury repair

RSD. Dyer^{1,2}, JCF. Kwok^{1,3,4}, SP. Wilshaw⁵, HE. Berry^{1,3}, RM. Hall², RM. Ichiyama³

¹*Institute of Medical and Biological Engineering*; ²*School of Mechanical Engineering*;
³*School of Biomedical Sciences; University of Leeds, UK* ⁴*Institute of Experimental Medicine, Czech Academy of Sciences, Czech Republic* ⁵*School of Pharmacy and Medical Sciences, University of Bradford, UK*

INTRODUCTION: Decellularised nerve grafts have become a popular tool to repair peripheral nerve injuries (Azouz et al., 2018). Nerve extracellular matrix (ECM) is intrinsically capable of guiding axon growth, while removal of cells and DNA from donor tissue prevents rejection. However, the irregularity of lesion sites in spinal cord injuries makes graft transplantation impossible.

Development of a thermosetting decellularised nerve hydrogel, which could be injected as a solution and then form a gel under physiological conditions, could provide a way to promote neuroregeneration in spinal cord injuries. This study aimed to produce thermosetting decellularised nerve hydrogels with a range of ECM concentrations.

METHODS: Porcine sciatic nerve branches were decellularised by washing in SDS (0.1 % w/v), EDTA, endonuclease, hypotonic and hypertonic solutions.

Decellularisation was validated through H&E and DAPI staining, DNA quantification, contact cytotoxicity, and thioglycollate broth sterility testing.

Decellularised nerve segments were digested in 1 mg.ml⁻¹ pepsin-HCl for 120 hours, followed by neutralisation with NaOH. Isotonic balancing with 10x PBS and dilution with 1x PBS produced decellularised nerve solutions containing 0.5-25 mg.ml⁻¹ ECM. Gelation was induced at 37°C.

RESULTS: After decellularisation, nerves retained their epineurial, perineurial and endoneurial layers. Cell nuclei were removed, and DNA concentrations were reduced by 95% (to 26 ng.mg⁻¹). Decellularised nerves were sterile, and non-toxic to epithelial and fibroblast cell lines.

When nerve ECM solutions were incubated at 37°C, 2-25 mg.ml⁻¹ ECM solutions formed gels within 20 minutes, while 0.5-1 mg.ml⁻¹ ECM

solutions displayed partial gelation after 60 minutes.

DISCUSSION & CONCLUSIONS: Successful development of thermosetting hydrogels from decellularised porcine peripheral nerves with a range of ECM concentrations.

Future work will assess the ability of nerve ECM hydrogels to support neuronal and glial cell growth in culture, to assess their potential to support regeneration in the injured spinal cord.

REFERENCES: Azouz, S.M., Lucas, H.D., Mahabir, R.C. and Noland, S.S. 2018. A Survey of the Prevalence and Practice Patterns of Human Acellular Nerve Allograft Use. Plastic and reconstructive surgery. Global open. 6(8), pp.e1803-e1803.

TISSUE CULTURE BIOREACTOR OPTIMISATION USING COMPUTATIONAL FLUID DYNAMICS TECHNIQUES

K. Chaplin¹, AJ. Capel¹, SDR. Christie², HCH. Bandulasena³, MP. Lewis¹

¹*School of Sport, Exercise and Health Sciences, Loughborough University, UK* ²*Department of Chemistry, School of Science, Loughborough University, UK* ³*Department of Chemical Engineering, Loughborough University, UK*

INTRODUCTION: Tissue culture bioreactors enable the consistent replenishment and removal of medium, preventing fluctuations in the concentration of nutrients resulting in more *in vivo* like culture of 3D tissue. Long-term perfusion cultures have the potential to be used for pharmaceutical drug discovery, toxicology studies and high throughput screening applications. The design of bioreactors is crucial in achieving a balance between high rates of mass transport and minimising potentially damaging shear stress [1]. Computational Fluid Dynamics (CFD) simulations enable flow characteristics and mass transfer to be rapidly evaluated.

METHODS: Bioreactor models were developed in Comsol Multiphysics (COMSOL AB, Stockholm, Sweden) to model the perfusion culture of tissue engineered skeletal muscle. Full geometry of a perfusion bioreactor was used as the computational domain for the simulations. Governing equations of continuity and incompressible Navier-Stokes equation for laminar flow were used to model the effect of flowrates (0.25mL/hr to 2 mL/hr) on fluid flow.

RESULTS: Continuous flow through the bioreactor enables the constant perfusion of skeletal muscle constructs with no stagnation zones that would limit convective mass transport. Shear stress on the skeletal muscle construct is low with a maximum of 3.3×10^{-3} Pa at 2 mL/hr, this unlikely to influence cell behaviour or proliferation. Fluid flow within the bioreactor is influenced by the dimensions of the scaffold used to produce the muscle tissue. The pseudo tendon posts used within this scaffold partially obstruct the velocity of flow onto the tissue. An increased flowrate results in the same convective mass transport limitations due to the low flowrate directly adjacent to the tissue. In this system a redesign of the bioreactor configuration could be more beneficial than increasing the flowrate.

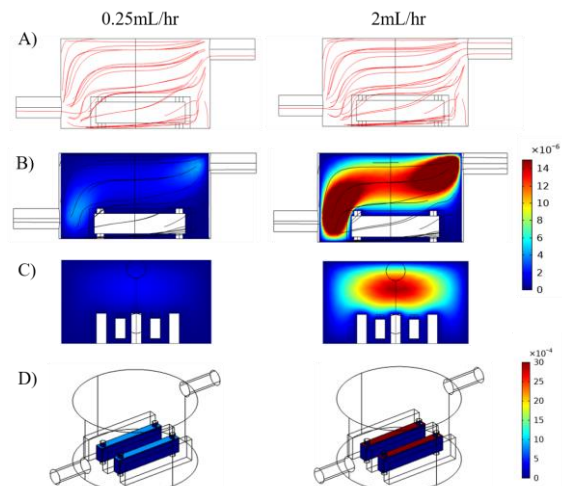


Figure 1. CFD models of A) fluid flow streamlines B) fluid velocity over the TE constructs (m/s) C) fluid velocity over the middle of the constructs D) shear stress on the surface of the constructs (Pa)

DISCUSSION & CONCLUSIONS: CFD modelling can be used to improve mass transfer and control shear stress in bioreactor design. CFD allows the user to visualise the effect of scaffold design on perfusion of tissue and understand potential limitations of system design, enabling design iterations to be rapidly evaluated. Combined with additive manufacturing (3D printing) techniques this could be used to produce bespoke bioreactors optimised for specific cell types.

ACKNOWLEDGEMENTS: The authors would like to acknowledge Loughborough University, EPSRC (grant reference EP/N509516/1) for funding and support.

REFERENCES:

- [1] D. Mazzei, M. A. Guzzardi, S. Giusti, and A. Ahluwalia, "A low shear stress modular bioreactor for connected cell culture under high flow rates," *Biotechnol. Bioeng.*, vol. 106, no. 1, pp. 127–137, 2010.

Tissue Engineering the tendon synovial sheath for anti-adhesive properties

A. Imere¹, J.K.F. Wong², M. Domingos³, S.H. Cartmell¹

¹*School of Materials, The University of Manchester, Manchester, UK* ²*Plastic Surgery Research, Institute of Inflammation and Repair, The University of Manchester, Manchester, UK* ³*School of Mechanical, Aerospace and Civil Engineering, The University of Manchester, Manchester, UK*

INTRODUCTION: The clinical treatments for tendon lacerations can be compromised by adhesion formation [1,2] due to tendon synovial sheath disruption and aberrant healing. Hence, there is the need for development of novel anti-adhesion systems capable of allowing tendons to glide. One of the most promising approaches relies on the introduction of a biomembrane that acts as a physical barrier for adhesion-forming cells whilst regenerating tendon synovial sheath [3]. Here, we propose a novel hybrid approach that combines electrospinning and 3D bioprinting techniques to produce a bilayer biomembrane for the restoration of tendon synovial sheath integrity and the prevention of post-operative adhesions.

METHODS: Polymeric meshes were prepared by electrospinning, using a 10% w/v solution of poly(ϵ -caprolactone) (PCL) (Mn=50,000) in 1,1,1,3,3,3-hexafluoro-2-propanol with process parameters of 1ml/h (flow rate), 20kV (voltage) and 20cm (needle-collector distance) for 1h. Mesh morphology was assessed via Scanning Electron Microscopy (SEM) and fibre diameter and pore size evaluated with ImageJ. Tensile testing of PCL meshes was performed using an Instron 3344 equipped with a 10N load cell at 5mm/min strain rate. HIG-82s (synoviocytes) were encapsulated in Alpha4 self-assembling peptide hydrogel (SAPH) (4×10^6 cells/ml) and cell-laden constructs were printed using a 3D Discovery. Cell viability and metabolic activity was evaluated at 1h, 1, 3 and 7 days via LIVE/DEAD and AlamarBlue assays respectively.

RESULTS: Electrospinning produced nanofibrous PCL meshes (Mean=0.254 μ m), with pores <3 μ m (Fig. 1A) and high mechanical properties (Fig. 1B). Cell-laden constructs with high reproducibility, geometrical and dimensional accuracy were obtained. Good cell viability and proliferation was detected at day 7 post-encapsulation (Fig. 1D), with increased cell metabolic activity over

time (Fig. 1C). PCL mesh and cell-laden SAPH constructs can be combined to create a bilayer biomembrane for restoration of tendon lubrication and prevention of adhesions, as shown in Fig. 1E.

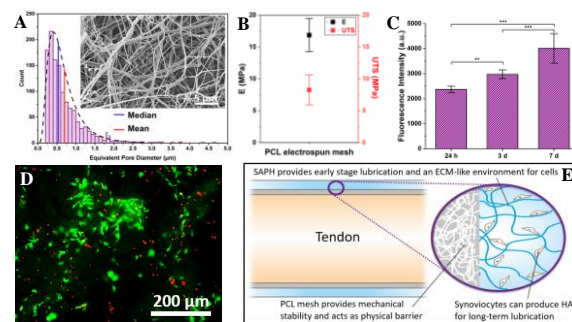


Fig. 1: A) SEM image and equivalent pore diameter distribution of PCL mesh. B) E and UTS of PCL mesh. C) Metabolic activity of HIG-82s upon encapsulation. D) Cell viability after 7 days. E) Proposed bilayer biomembrane (ECM: extracellular matrix, HA: hyaluronic acid).

DISCUSSION & CONCLUSIONS: In the proposed biomembrane model, a physical barrier with good structural integrity can be achieved as result of small pores and high mechanical properties shown by the PCL mesh. 3D bioprinting allows accurate spatial distribution of the hydrogel phase without affecting cell viability and metabolic activity. Moreover, Alpha4 SAPH provides a substrate that, mimicking the native tissue ECM, can potentially stimulate cells to produce HA for long-term lubrication. Future work will include anti-adhesion mechanical tests to investigate the anti-adhesive properties of the final product.

ACKNOWLEDGEMENTS: The authors thank EPSRC & MRC for funding (grant no. EP/L014904/1).

REFERENCES: [1] Rawson S et al. *MLTJ*. 2013; 3:220–228. [2] Wong JKF et al. *Am. J. Pathol.* 2009; 175: 1938–1951. [3] Khanna A et al. *Br. Med. Bull.* 2009; 90:85–109.

Tissue-engineered models to study extracellular matrix: tumour interactions in oral cancer

AL Harding¹, D Frankel², DW Lambert¹, HE Colley¹

¹*Ibio research group, School of Clinical Dentistry, Sheffield University, UK*

²*School of engineering, Newcastle University, UK*

INTRODUCTION: Tumours are capable of initiating the activation of the host stroma via a desmoplastic response; a fibrotic state that is characterised by an altered organisation and composition of ECM proteins. Tumour stroma consists of immune cells, blood vessels, and activated fibroblasts known as cancer associated fibroblasts (CAF). Within the tumour niche, abnormal ECM affects cancer progression by supporting a tumour permissive microenvironment, cellular transformation and metastasis. Although considerable evidence exists demonstrating a role for CAF in oral squamous cell carcinoma (OSCC), little is known about their influence on ECM: tumour interactions. Therefore, the objective is to generate a novel tissue-engineered mucosa model to study the CAF-derived ECM in oral squamous cell carcinoma (OSCC) progression.

METHODS: Utilising a transwell technique, culture conditions were optimised to stimulate normal oral fibroblast (NOF-) and cancer associated fibroblast (CAF-) derived matrix (DM) deposition. Full-thickness oral mucosa models were produced by culturing normal (FNB6) or OSCC (H357) cell lines seeded onto FDM at an air to liquid interface for 12 days. Atomic force microscopy (AFM) determined the soft matter properties and biomechanical stiffness of FDM. Live-cell imaging microscopy (LCIM) was used to examine the effects of different fibroblast-DM on the migration, adhesion and proliferation of cancer cells.

RESULTS: NOF stimulated to produce ECM, over a four-week culture period, generated an organised matrix with an average thickness of ~200 µm compared to CAFs which produced a thicker (350 µm), highly irregular ECM. Addition of FNB6 and H357 cells generated a stratified epithelial layer histologically resembling normal and cancerous tissue *ex vivo* (Figure 1). AFM determined the

micromechanical properties of the ECM and alterations of tissue stiffness, in disease progression. LCIM showed increased migration and proliferation of FNB6 and H357 cells on CAF-DM compared to NOF-DM (Figure 2).

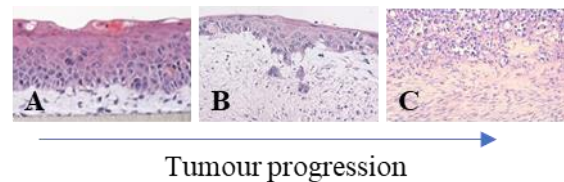


Fig. 1: H&E staining of fibroblast-derived matrices depicting OSCC disease progression. FNB6 on NOF matrix (A), FNB6 on CAF matrix (B), and H357 on CAF matrix (C). Mag x20.

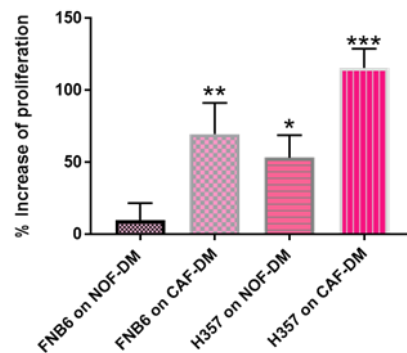


Fig. 2 Analysis of the proliferation rates of H357 and FNB6 cells on fibroblast-derived matrices by LCIM. $P^{**} = 0.0048$, $P^{*} = 0.0268$ and $P^{***} < 0.0001$ by one-way ANOVA.

DISCUSSION&CONCLUSIONS: Utilising *in vitro* tissue-engineering techniques it is possible to model FD-ECM deposition providing a novel, physiologically relevant tool for the study of OSCC progression.

ACKNOWLEDGEMENTS: I would like to generously thank Professor K Hunter, Dr R Bolt and Dr H Colley for the collection and ethics pertaining to the collection of oral tissue.

DEVELOPMENT OF A FULLY IMPLANTABLE BIODEGRADABLE SENSOR FOR THE ELECTROCHEMICAL MONITORING OF THERAPEUTICS

Steven Gibney*,¹ P Smith,¹ A Hook,¹ P Hoelig,² C Moers,² A Bernhardt,² F Rawson,¹

¹School of Pharmacy, University of Nottingham; ²Evonik Nutrition & Care GmbH, Darmstadt, Germany

*Steven.gibney@Nottingham.ac.uk – PhD student (1st year)

Introduction

Recent advances in biomaterial development have made it possible to explore a number of novel avenues concerning the emerging field of bioelectronics. Specifically, in relation to the field of biosensors the identification of new materials has made the possibility of developing a sensor platform capable of functioning *in vivo* is now a realistic possibility. The ability to measure an analyte of interest *in vivo* is seen as a major leap forward in therapeutic monitoring; current therapeutic monitoring involves recurring and difficult sampling procedures making data acquisition inconvenient, expensive and potentially inaccurate [1]. The successful development of a functioning *in vivo* sensor would overcome these limitations, however a number of challenges remain before this goal can be achieved. The largest of such challenges include poor biocompatibility, loss of functionality over time, and loss of sensitivity when placed in a complex environment [2]. To overcome these challenges a multidiscipline approach must be undertaken. Based on this, a combination of electrochemistry, polymer chemistry and biomaterial development will be used to develop a novel nano/micro-sensor capable of detecting and accurately monitor the systemic concentration of antidepressants.

Materials and Methods

A range of surface characterization techniques have been used to characterise blended-polymer films constructed from the conductive polymer poly(3,4-ethylenedioxythiophene): polystyrene sulfonate (PEDOT:PSS) and a range of commercial biodegradable polymers. Films were formed using either drop or spin coating techniques. The techniques used to characterise these films include Time of Flight Secondary Ion Mass Spectrometry (ToF-SIMS) to determine the distribution of polymers at the surface of the film, as well as Atomic Force Microscopy (AFM) to determine the topographic structure of the films. Finally, cyclic voltammetry and electrochemical impedance spectroscopy (EIS) have been used in order to understand the films conductive properties. Similarly, investigation has been carried out in to the redox behavior of potential therapeutic analytes. This primarily relied on electrochemical techniques, such as cyclic voltammetry, to determine the specific signal produced by therapeutic compounds when interrogated at various electrode surfaces in both simple and complex media. Furthermore, the effect of potential interferents, such as ascorbic acid, uric acid and glucose, was assessed to determine the feasibility of detecting tricyclic antidepressants (TCA's) in a complex environment.

Results and Discussion

Thus far, surface characterization of PEDOT films has shown that while PEDOT films can be easily manufactured the properties of the resulting films are influenced by the composition and technique used to create the film. Furthermore, electrochemical study has demonstrated that while the films are electroactive they require further optimization to achieve the resolution needed to be used as a sensor platform.

Secondly, electrochemical characterization of the redox behavior of certain TCAs indicates that specific signals are detectable using both glassy carbon electrodes (GCE) and gold electrodes. However, the results differ from those published previously and further work is required to determine how the electrode surface and electrolyte solution influence the analytes redox behavior [3].

Conclusions

Overall, results indicate that the detection of TCAs is possible however further optimization of electrode surfaces and study of the reaction kinetics is required. Likewise, while PEDOT is a promising material further work is necessary to understand how PEDOT interacts with both other polymers and electrode surfaces. If successful this project would act as a proof-of-concept for a novel sensor platform which would provide a step forward for translational research and contribute towards the growing fields of bioelectronics, therapeutic monitoring and personalised medicine.

References

1. Fiaturi N, Greenblatt DJ. *Handb. Exp. Pharmacol.* 1–19, 2018.
2. Rong G, et al. *ACS Sens.* 2: 327–338, 2017.
3. Sanghavi BJ, Srivastava AK. *Analyst.* 138: 1395–1404, 2013.

TOWARDS TRANSMUCOSAL PEPTIDE DELIVERY: INCORPORATION OF AN ACTIVE MODEL PROTEIN INTO A MUCODHESIVE NANOFIBRE PATCH USING UNIAXIAL ELECTROSPINNING

Jake G. Edmans*¹, Lars S. Madsen², Craig Murdoch¹, Martin E. Santocildes-Romero², Sebastian G. Spain¹, Paul V. Hatton¹, and Helen E. Colley¹

¹The University of Sheffield, ²AFYX Therapeutics, Copenhagen, Denmark
 Corresponding author: jedmans1@sheffield.ac.uk – PhD student (1st year)

Introduction

The oral delivery of peptides is challenging because of degradation in the gastrointestinal tract. Transmucosal drug delivery is an attractive alternative due to avoidance of the gastrointestinal tract and hepatic first-pass metabolism, and favourable ease of administration and patient compliance in comparison to subcutaneous parenteral delivery. However, significant obstacles remain for the development of effective formulations including permeation through the epithelial barrier and loss of biological activity. We have developed a biodegradable, mucoadhesive oral patch¹ that demonstrates long residence times *in vivo*² and is currently involved in a stage 2 clinical trial. The patches are comprised of a two-layer electrospun polymer system composed of a highly bio-adhesive inner layer and an outer saliva-resistant, durable but flexible protective layer. This research aims to further develop the patch for transmucosal delivery of therapeutic peptides.

Materials and Methods

Lysozyme, an antimicrobial enzyme, was incorporated into poly(vinylpyrrolidone)/Eudragit RS100 polymer nanofiber patches as a model protein using a variety of ethanol/water mixtures as solvents and uniaxial electrospinning. Loading rates, bioactivity, and release profile were investigated by soaking the patches in PBS to release the enzyme and then analysing the supernatant using enzyme kinetics and protein assays. The nanofiber morphology was analysed using scanning electron microscopy. The hydrophobic backing layer was produced by electrospinning an additional poly(caprolactone) layer and melting at 65 °C to produce a continuous film. Residence times were evaluated using a simple *in vitro* test and agar disc diffusion assays were used to assess any antimicrobial effect against oral bacteria strains.

Results and Discussion

For solvent mixtures in the range of 97 - 40 wt% ethanol, the bioactivity of the released enzyme was above 90 % and there was no significant difference between solvents. The loading efficiencies ranged from 70 – 100 % with no significant difference between solvents. The average fibre diameter is significantly decreased at 60 and 40 wt% ethanol due to higher solution conductivity and lower viscosity. Samples were taken from different parts of the patches, showing that the distribution of lysozyme is homogenous. The release profile showed that 87 % was released within 1 hour, which is desirable given that the existing patches show residence times of around 2 hours. There was no significant decrease in bioactivity after melting the backing layer at 65 °C.

Conclusions

The resulting protein-loaded patches displayed high bioactivity and clinically relevant release rates making them a promising proof of concept for the delivery of bioactive peptides to the oral mucosa. Additionally, lysozymes' antimicrobial properties may give the patches a potential application as antiseptic dressings for oral wounds.

References

1. Santocildes-Romero M. E. *et al.* ACS Appl. Mater. Interfaces. 9: 11557-11567, 2017.
2. Colley H. E. *et al.* Biomaterials 178: 134-136, 2018

Acknowledgements

This research was funded by the EPSRC Centre for Doctoral Training in Polymers, Soft Matter and Colloids (EP/L016281/1) and AFYX Therapeutics.

Towards understanding why nanoclays are osteogenic

Mohamed Mousa¹, Oscar Kelly², Jane Doyle², Nicholas D. Evans¹, Richard O. C. Oreffo¹ and Jonathan I. Dawson¹

¹B & J Research Group, Stem Cells & Regeneration, Institute of Developmental Sciences, University of Southampton, Southampton, SO16 6YD, United Kingdom

²BYK Additives Ltd., Moorfield Road, Widnes, Ceshire WA8 3AA, Great Britain

INTRODUCTION: Laponite clay nanoparticles are emerging as a new class of biomaterials with exciting opportunities for regenerative medicine applications[1]. High-profile studies have demonstrated[2] the osteogenic properties of Laponite, however, the mechanism(s) underlying nanoclay bioactivity remain poorly understood. Cell uptake and release of degradation products such as Li⁺ are frequently cited mechanisms.

In this work, we investigated the effect of Laponite clay nanoparticles on osteogenic differentiation of Human Bone Marrow Stromal Cells (HBMSCs) and the role of these frequently proposed mechanisms for clay bioactivity.

METHODS: *i) role of Laponite degradation products:*

Various Li⁺ modified Laponite formulations were generated and their effect on HBMSCs osteogenic differentiation was investigated at both basal and osteogenic medium conditions at clay doses of 0 – 100 µg/mL

ii) Role of Laponite endocytosis: HBMSCs were pre-treated with chlorpromazine hydrochloride (CPZ), a clathrin-mediated endocytosis inhibitor, for 2 hours, then incubated with both CPZ (5 µg/mL) and Laponite (0 – 100 µg/mL) in basal and osteogenic conditions for 72 hours. At day 3, ALP activity of HBMSCs was measured. Confocal microscopy was used to track interaction of Rhodamine B-labelled Laponite nanoparticles with HBMSCs.

RESULTS: Laponite nanoparticles induced osteogenic differentiation of HBMSCs at an early stage in a dose-dependent manner. This was confirmed by a significant increase in ALP Activity and upregulation of osteogenic genes (e.g. RUNX2 & Collagen I) at day 3, as well as enhanced Ca-P mineral deposition at day 14.

Modified Laponite chemistries achieved variation in their Li⁺ content. However no attenuation or increase in clay bioactivity was observed between the modified clays tested.

Finally, Laponite nanoparticles strongly interact with HBMSCs, but the addition of CPZ did not show significant effect on the dose

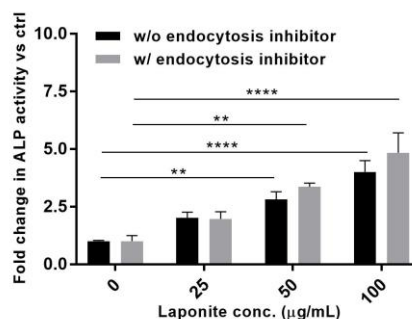


Figure 1: Addition of endocytosis-inhibitor did not affect Laponite dose effect on ALP activity at day 3.

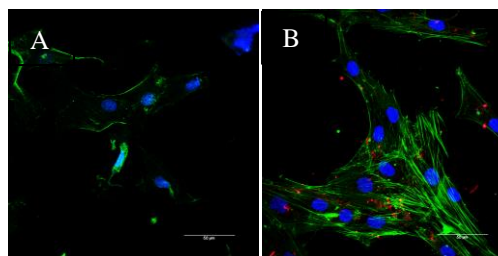


Figure 2: Laponite nanoparticles strongly interact with HBMSCs without affecting cell morphology. A = without Laponite; B = with Laponite. Scale bar = 50µm.

dependent (0 – 100 µg/mL) osteogenic effect of Laponite on the cells.

DISCUSSION & CONCLUSION: Cellular uptake of clay nanoparticles and their subsequent degradation, has been frequently cited as the main mode of action for clay bioactivity[3]. Our data, however, indicate that clay exert their osteogenic properties extracellularly and independent of their degradation products. This suggests a role for biophysical models, such as, clay-cell membrane and clay-ion interactions in cell culture medium[1]. Studies seeking to elucidate these mechanism(s) are ongoing.

REFERENCES:

- [1] M. Mousa *et al.* *Biomaterials*, vol. 159. pp. 204–214, 2018.
- [2] A. K. Gaharwar *et al.* *Adv. Mater.*, vol. 25, no. 24, pp. 3329–3336, 2013.
- [3] J. K. Carrow *et al.* *Proc. Natl. Acad. Sci.*, p. 201716164, 2018.

Tuning adenosine release from biodegradable microspheres for bone regeneration

Hadi Hajiali¹, James Hughes¹, Manuel Salmerón-Sánchez², Matthew J. Dalby², Felicity R. A.J. Rose¹,

¹ *Division of Regenerative Medicine and Cellular Therapies, Centre for Biomolecular Sciences, School of Pharmacy, University of Nottingham, Nottingham, NG7 2RD, UK.* ² *Centre for the Cellular Microenvironment, University of Glasgow, Glasgow, G12 8LT, UK.*

INTRODUCTION: There have been many studies conducted into the delivery of factors, such as small molecules, to support and augment new bone formation. It is essential to control the spatio-temporal release kinetics of such factors in order to enhance their efficiency and reduce the side effects of their high dose.[1] Recently, it has been demonstrated that human pluripotent stem cells can be differentiated into functional osteoblasts through the supplementation of adenosine in the culture media.[2] In this project, we aimed to investigate the encapsulation of adenosine into biodegradable polymer microspheres for bone regeneration and to tune the release profile by using different Poly(lactic-co-glycolic acid) (PLGA) polymers with various ratio of lactic acid to glycolic acid. Furthermore, it has been also shown that Pluronic F127 as a surfactant can modify the release profile [3]. Therefore, this study investigated the effect of the ratio of lactic acid to glycolic acid and Pluronic F127 on the adjustment of adenosine release for bone tissue engineering applications.

METHODS: In the first step, the microspheres were formed using a solid-in-oil-in water (s/o/w) emulsion. In the s/o/w system, the adenosine was added into the PLGA solution (PLGA with various ratio of lactic acid to glycolic acid: 75-25, 80-20, and 85-15 dissolved in the dichloromethane) directly in the solid phase. The emulsion was transferred to a poly(vinyl alcohol) solution and was homogenised. It was stirred to evaporate the dichloromethane, and then filtered, washed and lyophilized until dry. In the next step, Pluronic F127 was added to the optimised polymer solution and then the previous procedures followed. After the microspheres were prepared, their morphology, adenosine encapsulation efficiency, and the release profile were investigated.

RESULTS: The morphology of the microspheres were evaluated by scanning electron microscopy (SEM) (Fig. 1). To measure the encapsulation efficiency (the ratio of actual and theoretical adenosine loading), the microspheres first were

dissolved in dimethyl sulfoxide and analysed for adenosine content by UV spectroscopy.

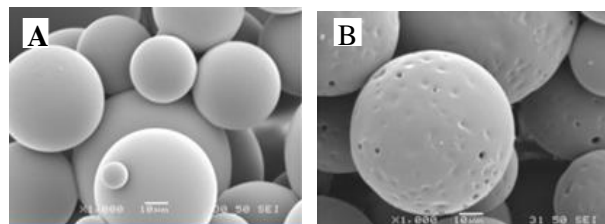


Fig.1: SEM Image of A: Adenosine encapsulated PLGA microspheres; B: Adenosine encapsulated PLGA-Pluronic F127 microspheres.

The data showed that the release of adenosine can be completed in 4 weeks by using PLGA 80-20 that can be more applicable for bone regeneration; in contrast, slower delivery of adenosine was observed in the PLGA 75-25 and PLGA 85-15; complete release was achieved in more than 6 weeks. The addition of Pluronic F127 to the PLGA 80-20 can also reduce the encapsulation efficiency and accelerate the release rate in the first week of study.

DISCUSSION & CONCLUSIONS: In this study, adenosine release was adjusted by using PLGA with various ratio of lactic acid to glycolic acid. The lower inherent viscosity (IV) and molecular weight (MW) of PLGA 80-20 compared to the IV and MW of PLGA 75-25 and PLGA 85-15 enhances the degradation rate of polymers and as a result, increases the rate of adenosine release from the microspheres that can be completed in 4 weeks. The delivery of adenosine can be also tuned by adding of Pluronic F127 to s/o/w system through the providing several pores into the microspheres. Finally, the adjusted delivery system for adenosine can be developed for bone tissue engineering applications.

REFERENCES: ¹ L. J. White, et al (2013) *Materials science & engineering. C, Materials for biological applications* **33**: 2578-2583. ² H. Kang, et al (2016) *Science advances* **2**: e1600691. ³ P. Wang et al (2016) *Colloids and Surfaces B: Biointerfaces* **147**: 360–367.

ULTRA-SHORT CONSTRAINED BETA-SHEET FORMING PEPTIDES FOR THE FABRICATION OF VERSATILE SOFT BIOMATERIALS

Mohamed Elsayw,^{1*} Ronak Patel¹, Jacek Wychowanec², James Leach¹, Claire-Marie Nuttegg³, Araida-Hidalgo-Bastida³

¹School of Pharmacy and Biomedical Sciences, University of Central Lancashire, ²School of Chemistry, University College Dublin, ³Centre for Biomedicine, School of Healthcare Science, Manchester Metropolitan University

*Corresponding author: melsawy@uclan.ac.uk

Introduction: Nature has exploited molecular self-assembly to develop the complex higher macromolecular structures of both the genome and proteome. Inspired by nature, we have recently developed *de novo* ultra-short constrained amphiphilic peptides that self-assemble into bioinspired β -sheet nanofibers.^{1,2} The amphiphilic nanofibers were used for the fabrication of various soft biomaterials, such as hydrogels in aqueous medium, emulgels in biphasic media as well as nanofibrillised microcages/microspheres (Fig. 1). The developed materials were used as scaffolds for dental pulp stem cells (DPSCs) and for the controlled delivery of 5-fluorouracil (5-FU).

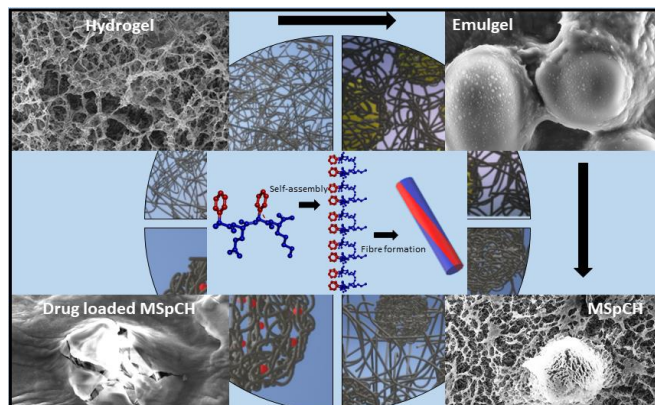


Figure 1: Self-assembly of the amphiphilic ultra-short peptide and the versatile systems fabricated from the nanofibers

Materials and Methods:

ATR-FTIR: molecular characterisation of self-assembly.

Oscillatory rheology: characterisation of the viscoelasticity of the fabricated materials.

AFM, SEM, TEM and SAXS: characterisation of nanofibrillar systems topology, morphology and structure.

Proliferation assay: alamar blue assay used to test the proliferation of DPSCs cultured on the hydrogel scaffolds.

Results and Discussion: FTIR showed that the ultra-short peptides self-assemble to form anti-parallel β -sheet structure in response to pH change of the aqueous solution, with prominent peaks at 1689, 1624 and 1524 cm^{-1} corresponding to an extended β -sheet conformation. AFM showed the formation of nanofibers with diameter size revealed to be of $\sim 9\text{nm}$ from SAXS Guinier analysis. Both SEM and TEM showed the formation of entangled nanofibre networks forming hydrogels in aqueous medium with critical gelation concentration of 3% W/V as revealed from the inverted vial test and oscillatory rheology (shear modulus ~ 4500). In biphasic media, the amphiphilic nanofibers formed stable O/W emulsions (Melissa oil phase) compared to commercial emulsifiers such as poloxamer, cetrimide, SDS and Tween 80 used at same molar concentrations under various environmental conditions (phosphate, chloride and thiocyanate salts; 60°C for 3 hrs; 3 weeks storage...etc.). AFM, TEM and SEM micrographs showed the formation of nanofibrillised microspheres at the O/W interface confirming that the emulsion stabilisation was mediated by the amphiphilic nanofibers (Fig. 1). Oscillatory rheology data showed the viscoelasticity and injectability of the formulated emulgels. The nanofibrillised microspheres were formulated from emulgels (chloroform oil phase) by vacuum evaporation and were loaded with 5-FU, which showed sustained release profiles compared to hydrogels, following Korsmeyer-Peppas (KP) release model. DPSC 2D culture on peptide hydrogel showed cell viability between 3 and 4 %W/V that was not significantly different from controls, suggesting that DPSC growth at these concentrations was comparable to growth on tissue culture treated control wells. However, at day 7, cells cultured on 5 %W/V scaffold showed a significant increase in viability ($p=0.0090$) compared to the control groups. Therefore 5 %W/V is an ideal concentration for further studies.

Conclusions: Ultra-short amphiphilic peptides were designed to self-assemble into bioinspired β -sheet nanofibers that formed the bases for the fabrication of various soft materials with great potential for biomedical (ECM scaffolds for tissue regeneration, anti-infective materials...etc.) and pharmaceutical (emulsifiers, drug delivery vehicles...etc.) applications.

References

1. Elsayw M *et al.* Langmuir, 32: 4917–4923, 2016.
2. Gao J *et al.* Biomacromolecules, 18: 826–834, 2017.

Acknowledgments: Diamond for beam time award (SM17102) and all the staff on beamline I22 at Diamond for their support with the SAXS experiments. Staff in the EM facility of the University of Manchester, for their assistance, and the Wellcome Trust for equipment grant support to the EM facility.

Uncovering the Role of Heparan Sulphate Proteoglycans in Extracellular Vesicle Biogenesis: Potential Tools for Improved Therapies

R. Morgan^{1,2}, R. Holley³, J. Webber⁴, D. Onion⁵, C. Merry², O. Kehoe¹

¹Rheumatology Research Laboratory, Keele University, UK. ²Stem Cell Glycobiology, University of Nottingham, UK. ³Cell Matrix Biology & Regenerative Medicine, University of Manchester, UK. ⁴Tissue Microenvironment, Cardiff University, UK. ⁵Flow Cytometry Facility, University of Nottingham, UK.

INTRODUCTION: Many cell types deliver therapeutic effects by secreting small extracellular vesicles (sEVs). Therefore, sEVs could be used as an alternative approach to cell-based therapies, overcoming many cell-associated challenges. sEVs may be optimised to generate potent therapies through manipulating sEVs biogenesis mechanisms. We aim to prove this concept by altering the global heparan sulphate (HS) present in MCF-7 cells. HS is a glycosaminoglycan found covalently attached to a protein core to form proteoglycans. One such HS proteoglycan is syndecan, a key component in the syndecan-syntenin-ALIX mechanism for EV production^{1,2}. We predict that HS may be involved in sEV cargo selection, due to its ability to form interactions with a wide range of factors. In addition, the structure of HS influences the activity of heparanase, a regulator in the rate of sEV production³. Therefore, structural alterations to HS could allow the cargo (thus therapeutic activity) to be modulated, whilst simultaneously increasing sEV yields.

METHODS: MCF-7s with knockouts in key HS biosynthetic enzymes were generated using CRISPR-Cas9. Subsequent alterations to HS structures were assessed using SAX-HPLC and flow cytometry. Wild type and mutant MCF-7s were cultured in CELLine bioreactors and sEVs were isolated by differential ultracentrifugation. sEVs were then compared using transmission electron microscopy, nanoparticle tracking analysis and western blotting. A bead-free flow cytometry-based method is under development to characterise and sort sEVs sub-populations based on their displayed HS. The effect of a heparanase inhibitor (OGT2115) was also assessed based on changes in HS levels and composition, and sEV size and concentration.

RESULTS: Flow cytometry and SAX-HPLC has allowed for differences in HS composition and display of protein binding epitopes to be distinguished among HS biosynthetic knockout cell lines, and different MCF-7 preparations and culture conditions. CELLine bioreactors have

enabled large quantities of EVs to be obtained. Bead-free flow cytometry has successfully identified EV populations using antibodies for EV and MCF-7 markers, and a biotinylated HS antibody (10E4) (**Figure 1**). Addition of OGT2115 inhibitor led to a decrease in sEV levels.

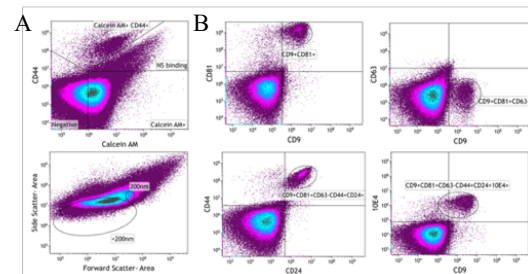


Fig. 1: Characterisation of sEVs using Bead-free flow cytometry. A. Dot plots to identify EV-like populations using Calcein AM staining and comparisons with 200 nm sizing bead calibrations. B. Expression of various markers within population identified in A.

DISCUSSION & CONCLUSIONS: Bead-free flow cytometry has successfully identified a 10E4 positive EV population. Next steps will be to include the full HS antibody repertoire into analysis. The sorting capabilities of the Astrios will be utilised to isolate and characterise distinct EV populations before and after HS manipulations using these HS antibodies. The use of the heparanase inhibitor: OGT2115 has demonstrated that sEV production can be manipulated by targeting HS, supporting our hypothesis.

ACKNOWLEDGEMENTS: Thank you to the Stem Cell Glycobiology Group, Prof Ian Kerr, the nmRC and the Flow Facility at the University of Nottingham.

REFERENCES: 1. Baietti *et al.*, Nat. Cell. Bio. 7: 677–85, 2012. 2. Roucourt *et al.*, Cell Res. 4: 412-28, 2015. 3. Thompson *et al.*, J. Biol. Chem. 14: 10093–9, 2013. 4. Kuppevelt *et al.*, J Biol Chem. 22: 12960-6,1998.

UNDERSTANDING AMELOBLASTOMA-INDUCED BONE REMODELLING

Bakkalci. D¹, Malik. K, ¹ Jell G¹, Fedele. S¹, Cheema. U¹

¹Department of Surgical and Interventional Sciences, University College London (UCL), UK

Corresponding author: deniz.bakkalci.16@ucl.ac.uk

INTRODUCTION

Bone resorption removes the mineral and organic constituents of the bone matrix, this process is mediated by osteoclasts³. Previous studies indicated that receptor activator of nuclear factor kappa-B ligand (RANKL) and its receptor are involved in bone resorption caused by AM cells. RANKL is a key regulator of osteoclast differentiation, recruitment, activation, and survival, this is achieved by binding to the receptor RANK expressed on osteoclasts⁴. This study focuses on investigating possible role of bone resorptive markers such as matrix metalloproteinases in AM-induced bone resorption.

METHODS

Plexiform AM cells (AM-1), follicular AM cells (AM-3) and human osteosarcoma cells (SaOS-2) were cultured in 96-well plates as monolayers (2D). RAFTTM3D Cell Culture system was used to create artificial cancer mass (ACM), where 50 000 cells were seeded within tissue-engineered biomimetic environment composed of monomeric collagen I. The gels were compressed via RAFT absorbers to remove excess fluid. Media culture supernatants from all cultures for day 1, 3 and 7 were collected and stored in -80°C for ELISA assay. To detect pro-MMP-2 and active MMP-2 protein levels, human MMP-2 ELISA assay was performed on culture media supernatant. Cells were fixed in 4% paraformaldehyde for immunofluorescence staining.

RESULTS

MMP-2 protein expression levels of AM-1, AM-3 and SaOS-2 cells were compared in 2D and 3D for day 1, 3, and 7. MMP-2 levels were not detectable in day 1 of cell lines cultured in 2D and 3D. By day 3 AM-3 and SaOS-2 cells seemed to release MMP-2 to cell culture media (Figure 1). Expression levels increased by day 7. Whereas, AM-1 cells did not express MMP-2 both in 2D and 3D throughout 7-day culture. 3D cell culture increased MMP-2 expression for AM-3 and SaOS-2 cells in day 3 and day 7 in comparison with 2D.

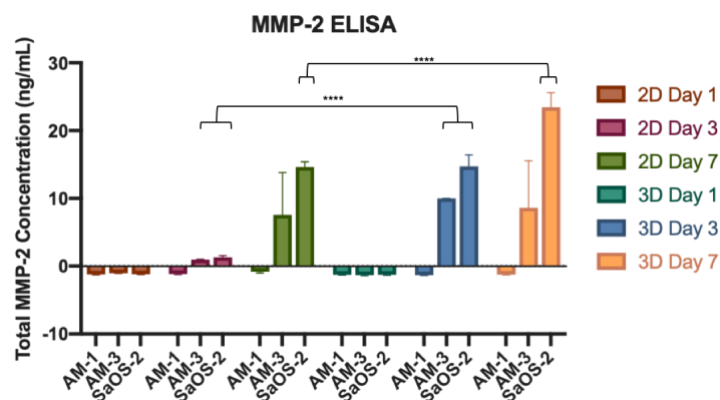


Figure 1: MMP-2 ELISA assay performed on AM-1, AM-3 and SaOS-2 cells. Calibrated by TECAN Plate Reader the infinite 200 Pro (n=3) (****<0.0001, one-way ANOVA).

DISCUSSION & CONCLUSION

MMP-2 is involved in matrix remodelling, thereby tumour invasion and bone resorption. In previous studies, MMP-2 inhibitor I (MMP-2I), decreased ameloblastoma cell invasion⁵. The gelatinase property of MMP-2 can be associated with bone resorptive effect of AM cells. Our results indicate that AM-3 cells might be expressing MMP-2. Further gene expression studies would support our results. As it is possible that there are other factors involved in AM-induced bone resorption such as MMP-9 and RANKL. Testing different markers may help to outline possible mechanisms of how AM cells cause bone resorption.

REFERENCES

1. Qian Y et al. The role of RANKL and MMP-9 in the bone resorption caused by ameloblastoma. *J Oral Pathol Med.* 2010;39(8):592-8.
2. Erikson TM, Day RM, Fedele S, Salih VM. The regulation of bone turnover in ameloblastoma using an organotypic in vitro culture model. *J Tissue Eng.* 2016;7.
3. Anne R et al. Evaluation of bone resorption amongst solid ameloblastoma subtypes. *Int J Oral Maxillofac Surg.* 2017;46:140-1
4. Park JH et al. Current Understanding of RANK Signaling in Osteoclast Differentiation and Maturation. *Mol Cells.* 2017;40(10):706-13.
5. Wang A, Zhang B, Huang H, Zhang L, Zeng D, Tao Q, et al. Suppression of local invasion of ameloblastoma by inhibition of matrix metalloproteinase-2 in vitro. *BMC cancer.* 2008;8:182-.

Understanding Cadherin Mechanisms Using Single Molecule Force Spectroscopy

A.Studd¹, P.Williams¹, C.Merry², S.Allen¹

¹School of Pharmacy, University of Nottingham, Nottingham, England, ²Stem Cell Glycobiology, School of Medicine, University of Nottingham, Nottingham, England

INTRODUCTION: Cadherins (named due to their ‘calcium dependant adhesion’) are a family of intercellular adhesion proteins that are present on some cell membranes, and have been shown to assist in cell-cell adhesion processes and cell signalling functions. E-cadherin is expressed by epithelial cells and embryonic stem cells, and has been shown to have great importance in the regulation of naive pluripotency in mouse embryonic stem cells (mESCs)¹. Recently developed peptide sequences targeting E-cadherin have been shown to affect both physical and biological cadherin functions². However, the relationship between the physical and biological effects actioned by these peptides is not yet understood, with this research aiming to bridge this gap and further our understanding of E-cadherin mechanisms in mESCs.

METHODS: Silicon wafers and silicon nitride cantilevers were prepared via vapour silanisation, followed by functionalisation with extracellular E-cadherin protein fragment (E2153, Sigma-Aldrich). Atomic force microscopy (AFM) was used to obtain force-distance data. Mouse embryonic stem cells were stained using primary antibodies targeting E-cadherin, N-cadherin, and OCT4. Where applicable, Epep (H-SWELYYPLRANL-NH2) and EpepW2R (H-SRELYYPLRANL-NH2) peptides were added at 10 μ M concentration to the functionalised Si wafers or cell culture medium.

RESULTS:

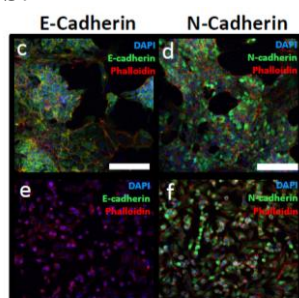


Figure 1: Confocal microscopy images of E14 (top) and *Ecad*^{-/-} (bottom) mES cells, following commencement of spontaneous differentiation. Scale bars represent 200 μ m.

The presence of E-cadherin and N-cadherin is highlighted in E14 and *Ecad*^{-/-} mES cell lines respectively (figure 1).

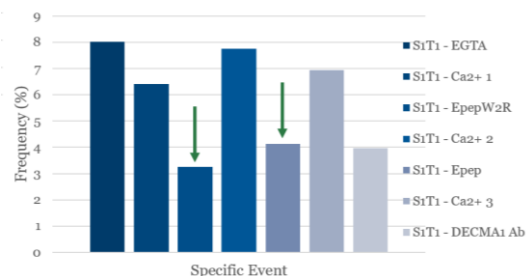


Figure 2: Frequency of adhesion during AFM testing of E-cadherin functionalised Si wafers and cantilevers. DECMA-1 antibody was used for a positive block control, and the peptides Epep and EpepW2R were applied at a concentration of 10 μ M.

E-Cadherin functionalised Si wafers showed success as a precursor for testing the effect of peptides on E-cadherin binding (figure 2).

DISCUSSION & CONCLUSIONS: Confocal imaging of cell samples (figure 1) highlighted the presence of E-cadherin and N-cadherin proteins, in agreement with previously published data on these cell lines. Treatment of E-cadherin functionalised Si wafers with Epep and EpepW2R peptides demonstrates a reduction in binding frequency during AFM testing (figure 2). This indicates both peptides act to inhibit binding, despite previous literature only attributing this effect to the Epep sequence. Further work is required to confidently determine the effects of these peptides, using mES cell monolayers in place of functionalised Si wafers.

ACKNOWLEDGEMENTS: The authors would like to gratefully acknowledge funding by the EPSRC & MRC via the CDT Regenerative Medicine programme.

REFERENCES:

- [1] - Maître, J. L. & Heisenberg, C. P. *Curr. Biol.* 23, 626–633 (2013). [2] - Segal, J. M. & Ward, C. M. *Sci. Rep.* 7, 41827 (2017).

UNDERSTANDING CELLULAR UPTAKE OF SILICATE SPECIES IN BONE CELLS

Joel Turner^{1*}, Azadeh Rezaei¹, Akiko Obata³, Julian Jones², Gavin Jell¹

¹Division of Surgery and Interventional Sciences/ University College London, ²Department of materials/ Imperial College London, ³Department of Life Science and Applied Chemistry/ Nagoya Institute of Technology
joel.turner.17@ucl.ac.uk – PhD 1st year

Introduction:

Silicate based bioactive glasses (BG) are used clinically to regenerate bone [1] [2]. Previous literature has demonstrated the therapeutic importance of BG dissolution products for bone repair and regeneration [3]. There remains, however, a lack of understanding on how soluble silica species interact with cells. This includes how silica species are internalised (and possibly excreted), the intracellular concentration and location of these ions. A greater understanding of silicate cellular internalisation will help in the optimisation of bioactive glass ion release rates for more precise control of cell behaviour. As such, this study aims to investigate silicate ion uptake dynamics in osteoblasts whilst examining some the roles these ions may play in bone regeneration.

Methods and Materials:

Osteoblast-like (SaOS-2) cells were cultured at 10,000/cm² in McCoy's Glutamax 5A medium containing 1mM sodium silicate hydrate. To assess if cytotoxicity was induced by different silicate concentrations and uptake inhibitors, proliferation, metabolic activity and cellular morphology were assessed by total DNA, Alamar blue and light microscopy assessment, respectively. Quantification of Si uptake was performed by ICP-OES, following lysing cells in 1M nitric acid at 85°C and filtration (after 6-96 h cell culture). Inhibition of silicate uptake mechanisms were evaluated by the use of chemical inhibitors of the sodium bicarbonate co-transporter protein by S0859 (Merck). To locate intracellular Si, cultured cells were fixed in 2% paraformaldehyde resin, stained with 1% osmium tetroxide. Scanning Transmission electron microscopy (STEM) (JEOL 2100 Plus) was used to image the cells and energy dispersive X-ray spectroscopy (EDXS) was used to locate and quantify Si content. Si uptake experiments were performed in triplicate. Data was statistically analysed using a Tau-Thompson assessment for anomalies and a student's t-test for statistical significance.

Results and Discussion:

A total increase in intracellular Si uptake was observed up to 48h (whilst the amount of uptake rate per hour decreased over time) (fig. 1A/B). Upon the replacement of Si containing serum with a control (no Si containing media) the concentration of Si decreased ($p < 0.05$), suggesting the excretion of Si from the cells (Fig. 1C). The inhibition of sodium-bicarbonate co-transporter protein decreased ion uptake (without effecting cell number) suggesting a potential mechanism of uptake (Fig 1D). STEM/EDX point analysis showed Si to be evenly distributed within the cell. Higher concentrations were seen to be localised within vesicle-like structures suggesting an active movement of Si throughout the cell.

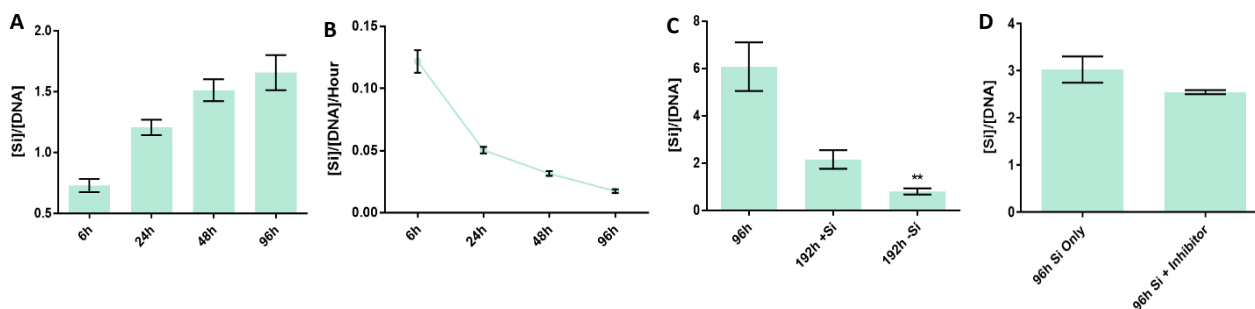


Figure 1. Si uptake by osteoblast-like SaOS-2 cells as determined by ICP-OES. (A) Intracellular Si concentration increased/ μg DNA up to 48hrs, (B) Si ion uptake rate decreases as a function of time, (C) replacing culture medium with Si and non-Si conditioned mediums causes a significant decrease in Si, (D) intracellular Si ion concentration decreases following inhibition of sodium-bicarbonate uptake channels. $N=3$, error presented as \pm SD, * = $P < 0.05$, ** = $P < 0.01$

Conclusions:

Osteoblast-like cells reach a maximum uptake of Si ions over time. Our study suggested that the cells may begin excreting ions at specific stages during their proliferation. Further experiments showed that sodium-bicarbonate channels may play a role in the cellular uptake of these ions. As such, new BG materials should be tailored to release silicate and other ions to target specific cell types dependent on their uptake rates and mechanisms.

1. Logroscino G. Journal of Materials Science; 25(10):2445-2461. 2014
2. Hench L. Journal of Materials Science: 17(11):967-978. 2006
3. Xynos I. Journal of Biomedical Materials Research; 55(2):151-157. 2001

UNDERSTANDING NEURAL NETWORKS: THE DEVELOPMENT OF SINGLE NEURON-NEURON BRAIN-ON-A-CHIP MODELS

James Kinsella, Dr S Christie, Dr P Roach
 Chemistry/Loughborough University,

Corresponding author: j.a.kinsella@lboro.ac.uk -PhD student (2nd year)

Introduction

Understanding the structure of complex neural networks and how these interactions result in such a wide array of functions has been of wide interest across the sciences. Owing to its complexity, understanding the brain has yielded multiple approaches. Largely due to an increase in life expectancy with higher risk of age-related neurological disorders, there is a growing need to better understand the brain, how it functions and dysfunctions and how we can aim to treat such illness. To treat such disorders, advanced *in vitro* models need to be developed in order that pharmaceuticals and cell therapies can be assessed at a higher level before clinical trials. However, owing to neural complexity and physical structure, studying and understanding large neural networks is difficult. Developing *in vitro* models that focus on analysing small neural networks via multi-electrode arrays (MEAs) could help improve our understanding and therefore improve treatment development. The work presented here is aimed towards this goal, being focused on chemical patterning to position and control the development of engineered neural architecture.

Materials and Methods

Oxygen plasma-cleaned coverslips were prepared with a cell-phobic polymer brush structure presented in patterns to control the quantity, location and direction of neuron growth. Model MEA surfaces were also prepared by spin coating a thin layer of SU8-10 onto coverslips; this is an epoxy-based negative photoresist that is used to insulate the top surface of MEAs. S1813 (positive photoresist) was used as a sacrificial template around which chemical brushes were generated via a surface-bound ATRP reaction.

SU8-10 was applied via the use of a pre-coater (GLYMO) spin coater rotating first at 500 rpm then 3000 rpm. Coverslips were baked at 95 °C for 60 seconds, exposed to i-line UV, baked again at 65 °C (60 seconds), 95 °C (60 seconds), 130 °C (120 seconds) and then left to cool slowly. S1813 was spun on at 500 rpm (30 seconds) 3000 rpm (60 seconds), prebaking at 110 °C for 75 seconds and exposed to i-line UV before developing. Patterns were post-baked at 110 °C for 10 minutes.

Polymer brushes were generated via three stages: 3-aminopropyl triethoxysilane (ATPES) was first applied, onto which α -bromoisobutryl bromide (BIBB) was then bound, followed by the 3-sulfopropyl methacrylate potassium salt (pKSPMA) being used as a monomer to grow the polymer brush. Chemical patterning was adapted from Pardo-Figuerez, et al.^[1] Surface chemistry and patterning were analysed by x-ray photoelectron spectroscopy (XPS), drop shape analysis (DSA) and fluorescent staining (conjugation of FITC). A neuroblastoma cell line, SH-SY5Y, were cultured onto treated coverslips and analysed via brightfield and fluorescent microscopy.

Results/ Discussion

Chemical patterning onto glass and SU8-coated coverslips was confirmed by multiple methods, with cells demonstrating preferential attachment and direction growth control following these patterns down to a few microns in feature size. Cell seeding densities showed some control over pattern conformity, with organization of neural networks being demonstrated towards the single cell-cell level.

Conclusion

Chemical patterning can be used to control the localization and controlled connectivity of neuronal cells, towards the production of specifically designed neural network architectures. This ability to control cell growth combined with reduced cell seeding density will enable the development of single neuronal networks onto multiple platforms starting with SU8-10/S1813 combination and then eventually leading to chemical patterning of MEAs.

Reference

[1] Pardo-Figuerez, M. et al, ACS Biomaterials Science & Engineering, **4**, 98-106s, 2018,

Unique patterns of elastin degradation in ascending aortic aneurysms in bicuspid aortic valve patients

Ya Hua Chim¹, Hannah Davies², Mark Field³, Jill Madine², Riaz Akhtar^{*1}

¹School of Engineering, University of Liverpool, ²Institute of Integrative Biology, University of Liverpool, ³Liverpool Heart and Chest Hospital

Corresponding author: r.akhtar@liverpool.ac.uk

Introduction

Bicuspid aortic valve patients (BAV) are associated with increased risk of ascending aortic aneurysms. However, it is unclear whether matrix degradation varies in different ascending aneurysm aetiologies. Here, we measured the micromechanical and biochemical properties and characterised elastin microstructure within the aortic tissue of two specific aneurysmal groups; BAV with associated aneurysm (BAV-A) and idiopathic degenerative aneurysm (DA). Aneurysmal tissues are compared against control tissue.

Methods

Aortic tissue was obtained from patients undergoing aneurysmal repair surgery (BAV-A; n=15 and DA; n=15). Control tissue was punch biopsies obtained during coronary artery by-pass graft (CABG; n=9). The elastic modulus (E) was measured with nanoindentation for the medial layer. Glycosaminoglycan (GAG), collagen and elastin levels were measured using biochemical assays. Verhoeff Van Gieson-stained sections were imaged for elastin microstructural quantification.

Results

BAV-A had over 20% higher E relative to control and DA. No significance between DA and control due to tissue heterogeneity. Collagen level of BAV-A ($36.9 \pm 7.4 \mu\text{g}/\text{mg}$) and DA ($49.9 \pm 10.9 \mu\text{g}/\text{mg}$) was higher compared to the control ($30.2 \pm 13.1 \mu\text{g}/\text{mg}$). GAG and elastin levels were not significant between the groups. Elastin segments were uniform in controls. Aneurysmal tissues had loss of segments close to the intima and adventitia layers. Although BAV-A and DA had more elastin segments compacted in the media, elastin segments were highly fragmented in DA.

Conclusions

BAV-A has increased stiffness within the aortic wall relative to DA and control tissue. Although elastin levels were equal for all groups, spatial distribution of elastin provided us with a unique profile of matrix degradation for BAV-A. The findings of this work are important for the development of future clinical treatment of BAV-A treatment.

Utilising self-assembling peptide hydrogels for MSC mechanobiology research

Joshua E. Shaw¹, Mhairi M. Harper², Joe Swift¹ and Stephen M. Richardson¹

¹ University of Manchester, UK, ² Biogelx Ltd, Glasgow, UK

INTRODUCTION: Understanding how bone marrow mesenchymal stem cells (BMMSCs) interpret and respond to mechanical stimuli is critical to understand the role of tissue mechanics on stem cell fate. Recent publications have highlighted the morphological and phenotypic response of BMMSCs to the stiffness of the culture surface. However, the synthetic polymer hydrogels used do not allow progression to more physiologically relevant 3D culture and rely on biochemical functionalisation for cell adhesion. To overcome these limitations with existing technologies, a self-assembling peptide (Fmoc-FF/S) hydrogel with tunable stiffness was investigated to establish whether BMMSCs display the characteristic morphological response to stiffness in the absence of biochemical functionalization(1-3).

METHODS: Fmoc-FF/S hydrogels were created at set range of concentrations: 5-40mM. The storage and loss modulus of the hydrogels was analysed using oscillatory rheology. Gel layers were formed in Mattek dishes and seeded with primary human BMMSCs ($2.2 \times 10^3/\text{cm}^2$). Viability was assessed after 24 hours using a fluorescent LIVE/DEAD assay. After 96 hours the BMMSCs were fixed, stained with Phalloidin 488 and Hoechst 33342 before fluorescent imaging. High throughput morphometric analysis was performed using CellProfiler to determine cell spread area, nuclear area and cell eccentricity.

RESULTS: Oscillatory rheology confirmed storage moduli of the hydrogel between 0.5 and 30kPa. LIVE/DEAD staining confirmed equal viability and density of BMMSCs bound to all stiffness of the hydrogels. Morphometric analysis revealed an increase in cell area, nuclear area and eccentricity of BMMSCs cultured on increasing hydrogel stiffness despite the lack of biochemical functionalisation of the hydrogel.

DISCUSSION & CONCLUSIONS: Together, these data highlight the biocompatibility of the peptide hydrogel for BMMSC culture and its suitability for future mechanobiology experiments with 3D culture.

ACKNOWLEDGEMENTS: JES would like to acknowledge funding from the BBSRC (GRANT #: BB/M01120B/1) and our collaboration with Biogelx Ltd.

REFERENCES: (1) Engler A, Sen S, Sweeney H, Discher D. Matrix elasticity directs stem cell lineage specification. *Cell*. 2006;126(4):677–89. (2) Zhou M, Smith AM, Das AK, Hodson NW, Collins RF, Ulijn RV, Gough JE. Self-assembled peptide-based hydrogels as scaffolds for anchorage-dependent cells. *Biomaterials*. 2009 May;30(13):2523-30. (3) Jayawarna V, Richardson SM, Hirst AR, Hodson NW, Saiani A, Gough JE, Ulijn RV. Introducing chemical functionality in Fmoc-peptide gels for cell culture. *Acta Biomater*. 2009 Mar;5(3):934-43.

Vascularisation Bioreactor: A step towards “plug-and-play” vascularised tissue

R. Balint¹, L. A. Hidalgo-Bastida^{2,3,4}

¹Manchester Institute of Biotechnology (MIB), University of Manchester, United Kingdom,

²Centre for Biomedicine, ³Centre for Advanced Materials and Surface Engineering, ⁴Centre for Musculoskeletal Science and Sports Medicine, Manchester Metropolitan University, UK

INTRODUCTION: In the human body, cells are no further than 200 μm from capillaries, ensuring effective blood supply of nutrients and oxygen. In contrast, in laboratory-grown tissues there is no such blood supply, and cells rely on simple diffusion for nourishment. Even, if pre-capillarised or grown in a perfusion bioreactor, upon implantation, it takes several days for the patient’s own blood supply to begin nourishing the laboratory-grown tissue either through inoculation or neovascularisation. Surgeons, when preparing tissue grafts, retain appropriate vasculature in order to enable immediate connection to the patient’s blood vessels, and would require the same from engineered tissue. Hence, this study aimed to design a bioreactor system that allows the co-culture and *in vitro* inoculation of a perfused artificial blood vessel (ABV) with a pre-capillarised tissue construct.

METHODS: Bioreactor chambers were designed and optimised in CAD software. *In silico* Finite Element Models were created of glucose and oxygen levels within the bioreactor chamber, taking into account diffusion through and uptake within the ABV and the pre-capillarised tissue. ABVs were formed *in vitro* by either casting or electrospinning pure or composited polycaprolactone (PCL) and polyurethane (PU). Biocompatibility of the ABVs was assessed with human umbilical vein endothelial cells (HUVECs) using the PicoGreen assay, and CellMask Orange staining with confocal microscopy. In a second iteration, collagen gel containing human aortic smooth muscle cells (aSMCs) at 1 mi cells/ml was cast around electrospun PCL-PU scaffolds, while HUVECs were seeded into the lumen of the gel at 200k cells/cm². Experiments were also performed with ABVs without the electrospun PCL-PU support. ABVs were grown for up to 14 days and imaged using confocal microscopy. Pre-capillary formation was optimised in collagen gel by combining HUVECs (200-1000k per ml), aSMCs (100-200k cells/ml) and human adipose derived stem cells (ADSCs)

(200-800k cells/ml) in M199 or EGM2 medium. The cells were pre-stained with Vybrant Multicolor dyes and capillary formation was tracked over 14 days using confocal microscopy. The addition of cell pellets or hanging drops into the gel as a starting site for capillary formation was also investigated. Frames to support the collagen gel inside the bioreactor were CAD designed and 3D printed.

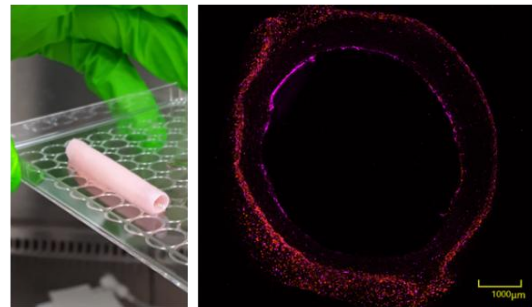


Fig. 1: ABV formed from aSMCs and HUVECs. Left – photo; Right – Confocal image of cross section (purple indicates HUVECs, while red indicates aSMCs.)

RESULTS: FEM models show a gradient of glucose and oxygen within the pre-capillarised graft. aSMCs contracted the collagen gel around the PCL-PU scaffold by day 10, forming an ABV with an outer layer of aSMCs and a clear inner lumen covered with HUVECs. Ideal cell concentration for pre-capillary formation was optimised to be 200-400k cells/ml HUVECs and ADSCs with 100k cells/ml aSMCs. Initial tests were run with the bioreactor system.

DISCUSSION & CONCLUSIONS: The bioreactor system, ABV and pre-capillarised tissue have been optimised. Extensive experimentation testing the efficacy of the bioreactor system will follow.

ACKNOWLEDGEMENTS: We thank the EPSRC Doctoral Prize Fellowship and the EPSRC Postdoctoral Fellowship (EP/P016898 /1) funding for financial support, and the Royce Institute for use of the CQ1 confocal microscope.

Authors Index

Abeygunawardana, V.	124	Basnett, P.	29
Addison, O.	59	Bate, T.	116
Aguilar-Agon, K.	112	Baynham, P.	45
Ahmed, I.	22, 110	Bayston, R.	31
Akhtar, R.	155	Beattie, L.	83
Al Hosni, R.	70	Beeken, L.	41
Alderson, A.	35	Behbehani, M.	29
Alexander, C.	6, 41	Bensidhoum, M.	24
Alexander, M.	6, 23, 27, 44, 94, 105, 106, 115	Bernhardt, A.	145
Ali, A.	122, 124	Berry, H.	141
Allen, C.	31	Best, S.	113, 133
Allen, S.	152	Bhangra, K.	86, 131
Almquist, B.	3	Birchall, M.	15, 77
Alobaid, M.	94	Black, K.	129
Alotaibi, N.	100	Blaker, J.	20, 98
Alvarez Paino, M.	6	Blanford, C.	50, 76
Amer, M.	6	Bonalumi, F.	40
Angkawinitwong, U.	18, 60	Bosworth, L.	8
Anneren, C.	101	Bowen, J.	15
Arkill, K.	134	Bowker, L.	139
Ashford, M.	75	Britchford, E.	31
Ashraf, W.	31	Budyn, E.	24
Ashworth, J.	21, 44, 134	Bullock, G.	37
Atkinson, S.	49	Burke, G.	136
Attallah, M.	59	Burova, I.	111
Aveyard, J.	7, 19, 47, 66, 102	Buttery, L.	63
Aviles Milan, J.	117		
Ayoub, A.	100	Callanan, A.	2, 52, 82, 108, 109, 116
		Cameron, R.	113, 133
Badylak, S.	8, 15	Campbell Ritchie, A.	79
Bakkalci, D.	90, 151	Campora, S.	27
Balestri, W.	118	Cantini, M.	9
Balint, R.	14, 157	Canty-Laird, E.	61
Bance, M.	96	Capel, A.	112, 119, 142
Bandulasena, H.	142	Cartmell, S.	20, 98, 143
Banks, C.	72	Carugo, D.	28, 34
Baranov, P.	67	Celiz, A.	62
Barcelona, E.	9	Chan, M.	11
Barrera, V.	8, 39, 104	Chan, W.	75
Barrett, P.	103	Chang, J.	15
Bartolacci, J.	15	Chaplin, K.	142
Baskapan, B.	109	Cheema, U.	70, 77, 90, 132, 140, 151

Childs, P.	121	Fedele, S.	90, 151
Chim, Y.	155	Felfel, R.	110
Choi, D.	131	Fermor, H.	92
Choreño Machain, T.	132	Ferri, S.	28, 34
Christie, S.	142, 154	Fest-Santini, S.	40
Cinquin, B.	24	Fisher, K.	88
Claeyssens, F.	42, 56	Fleming, G.	7
Clements, D.	75	Forbes, S.	116
Colley, H.	13, 144, 146	Foster, N.	128
Cooper, P.	58	Fothergill, J.	7
Cox, S.	12, 57, 59	Frankel, D.	144
Crua, C.	40		
Crucitti, V.	115	gao, y.	82
Cui, Z.	80	Gellert, P.	75
Curran, J.	4, 47, 123	Gerigk, M.	114
		Ghaemmaghami, A.	94, 105, 106, 115
D'Sa, R.	7, 8, 19, 47, 66, 102	Ghevaert, C.	113
Dalby, M.	9, 36, 100, 121, 148	Gibney, S.	145
Davies, H.	155	Gibson, I.	69, 138
Davies, N.	40, 120	Gibson, M.	94
Dawson, J.	26, 117, 147	Gill, R.	99
De Coppi, P.	77	Goldfinch, J.	107
De Grazia, A.	51	Gough, J.	50, 76, 97
de la Raga, F.	91	Grant, D.	22, 49, 110
Deller, R.	19, 66	Grant, H.	83
Denning, C.	27, 101	Graute, M.	87
Dixon, D.	136	Green, N.	68, 126
Dixon, J.	64, 89	Gregory, H.	18, 60
Doherty, K.	8	Grillo, A.	78
Domingos, M.	88, 143	Grover, L.	12, 59, 128
Dowding, K.	44		
Doyle, J.	147	Hague, R.	23, 27
Duffy, G.	129	Hajjali, H.	148
Duffy, P.	133	Hall, C.	139
Dundas, A.	115	Hall, R.	141
Dye, J.	80	Hanaei, S.	46
Dyer, R.	141	Haneef, A.	5
		Harding, A.	144
Edirisinghe, M.	29	Hardy, J.	20
Edmans, J.	146	Harper, M.	156
Eisenstein, N.	59	Harrison, C.	10
El Haj, A.	128	Hatton, P.	146
Elsawy, M.	149	Havins, L.	74
Emberton, M.	140	Haycock, J.	29, 56
Engstrom, D.	119	Hearnden, V.	37, 68, 95, 126
Evans, N.	26, 28, 34, 51, 135, 147	Henderson, C.	83
		Henstock, J.	4
bath.ac.uk, P.	99	Hernandez Miranda, M.	135
Farnie, G.	21		

Hidalgo-Bastida, A.	14, 72, 149, 157	Kellaway, S.	84, 85
Higginbotham, S.	68	Kelly, O.	147
Ho, J.	77	Kinsella, J.	154
Hoelig, P.	145	Knowles, J.	131
Hogg, P.	39	Koduri, M.	4
Holley, R.	150	Konan, S.	132
Hook, A.	145	Kotani, E.	33
Hooper, N.	88	Kret, K.	79
Hopkinson, A.	31, 65	Kuehne, S.	57
Hoppler, S.	69	Kureshi, A.	78
Hossain, K.	22	Kwok, J.	141
Howard, D.	113		
Huang, Y.	96, 114	Lace, R.	19
Hunt, J.	4, 118, 139	Lambert, D.	68, 144
		Lanham, S.	28
Ichiyama, R.	141	Laranjeira, S.	86
Illangakoon, E.	29	Latif, A.	115
Imere, A.	143	Lawson-Statham, P.	92
Ingavle, G.	120	Le Maitre, C.	35
Ingham, E.	104	Lee-Reeves, C.	43
Irvine, D.	23, 115	Lei, I.	96
Izon, M.	92	Levis, H.	61
		Lewis, L.	101
Jabbari, S.	57	Lewis, M.	16, 112, 119, 125, 142
Jalan, R.	120	Li, M.	47
James, J.	134	Li, Y.	25, 130
Jamshidi, P.	59	Louth, S.	59
Jayash, S.	58	Lowdell, M.	77
jell, g.	25, 90, 130, 151, 153	Lowther, M.	12
Jenkins, S.	107	Lu, Y.	76
Jenner, D.	51	Lukasiewicz, B.	29
Jennings, L.	92		
Jiang, C.	96	Ma, J.	20
Jiang, L.	27	Macia, M.	17, 87
Jiang, Z.	80	Mackay, S.	83
Johnson, S.	15, 75	Macnaughtan, J.	120
Jones, E.	92	MacNeil, S.	42, 126
Jones, J.	84, 153	Macri-Pellizzeri, L.	22
Jones, M.	33, 67	Madine, J.	155
Jordan-Mahy, N.	35	Madsen, L.	146
Joseph, A.	39	Mahalingam, S.	29
		Majewski, C.	10
Kabiri, B.	107	Malik, K.	151
Kammerling, L.	106	Mann, K.	102
Kanczler, J.	28	Mantovani, G.	75
Keane, T.	11, 43	Mardling, P.	35
Kearney, J.	39, 104	Marsit, N.	31, 65
Kearns, V.	61	Martin, N.	112
Kehoe, O.	150		

Martin, S.	119	Obata, A.	153
Maruta, R.	33	Obenza Otero, R.	75
May, J.	28, 34	Oliva Jorge, N.	3
Mbadugha, C.	105	Ollington, B.	13
McBride, F.	7, 47	omran, m.	10
McCormick, R.	5	Onion, D.	150
McDonald, A.	2, 108	Oosterbeek, R.	133
McIntosh, O.	31, 65	Orapiriyakul, W.	121
McKechnie, A.	37	Oreffo, R.	26, 121, 147
McLAREN, J.	22	Orozco Gil, L.	65
McMahon, S.	133	Ortega Asencio, I.	42
Medina-Fernandez, I.	62	Oswald, J.	67
Meek, D.	121	Ozulumba, T.	120
Meenagh, A.	54	Pape, J.	140
Meenan, B.	54, 93	Parmenter, C.	16
Mehrban, N.	15	Patel, R.	149
Menagh, G.	136	Patel, U.	22
Merry, C.	21, 44, 101, 134, 150, 152	Paxton, J.	17, 87
Merryweather, D.	16	Pearce, I.	5
Miller, A.	97	Pegg, E.	99
miller, c.	10, 37	Penuelas Alvarez, A.	95
Moakes, R.	128	Perea Ruiz, S.	73
Moers, C.	145	Pernstich, C.	33, 67
Moore, M.	93	Perry, C.	46
Moorehead, R.	10	Petaroudi, M.	36
Morgan, R.	150	Petta, S.	25
Mori, H.	33	Phamornnak, C.	20
Morris, R.	118	Phillips, J.	18, 43, 60, 85, 86, 131
Mortimer, J.	17, 87	Pijuan-Galitó, S.	44, 101
Mountcastle, S.	57	Pineda Molina, C.	8, 15
Mousa, M.	147	Pitt, G.	102
Moxon, S.	88	Player, D.	103, 112
Mudera, V.	78, 103	Polydorou, A.	28, 34
Munir, N.	108	Poologasundarampillai, G.	58
Murdoch, C.	13, 146	Porges, E.	51
Murukesan, D.	134	Porter, A.	153
Nai, K.	59	Portier, H.	24
Naudi, K.	100	Potjewyd, G.	88
Needham, D.	6	Quijano, L.	15
Newman, T.	51	Radu, A.	130
Ng, T.	138	Ramis, J.	63
Niu, X.	117	Ramnarine, R.	26
Nuttegg, C.	149	Ramos Rodriguez, D.	42
O'Dowd, J.	114	Rance, G.	27
O'Loughlin, D.	61	Rathbone, S.	104
Oakley, S.	125	Raval, R.	7, 47

Rawson, F.	27, 145	Shaw, D.	63
Rehmani, S.	89	Shaw, J.	156
Reid, A.	76	Shelton, R.	57, 58
Reid, J.	2	Shepherd, D.	59
Reid, S.	121	Shepherd, J.	10, 95, 113
Reinwald, Y.	46, 118, 122, 124	Sheridan, C.	61
Rezaei, A.	25, 130, 153	Shiple, R.	86, 111, 131
Richards, D.	30	Sidney, L.	31, 41, 65
Richards, I.	123	Skakle, J.	138
Richards, S.	94	Slater, C.	21
Richardson, S.	156	Slinn, I.	72
Riches, P.	83	Smith, A.	137
Roach, P.	16, 45, 74, 125, 154	Smith, L.	64
Robertson, V.	18, 60	Smith, P.	145
Roberts, C.	23	Smith, R.	11
Roberts, S.	70	Snuggs, J.	55
Rodrigo-Navarro, A.	36	Sottile, V.	22
Roe, J.	45	Spain, S.	146
Rooney, P.	8, 39, 104	Srisubin, T.	50
Rose, F.	6, 41, 48, 63, 148	Stening, J.	48
Ross, E.	36	Stevens, M.	11, 43
Rowland, C.	51	Storey, K.	107
Roy, I.	29	Stride, E.	28, 34
Ruiz, L.	23	Stuart, B.	49
Rumney, R.	28	Studd, A.	152
Russo, E.	75	Sturtivant, A.	52
Rust, P.	17, 87	Sutcliffe, C.	123
Saiani, A.	97	Swift, J.	156
Salam, N.	69	Takaki, K.	33
Sallstrom, N.	119	Tamm, C.	101
Salmeron-Sanchez, M.	9, 36, 100, 121, 148	TANDON, B.	98
Sammons, R.	57	Tanner, E.	121
sandeman, s.	40, 120	Tare, R.	117
Sandoval, A.	56	Taresco, V.	23
Sanjuan Alberte, P.	27	Tatler, A.	63, 64
Santini, M.	40	Taylor, A.	51
Santocildes-Romero, M.	146	Taylor, C.	29
Santos, L.	46	Tew, S.	123
Saso, S.	11	Thomas, K.	49
Savina, I.	40	Thompson, A.	134
Scammell, B.	22	Thompson, J.	44, 101
Scotchford, C.	49, 79	Tseng, F.	4
Scott, A.	15	Tsimbouri, P.	121
Sengers, B.	135	Tuck, C.	23, 27
Senior, J.	137	Turgut, B.	110
Shakesheff, K.	6, 64, 89	Turner, J.	130, 153
Shakib, K.	25		

Vadibeler, S.	87	Wildman, R.	23, 27, 115
Vaithilingam, J.	27	Willcock, H.	45
Varley, I.	10	Williams, G.	18, 60
Velazquez, M.	127	Williams, P.	152
Vonk, N.	17	Williams, R.	8, 19, 66, 129
Vyas, N.	57	Wilshaw, S.	141
		Wilson, A.	38
Wadge, M.	110	Wong, J.	143
Wall, I.	111	Woolfson, D.	15
Walmsley, D.	57	Workman, V.	68, 126
Wang, T.	88	Wright, A.	134
Warren, J.	92	Wu, Q.	34
Webber, J.	150	Wychowaniec, J.	149
Webber, M.	59		
Webster, G.	39	Xin, Y.	97
Wellings, D.	129	Zaib, J.	28
West, J.	117	Zelzer, M.	75
Weston, N.	16	Zhang, W.	88
White, L.	8, 48, 84, 85	Zhang, X.	133
Whitty, C.	67	Zhou, Z.	23
